University of Szeged

Faculty of Pharmacy

Department of Pharmacodynamics and Biopharmacy

Ph.D. Thesis

Antiproliferative and antimetastatic properties of A- or D-ring Modified Estrone Analogs

Seyyed Ashkan Senobar Tahaei Pharm.D.

Supervisor:

István Zupkó Ph.D., D.Sc.

2023

SCIENTIFIC PUBLICATIONS RELATED TO THE SUBJECT OF THE THESIS

I. **Senobar Tahaei SA**, Kulmány Á, Minorics R, Kiss A, Szabó Z, Germán P, Szebeni GJ., Gémes N, Mernyák E, Zupkó I: Antiproliferative and antimetastatic properties of 16-azidomethyl substituted 3-*O*-benzyl estrone analogs.
Int J Mol Sci, 2023; 24, 13749
IF: 5.600 / Q1   doi: 10.3390/ijms241813749

II. Jójárt R, **Senobar Tahaei A**, Trungel-Nagy P, Kele Z, Minorics R, Paragi G, Zupkó I, Mernyák E: Synthesis and evaluation of anticancer activities of 2- or 4-substituted 3-(*N*-benzyltriazolylmethyl)-13α-oestrone derivatives.
J Enzyme Inhib Med Chem, 2021; 36: 58-67
IF: 5.756 / Q1   doi: 10.1080/14756366.2020.1838500

III. Kiss A, Wölfling J, Mernyák E, Frank É, Benke Z, **Senobar Tahaei A**, Zupkó I, Mahó S, Schneider G: Stereocontrolled synthesis of the four possible 3-methoxy and 3-benzyloxy-16-triazolyl-methyl-estra-17-ol hybrids and their antiproliferative activities
Steroids, 2019; 152: 108500
IF: 1.948 / Q2   doi: 10.1016/j.steroids.2019.108500

ADDITIONAL PUBLICATIONS

1. Bamou FZ, Le TM, Tayeb BA, **Tahaei SAS**, Minorics R, Zupkó I, Szakonyi Z: Antiproliferative activity of (−)-isopulegol-based 1,3-oxazine, 1,3-thiazine and 2,4-diaminopyrimidine derivatives. ChemistryOpen 11: e202200169 (2022)
   IF: 2.630 / Q2   doi: 10.1002/open.202200169

2. **Senobar Tahaei SA**, Stájer A, Barrak I, Ostorházi E, Szabó D, Gajdács M: Correlation Between Biofilm-Formation and the Antibiotic Resistant Phenotype in *Staphylococcus aureus* Isolates: A Laboratory-Based Study in Hungary and a Review of the Literature. Infect Drug Resist. 23;14:1155-1168 (2021)
   IF: 4.177 / Q1   doi: 10.2147/IDR.S303992

3. Csupor D, Kurtán T, Vollár M, Kúsz N, Kövér KE, Mándi A, Szűcs P, Marschall M, **Senobar Tahaei SA**, Zupkó I, Hohmann J: Pigments of the moss Paraleucobryum longifolium: Isolation and structure elucidation of prenyl-substituted 8,8'-linked 9,10-phenanthrenequinone dimers. J Nat Prod 83: 268-76 (2020)
   IF: 4.050 / Q1   doi: 10.1021/acs.jnatprod.0c00243

4. Bús C, Kúsz N, Jakab G, **Senobar Tahaei SA**, Zupkó I, Endrész V, Bogdanov A, Burián K, Csupor-Löffler B, Hohmann J, Vasas A: Phenanthrenes from Juncus compressus Jacq. with promising antiproliferative and anti-HSV-2 activities. Molecules 23: 2085 (2018)
   IF: 3.060 / Q1   doi: 10.3390/molecules23082085

Cumulative Impact Factor : 27.221

Table of Contents

1. Introduction

1.1. Epidemiology of Cancer

Cancer has emerged as a significant and noteworthy contributor to mortality across many countries, demonstrating mortality rates comparable to those attributed to stroke and coronary heart disease. This ongoing trend is exemplified in the latest update emanating from the International Agency for Research on Cancer (IARC) database. According to this update, the year 2020 witnessed the global landscape being marked by the emergence of 19.3 million new instances of cancer, tragically resulting in nearly 10 million deaths that could be directly attributed to cancer-related causes. These figures underscore the undeniable gravity of the situation, prompting a collective call to action[1].

Moreover, insights derived from the IARC database offer projections that spotlight the potential trajectory of the cancer burden on a global scale. These projections indicate an impending escalation, with the worldwide incidence of cancer anticipated to rise to a staggering 28.4 million cases by 2040. This projection underscores a notable 47% increase from the preceding numerical value. This serves as a reminder of the magnitude of the challenge ahead and underscores the imperative to prioritize and mobilize resources for effective prevention, early detection, and comprehensive treatment strategies. Examining the specific facets of this complex issue, it becomes evident that lung cancer is the leading cause of cancer-related deaths, accounting for a significant 18% of mortality attributed to tumors. Lung cancer is closely followed by colorectal cancer (responsible for 9.4% of such deaths), liver cancer (attributed to 8.3%), stomach cancer (contributing to 7.7%), and female breast cancer (playing a role in 6.9% of these fatalities). These sobering statistics underscore the diverse cancer types that demand comprehensive research, improved diagnostic tools, and innovative treatment modalities[1,2].

Shifting the focus to the demographic distribution of these challenging realities, it is noteworthy that breast cancer emerges as the most frequently diagnosed malignancy among female patients, accounting for an alarming 24.5% of new cases. This fact highlights the urgent need for enhanced awareness campaigns, accessible screening programs, and dedicated research efforts to improve breast cancer prevention and early intervention measures[1].

Taking a holistic view, a significant 38.9% of newly diagnosed cancers in females are attributed to gynecological malignancies. This highlights the intricate and multifaceted nature of cancer, which necessitates a comprehensive and multi-pronged approach to tackle its challenges. The confluence of these statistics underscores the need for continued collaboration among researchers,

medical professionals, policymakers, and communities to collectively address the escalating cancer burden and strive toward improved outcomes for patients worldwide [1].

The distribution of the 2.26 million female breast cancer cases identified in 2020 reveals a notable disparity across geographical regions, emphasizing an unequal landscape. This is particularly evident when assessing the age-standardized incidence rates, which exhibit a discernible range. Europe is the region with the highest incidence rate, at 69.7 cases per 100,000 individuals. In contrast, South-East Asia records the lowest incidence rate at 28.3 cases per 100,000 individuals. These figures underscore the influence of regional factors and dynamics on the prevalence and manifestation of female breast cancer.

A noteworthy and statistically significant trend emerges when delving into the relationship between the mortality-to-incidence ratio (MIR) and the human development index (HDI). This correlation elucidates an intriguing pattern: a discernible inverse relationship between these two variables. The MIR, which serves as an indicator of the prognosis and outcomes for patients with breast cancer, exhibits a tendency to be higher in regions with a lower HDI. This statistical association accentuates the challenging reality faced by patients residing in less developed areas of the world, where access to advanced healthcare resources, early detection initiatives, and comprehensive treatment options might be comparatively limited.

This interplay between MIR and HDI underscores the complexity of the global health landscape and highlights the multifaceted nature of factors that impact cancer-related outcomes. While medical advancements and improved healthcare infrastructure have led to more favorable prognoses in more developed regions, the data reflect the urgent need to address healthcare disparities on a global scale. By acknowledging and actively managing the connections between healthcare access, socio-economic development, and cancer outcomes, we can strive for a more equitable distribution of resources and interventions, ultimately working towards better outcomes for all individuals affected by breast cancer, regardless of their geographical location [2].

All these epidemiological results suggest that the prevention and treatment of female breast cancer are not yet solved despite the impressive therapeutic progress of the latest decades.

1.2. Awareness and Contemporary Insights into Breast Cancer

Breast cancer is the prevalent form of cancer, the foremost cause of cancer-related fatalities among females globally. In 2008, around 1.38 million fresh instances of breast cancer were identified, wherein nearly half of all breast cancer patients and approximately 60% of associated mortalities emanated from developing nations. The spectrum of breast cancer survival rates diverges

significantly globally, ranging from a projected 5-year survival rate of 80% in developed regions to below 40% for their developing counterparts[3].

Nations in the developing phase encounter limitations in terms of resources and infrastructure, which pose significant obstacles to the overarching goal of enhancing breast cancer outcomes through the prompt identification, diagnosis, and effective management of the disease[4].

In well-developed countries such as the United States, it is estimated that approximately 232,340 females will receive diagnoses of breast cancer, leading to the unfortunate loss of 39,620 lives among females due to this condition in the year 2013[5].

The substantial reduction in breast cancer-related mortality in the United States between 1975 and 2000 is attributed to continuous advancements in screening mammography and treatment approaches[6].

As per the World Health Organization (WHO), the fundamental approach to improving breast cancer outcomes and survival remains rooted in early detection. Various contemporary medications are prescribed for the treatment of breast cancer. Medical intervention for breast cancer involving antiestrogens like raloxifene or tamoxifen can potentially prevent the onset of breast cancer in individuals at an elevated risk of its development. Additionally, a preventive measure involving surgery on both breasts is considered for those at an escalated risk of female cancer occurrence. For patients diagnosed with breast tumors, a range of management strategies is employed, encompassing targeted therapy, hormonal therapy, radiation therapy, surgical procedures, and chemotherapy. In cases where distant metastasis is present, interventions are typically directed toward enhancing the quality of life and overall survival rate[7].

In 2012, a total of 1.67 million fresh instances of breast cancer were diagnosed, constituting a noteworthy 25% of all cancer diagnoses among women. This global distribution revealed that 883,000 cases emerged within less developed countries, while 794,000 cases were reported in more developed countries. Based on available data, the incidence of breast cancer stands at 145.2 women per 100,000 in Belgium and 66.3 women per 100,000 in Poland.

Further statistics indicate that the United States witnesses an incidence of one out of every eight women being affected by breast cancer. In the Asian context, the prevalence is notably lower, with one woman out of 35 facing a breast cancer diagnosis. In Iran, the figures point to an incidence rate of 10 cases per 100,000 individuals, with an annual report of approximately 7,000 new cases[8–10].

1.3. Types of Breast Cancer

1.3.1. Non-Invasive Breast Cancer

This form of cancer remains localized within the lobules or ducts where it originates and has not spread to distant areas. An illustrative instance of this non-invasive breast cancer is ductal carcinoma in situ, which materializes when atypical cells emerge within the milk ducts yet do not invade the adjacent tissues or extend beyond. The term "in situ" signifies "in place." Although the atypical cells remain confined within the lobules or ducts and do not invade surrounding tissues, they possess the potential to evolve into invasive breast cancer.

Lobular carcinoma in situ is recognized more as an indicative risk factor than a precursor to subsequent invasive cancer growth. Consequently, additional surgical intervention is unnecessary once the diagnosis is made, with sequential follow-up recommended. Regarding the management of ductal carcinoma in situ, it is noteworthy that preserving the breast is currently considered the optimal approach for treating breast cancer, the ailment being addressed. The limitations associated with management recommendations grounded in retrospective data are acknowledged, underscoring clinical studies need to establish the most effective beneficial treatment strategies for non-invasive breast cancer[11–13].

1.3.2. Lobular Carcinoma in situ (LCIS)

This variant of breast cancer originates within the breast lobules. Importantly, this type of breast cancer remains confined within the lobules and does not extend beyond them into the surrounding breast tissue. Commonly referred to as non-invasive breast cancer, lobular carcinoma in situ is a distinctive diagnostic classification[14,15].

1.3.3. Ductal Carcinoma in situ

Ductal carcinoma in situ represents the most prevalent form of non-invasive breast cancer, primarily confined within the breast ducts. An illustrative instance of this type is ductal comedocarcinoma[16].

1.3.4. Invasive Breast Cancer

This phenomenon occurs when abnormal cells originating within the lobules or milk ducts extend into the immediate vicinity of breast tissue. The cancerous cells possess the capacity to disseminate from the breast to various body regions through the immune system or systemic circulation. This migration may occur early in the tumor's development when it is small or later when it has grown significantly. Invasive breast cancer ranks among the most prevalent forms of cancer in females.

Notably, the affluent populations of Australia and Europe exhibit regions with heightened susceptibility, wherein approximately 6% of females encounter invasive breast cancer before age 75. The incidence of breast cancer demonstrates a rapid increase with advancing age. When invasive breast cancer spreads to other organs, it assumes the classification of metastatic breast cancer. The brain, bones, lungs, and liver are among the most common organs to which these cells metastasize. Once again, these cells undergo irregular proliferation, creating new cancer formations. Although the newly arising cells are situated in different body parts, the condition is still classified as breast cancer[17–21].

1.3.5. Infiltrating Lobular Carcinoma

Infiltrating lobular carcinoma is equivalently identified as invasive lobular carcinoma. This variant, known as ILC, originates in the breast's milk-producing glands (lobules), often displaying a tendency to extend to distant regions within the body[22].

1.3.6. Infiltrating Ductal Carcinoma

Infiltrating ductal carcinoma is alternatively referred to as invasive ductal carcinoma. This form of carcinoma, denoted as IDC, originates within the breast's milk ducts and progresses to infiltrate the duct walls, subsequently invading the surrounding adipose tissues of the breast. Furthermore, the potential for extension exists in other anatomical regions of the body[23].

1.3.7. Medullary Carcinoma

Medullary carcinoma is invasive breast cancer characterized by forming a distinct boundary between normal and medullary tissue[24].

1.3.8. Mucinous Carcinoma

Colloid carcinoma, also known as mucinous carcinoma, is an infrequent form of breast cancer originating from mucus-producing cancer cells. Women afflicted with mucinous carcinoma typically experience a more favorable prognosis compared to those diagnosed with other, more prevalent forms of invasive carcinoma[25].

1.3.9. Tubular Carcinoma

Tubular carcinomas represent a distinct subtype of invasive breast carcinoma. Women diagnosed with tubular carcinoma typically exhibit a more favorable prognosis compared to those with other, more common forms of invasive carcinoma[26].

1.3.10. Inflammatory Breast Cancer

Inflammatory breast cancer is characterized by the pronounced swelling of the breasts, often accompanied by redness and warmth. Additionally, the skin over the breast might exhibit dimples or extensive ridges. These manifestations result from cancer cells obstructing lymph vessels or channels within the skin. Despite its rarity, inflammatory breast cancer displays an exceptional aggressiveness in its growth. Managing this condition necessitates a meticulous orchestration of multidisciplinary approaches, encompassing radiation therapy, surgery, chemotherapy, and imaging.

Since its application in this context, the introduction of neoadjuvant chemotherapy has significantly contributed to the enhancement of overall survival. Notably, neoadjuvant chemotherapy has played a pivotal role in augmenting general survival and rendering locoregional treatments, such as radiation and surgery, more effective. This convergence of treatment strategies has yielded sustained improvements in managing this ailment[27,28].

1.3.11. Paget's Disease of The Breast

It represents an infrequent subtype of breast cancer that often exhibits visible alterations affecting the nipple of the breast. Characterized by symptoms such as reddish and itchy rashes involving the nipple, this condition can sometimes extend to the surrounding normal skin. While sharing similarities with skin conditions like eczema and psoriasis, a distinguishing feature is that Paget's disease usually affects just one breast and typically initiates from the nipple rather than the areola. In contrast, other skin conditions tend to affect both breasts and may commence from the areola. Paget's disease of the breast accounts for approximately 1-3% of all breast cancers and can affect both men and women. Despite ongoing investigations, the precise underlying mechanisms behind its pathogenesis remain unclear. Various theories have been proposed in support of its development. Warning signs encompass nipple bleeding, discharge oozing, nipple flattening or inversion, and the presence of breast lumps. A diagnostic method known as punch biopsy is employed for confirmation.

The prognosis is generally favorable when Paget's disease remains confined within the nipple or breast ducts[29,30].

1.3.12. Phyllodes Tumor

Phyllodes tumors exhibit the potential to manifest as either benign or malignant growths. Emerging within the breast's connective tissues, phyllodes tumors can be managed through surgical excision. Notably, phyllodes tumors are sporadic, with fewer than 10 female fatalities [31–33].

1.3.13. Triple-Negative Breast Cancer

Breast cancer is presently comprehensively acknowledged as a heterogeneous condition, encompassing distinct subtypes delineated by their diverse pathological attributes, prognoses, and responsiveness to treatment. One such subtype is triple-negative breast cancer, characterized by the absence of expression of progesterone receptor, human epidermal growth factor receptor 2, and estrogen receptor. This variant exhibits a notably aggressive nature, predominantly observed among premenopausal women. Among white females, this subtype accounts for 10–15% of cases, constituting a significantly elevated occurrence rate[31,32].

Our study mainly concentrated on this kind of breast cancer because we tested our selected compounds, **16AABE** and **16BABE**, specifically against triple-negative cancer cells.

1.4. Pathogenesis of Breast Cancer

The breast, a complex tubulo-alveolar organ enveloped by an asymmetrical connective tissue matrix, undergoes dynamic changes throughout a woman's life. These alterations, evident during menstrual cycles and pregnancy, suggest the presence of precursor cells in mature tissue capable of generating new duct-lobular units. The breast's typical histology comprises a stratified epithelium framed by a basement membrane and interwoven with blood vessels, lymphatics, and stromal cells. Immunohistochemical staining can discern myoepithelial and epithelial cells within the stratified epithelium. The cellular heterogeneity seen in breast carcinoma likely stems from the neoplastic transformations of these cell types or stem cells with differentiation potential. In breast cancer, neoplastic cells defy the regulated growth typical of normal tissues, characterized by prolonged proliferation independent of external cues. Distinct from normal cells, they override growth suppressor genes [33–38]

Breast cancer, a malignant disease originating in breast cells, results from genetic and environmental interplay. DNA damage, genetic mutations like BRCA1, BRCA2, and environmental estrogen exposure are among the contributors. While normal protective pathways prevent cell death, mutations impairing these mechanisms promote cancer formation. Dysfunctional growth factor signaling and interaction between epithelial and stromal cells can also fuel malignancy. Overexpressed leptin in breast adipose tissue promotes cell proliferation and cancer growth. Cancer cells, sustained by the enzyme telomerase, replicate without chromosomal shortening and induce angiogenesis for nutrient supply. They breach tissue boundaries, spreading through blood and lymphatic vessels to form secondary tumors[39–45].

1.5. Causative Factors

Breast, being sensitive to estrogen, can experience enlargement and tenderness due to birth control pills or estrogen replacement. Combined with a high-fat, low-fiber Western diet, this effect could potentially trigger breast cancer. Incidence is higher in women above 50, and epidemiological studies suggest that having more children may reduce risk. Breast cancer accounts for 10.04% of all cancers, mainly affecting women aged 40 to 50. Environmental factors like early childbirth before the age of 20 may decrease risk. The risk of breast cancer increases with age and may be amplified by certain genetic factors. Family history, particularly among close relatives, increases risk, as does a positive history of ovarian, endometrial, or colon cancer. Genetic mutations, such as the BRCA1 gene, play a role, but environmental factors also contribute, including obesity, deficiency of vitamin D, and exposure to certain pollutants. Hormone replacement therapy, obesity, and consumption of alcohol can enhance breast cancer risk[46–51].

1.6. Mortality of Breast Cancer

Breast cancer ranks as the fifth most common cause of cancer-related deaths. The mortality and age-standardized prevalence of breast cancer are notably higher in the United States compared to global statistics.The worldwide death toll from breast cancer was estimated at 519,000 by a study in 2004[52].

In the United States, approximately 1,208,000 cancer cases are reported annually, resulting in about 538,000 deaths from the disease, constituting nearly one-fifth of all annual deaths across various causes[53].

1.7. Treatment of Breast Cancer

1.7.1. Role of Estrogen and Progesterone Receptors in Treatment

The estrogen receptor assay has become a standard practice in managing complex breast cancer. Tumors lacking the estrogen receptor tend to respond less to endocrine treatment, while positive estrogen receptor status shows 50–60% response rates. Recent studies indicate that the estrogen receptor status of the primary tumor is a better predictor of endocrine dependence in metastatic cancers at the time of clinical progression. Furthermore, the absence of estrogen receptor in the primary tumor is a significant independent predictive factor for higher relapse rates and shorter survival.

Quantitative estrogen receptor assessment and progesterone receptor evaluation are methods to enhance the accuracy of selecting patients for hormonal therapy. Cancers with high quantitative estrogen receptor levels or positive progesterone receptor status exhibit the most favorable

response. Initial research suggests that progesterone receptors might better indicate hormone dependence than quantitative estrogen receptor levels[54].

1.7.2. Hormonal Therapy

Anti-estrogen therapy is pivotal in treating breast cancer, particularly in cases where hormones influence the tumor and possess hormone receptors like estrogen receptors. The most common category of drugs employed for breast cancer treatment is anti-estrogen therapy, which includes agents such as tamoxifen, raloxifene, and toremifene. Tamoxifen, for instance, works by inhibiting the entry of estrogen into breast cancer cells, effectively curbing their growth. It's suitable for females of various age groups, with a particular preference for those with estrogen receptor-positive breast carcinoma. Tamoxifen acts as a selective estrogen receptor modulator (SERM), exhibiting anti-estrogen properties in breast tissues while mimicking estrogen in other body areas like the uterus. Though the toxic effects of anti-estrogen therapy are relatively minimal compared to other cytotoxic drugs, some patients may discontinue treatment due to side effects such as hot flushes, gastrointestinal issues, or vaginitis. Conversely, fulvestrant is a complete estrogen antagonist with notable anti-neoplastic action in breast tissues. Notably, raloxifene and tamoxifen are both SERMs that selectively inhibit or stimulate estrogen-like activity in different tissues, affecting estrogen receptors. Tamoxifen's efficacy in reducing breast cancer risk has been established through extensive research, showing a 38% decrease in overall breast cancer occurrence among high-risk individuals when administered over 5 years[55–60].

However, various adverse effects have been associated with tamoxifen use, including venous thrombosis, cataracts, endometrial cancer, and menstrual disorders. Another drug, raloxifene, has also demonstrated a capacity to reduce breast cancer risk, although it may have certain side effects. Clinical studies have found raloxifene comparable to tamoxifen in lowering the risk of invasive breast cancer, with fewer incidences of cataracts and thromboembolism. Over the years, the FDA's approval of these drugs for breast cancer prevention has reinforced their significance in managing this disease[61,62].

1.7.3. Chemotherapy

Chemotherapy refers to the process of using specific medications to eliminate cancer cells. Depending on the patient's condition, it can be employed both before and after surgery. According to the American Cancer Society, chemotherapy medications include docetaxel, paclitaxel, platinum agents (cisplatin, carboplatin), vinorelbine, capecitabine, liposomal doxorubicin, cyclophosphamide, carboplatin, and more[63]. However, chemotherapy is associated with various side effects. Treating metastatic or secondary breast cancer is challenging but can be managed and

controlled for several years. Chemotherapy may be prescribed to control the progression of metastatic breast cancer, slow its growth, and alleviate certain symptoms. Other treatment options can also be employed with or before chemotherapy[64].

Epirubicin and doxorubicin are among the most frequently utilized medications in breast cancer treatment. Evidence suggests that anthracyclines, a class of drugs that includes these two, may be more effective in treating breast cancer than other types of chemotherapy medications[65].

1.8. Cancer and Steroids: Unveiling the Therapeutic Potential

Steroids encompass a group of endogenous compounds that exhibit multifaceted roles as potential agents for combating cancer. Within hormone-dependent tumors, including those found in breast, uterine, ovarian, prostate, and endometrial contexts, an elevated expression of steroid receptors has been implicated in the augmentation of cellular proliferation. Various strategies have been formulated to mitigate the growth-stimulating hormonal response of these cancerous cells, as discussed earlier in this study.

The realization of a substantial improvement in the global burden of cancer hinges on developing and deploying innovative therapeutic approaches, including the introduction of novel pharmaceutical compounds. Exploring the potential of compounds characterized by steroidal structures as effective agents against cancer has a rich history. This exploration of the anticancer properties of steroidal compounds has unfolded over many years. In recent decades, this endeavor has yielded noteworthy results, integrating several fresh steroid-based drugs into clinical practice. Among these breakthroughs, compounds like cyproterone, finasteride, exemestane, and fulvestrant have emerged as notable additions to cancer treatment options. The integration of these compounds has significantly reshaped the landscape of clinical oncology. Notably, exemestane, which operates as an aromatase inhibitor, has found application in treating postmenopausal breast cancer. Its distinctive mechanism of action has made it an asset in combating this specific type of cancer, offering renewed hope to patients in this demographic.

Another way of progress has been utilizing 5α-reductase inhibitors, exemplified by dutasteride, within clinical contexts. These inhibitors are pivotal in alleviating androgen-dependent cancers, representing a therapeutic possibility that has shown promise in addressing specific cancer types. This development signifies a stride forward in personalized treatment approaches, as it targets the unique characteristics of certain cancers driven by androgenic processes.

In addition, a broad spectrum of steroidal molecules has been either derived from natural reservoirs or meticulously formulated and synthesized. These compounds have garnered attention due to their reported efficacy against cancer cells, achieved through mechanisms distinct from

hormonal pathways. Notably, steroidal compounds possessing cytotoxic attributes influence various molecular targets. These targets encompass vital cellular components such as microtubules and topoisomerases. Through intricate interactions with these molecular entities, the cytotoxic steroids intricately disrupt cellular processes, often precipitating the cell cycle's arrest and ultimately prompting the complex cascade of programmed cell death called apoptosis. This multifaceted action on various cellular fronts underscores the potential of these steroidal entities as promising candidates for novel therapeutic interventions in the realm of cancer research[66]. Integrating these compounds into clinical practice exemplifies the ongoing commitment to advancing cancer treatment methodologies. By embracing the potential of these novel agents with steroidal scaffolds, the medical community continues to explore and uncover new avenues for combating various cancer types. These advancements stand as a testament to the relentless pursuit of effective therapeutic solutions that can profoundly impact patient's lives, ultimately contributing to the collective goal of reducing the global burden of cancer[67].

A pragmatic approach to developing innovative drug candidates entails strategically manipulating naturally occurring molecules through chemical modifications. This deliberate alteration results in the creation of semi-synthetic analogs that exhibit a range of distinct biological activities. This strategy capitalizes on the intricate understanding of the molecular structures and mechanisms inherent to endogenous compounds, using this knowledge as a foundation to craft novel compounds with enhanced or modified properties.

By building upon the existing scaffold of naturally occurring molecules, researchers can implement precise chemical modifications to achieve desired outcomes. This may encompass tailoring the compound's pharmacokinetic profiles, optimizing their interactions with biological targets, or introducing new functionalities that broaden their potential therapeutic applications. The resulting semi-synthetic analogs can encompass diverse biological activities, ranging from improved efficacy to reduced side effects[68].

Early incorporation of steroid-based compounds into anticancer strategies can be traced back to the utilization of diverse botanical extracts. Emerging evidence highlights the significance of steroid-like triterpenes, such as betulinic acid and oleanolic acid, and their derivatives in this context. These compounds exhibit compelling attributes, including potent proapoptotic effects (initiating programmed cell death) and antimigratory properties, across a range of human cancer cell lines.

Identifying these natural compounds as potential anticancer agents emphasizes the value of exploring nature's repertoire in drug discovery. Betulinic acid, oleanolic acid, and related derivatives offer promise as foundational components for future anticancer therapies, with their

demonstrated ability to induce cell death and inhibit cell migration, addressing crucial aspects of cancer treatment and metastasis prevention. This journey from traditional botanical knowledge to contemporary drug development highlights the fusion of traditional wisdom and modern scientific exploration in pursuing innovative cancer treatments[69–75].

Recent research has focused on exploring modifications to estrane-based compounds within rings A or D. Notably, the investigation of 16-triazolyl estranes has revealed their potential as promising agents with anticancer properties[76,77].

Studies have demonstrated that numerous core-modified estradiol analogs exhibit considerable antiproliferative activity against human cancer cell lines derived from gynecological malignancies[78]. The careful consideration of various factors, including the position, specific characteristics, size, and polarity of newly incorporated substituents within the molecule, has been observed to wield significant influence over the anticancer properties of the designed derivatives. This meticulous approach to molecular design underscores the intricacies of tailoring compounds for optimal therapeutic effects. Indeed, the tailored modifications play a pivotal role in dictating the compound's interactions with cellular components and signaling pathways, ultimately shaping their ability to combat cancerous growth.

Intriguingly, certain core-modified estrones have showcased a distinct antiproliferative mechanism that directly engages with the tubule-microtubule system, a crucial component in cell division and replication processes. This interaction leads to discernible consequences as the rates of tubulin polymerization become disrupted. This disruption, in turn, interferes with the intricate balance required for proper cellular division, culminating in hindered cancer cell proliferation. This intricate dance between molecular design and cellular behavior underscores the potential of tailored core-modified estrones as agents that disrupt fundamental cellular processes, offering a promising avenue for targeted anticancer interventions[77,79].

We recently reported certain 16,17-functionalized 3-methoxy or 3-benzyloxy estrone derivatives as potent antiproliferative compounds[80]. The arrangement of substitutions on ring D and the type of protective group attached to C-3-O have been shown to impact the compound's ability to inhibit cell growth significantly. The intricate interplay of these factors has a pronounced effect on the compound's potential to impede cellular proliferation. Compounds featuring 3-benzyl ethers as protective groups have demonstrated notably more vigorous inhibitory activity, underlining their heightened potency in exerting anticancer effects[80]. The substituent's nature and orientation affected the antitumoral behavior .

Based on our promising results concerning the antiproliferative activities of 16,17-functionalized estrone or estradiol 3-ethers, the objective of this study is to assess the anticancer properties of four 16-azidomethyl-17-hydroxy derivatives (**SI–SIV**) (Figure 1), their triazolyl analogs (**TI– TXIII**) (Figure 2 and 3) and the 17-keto counterparts of 16-azidomethyl compounds (**16AABE** and **16BABE**) (Figure 1).

The present study aimed to assess the antiproliferative and antimetastatic properties of these novel substituted steroidal compounds.
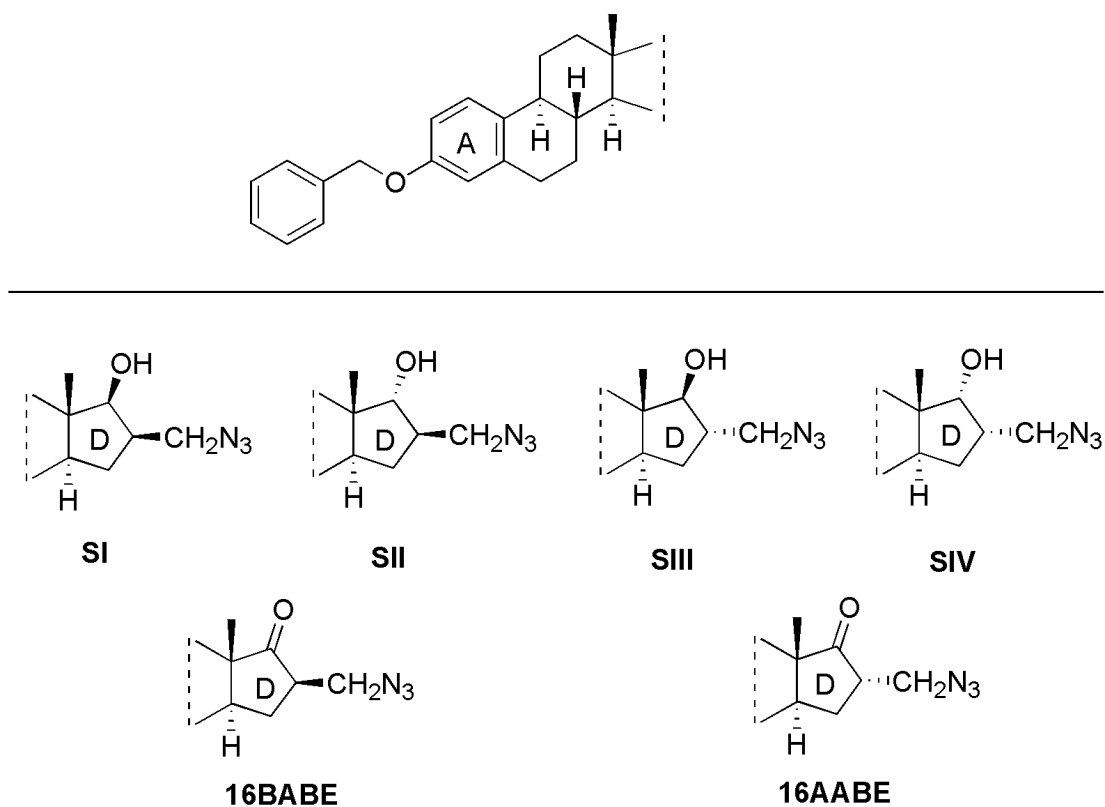

Figure 1. Structures of the tested starting compounds (SI–SIV) and the newly synthesized 16β-azidomethyl-3-O-benzyl estrone (16BABE) and 16α-azidomethyl-3-O-benzyl estrone (16AABE).

2. Aims of The Study

The primary aim of this study was to explore the potential antiproliferative and antimetastatic characteristics of these promising compounds. This investigation was conducted through in vitro experiments on cell lines associated with breast and gynecological tumors. Additionally, the study aimed to uncover the underlying mechanism that drives these compound's actions, providing insights into their mode of operation.

The performed experiments aimed to achieve the following objectives:

- The experiments are designed to elucidate the antiproliferative properties of the tested compounds on breast and gynecological cancer cell lines. Furthermore, the IC_{50} values of these compounds are being ascertained utilizing the established MTT assay protocol.

- The study encompasses the estimation of tumor selectivity indices across all examined cell lines, with a comparative reference to a non-cancerous cell line (NIH/3T3).

- In this study, the objective of performing the PI staining cell cycle by flow cytometry was to investigate the distribution of cells within different phases of the cell cycle. This method allows for a comprehensive understanding of cellular progression, aiding in assessing potential alterations induced by the experimental conditions and providing valuable insights into the mechanistic underpinnings of the observed effects.

- Conducting the tubulin polymerization assay serves as a method to evaluate the influence of the tested compounds on tubulin dynamics. This assay offers valuable insights into the potential implications for cell growth and migration, which are pivotal for comprehending their therapeutic prospects, particularly within cancer research.

- This investigation aims to assess the tested compound's inhibitory impacts on the initial stages of metastasis development, including migration and invasion. This objective will be achieved through the implementation of wound-healing and Boyden chamber assays, which collectively offer insights into the compound's potential to hinder these critical processes.

- Measuring the estrogenic activity of the test compounds using a transfected cell line provides valuable insights into the hormonal properties of the tested molecules.

3. Materials and Methods

3.1. Cell Culture and Chemicals

The utilized cell lines (HeLa, MDA-MB-231, MCF-7, A2780, and NIH/3T3) were obtained from ECACC (European Collection of Cell Cultures, Salisbury, UK). In contrast, SiHa and T47D-KBluc cells were obtained from ATCC (American Tissue Culture Collection, Manassas, VA, USA). All cell lines were cultured in Eagle's Minimum Essential Medium (EMEM) at 37 °C in a humidified atmosphere with 5% carbon dioxide. The medium was supplemented with 10% fetal bovine serum (FBS), 1% non-essential amino acid solution, and 1% penicillin, streptomycin, and amphotericin B mixture. All cell culture mediums and supplements were obtained from Lonza Group Ltd. (Basel, Switzerland). Chemicals for the described in vitro experiments were purchased from Merck Ltd. (Budapest, Hungary) unless stated otherwise.

3.2. Determination of Antiproliferative Activity (MTT Assay)

The antiproliferative effects of the presented compounds were evaluated on a panel of human gynecological cancer cell lines. MCF-7 and MDA-MB-231 cell lines were derived from breast cancers, while HeLa and SiHa cell lines originated from cervical cancers with different pathological backgrounds, while A2780 cells are from ovarian cancer. Non-cancerous human fibroblast cells (NIH/3T3) were used exclusively to assess the selectivity of the two azidomethyl compounds.

Cancer cells were seeded in a 96-well microplate for the proliferation assay at 5000 cells/well density. After 24 hours of incubation, 200 µL of new medium containing the tested compounds at 10 or 30 µM concentrations was added.

Following incubation for 72 hours at 37 °C in a humidified atmosphere containing 5% CO_2, cell viability was assessed by adding 20 µL of a 5 mg/ml 3-(4,5-dimethylthiazol-2-yl)-2,5-diphenyltetrazolium bromide (MTT) solution. The yellow MTT solution was converted to violet crystals by mitochondrial reductases in viable cells after a 4-hour incubation. Subsequently, the medium was removed, and the formazan crystals were dissolved in 100 µL of DMSO with shaking at 37 °C for 60 minutes.

The absorbance of the reduced MTT solution was measured at 545 nm using a microplate reader, with untreated cells serving as the negative control [31]. In the case of active compounds (i.e., higher than 50% cell growth inhibition at 10 or 30 µM), the assay was repeated with a series of dilutions, and sigmoidal dose-response curves were fitted to the obtained data. The IC_{50} values, representing the concentration at which cell proliferation was reduced by 50% compared to the

untreated control, were calculated using GraphPad Prism 5 (GraphPad Software, San Diego, CA, USA). Each in vitro experiment was conducted on two microplates with a minimum of five parallel wells. Stock solutions of the tested substances (10 mM) were prepared in DMSO, with the highest DMSO concentration in the medium not exceeding 0.3%, which did not significantly affect cell proliferation. Cisplatin was used as the reference agent.

3.3. Propidium Iodide-Based Cell Cycle Analysis

Cell cycle analysis was conducted to investigate the mechanism of action of azidomethyl compounds in human breast cancer cell lines. Specifically, MDA-MB-231 cells were seeded in 24-well plates at a density of 80,000 cells per well. The cells were treated with six concentrations of **16AABE** (0.5, 1 and 2 μM) and **16BABE** (2, 4 and 8 μM) for 24 hours.

After treatment, the cells were washed with phosphate-buffered saline (PBS) and harvested using trypsin. The harvested cells were combined with the supernatants and PBS from the washing process. Subsequently, centrifugation at 1,700 rpm for 5 minutes at room temperature was performed, followed by resuspending the cell pellets in a DNA staining solution. The DNA staining solution consisted of 10 μg/mL propidium iodide (PI), 0.1% Triton-X, 10 μg/mL RNase A, and 0.1% sodium citrate dissolved in PBS. The resuspended cells were then incubated in the dark at room temperature for 30 minutes.

At least 20,000 events per sample were analyzed using a FACSCalibur flow cytometer to assess the DNA content. The data obtained were analyzed using ModFit LT 3.3.11 software (Verity Software House, Topsham, ME, USA). Untreated cells were the control, and a hypodiploid (subG1) phase indicated the apoptotic cell population[81].

3.4. Tubulin Polymerization Assay

Following the manufacturer's instructions, a tubulin polymerization assay kit (Cytoskeleton Inc., Denver, CO, USA) was employed to assess the cell-independent direct effects of **16AABE** and **16BABE** on tubulin polymerization in vitro. Initially, 10 μL of a 500 μM solution of the desired compound was added to a UV-transparent microplate prewarmed to 37°C. Positive control samples containing 10 μL of 10 μM paclitaxel and untreated controls with general tubulin buffer (80 mM PIPES pH 6.9, 2 mM $MgCl_2$, 0.5 mM EGTA) were also prepared. Next, 100 μL of a 3.0 mg/mL tubulin solution dissolved in polymerization buffer (80 mM PIPES pH 6.9, 2 mM $MgCl_2$, 0.5 mM EGTA, 1 mM GTP, 10.2% glycerol) was added to each sample well in separate wells of a 96-well plate. The plate was immediately placed in an ultraviolet spectrophotometer (SPECTROstarNano, BMG Labtech, Ortenberg, Germany) prewarmed to 37°C. A 60-minute

kinetic reaction was initiated, during which the absorbance was measured at 340 nm every minute to evaluate the effects of the tested compounds. The tubulin polymerization curve was constructed by plotting the optical density against time. The maximum reaction rate (Vmax; Δabsorbance/min) was calculated based on the highest difference in absorbance observed over three consecutive time points on the kinetic curve.

3.5. Migration Assay

As previously described, MCF-7 cell suspension was prepared in a supplemented EMEM. The cells were then seeded onto 12-well plates using specialized silicone inserts (Ibidi GmbH, Grafelfing, Germany) at a concentration of 25,000 cells per well. The silicone inserts were gently removed after overnight incubation, and the cells were washed with PBS. Subsequently, the cells were subjected to a wound healing assay by treating them with low concentrations of compounds (1.5 and 3 μM) prepared in EMEM medium with reduced serum content (2% FBS).

The antimigratory effect of the compounds was assessed by measuring the size of the cell-free areas. Images of the cell monolayer were captured at 0, 24, and 48 hours using the QCapture Pro software. Based on the captured images, the size of the cell-free areas was determined using the ImageJ software (National Institutes of Health, Bethesda, MD, USA).

3.6. Invasion Assay

To assess the impact of our compounds on the invasion capacity of malignant MDA-MB-231 cells, we employed Boyden chambers equipped with a reconstituted membrane that mimics the basement membrane. The treated cells were carefully pipetted onto the hydrated membranes in the upper chamber. In the lower chamber, EMEM supplemented with 10% FBS served as a chemoattractant. After a 24-hour incubation period, the supernatants were removed, and non-invading cells on the upper side of the membrane were gently wiped away using a cotton swab. The membrane was then rinsed twice with PBS and fixed with ice-cold 96% ethanol. Subsequently, invading cells were stained with a 1% crystal violet dye solution for 30 minutes in the dark at room temperature. Multiple images (at least three per insert) were captured using a Nikon Eclipse TS100 microscope. Finally, the invading cells were quantified and compared to untreated control samples.

3.7. Determination of Estrogenic Activity

T47D human breast adenocarcinoma cells expressing endogenous estrogen receptor (ERα) modified with an estrogen-responsive luciferase (Luc) reporter gene (T47D-KBluc) were used to assess the estrogenic activity of **16AABE** and **16BABE**[82]. Cells were maintained in phenol red-free MEM with 2 mM L-glutamine, 1 g/L glucose, 10% FBS and penicillin-streptomycin antibiotics. Before testing the compound's effect, cells were maintained in the same medium above but supplemented with 10% charcoal dextran-treated FBS for at least six days. Cells were seeded at a density of 50,000 per well in 200 µl of the medium above in a 96-well white flat bottom plate (Greiner Bio-One, Mosonmagyaróvár, Hungary) and allowed to attach for 72 h. Then the indicated concentrations of the test compounds and the reference agent 17β-estradiol were added (less than 0.1% DMSO in the final concentration). Plates were incubated at 37°C in a humidified 5% CO_2 incubator before measuring luciferase activity. After 24 h incubation, the dosing media was removed entirely, and 30 µl of One-Glo firefly luciferase reagent (Promega, Madison, WI, USA) per well was added to the plate and then incubated for 3 minutes at room temperature according to the manufacturer protocol and the luminescence signal was quantified (FLUOstar Optima, BMG Labtech, Ortenberg, Germany).

3.8. Statistical Analysis

The statistical analysis of the obtained results was conducted using the GraphPad Prism 5 software (GraphPad, San Diego, CA, USA). One-way analysis of variance (ANOVA) was employed, followed by the Dunnett posttest, to assess the significance of the observed differences. Data are expressed as mean values ± standard error of the mean (SEM).

4. Results

4.1. Antiproliferative Assay

4.1.1. Antiproliferative Activity of Triazolyl Compounds

In a preceding endeavor within our ongoing research trajectory, an earlier investigation focused on compounds closely resembling the present subject of interest. This earlier study meticulously centered on a diverse collection of hydroxyl analogs, similar to the compounds **16AABE** and **16BABE** that currently form the core of our inquiry. This prior exploration was designed to reveal latent antiproliferative efficacy inherent within these hydroxyl analogs.
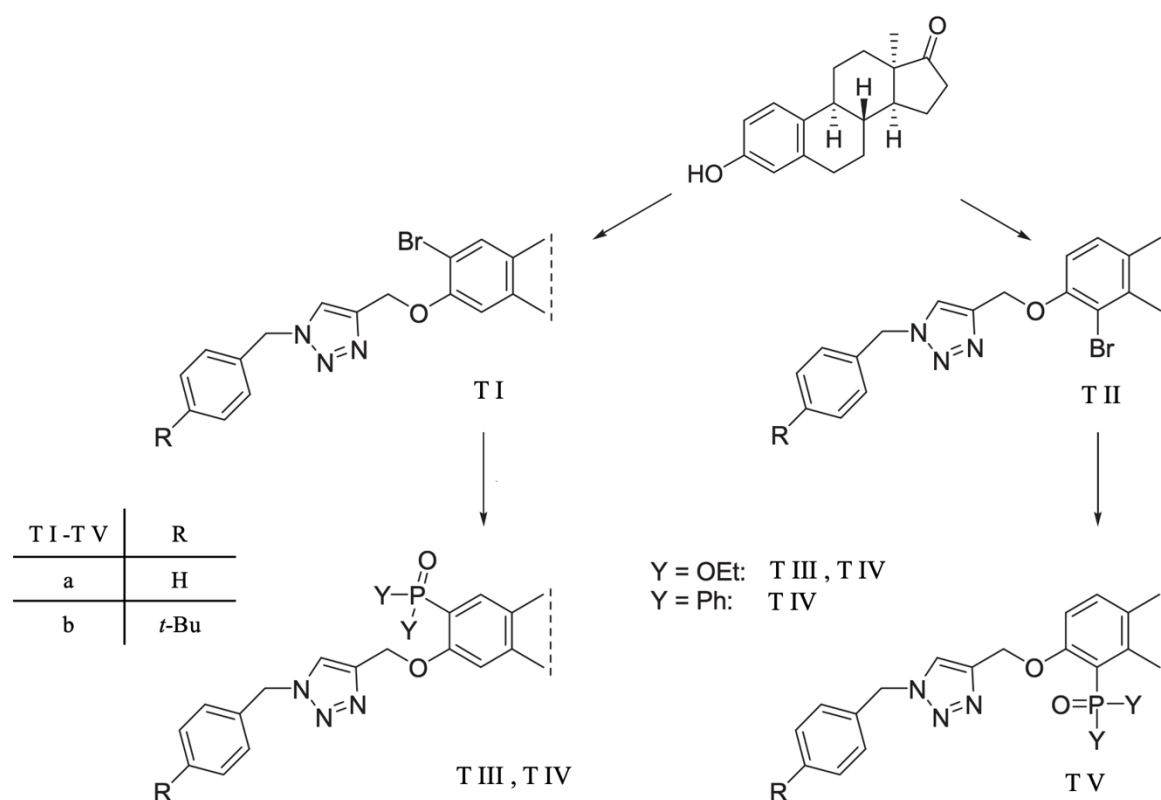

Figure 2. Structures of the steroidal 17-hydroxyl analogs (TI – TV) of investigated compounds.

	R^2		
a	Cyclopropyl		
b	Cyclopentyl		
c	Cyclohexyl		
d	Phenyl		
e	Nitro-benzoyloxymethyl		
f	Hydroxymethyl		

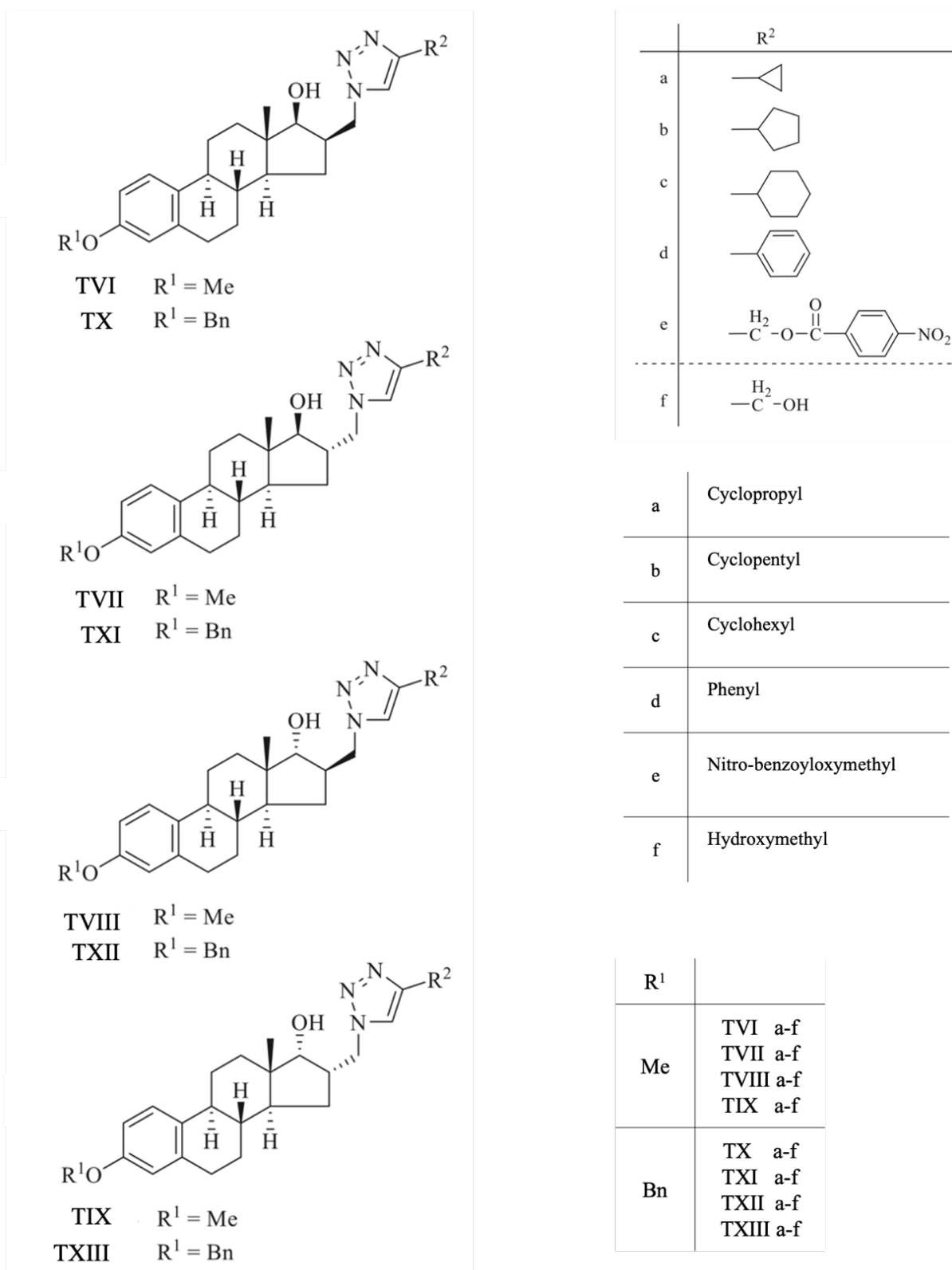| R^1	
Me	TVI a-f TVII a-f TVIII a-f TIX a-f
Bn	TX a-f TXI a-f TXII a-f TXIII a-f

Figure 3. Structures of the steroidal 17-hydroxyl analogs (TVI - TXIII) of investigated compounds.

Looking back at this previous attempt the investigative scope encompassed an array of cancer cell lines, strategically selected to extract the nuanced effects of the hydroxyl compounds on cellular proliferation dynamics. The outcomes derived from this preliminary investigation revealed a promising view of antiproliferative attributes embedded within these hydroxyl analogs. Their inherent capacity to impede the progression of cellular proliferation emerged as a noteworthy thematic thread, thus offering a potential avenue for targeted therapeutic intervention. Anchored upon these initial findings, our current inquiry expands the previous research, aiming to illuminate the broader pharmacological foundations intrinsic to the compounds **16AABE** and **16BABE**. This collective effort seeks to distill a comprehensive comprehension of the potential implications encapsulated within these compounds, enhancing our overall insight into their therapeutic viability.

Regarding the arrangement of substituents at positions C-16 and C-17, the 16β,17β-derivatives showcased remarkable inhibitory prowess over cellular growth in our studies. Notably, two derivatives carrying analogous cycloalkyl groups at position C-4' exhibited significant and selective antiproliferative effects specifically against the triple-negative breast cancer cell line MDA-MB-231, with IC_{50} values falling within the lower micromolar spectrum.

The following data (Table 2), encapsulates the observed effects on cellular proliferation, offering a quantitative snapshot of the potency wielded by the hydroxyl bearing group of the analog compounds across diverse cancer cell lines.

Table 1. Antiproliferative activity of steroidal 17-hydroxyl analogs (TVI – TIX) of the investigated compounds.

Growth Inhibition, % ± SEM [calculated IC$_{50}$]

Compound	Conc. (μM)	HeLa	SiHa	MCF-7	MDA-MB-231
TVI					
a	10	< 20	21.28± 1.88	< 20	< 20
	30	< 20	28.71± 2.20	46.42± 1.47	< 20
b	10	< 20	< 20	< 20	< 20
	30	39.86± 0.38	< 20	57.42± 1.77	29.88 ± 1.57
c	10	< 20	< 20	< 20	< 20
	30	40.22± 1.02	< 20	70.84± 1.55	37.96 ± 1.55
d	10	< 20	< 20	< 20	< 20
	30	44.16± 0.48	< 20	54.93± 1.78	38.28 ± 1.84
e	10	< 20	23.91± 1.61	34.23± 3.10	< 20
	30	37.18± 1.65	54.72± 0.48	76.26± 0.72	35.93 ± 2.13
f	10	< 20	28.06± 1.99	29.45± 1.67	< 20
	30	41.03± 0.77	57.69± 1.12	70.23± 1.35	34.81 ± 2.88
TVII					
a	10	< 20	25.55± 1.01	< 20	< 20
	30	< 20	34.78± 2.47	57.43± 1.91	< 20
b	10	< 20	< 20	< 20	< 20
	30	< 20	26.57± 2.26	67.59± 1.65	< 20
c	10	< 20	< 20	< 20	< 20
	30	< 20	29.90± 2.59	69.68± 0.77	< 20
d	10	< 20	< 20	< 20	< 20
	30	< 20	29.96± 1.79	70.75± 1.05	14.54 ± 1.32
e	10	< 20	< 20	< 20	< 20
	30	< 20	38.69± 2.09	63.12± 2.14	< 20
f	10	< 20	< 20	22.02± 1.61	< 20
	30	< 20	37.79± 1.04	50.94± 1.55	< 20
TVIII					
a	10	< 20	< 20	< 20	< 20
	30	31.14± 1.28	< 20	28.72± 0.93	25.08 ± 3.15
b	10	< 20	< 20	< 20	< 20
	30	58.25± 2.03	< 20	48.01± 1.31	< 20
c	10	< 20	30.97± 2.69	< 20	< 20
	30	< 20	33.89± 2.35	< 20	< 20
d	10	< 20	< 20	< 20	< 20
	30	26.90± 2.15	< 20	63.27± 0.82	< 20
e	10	< 20	< 20	< 20	< 20
	30	< 20	37.53± 3.00	33.94± 0.75	28.19 ± 0.96
f	10	< 20	29.13± 1.59	< 20	< 20
	30	26.61± 0.57	43.85± 3.32	38.45± 1.93	43.80 ± 3.16
TIX					
a	10	< 20	< 20	< 20	< 20
	30	89.01± 0.47	< 20	78.65± 0.78	46.21 ± 1.54
b	10	< 20	< 20	< 20	< 20
	30	34.18± 0.81	< 20	31.07± 2.36	< 20
c	10	< 20	< 20	< 20	< 20
	30	49.11± 0.55	< 20	43.22± 1.52	< 20
d	10	< 20	< 20	< 20	< 20
	30	42.13± 1.66	< 20	55.41± 0.76	< 20
e	10	< 20	< 20	< 20	< 20
	30	83.66± 0.34	42.06± 2.50	70.11± 1.06	50.27 ± 2.00
f	10	< 20	< 20	22.34± 2.06	< 20
	30	84.77± 1.18	29.80± 1.66	68.27± 1.19	47.74 ± 1.21
cisplatin	10	42.61± 2.33	86.84± 0.50	53.03± 2.29	20.84 ± 0.81
	30	99.93± 0.26	90.18± 1.78	86.90± 1.24	74.47 ± 1.20
		[12.43]	[7.84]	[5.78]	[19.13]

Table 2. Antiproliferative activity of steroidal 17-hydroxyl analogs (TX – TXIII) of the investigated compounds.
Growth Inhibition, % ± SEM [calculated IC$_{50}$]

Compound	Conc. (µM)	HeLa	SiHa	MCF-7	MDA-MB-231	NIH-3T3
TX						
a	10	44.94 ± 1.04	21.17 ± 2.05	41.71 ± 0.64	47.32 ± 1.15	44.91 ± 1.36
	30	52.45 ± 2.39	66.23 ± 0.86	64.32 ± 0.56	71.49 ± 0.75	91.28 ± 0.50
b	10	51.49 ± 3.62	49.36 ± 1.69	44.58 ± 1.50	93.00 ± 0.26	44.81 ± 1.50
	30	62.58 ± 2.21	73.94 ± 2.04	50.52 ± 3.26	93.71 ± 0.09	59.09 ± 0.73
					[3.33]	
c	10	54.70 ± 1.88	49.58 ± 2.11	44.04 ± 3.32	77.13 ± 1.07	
	30	53.66 ± 2.56	61.83 ± 2.77	59.33 ± 2.99	88.81 ± 0.55	
					[5.91]	
d	10	64.14 ± 0.86	70.88 ± 1.03	73.41 ± 1.22	95.04 ± 0.16	95.60 ± 0.25
	30	90.12 ± 0.99	94.14 ± 0.29	80.16 ± 3.40	95.60 ± 0.06	98.22 ± 0.04
		[2.28]	[4.05]	[3.91]	[3.65]	[3.34]
e	10	< 20	< 20	41.63 ± 2.83	21.96 ± 0.73	
	30	92.12 ± 0.25	89.25 ± 0.68	97.00 ± 0.11	95.22 ± 0.91	
f	10	45.08 ± 0.72	41.26 ± 1.25	55.41 ± 1.26	55.57 ± 1.50	
	30	39.39 ± 0.49	52.60 ± 1.31	62.52 ± 0.67	88.92 ± 0.99	
TXI						
a	10	37.98 ± 2.68	< 20	72.42 ± 2.19	46.43 ± 2.05	85.50 ± 1.22
	30	96.56 ± 0.11	96.71 ± 0.17	98.72 ± 0.09	97.96 ± 0.17	97.63 ± 0.12
				[6.11]		[5.97]
b	10	38.55 ± 1.32	< 20	31.80 ± 1.35	17.13 ± 2.36	
	30	43.97 ± 2.23	< 20	84.44 ± 0.71	37.72 ± 2.28	
c	10	36.30 ± 1.45	< 20	24.95 ± 2.15	< 20	
	30	35.53 ± 1.24	< 20	74.73 ± 1.00	< 20	
d	10	< 20	< 20	47.25 ± 1.78	45.55 ± 2.63	
	30	22.15 ± 1.29	< 20	57.30 ± 0.77	59.79 ± 1.22	
e	10	< 20	< 20	68.51 ± 0.71	89.24 ± 0.70	31.41 ± 2.21
	30	96.98 ± 0.33	96.91 ± 0.14	99.12 ± 0.07	97.73 ± 0.23	99.01 ± 0.05
				[6.53]	[5.69]	[11.75]
f	10	21.62 ± 3.46	< 20	29.14 ± 2.06	40.46 ± 2.98	10.00 ± 1.01
	30	30.79 ± 2.92	27.28 ± 1.90	43.28 ± 1.53	76.93 ± 1.60	23.40 ± 0.60
TXII						
a	10	24.26 ± 2.63	34.00 ± 1.43	58.38 ± 3.20	56.24 ± 0.98	25.56 ± 2.21
	30	85.22 ± 1.32	82.68 ± 1.25	97.21 ± 0.10	84.18 ± 0.44	99.24 ± 0.07
b	10	37.10 ± 1.77	39.59 ± 1.17	51.92 ± 1.00	56.44 ± 0.98	
	30	52.08 ± 2.08	69.54 ± 1.24	65.12 ± 1.91	71.81 ± 0.96	
c	10	38.89 ± 2.60	64.05 ± 1.24	49.68 ± 1.66	72.37 ± 1.27	13.99 ± 1.79
	30	55.93 ± 2.39	83.34 ± 1.31	61.26 ± 1.72	85.81 ± 1.04	29.56 ± 1.17
			[9.29]		[6.74]	
d	10	34.23 ± 1.39	30.04 ± 2.07	47.03 ± 1.25	55.77 ± 1.03	
	30	47.74 ± 0.78	39.96 ± 2.34	42.43 ± 1.69	57.71 ± 1.00	
e	10	< 20	21.53 ± 1.81	35.74 ± 1.33	< 20	
	30	99.06 ± 0.09	96.91 ± 0.06	98.50 ± 0.93	99.01 ± 0.52	
f	10	< 20	24.65 ± 1.46	25.50 ± 2.93	24.79 ± 2.20	
	30	98.72 ± 0.13	96.04 ± 0.25	98.41 ± 0.15	98.79 ± 0.16	
TXIII						
a	10	35.48 ± 1.91	46.07 ± 1.13	52.88 ± 0.82	25.61 ± 2.84	
	30	63.44 ± 1.79	69.86 ± 0.55	73.39 ± 0.74	52.16 ± 2.52	
b	10	39.75 ± 2.45	< 20	43.51 ± 1.85 42.28 ± 1.44	44.86 ± 0.93	
	30	47.34 ± 1.62	< 20		43.73 ± 2.25	
c	10	56.71 ± 0.57	39.93 ± 3.14	48.56 ± 0.48	30.30 ± 1.64	
	30	58.21 ± 0.73	31.15 ± 2.86	49.93 ± 1.33	31.60 ± 3.08	
d	10	74.18 ± 1.15	76.88 ± 0.49	75.97 ± 0.89	86.12 ± 0.33	70.18 ± 1.15
	30	91.17 ± 0.33	87.39 ± 0.86	88.99 ± 0.25	90.72 ± 1.00	91.12 ± 1.64
		[2.30]	[4.14]	[3.87]	[3.89]	[3.71]
e	10	27.42 ± 2.16	< 20	52.86 ± 1.30	29.58 ± 1.69	
	30	92.94 ± 0.17	91.91 ± 0.23	96.38 ± 0.07	94.09 ± 0.43	
f	10	30.97 ± 1.02	39.85 ± 1.24	50.60 ± 0.65	31.89 ± 2.92	
	30	91.88 ± 0.26	90.94 ± 0.18	95.12 ± 0.10	92.56 ± 0.34	
cisplatin	10	42.61 ± 2.33	86.84 ± 0.50	53.03 ± 2.29	20.84 ± 0.81	94.20 ± 0.39
	30	99.93 ± 0.26	90.18 ± 1.78	86.90 ± 1.24	74.47 ± 1.20	96.44 ± 0.17
		[12.43]	[7.84]	[5.78]	[19.13]	[3.23]

23

Table 3. Anti proliferative activity of four starting molecules 16α-azidomethyl and 16β-azidomethyl bearing 17α-hydroxyl and 17β -hydroxyl.
*Growth Inhibition, % ± SEM.
The inhibition values less than 20 percent are not given numerically.

Compound	Concentration	HeLa	SiHa	MCF-7	MDA-MB-231
SI	10	33.97 ± 0.33	<20*	38.82 ± 0.81	34.07 ± 0.27
	30	93.10 ± 0.21	89.93 ± 0.20	92.64 ± 0.22	92.92 ± 0.09
SII	10	29.15 ± 1.06	<20	20.22 ± 2.19	45.06 ± 1.69
	30	55.54 ± 2.06	43.16 ± 2.58	51.86 ± 1.85	64.22 ± 1.39
SIII	10	24.96 ± 2.26	<20	27.33 ± 1.28	33.50 ± 2.92
	30	93.35 ± 0.32	86.46 ± 0.36	92.55 ± 0.18	89.05 ± 0.90
SIV	10	26.63 ± 1.78	<20	<20	25.14 ± 2.83
	30	52.89 ± 0.49	31.91 ± 0.69	52.42 ± 2.50	57.32 ± 0.98

4.1.2. Antiproliferative Activity of Azidomethyl Compounds

The antiproliferative capacity of the prepared compounds was determined by employing the MTT assay against a panel of human adherent cancer cell lines isolated from breast (MCF-7 and MDA-MB-231) or cervical (HeLa and SiHa) tumors. All compounds were tested at two concentrations (10 and 30 μM). When more than 50% was obtained at 10 μM, the assays were repeated with a broader concentration range (0.1–30 μM), and IC_{50} values were calculated. Starting molecules **SI**–**SIV** exerted negligible action at 10 μM, but substantial cell growth inhibitions were observed at the higher concentration. On the other hand, the 17-keto analogs (**16AABE** and **16BABE**) elicited higher than 90% inhibition even at the lower concentration, and their calculated IC_{50} values were lower than those of reference agent cisplatin. The MTT assays were performed against non-cancerous fibroblast cell line NIH/3T3 to obtain preliminary data concerning the cancer selectivity of the antiproliferative properties of **16AABE** and **16BABE**. The fibroblast cells proved less sensitive, and calculated IC_{50} values were above 10 μM. The ratios of IC_{50} values obtained against cancer cells and fibroblasts are between 0.2 and 0.5, indicating a substantial cancer selectivity of the two compounds (Table 5).

Compound	Conc.	HeLa	SiHa	MDA-MB-231	MCF-7	NIH/3T3
SI	10 µM					n.d.
	30 µM					
SII	10 µM					n.d.
	30 µM					
SIII	10 µM					n.d.
	30 µM					
SIV	10 µM					n.d.
	30 µM					
16AABE	10 µM					
	30 µM					
16BABE	10 µM					
	30 µM					
cisplatin*	10 µM					
	30 µM					

Cancer cell growth inhibition: 20% or less
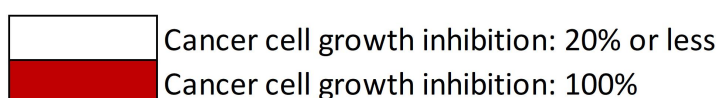
Cancer cell growth inhibition: 100%

Figure 4. Antiproliferative properties of the investigated molecules. Inhibition values lower than 20% are considered negligible and not given numerically. n.d.: not determined. *Cisplatin data were obtained from our previous study.

Table 4. Growth Inhibition, % ± SEM and IC50 values of 16AABE and 16BABE [µM]

*Cisplatin data were obtained from our previous study.

Compound		Concentration	**16 AABE**	**16 BABE**	Cisplatin*
HeLa	Inhibition %	10 µM	93.40±0.13	93.22±0.92	42.61 ± 2.33
		30 µM	94.33±0.32	93.96±0.23	99.93 ± 0.26
	Calculated IC$_{50}$ (µM)		[4.60]	[5.01]	[12.43]
SiHa	Inhibition %	10 µM	90.73±0.53	90.10±0.66	86.84 ± 0.50
		30 µM	91.08±0.55	91.48±0.55	90.18 ± 1.78
	Calculated IC$_{50}$ (µM)		[3.85]	[4.10]	[7.84]
MCF-7	Inhibition %	10 µM	92.94±0.37	91.73±0.71	53.03 ± 2.29
	Calculated IC$_{50}$ (µM)	30 µM	93.79±0.40	93.85±0.22	86.90 ± 1.24
			[3.15]	[3.13]	[5.78]
MDA-MB-231	Inhibition %	10 µM	93.65±0.24	93.35±0.17	20.84 ± 0.81
	Calculated IC$_{50}$ (µM)	30 µM	95.03±0.23	95.11±0.31	74.47 ± 1.20
			[8.13]	[4.72]	[19.13]
NIH 3T3	Inhibition %	10 µM	<20	<20	94.20 ± 0.39
	Calculated IC$_{50}$ (µM)	30 µM	94.79	98.29	96.44 ± 0.17
			[18.93]	[13.59]	[3.23]

Table 5. Tumor selectivity indices of 16AABE and 16BABE expressed as the ratio of IC50 values obtained against cancer cells and fibroblasts.

Cancer cell line	$\frac{\text{IC}_{50} \text{ of cancer cell line}}{\text{IC}_{50} \text{ of NIH/3T3}}$	
	16AABE	16BABE
HeLa	0.369	0.243
SiHa	0.302	0.203
MCF-7	0.230	0.166
MDA-MB-231	0.347	0.429

4.2. Propidium Iodide-Based Cell Cycle Analysis

16AABE and **16BABE** were subjected to propidium iodide-based cell cycle analysis by flow cytometry to better understand their mechanism of action. MDA-MB-231 cells were treated with various concentrations for 24 hours, and the DNA content of the cells was determined. **16AABE** resulted in a moderate but significant increase in the hypodiploid (subG1) population at 1 µM (Figures 5 and 6). At 2 µM, which is approximately the IC$_{50}$ value, a more profound cell cycle disturbance was observed with a pronounced increase of subG1 and G2/M populations at the expense of G1 and S phases. **16BABE**, conversely, caused a minor but significant accumulation of subG1 cells at 8 µM, a concentration roughly its IC$_{50}$, indicating the proapoptotic activity of the compound (Figure 5).
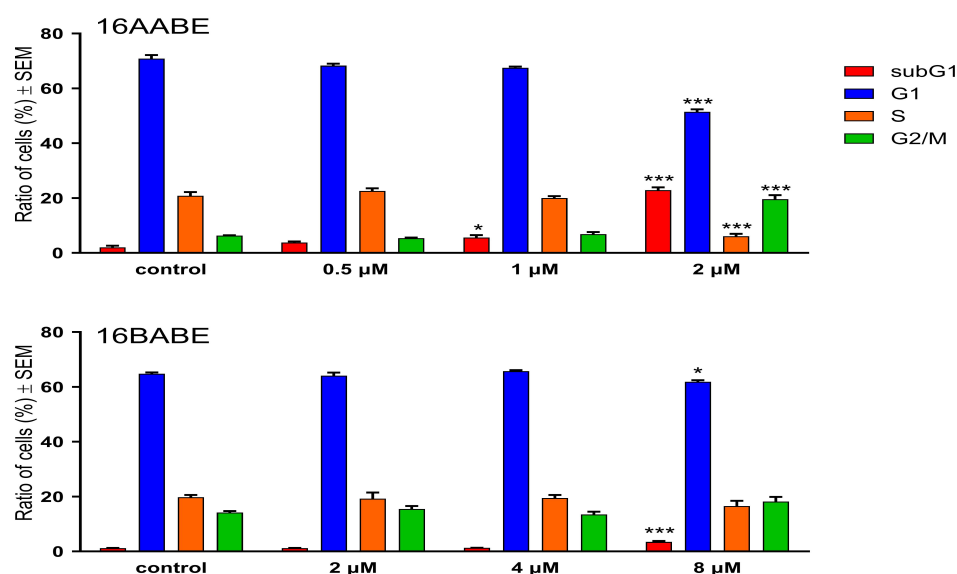

*Figure 5. Effects of 16AABE (upper panel) and 16BABE (lower panel) on cell cycle distribution of MDA-MB-231 cells treated with the indicated concentrations for 24 hours. * and *** indicate significant differences at p<0.05 and p<0.001, respectively. Data are from three independent experiments performed in triplicate.*
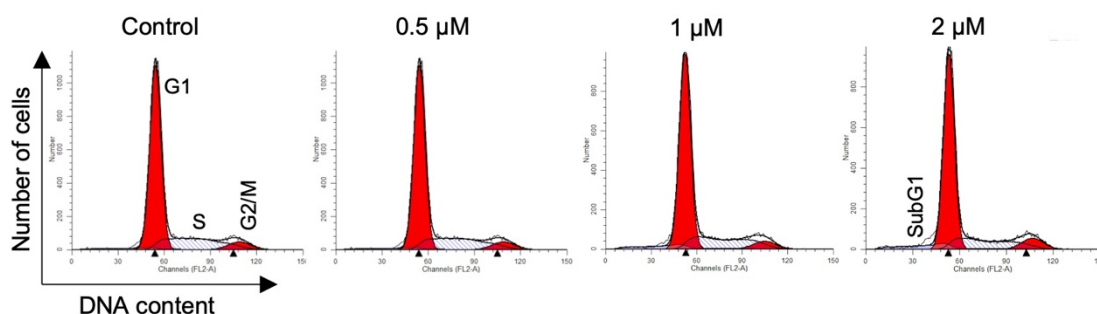
Figure 6. Representative histograms of MDA-MB-231 cells treated with 16AABE. Histograms were generated via ModFit LT 3.3.11 software.

4.3. Tubulin Polymerization Assay

The impact of **16AABE** and **16BABE** on microtubule polymerization was assessed using a cell-free system with a photometric kinetic determination. The concentrations of the test compounds were selected based on their IC_{50} values, as the kit's manufacturer recommended. Both compounds exhibited a stimulating effect on tubulin polymerization compared to the control samples. Notably, the calculated maximum tubulin polymerization (Vmax) rates were significantly higher than those observed in the control condition (Figure 7). It is worth mentioning that the Vmax values of the tested compounds were higher than that of the reference agent paclitaxel (PAC, 10 µM), indicating their profound activity on the polymerization of tubulin.
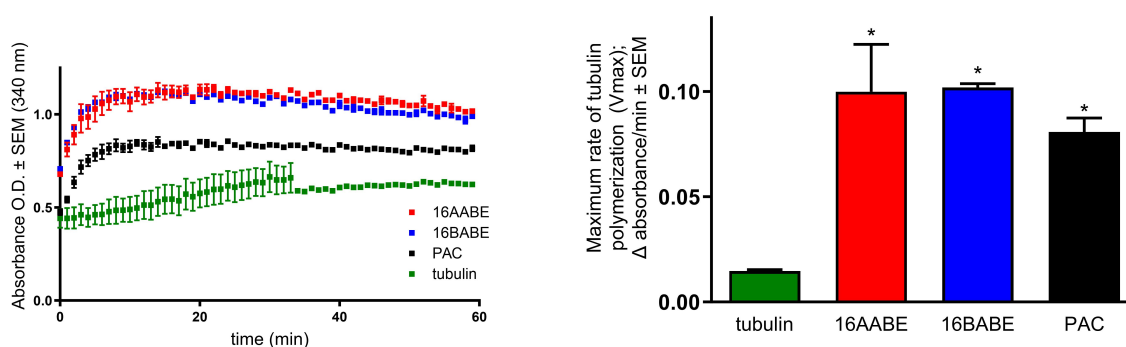

*Figure 7. Direct effects of 16AABE and 16BABE (500 µM for both) on tubulin polymerization. Left panel: recorded kinetic curves; paclitaxel (10 µM PAC) was included as a reference agent. Right panel: calculated maximum values for the rate of tubulin polymerization. * Indicate significance at p<0.05 compared to untreated tubulin – results from two independent experiments performed in duplicate.*

27

4.4. Wound Healing Assay

To investigate the antimigratory activity of our compounds, we conducted a wound-healing assay using the MCF-7 breast cancer cell line. The assay involved incubating the cells in a minimal serum-containing (2%) medium for 24 or 48 hours after creating a wound by removing silicone inserts. Microscope image analysis was employed to measure the reduction in cell-free areas, which served as an indicator of wound closure. Our findings demonstrated a significant decrease in the migratory capacity of cancer cells (Figures 8 and 9). Notably, both compounds exhibited remarkable antimigratory effects at subantiproliferative concentrations (1.5 μM), with **16BABE** demonstrating more pronounced action after 24 hours of incubation.
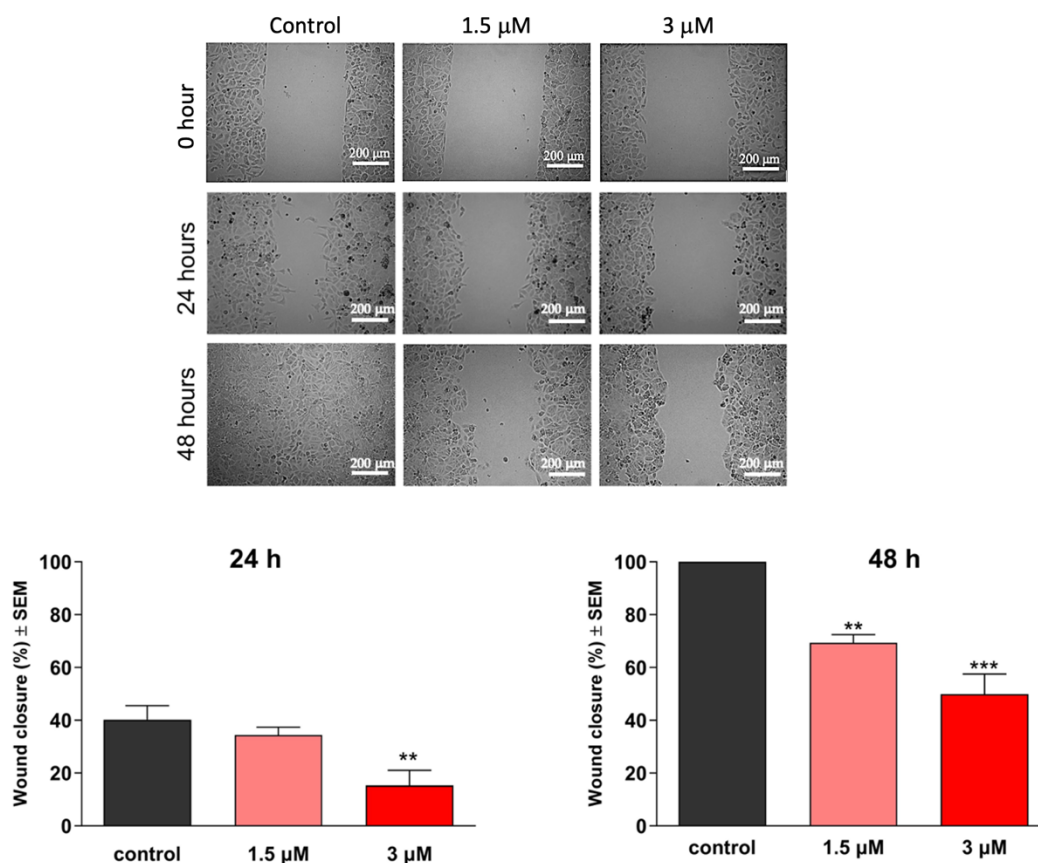

*Figure 8. Effects of 16AABE on the migration of MCF-7 cells. Upper panels: representative images taken at 24 or 48 h post-treatment with 16 16AABE. Lower panels: calculated wound closure values determined after 24 or 48 h post-treatment. ** and *** indicate significance at p<0.01 and p<0.001, respectively. Findings are based on the results of 4 independent experiments, all performed in triplicate.*
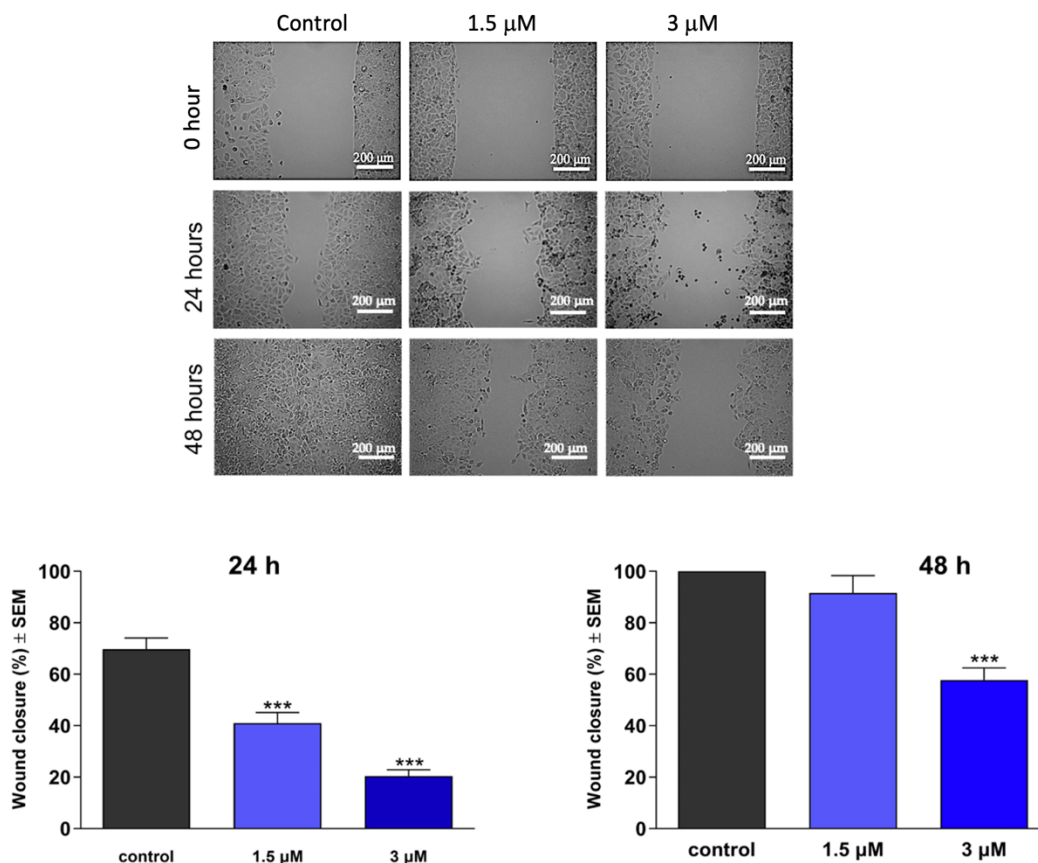
Figure 9. Effects of 16BABE on the migration of MCF-7 cells. Upper panels: representative images taken at 24 or 48 h post-treatment with 16 16BABE. Lower panels: calculated wound closure values determined after 24 or 48 h post-treatment. *** indicates significance at $p<0.001$. Findings are based on the results of 4 independent experiments, all performed in triplicate.

4.5. Boyden Chamber Assay

In addition to its impact on cell migration, the invasive capacity of cancer cells plays a pivotal role in their metastatic behavior, making it a crucial factor in assessing their antimetastatic potential. Boyden chambers with Matrigel Matrix-coated membranes (pore diameter: 8.0 μm) were employed to evaluate invasiveness, as they permit the passage of invasive cells while impeding the migration of non-invading cells. Remarkably, the tested compounds effectively hindered the invasion of MDA-MB-231 cells, even at low concentrations of 0.5 or 1 μM (Figures 10 and 11). Moreover, both compounds exhibited a significant decrease in invading cells after 48 hours of treatment, underscoring their remarkable anti-invasive potential.
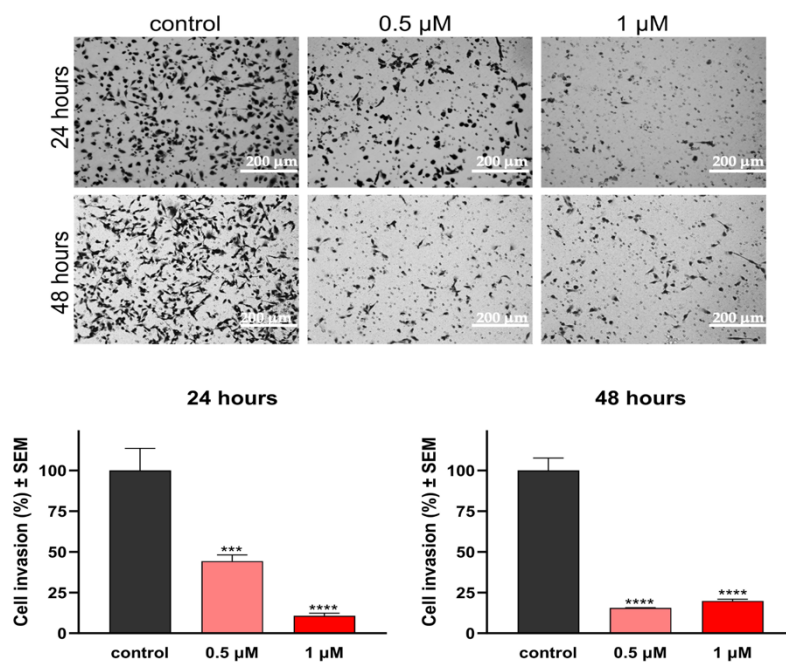
Figure 10. Effects of 16AABE on the invasion capacity of MBA-MD-231 cells. Upper panels: representative images taken at 24 or 48 h post-treatment with 16AABE. Lower panels: 16AABE significantly reduced invasion of MDA-MB-231 cells at 24-hour and 48-hour treatments. Findings are based on the results of at least 4 independent experiments performed in duplicate. *** and **** indicate significance at p<0.001 and p<0.0001, respectively.

Figure 11. Effects of 16BABE on the invasion capacity of MBA-MD-231 cells. Upper panels: representative images taken at 24 or 48 h post-treatment with 16BABE. Lower panels: 16BABE significantly reduced invasion of MDA-MB-231 cells at 24-hour and 48-hour treatments. Findings are based on the results of at least 4 independent experiments performed in duplicate. *** and **** indicate significance at p<0.001 and p<0.0001, respectively.
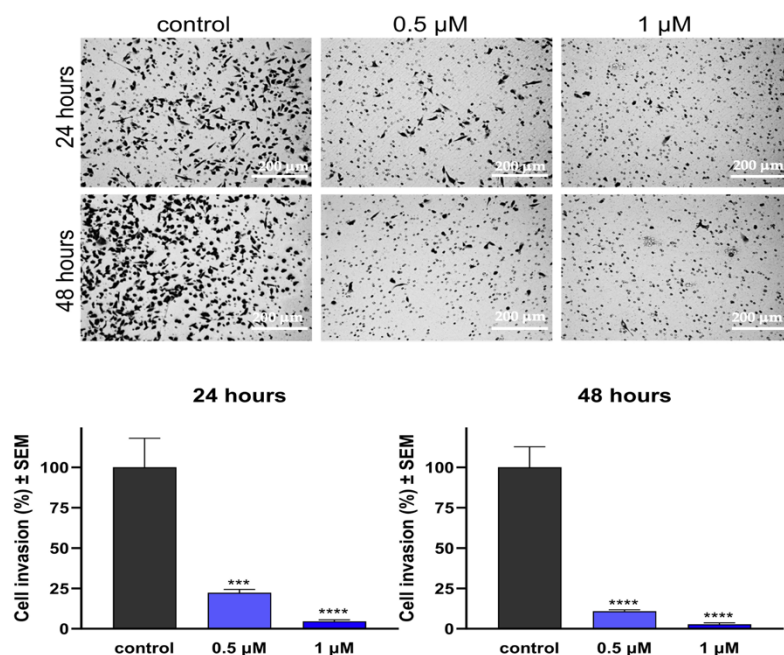
4.6. Estrogenic Activities of The Tested Compounds

Since **16AABE** and **16BABE** are structurally closely related to natural estrogen 17β-estradiol, their hormonal activities are considered crucial elements of their pharmacological profile. A T47D breast cancer cell line transfected with an estrogen-responsive luciferase reporter gene was utilized to clarify the estrogenic activity of the tested compounds (Figure 12). Treatment with both compounds resulted in estrogenic activity at concentrations several orders of magnitude higher than reference agents 17β-estradiol. The calculated concentrations eliciting 50% of maximum estrogenic stimulation were approximately 5.5 and 178 nM, respectively. These results indicate that these estrone analogs possess considerable hormonal activity at their antiproliferative or antimetastatic concentrations.
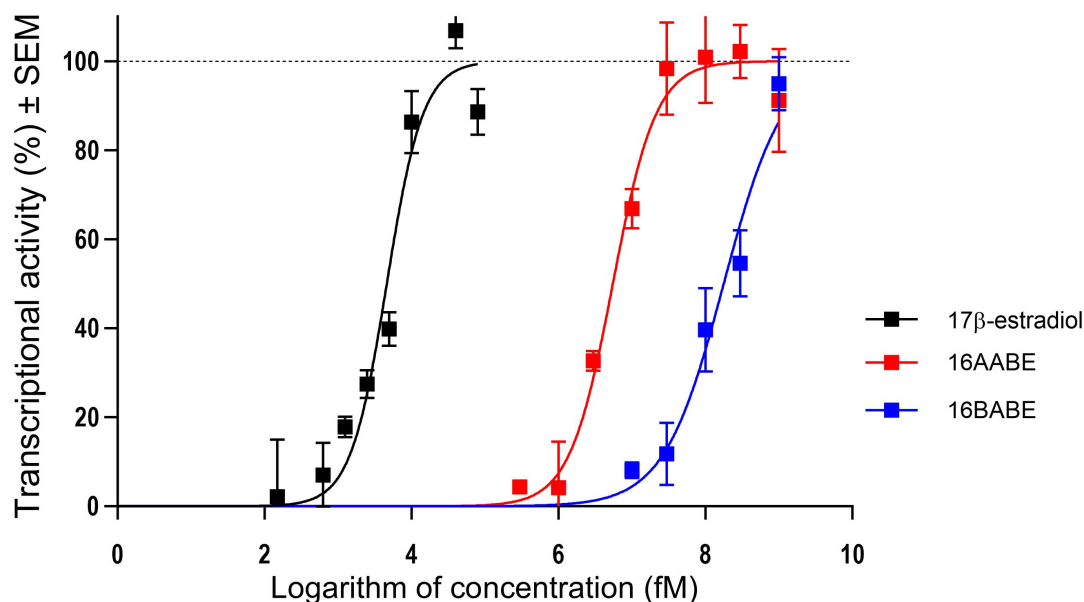

Figure 12. Estrogenic effects of 16AABE and 16BABE expressed as the intensity of the estrogen-responsive luciferase in transfected T47D breast cancer cell line. Findings are based on the results of 3 independent experiments performed in triplicate.

5. Discussion

Breast cancer holds a preeminent position as the most frequently diagnosed malignancy among women worldwide. Its emergence is characterized by a multifaceted etiology, wherein a convergence of genetic and environmental factors contributes to its intricate pathogenesis. This complex interplay underscores the multifactorial nature of the disease's origin, highlighting the necessity for a comprehensive understanding of its underlying mechanisms.

Amidst this complexity, various factors such as age, family history, hormones, marital status, and lifestyle choices intertwine to shape breast cancer's development. This amalgamation adds layers of complexity to understanding its emergence. An essential framework for comprehending breast cancer's heterogeneity lies in the classification system based on pivotal molecular markers. Specifically, the presence or absence of estrogen and progestin receptors, alongside the HER2 status, delineates major subtypes of the disease. These subtypes encompass hormone receptor-positive, HER2-positive, and triple-negative breast cancer (TNBC). Among these, TNBC, accounting for approximately 15-20% of cases, stands out with its distinct characteristics. Notably, TNBC's heightened prevalence in younger patients, particularly those below 40, paints a complex picture of age-related variations in breast cancer presentations[83–85].

This intricate framework illuminates the multi-faceted nature of breast cancer, spotlighting the need for a holistic approach that encompasses its clinical manifestations and its genetic, molecular, and environmental underpinnings. This multifactorial perspective is pivotal in driving advancements in diagnosis, treatment, and the overall management of breast cancer across its diverse array of presentations[83,84].

TNBC distinguishes itself through its aggressive behavior relative to other subtypes, contributing to a notably poorer prognosis for affected individuals. This heightened aggressiveness stems from the absence of specific molecular targets, necessitating a distinct therapeutic approach. Unfortunately, the absence of these targeted avenues constrains pharmacological interventions for TNBC, thereby limiting treatment options to conventional cytotoxic agents. As a result, addressing the unique challenges posed by TNBC remains a critical priority in improving patient outcomes[85].

Despite the widely recognized role of estrogens, including the natural hormone 17β-estradiol, in promoting cell growth, a noteworthy discovery has emerged: certain estrane-based molecules exhibit remarkable potential as potent candidates for anticancer drugs. This intriguing finding challenges conventional assumptions and underscores the complexity of molecular interactions, paving the way for novel therapeutic strategies in the fight against cancer[78].

The category of 16-substituted triazolyl estranes stands out as a distinct class of compounds characterized by a distinctive structural framework that combines an estrane scaffold with a triazole ring. The construction and synthesis of these compounds involve the strategic application of click chemistry, complemented by meticulous structure-activity relationship studies aimed at refining their pharmacological attributes. Based on a study by Molnár J. *et al.,* a diverse and innovative collection of compounds characterized by a steroidal framework featuring the pharmacophore triazole ring at distinct positions on ring D has been subjected to rigorous testing for their potential antiproliferative properties. Among these compounds, those bearing a 17α-triazolyl group exhibited relatively limited activity, while their counterparts with 15- and 16-triazolyl substitutions demonstrated considerable and noteworthy effects, warranting comprehensive further exploration [76]

Remarkably, certain compound members displayed in vitro potencies rivaling cisplatin, a widely employed reference compound in clinical contexts. Encouraged by these outcomes, the most potent analogs were subjected to an in-depth investigation in order to elucidate the precise mechanisms underpinning their effects.

The activation of the intrinsic pathway of apoptosis was substantiated by identifying pertinent biochemical markers and observing corresponding morphological changes within the affected cells. Additionally, the impediment of the cell cycle progression at the G2–M transition point was confirmed, further contributing to understanding the compound's mode of action.

This comprehensive study sheds light on the promising potential of these innovative steroidal derivatives, serving as a foundation for potential therapeutic applications in the realm of proliferative disorders and necessitating continued and nuanced research efforts to fully unravel their intricate pharmacological mechanisms and clinical utility[76,77].

Based on another study conducted in 2013, the existing methods for synthesizing steroidal compounds derived from sex hormones, which exhibit notable inhibitory effects on the growth of various cancer cell lines, have been examined. The outcomes obtained thus far underscore that incorporating either basic substituents or heterocyclic elements can substantially alter the original compound's biological activities. Consequently, both a design approach grounded in the structure of the compounds and a more exploratory pursuit for efficacious variations appear to warrant careful consideration in the pursuit of pioneering steroidal agents with anticancer properties. As the novel compounds explored in this study served as the foundational compounds for our research, the pronounced antiproliferative effects exhibited by these substances prompted the continuation of our investigation. Considering this study's findings, we decided to proceed with

our own research, focusing on compounds sharing a similar structural framework but featuring distinct modifications[86].

In our comprehensive pursuit of antiproliferative activity, we extended our investigation to encompass two estrone congeners, specifically **16AABE** and **16BABE**. Intriguingly, we observed that compounds featuring a 17-keto function displayed heightened activity compared to the reference agent cisplatin. The calculated ratios of IC_{50} values obtained against cancer cells compared to NIH/3T3 fibroblasts consistently yielded values below 1 (ranging between 0.166 and 0.429), signifying a dependable cancer-selective behavior. In contrast, their 17-hydroxy analogs exhibited only modest effects. Notably, our scrutiny of the stereochemical aspect, specifically focusing on the configuration of the 16-azidomethyl group, revealed that this factor does not wield a critical influence on the compound's activity.

Building upon these impactful findings, we embarked on a more detailed exploration of the anticancer attributes of the two estrone derivatives. Employing a fundamental approach, cell cycle analysis, we sought to uncover insights into the mechanisms underlying their intervention in cell proliferation. Remarkably, both selected compounds, **16AABE** and **16BABE**, demonstrated the capability to disrupt the cell cycle of MDA-MB-231 TNBC cells. Remarkably, following a 24-hour treatment with **16AABE**, we observed a concentration-dependent elevation in the hypodiploid (subG1) population. This action was detectable even at concentrations below the IC_{50} (1 and 2 μM), underscoring the compound's proapoptotic potential[81].

Furthermore, a marked accumulation of cells in the G2/M phase was noted, resulting in a discernible reduction in the G1 and S populations. Conversely, **16BABE** exhibited an evident alteration in cell cycle distribution solely at its IC_{50} concentration (8 μM), manifesting as a measured increase in the subG1 population coupled with a decline in the G1 population.

Considering the cell cycle perturbations engendered by the investigated compounds, it appeared prudent to undertake an exploration of tubulin polymerization. Microtubules, dynamic filamentous proteins integral to the cytoskeleton, hold a pivotal status as significant targets for interventions in cancer therapy. This investigation holds the potential to uncover the intricate mechanisms by which the tested compounds exert their effects, shedding light on their precise mode of action and therapeutic implications[87].

Both compounds showcased a notable elevation in tubulin polymerization rate at a concentration of 500 μM, implying their capacity to promote microtubule assembly and stability. Notably, these effects stood on par with or exceeded those observed with the positive control paclitaxel. This underscores the pivotal role of direct interaction with tubulin as a crucial facet of the compound's pharmacological characteristics.

In line with epidemiological insights, it's intriguing that roughly 90% of human cancer-related fatalities are attributed to the intricate phenomenon of metastases. This statistic underscores the imperative of addressing the challenges posed by metastatic dissemination, given its significant impact on cancer prognosis and overall patient outcomes[88]. This intricate cascade of events encompasses multiple stages, encompassing local migration and invasion of tumor cells into adjacent tissues, subsequent penetration into the vascular system, survival and evasion within the circulatory system, and eventually proliferation within distant organs. These orchestrated processes collectively culminate in establishing metastatic colonies, underscoring the complexity of metastasis as a multistep phenomenon[89]. Epidemiological data emphasizes the notable occurrence of the invasive variant of cervical cancer, positioning it as the fourth most prevalent cancer among women globally. This ranking follows breast, colon, and lung cancers, further underlining their substantial impact. The process of metastasis in cervical carcinomas can manifest through two primary routes: the hematogenous and lymphatic pathways. Notably, patients with hematogenous metastases generally exhibit lower survival rates compared to those with lymphatic metastases. This intricate understanding of metastatic routes and their distinct implications adds depth to our comprehension of cervical cancer's progression and underscores the diverse challenges associated with its management[90–93].

These epidemiological findings illustrate the importance of antimetastatic compounds as emerging drug candidates.

Both **16AABE** and **16BABE** have demonstrated significant inhibitory effects on the migration of MDA-MB-231 cells. Their impact is evident in both time- and concentration-dependent manners, as evidenced by the wound healing assay. Notably, this effect is observed at a concentration as low as 1.5 μM, a value considerably below any of the identified IC_{50} values associated with cell growth inhibition. This intriguing observation suggests that the compound's ability to impede cell migration might represent a distinct pharmacological attribute rather than being a simple consequence of their impact on cell growth.

As we delve further into comprehending the anti-invasive properties of these estrone analogs, the Boyden chamber assay emerges as a valuable tool for evaluation. In this context, a 24-hour treatment with both compounds yielded a highly significant reduction in breast cancer cell invasion, notable at concentrations of 0.5 μM and 1 μM. Furthermore, this anti-invasive action gained even more pronounced significance after a 48-hour incubation period. While a comprehensive mechanistic explanation of these elicited antimetastatic effects may lie beyond the scope of the present study, it is worth noting that a previous exploration of a group of 3-*O*-sulfamoyl-13α-estrone derivatives demonstrated a pharmacological profile with striking

similarities to the compounds under our current investigation. This congruence in outcomes adds an interesting layer of consistency to our findings, encouraging further exploration and potential avenues for future research. To gain insight into the binding characteristics of the three 13α-estrones, molecular docking studies have been conducted to understand their interactions with β-tubulin[94]. Intriguingly, the observed binding affinities exhibited a correlation with their positive impact on tubulin polymerization. This intriguing linkage suggests that β-tubulin could potentially serve as the site of action for **16AABE** and **16BABE**, shedding light on their mechanism of action. Given that the functions of microtubules extend beyond their role in constructing the mitotic spindle, a compound capable of disrupting tubulin dynamics might potentially exert additional effects beyond the anticipated antimitotic properties. The dynamic nature of tubulin is intricately intertwined with the mobility of cancer cells. Thus, pharmacological interventions that influence the polymerization of the peptide might have the potential to impact the metastatic potential of cancer cells. This effect could manifest independently of the direct cytotoxicity of the agent, offering a novel perspective on the multifaceted roles that tubulin disruptors might play in the complex landscape of cancer progression[95].

The utilization of the estrane skeleton provided a logic for exploring the estrogenic activity of the tested analogs. Our findings reveal that both **16AABE** and **16BABE** demonstrated considerable hormonal activity at nanomolar concentrations, a range that aligns with their antiproliferative and antimetastatic effects. However, it's important to note that a drug exhibiting estrogenic hormonal effects could potentially stimulate the proliferation of cancer cells, which might be detrimental in many gynecological cancers.

Nevertheless, a theoretical scenario exists wherein a subset of hormone-independent malignancies, such as triple-negative breast cancer, might remain unaffected by the hormonal agonist action. This would imply that the hormonal aspect does not impede the utility of such agents in these specific cancer types. Consequently, the estrone analogs we have presented here hold promise as innovative drug candidates for cancerous disorders that are not influenced by hormonal effects, offering a potentially magnificent way of treatment for these hormone-neutral malignancies. This intriguing prospect underscores the need for nuanced approaches considering the complex interplay between hormonal actions and cancer progression.

6. Summary

In conclusion, our findings provide compelling experimental evidence supporting the relevance of 16-azidomethyl-estrone analogs as drug candidates with anticancer properties. The observed tumor-selective antiproliferative and antimetastatic effects, combined with their ability to induce cell cycle disturbances and exhibit tumor selectivity, highlight the promising prospects of these compounds as innovative anticancer agents. Furthermore, their potent antimigratory and anti-invasive properties are exerted below their growth-inhibitory concentrations. The tested compounds substantially increased the polymerization of tubulin, which may be the basis of their actions. Since **16AABE** and **16BABE** possess estrogenic activity, their further development seems rational for treating hormone-independent malignancies.

7. Glossary of Acronyms and Abbreviations

ANOVA	Analysis of variance
ATCC	American Type Culture Collection
BRCA1	Breast cancer type 1 susceptibility protein gene
BRCA2	Breast cancer type 2 susceptibility protein gene
CO_2	Carbon dioxide
DMSO	Dimethyl sulfoxide
DNA	Deoxyribonucleic acid
EGTA	Ethylene glycol-bis(β-aminoethyl ether)-N,N,N′,N′-tetraacetic acid
FBS	Fetal bovine serum
FDA	Food and drug administration
G1	First growth phase in cell cycle
G2/M	Second growth phase in cell cycle with double DNA content / mitotic phase
GLOBOCAN	Global Cancer Observatory
HER2	Human epidermal growth factor receptor 2
IC50	Half maximal inhibitory concentration
IDC	Infiltrating ductal carcinoma
ILC	Infiltrating lobular carcinoma
MEM	Minimum Essential Medium
MTT	3-(4,5-dimethylthiazol-2-yl)-2,5-diphenyltetrazolium bromide
OEt	Ethoxy
PBS	Phosphate buffer solution
Ph	Phenyl
PI	Propidium Iodide
PIPES	Piperazine-N,N′-bis(2-ethanesulfonic acid)
S	Phase of DNA replication
SEM	Standard error of mean
Sub-G1	Hypodiploid cell fraction
t-Bu	Tert-butyl
TNBC	Triple negative breast cancer
WHO	World Health Organization

8. References

1. Sung, H.; Ferlay, J.; Siegel, R.L.; Laversanne, M.; Soerjomataram, I.; Jemal, A.; Bray, F. Global Cancer Statistics 2020: GLOBOCAN Estimates of Incidence and Mortality Worldwide for 36 Cancers in 185 Countries. *CA Cancer J Clin* **2021**, *71*, 209–249, doi:10.3322/caac.21660.

2. Azadnajafabad, S.; Saeedi Moghaddam, S.; Mohammadi, E.; Delazar, S.; Rashedi, S.; Baradaran, H.R.; Mansourian, M. Patterns of Better Breast Cancer Care in Countries with Higher Human Development Index and Healthcare Expenditure: Insights from GLOBOCAN 2020. *Front Public Health* **2023**, *11*, doi:10.3389/fpubh.2023.1137286.

3. Coleman, M.P.; Quaresma, M.; Berrino, F.; Lutz, J.-M.; De Angelis, R.; Capocaccia, R.; Baili, P.; Rachet, B.; Gatta, G.; Hakulinen, T.; et al. Cancer Survival in Five Continents: A Worldwide Population-Based Study (CONCORD). *Lancet Oncol* **2008**, *9*, 730–756, doi:10.1016/S1470-2045(08)70179-7.

4. Anderson, B.O.; Yip, C.-H.; Smith, R.A.; Shyyan, R.; Sener, S.F.; Eniu, A.; Carlson, R.W.; Azavedo, E.; Harford, J. Guideline Implementation for Breast Healthcare in Low-Income and Middle-Income Countries. *Cancer* **2008**, *113*, 2221–2243, doi:10.1002/cncr.23844.

5. Siegel, R.; Naishadham, D.; Jemal, A. Cancer Statistics, 2013. *CA Cancer J Clin* **2013**, *63*, 11–30, doi:10.3322/caac.21166.

6. Berry, D.A.; Cronin, K.A.; Plevritis, S.K.; Fryback, D.G.; Clarke, L.; Zelen, M.; Mandelblatt, J.S.; Yakovlev, A.Y.; Habbema, J.D.F.; Feuer, E.J. Effect of Screening and Adjuvant Therapy on Mortality from Breast Cancer. *New England Journal of Medicine* **2005**, *353*, 1784–1792, doi:10.1056/NEJMoa050518.

7. Peng, J.; Sengupta, S.; Jordan, V.C. Potential of Selective Estrogen Receptor Modulators as Treatments and Preventives of Breast Cancer. *Anticancer Agents Med Chem* **2009**, *9*, 481–499, doi:10.2174/187152009788451833.

8. Ferlay, J.; Soerjomataram, I.; Dikshit, R.; Eser, S.; Mathers, C.; Rebelo, M.; Parkin, D.M.; Forman, D.; Bray, F. Cancer Incidence and Mortality Worldwide: Sources, Methods and Major Patterns in GLOBOCAN 2012. *Int J Cancer* **2015**, *136*, E359–E386, doi:10.1002/ijc.29210.

9. Bien, A.M.; Korzynska-Pietas, M.; Iwanowicz-Palus, G.J. Assessment of Midwifery Student Preparation for Performing the Role of Breast Cancer Educator. *Asian Pacific Journal of Cancer Prevention* **2014**, *15*, 5633–5638, doi:10.7314/APJCP.2014.15.14.5633.

10. Haghighat, S.; Akbari, M.E.; Ghaffari, S.; Yavari, P. Standardized Breast Cancer Mortality Rate Compared to the General Female Population of Iran. *Asian Pacific Journal of Cancer Prevention* **2012**, *13*, 5525–5528, doi:10.7314/APJCP.2012.13.11.5525.

11. West, A.-K.V.; Wullkopf, L.; Christensen, A.; Leijnse, N.; Tarp, J.M.; Mathiesen, J.; Erler, J.T.; Oddershede, L.B. Dynamics of Cancerous Tissue Correlates with Invasiveness. *Sci Rep* **2017**, *7*, 43800, doi:10.1038/srep43800.

12. Posner, M.C.; Wolmark, N. Non-Invasive Breast Carcinoma. *Breast Cancer Res Treat* **1992**, *21*, 155–164, doi:10.1007/BF01974998.

13. Hang, J.A.; Sim, L.; Zakaria, Z. Non-Invasive Breast Cancer Assessment Using Magnetic Induction Spectroscopy Technique. *International Journal of Integrated Engineering* **2017**, *9*.

14. Clauser, P.; Marino, M.A.; Baltzer, P.A.T.; Bazzocchi, M.; Zuiani, C. Management of Atypical Lobular Hyperplasia, Atypical Ductal Hyperplasia, and Lobular Carcinoma in Situ. *Expert Rev Anticancer Ther* **2016**, *16*, 335–346, doi:10.1586/14737140.2016.1143362.

15. Chuba, P.J.; Hamre, M.R.; Yap, J.; Severson, R.K.; Lucas, D.; Shamsa, F.; Aref, A. Bilateral Risk for Subsequent Breast Cancer After Lobular Carcinoma-In-Situ: Analysis of Surveillance, Epidemiology, and End Results Data. *Journal of Clinical Oncology* **2005**, *23*, 5534–5541, doi:10.1200/JCO.2005.04.038.

16. Nakhlis, F.; Morrow, M. Ductal Carcinoma in Situ. *Surgical Clinics of North America* **2003**, *83*, 821–839, doi:10.1016/S0039-6109(03)00072-0.

17. Harris, L.N.; Ismaila, N.; McShane, L.M.; Andre, F.; Collyar, D.E.; Gonzalez-Angulo, A.M.; Hammond, E.H.; Kuderer, N.M.; Liu, M.C.; Mennel, R.G.; et al. Use of Biomarkers to Guide Decisions on Adjuvant Systemic Therapy for Women With Early-Stage Invasive Breast Cancer: American Society of Clinical Oncology Clinical Practice Guideline. *Journal of Clinical Oncology* **2016**, *34*, 1134–1150, doi:10.1200/JCO.2015.65.2289.

18. Ziperstein, M.J.; Guzman, A.; Kaufman, L.J. Breast Cancer Cell Line Aggregate Morphology Does Not Predict Invasive Capacity. *PLoS One* **2015**, *10*, e0139523, doi:10.1371/journal.pone.0139523.

19. Prabhakaran, S.; Rizk, V.T.; Ma, Z.; Cheng, C.-H.; Berglund, A.E.; Coppola, D.; Khalil, F.; Mulé, J.J.; Soliman, H.H. Evaluation of Invasive Breast Cancer Samples Using a 12-Chemokine Gene Expression Score: Correlation with Clinical Outcomes. *Breast Cancer Research* **2017**, *19*, 71, doi:10.1186/s13058-017-0864-z.

20. Stevanovic, A.; Lee, P.; Wilcken, N. Metastatic Breast Cancer. *Aust Fam Physician* **2006**, *35*, 309–312.

21. Page, K.; Guttery, D.S.; Fernandez-Garcia, D.; Hills, A.; Hastings, R.K.; Luo, J.; Goddard, K.; Shahin, V.; Woodley-Barker, L.; Rosales, B.M.; et al. Next Generation Sequencing of Circulating Cell-Free DNA for Evaluating Mutations and Gene Amplification in Metastatic Breast Cancer. *Clin Chem* **2017**, *63*, 532–541, doi:10.1373/clinchem.2016.261834.

22. Arpino, G.; Bardou, V.J.; Clark, G.M.; Elledge, R.M. Infiltrating Lobular Carcinoma of the Breast: Tumor Characteristics and Clinical Outcome. *Breast Cancer Research* **2004**, *6*, R149, doi:10.1186/bcr767.

23. Somiari, R.I.; Sullivan, A.; Russell, S.; Somiari, S.; Hu, H.; Jordan, R.; George, A.; Katenhusen, R.; Buchowiecka, A.; Arciero, C.; et al. High-Throughput Proteomic Analysis of Human Infiltrating Ductal Carcinoma of the Breast. *Proteomics* **2003**, *3*, 1863–1873, doi:10.1002/pmic.200300560.

24. Mateo, A.M.; Pezzi, T.A.; Sundermeyer, M.; Kelley, C.A.; Klimberg, V.S.; Pezzi, C.M. Chemotherapy Significantly Improves Survival for Patients with T1c-T2N0M0 Medullary Breast Cancer: 3739 Cases From the National Cancer Data Base. *Ann Surg Oncol* **2017**, *24*, 1050–1056, doi:10.1245/s10434-016-5649-6.

25. Anuradha, D.; Lakshmi, A. Mucinous Carcinoma of Breast with Neuroendocrine Differentiation: A Rare Case Report with Review of Literature. *Int J Res Med Sci* **2014**, *2*, 1751, doi:10.5455/2320-6012.ijrms201411102.

26. Priya, V.S.L.; Prasaad, P.R. Tubulo- Lobular Carcinoma: A Rare Mixed Invasive Carcinoma Of. *Int J Res Med Sci* **2017**, *5*, 2818, doi:10.18203/2320-6012.ijrms20172496.

27. Joglekar-Javadekar, M.; Van Laere, S.; Bourne, M.; Moalwi, M.; Finetti, P.; Vermeulen, P.B.; Birnbaum, D.; Dirix, L.Y.; Ueno, N.; Carter, M.; et al. Characterization and Targeting of Platelet-Derived Growth Factor Receptor Alpha (PDGFRA) in Inflammatory Breast Cancer (IBC). *Neoplasia* **2017**, *19*, 564–573, doi:10.1016/j.neo.2017.03.002.

28. Cariati, M.; Bennett-Britton, T.M.; Pinder, S.E.; Purushotham, A.D. "Inflammatory" Breast Cancer. *Surg Oncol* **2005**, *14*, 133–143, doi:10.1016/j.suronc.2005.07.004.

29. Errichetti, E.; Avellini, C.; Pegolo, E.; De Francesco, V. Dermoscopy as a Supportive Instrument in the Early Recognition of Erosive Adenomatosis of the Nipple and Mammary Paget's Disease. *Ann Dermatol* **2017**, *29*, 365, doi:10.5021/ad.2017.29.3.365.

30. Merrill, A.Y.; White, A.; Howard-McNatt, M. Paget's Disease of the Breast: An Institutional Review and Surgical Management. *Am Surg* **2017**, *83*, e96-98.

31. Liedtke, C.; Mazouni, C.; Hess, K.R.; André, F.; Tordai, A.; Mejia, J.A.; Symmans, W.F.; Gonzalez-Angulo, A.M.; Hennessy, B.; Green, M.; et al. Response to Neoadjuvant Therapy and Long-Term Survival in Patients With Triple-Negative Breast Cancer. *Journal of Clinical Oncology* **2008**, *26*, 1275–1281, doi:10.1200/JCO.2007.14.4147.

32. Foulkes, W.D.; Smith, I.E.; Reis-Filho, J.S. Triple-Negative Breast Cancer. *New England Journal of Medicine* **2010**, *363*, 1938–1948, doi:10.1056/NEJMra1001389.

33. Stingl, J.; Raouf, A.; Emerman, J.T.; Eaves, C.J. Epithelial Progenitors in the Normal Human Mammary Gland. *J Mammary Gland Biol Neoplasia* **2005**, *10*, 49–59, doi:10.1007/s10911-005-2540-7.

34. Villadsen, R.; Fridriksdottir, A.J.; Rønnov-Jessen, L.; Gudjonsson, T.; Rank, F.; LaBarge, M.A.; Bissell, M.J.; Petersen, O.W. Evidence for a Stem Cell Hierachy in the Adult Human Breast. *J Cell Biol* **2007**, *177*, 87–101, doi:10.1083/jcb.200611114.

35. Gusterson, B.A.; Warburton, M.J.; Mitchell, D.; Ellison, M.; Neville, A.M.; Rudland, P.S. Distribution of Myoepithelial Cells and Basement Membrane Proteins in the Normal Breast and in Benign and Malignant Breast Diseases. *Cancer Res* **1982**, *42*, 4763–4770.

36. Evan, G.I.; Vousden, K.H. Proliferation, Cell Cycle and Apoptosis in Cancer. *Nature* **2001**, *411*, 342–348, doi:10.1038/35077213.

37. Graña, X.; Reddy, E.P. Cell Cycle Control in Mammalian Cells: Role of Cyclins, Cyclin Dependent Kinases (CDKs), Growth Suppressor Genes and Cyclin-Dependent Kinase Inhibitors (CKIs). *Oncogene* **1995**, *11*, 211–219.

38. Stingl, J.; Raouf, A.; Eirew, P.; Eaves, C.J. Deciphering the Mammary Epithelial Cell Hierarchy. *Cell Cycle* **2006**, *5*, 1519–1522, doi:10.4161/cc.5.14.2983.

39. Hartwell, L.H.; Kastan, M.B. Cell Cycle Control and Cancer. *Science (1979)* **1994**, *266*, 1821–1828, doi:10.1126/science.7997877.

40. LEIGHTON, J.; KALLA, R.L.; TURNER, J.M.; FENNELL, R.H. Pathogenesis of Tumor Invasion. II. Aggregate Replication. *Cancer Res* **1960**, *20*, 575–586.

41. Cavalieri, E.; Chakravarti, D.; Guttenplan, J.; Hart, E.; Ingle, J.; Jankowiak, R.; Muti, P.; Rogan, E.; Russo, J.; Santen, R.; et al. Catechol Estrogen Quinones as Initiators of Breast and Other Human Cancers: Implications for Biomarkers of Susceptibility and Cancer Prevention. *Biochimica et Biophysica Acta (BBA) - Reviews on Cancer* **2006**, *1766*, 63–78, doi:10.1016/j.bbcan.2006.03.001.

42. Jardé, T.; Perrier, S.; Vasson, M.-P.; Caldefie-Chézet, F. Molecular Mechanisms of Leptin and Adiponectin in Breast Cancer. *Eur J Cancer* **2011**, *47*, 33–43, doi:10.1016/j.ejca.2010.09.005.

43. Hanahan, D.; Weinberg, R.A. The Hallmarks of Cancer. *Cell* **2000**, *100*, 57–70, doi:10.1016/S0092-8674(00)81683-9.

44. Jain, R.K. Normalization of Tumor Vasculature: An Emerging Concept in Antiangiogenic Therapy. *Science (1979)* **2005**, *307*, 58–62, doi:10.1126/science.1104819.

45. Gupta, G.P.; Massagué, J. Cancer Metastasis: Building a Framework. *Cell* **2006**, *127*, 679–695, doi:10.1016/j.cell.2006.11.001.

46. Harirchi, I.; Karbakhsh, M.; Kashefi, A.; Momtahen, A.J. Breast Cancer in Iran: Results of a Multi-Center Study. *Asian Pac J Cancer Prev* **2004**, *5*, 24–27.

47. Alegre, M.M.; Knowles, M.H.; Robison, R.A.; O'Neill, K.L. Mechanics behind Breast Cancer Prevention - Focus on Obesity, Exercise and Dietary Fat. *Asian Pacific Journal of Cancer Prevention* **2013**, *14*, 2207–2212, doi:10.7314/APJCP.2013.14.4.2207.

48. Zainal, N.Z.; Nik-Jaafar, N.R.; Baharudin, A.; Sabki, Z.A.; Ng, C.G. Prevalence of Depression in Breast Cancer Survivors: A Systematic Review of Observational Studies. *Asian Pacific Journal of Cancer Prevention* **2013**, *14*, 2649–2656, doi:10.7314/APJCP.2013.14.4.2649.

49. do Carmo França-Botelho, A.; Ferreira, M.C.; França, J.L.; França, E.L.; Honório-França, A.C. Breastfeeding and Its Relationship with Reduction of Breast Cancer: A Review. *Asian Pac J Cancer Prev* **2012**, *13*, 5327–5332.

50. Alco, G.; Igdem, S.; Dincer, M.; Ozmen, V.; Saglam, S.; Selamoglu, D.; Erdogan, Z.; Ordu, C.; Pilanci, K.N.; Bozdogan, A.; et al. Vitamin D Levels in Patients with Breast Cancer: Importance of Dressing Style. *Asian Pacific Journal of Cancer Prevention* **2014**, *15*, 1357–1362, doi:10.7314/APJCP.2014.15.3.1357.

51. Zhao, M.; Howard, E.W.; Parris, A.B.; Guo, Z.; Zhao, Q.; Yang, X. Alcohol Promotes Migration and Invasion of Triple-Negative Breast Cancer Cells through Activation of P38 MAPK and JNK. *Mol Carcinog* **2017**, *56*, 849–862, doi:10.1002/mc.22538.

52. Shaukat, U.; Ismail, M.; Mehmood, N. Epidemiology, Major Risk Factors and Genetic Predisposition for Breast Cancer in the Pakistani Population. *Asian Pacific Journal of Cancer Prevention* **2013**, *14*, 5625–5629, doi:10.7314/APJCP.2013.14.10.5625.

53. Kadivar, M.; Mafi, N.; Joulaee, A.; Shamshiri, A.; Hosseini, N. Breast Cancer Molecular Subtypes and Associations with Clinicopathological Characteristics in Iranian Women, 2002-2011. *Asian Pacific Journal of Cancer Prevention* **2012**, *13*, 1881–1886, doi:10.7314/APJCP.2012.13.5.1881.

54. Osborne, C.K.; Yochmowitz, M.G.; Knight, W.A.; McGuire, W.L. The Value of Estrogen and Progesterone Receptors in the Treatment of Breast Cancer. *Cancer* **1980**, *46*, 2884–2888, doi:10.1002/1097-0142(19801215)46:12+<2884::aid-cncr2820461429>3.0.co;2-u.

55. Visvanathan, K.; Chlebowski, R.T.; Hurley, P.; Col, N.F.; Ropka, M.; Collyar, D.; Morrow, M.; Runowicz, C.; Pritchard, K.I.; Hagerty, K.; et al. American Society of Clinical Oncology Clinical Practice Guideline Update on the Use of Pharmacologic Interventions Including Tamoxifen, Raloxifene, and Aromatase Inhibition for Breast Cancer Risk Reduction. *Journal of Clinical Oncology* **2009**, *27*, 3235–3258, doi:10.1200/JCO.2008.20.5179.

56. Nayfield, S.G.; Karp, J.E.; Ford, L.G.; Dorr, F.A.; Kramer, B.S. Potential Role of Tamoxifen in Prevention of Breast Cancer. *JNCI Journal of the National Cancer Institute* **1991**, *83*, 1450–1459, doi:10.1093/jnci/83.20.1450.

57. JORDAN, V. New Insights into the Metabolism of Tamoxifen and Its Role in the Treatment and Prevention of Breast Cancer. *Steroids* **2007**, *72*, 829–842, doi:10.1016/j.steroids.2007.07.009.

58. Fisher, B.; Costantino, J.P.; Wickerham, D.L.; Redmond, C.K.; Kavanah, M.; Cronin, W.M.; Vogel, V.; Robidoux, A.; Dimitrov, N.; Atkins, J.; et al. Tamoxifen for Prevention of Breast Cancer: Report of the National Surgical Adjuvant Breast and Bowel Project P-1 Study. *JNCI: Journal of the National Cancer Institute* **1998**, *90*, 1371–1388, doi:10.1093/jnci/90.18.1371.

59. Vogel, V.G. Effects of Tamoxifen vs Raloxifene on the Risk of Developing Invasive Breast Cancer and Other Disease Outcomes<SUBTITLE>The NSABP Study of Tamoxifen and Raloxifene (STAR) P-2 Trial</SUBTITLE> *JAMA* **2006**, *295*, 2727, doi:10.1001/jama.295.23.joc60074.

60. Cuzick, J.; Powles, T.; Veronesi, U.; Forbes, J.; Edwards, R.; Ashley, S.; Boyle, P. Overview of the Main Outcomes in Breast-Cancer Prevention Trials. *The Lancet* **2003**, *361*, 296–300, doi:10.1016/S0140-6736(03)12342-2.

61. Vogel, V.G. Chemoprevention Strategies 2006. *Curr Treat Options Oncol* **2007**, *8*, 74–88, doi:10.1007/s11864-007-0019-z.

62. Land, S.R.; Wickerham, D.L.; Costantino, J.P.; Ritter, M.W.; Vogel, V.G.; Lee, M.; Pajon, E.R.; Wade, J.L.; Dakhil, S.; Lockhart, J.B.; et al. Patient-Reported Symptoms and Quality of Life During Treatment With Tamoxifen or Raloxifene for Breast Cancer Prevention. *JAMA* **2006**, *295*, 2742, doi:10.1001/jama.295.23.joc60075.

63. Benson, A.B.; Schrag, D.; Somerfield, M.R.; Cohen, A.M.; Figueredo, A.T.; Flynn, P.J.; Krzyzanowska, M.K.; Maroun, J.; McAllister, P.; Van Cutsem, E.; et al. American Society of Clinical Oncology Recommendations on Adjuvant Chemotherapy for Stage II Colon Cancer. *Journal of Clinical Oncology* **2004**, *22*, 3408–3419, doi:10.1200/JCO.2004.05.063.

64. Müller, A.; Homey, B.; Soto, H.; Ge, N.; Catron, D.; Buchanan, M.E.; McClanahan, T.; Murphy, E.; Yuan, W.; Wagner, S.N.; et al. Involvement of Chemokine Receptors in Breast Cancer Metastasis. *Nature* **2001**, *410*, 50–56, doi:10.1038/35065016.

65. O'Shaughnessy, J.; Miles, D.; Vukelja, S.; Moiseyenko, V.; Ayoub, J.-P.; Cervantes, G.; Fumoleau, P.; Jones, S.; Lui, W.-Y.; Mauriac, L.; et al. Superior Survival With Capecitabine Plus Docetaxel Combination Therapy in Anthracycline-Pretreated Patients With Advanced Breast Cancer: Phase III Trial Results. *Journal of Clinical Oncology* **2002**, *20*, 2812–2823, doi:10.1200/JCO.2002.09.002.

66. Gupta, A.; Kumar, B.S.; Negi, A.S. Current Status on Development of Steroids as Anticancer Agents. *J Steroid Biochem Mol Biol* **2013**, *137*, 242–270, doi:10.1016/j.jsbmb.2013.05.011.

67. Bansal, R.; Acharya, P.C. Man-Made Cytotoxic Steroids: Exemplary Agents for Cancer Therapy. *Chem Rev* **2014**, *114*, 6986–7005, doi:10.1021/cr4002935.

68. Newman, D.J.; Cragg, G.M. Natural Products as Sources of New Drugs over the Nearly Four Decades from 01/1981 to 09/2019. *J Nat Prod* **2020**, *83*, 770–803, doi:10.1021/acs.jnatprod.9b01285.

69. AlQathama, A.; Shao, L.; Bader, A.; Khondkar, P.; Gibbons, S.; M Prieto, J. Differential Anti-Proliferative and Anti-Migratory Activities of Ursolic Acid, 3-O-Acetylursolic Acid and Their Combination Treatments with Quercetin on Melanoma Cells. *Biomolecules* **2020**, *10*, 894, doi:10.3390/biom10060894.

70. Bednarczyk-Cwynar, B.; Ruszkowski, P.; Bobkiewicz-Kozlowska, T.; Zaprutko, L. Oleanolic Acid A-Lactams Inhibit the Growth of HeLa, KB, MCF-7 and Hep-G2 Cancer Cell Lines at Micromolar. *Anticancer Agents Med Chem* **2016**, *16*, 579–592, doi:10.2174/1871520615666150907095756.

71. Gheorgheosu, D.; Duicu, O.; Dehelean, C.; Soica, C.; Muntean, D. Betulinic Acid as a Potent and Complex Antitumor Phytochemical: A. *Anticancer Agents Med Chem* **2014**, *14*, 936–945, doi:10.2174/1871520614666140223192148.

72. Liu, J.; Wu, N.; Ma, L.N.; Zhong, J.T.; Liu, G.; Zheng, L.H.; Lin, X.K. P38 MAPK Signaling Mediates Mitochondrial Apoptosis in Cancer Cells Induced by Oleanolic Acid.

Asian Pacific Journal of Cancer Prevention **2014**, *15*, 4519–4525, doi:10.7314/APJCP.2014.15.11.4519.

73. Sun, H.; Lv, C.; Yang, L.; Wang, Y.; Zhang, Q.; Yu, S.; Kong, H.; Wang, M.; Xie, J.; Zhang, C.; et al. Solanine Induces Mitochondria-Mediated Apoptosis in Human Pancreatic Cancer Cells. *Biomed Res Int* **2014**, *2014*, doi:10.1155/2014/805926.

74. Wu, J.; Yang, C.; Guo, C.; Li, X.; Yang, N.; Zhao, L.; Hang, H.; Liu, S.; Chu, P.; Sun, Z.; et al. SZC015, a Synthetic Oleanolic Acid Derivative, Induces Both Apoptosis and Autophagy in MCF-7 Breast Cancer Cells. *Chem Biol Interact* **2016**, *244*, 94–104, doi:https://doi.org/10.1016/j.cbi.2015.11.013.

75. Yang, S.-J.; Liu, M.-C.; Xiang, H.-M.; Zhao, Q.; Xue, W.; Yang, S. Synthesis and in Vitro Antitumor Evaluation of Betulin Acid Ester Derivatives as Novel Apoptosis Inducers. *Eur J Med Chem* **2015**, *102*, 249–255, doi:https://doi.org/10.1016/j.ejmech.2015.08.004.

76. Molnár, J.; Frank, É.; Minorics, R.; Kádár, Z.; Ocsovszki, I.; Schönecker, B.; Wölfling, J.; Zupkó, I. A Click Approach to Novel D-Ring-Substituted 16α-Triazolylestrone Derivatives and Characterization of Their Antiproliferative Properties. *PLoS One* **2015**, *10*, e0118104, doi:10.1371/journal.pone.0118104.

77. Mernyák, E.; Kovács, I.; Minorics, R.; Sere, P.; Czégány, D.; Sinka, I.; Wölfling, J.; Schneider, G.; Újfaludi, Z.; Boros, I.; et al. Synthesis of Trans-16-Triazolyl-13α-Methyl-17-Estradiol Diastereomers and the Effects of Structural Modifications on Their in Vitro Antiproliferative Activities. *J Steroid Biochem Mol Biol* **2015**, *150*, 123–134, doi:10.1016/j.jsbmb.2015.04.001.

78. Minorics, R.; Zupko, I. Steroidal Anticancer Agents: An Overview of Estradiol-Related Compounds. *Anticancer Agents Med Chem* **2018**, *18*, 652–666, doi:10.2174/1871520617666171114111721.

79. Bózsity, N.; Minorics, R.; Szabó, J.; Mernyák, E.; Schneider, G.; Wölfling, J.; Wang, H.-C.; Wu, C.-C.; Ocsovszki, I.; Zupkó, I. Mechanism of Antiproliferative Action of a New D-Secoestrone-Triazole Derivative in Cervical Cancer Cells and Its Effect on Cancer Cell Motility. *J Steroid Biochem Mol Biol* **2017**, *165*, 247–257, doi:https://doi.org/10.1016/j.jsbmb.2016.06.013.

80. Kiss, A.; Mernyák, E.; Wölfling, J.; Sinka, I.; Zupkó, I.; Schneider, G. Stereoselective Synthesis of the Four 16-Hydroxymethyl-3-Methoxy- and 16-Hydroxymethyl-3-Benzyloxy-13 α -Estra-1,3,5(10)-Trien-17-Ol Isomers and Their Antiproliferative Activities. *Steroids* **2018**, *134*, 67–77, doi:10.1016/j.steroids.2018.02.008.

81. Vermes, I.; Haanen, C.; Reutelingsperger, C. Flow Cytometry of Apoptotic Cell Death. *J Immunol Methods* **2000**, *243*, 167–190, doi:10.1016/S0022-1759(00)00233-7.

82. Wilson, V.S. Development and Characterization of a Cell Line That Stably Expresses an Estrogen-Responsive Luciferase Reporter for the Detection of Estrogen Receptor Agonist and Antagonists. *Toxicological Sciences* **2004**, *81*, 69–77, doi:10.1093/toxsci/kfh180.

83. Sharma, J.D.; Khanna, S.; Ramchandani, S.; Kakoti, L.M.; Baruah, A.; Mamidala, V. Prevalence of Molecular Subtypes of Breast Carcinoma and Its Comparison between Two Different Age Groups: A Retrospective Study from a Tertiary Care Center of Northeast India. *South Asian J Cancer* **2021**, *10*, 220–224, doi:10.1055/s-0041-1731905.

84. Li, Y.; Zhang, H.; Merkher, Y.; Chen, L.; Liu, N.; Leonov, S.; Chen, Y. Recent Advances in Therapeutic Strategies for Triple-Negative Breast Cancer. *J Hematol Oncol* **2022**, *15*, 121, doi:10.1186/s13045-022-01341-0.

85. Derakhshan, F.; Reis-Filho, J.S. Pathogenesis of Triple-Negative Breast Cancer. *Annual Review of Pathology: Mechanisms of Disease* **2022**, *17*, 181–204, doi:10.1146/annurev-pathol-042420-093238.

86. Frank, É.; Schneider, G. Synthesis of Sex Hormone-Derived Modified Steroids Possessing Antiproliferative Activity. *J Steroid Biochem Mol Biol* **2013**, *137*, 301–315, doi:https://doi.org/10.1016/j.jsbmb.2013.02.018.

87. Dumontet, C.; Jordan, M.A. Microtubule-Binding Agents: A Dynamic Field of Cancer Therapeutics. *Nat Rev Drug Discov* **2010**, *9*, 790–803, doi:10.1038/nrd3253.

88. Mehlen, P.; Puisieux, A. Metastasis: A Question of Life or Death. *Nat Rev Cancer* **2006**, *6*, 449–458, doi:10.1038/nrc1886.

89. Eger, A.; Mikulits, W. Models of Epithelial–Mesenchymal Transition. *Drug Discov Today Dis Models* **2005**, *2*, 57–63, doi:https://doi.org/10.1016/j.ddmod.2005.04.001.

90. Bhatla, N.; Berek, J.S.; Cuello Fredes, M.; Denny, L.A.; Grenman, S.; Karunaratne, K.; Kehoe, S.T.; Konishi, I.; Olawaiye, A.B.; Prat, J.; et al. Revised FIGO Staging for Carcinoma of the Cervix Uteri. *International Journal of Gynecology & Obstetrics* **2019**, *145*, 129–135, doi:https://doi.org/10.1002/ijgo.12749.

91. Franco, E.L.; Schlecht, N.F.; Saslow, D. The Epidemiology of Cervical Cancer. *The Cancer Journal* **2003**, *9*, 348–359, doi:10.1097/00130404-200309000-00004.

92. Stolnicu, S.; Hoang, L.; Soslow, R.A. Recent Advances in Invasive Adenocarcinoma of the Cervix. *Virchows Arch* **2019**, *475*, 537–549, doi:10.1007/s00428-019-02601-0.

93. Vandeperre, A.; Van Limbergen, E.; Leunen, K.; Moerman, P.; Amant, F.; Vergote, I. Para-Aortic Lymph Node Metastases in Locally Advanced Cervical Cancer: Comparison

between Surgical Staging and Imaging. *Gynecol Oncol* **2015**, *138*, 299–303, doi:https://doi.org/10.1016/j.ygyno.2015.05.021.

94. Ali, H.; Traj, P.; Szebeni, G.J.; Gémes, N.; Resch, V.; Paragi, G.; Mernyák, E.; Minorics, R.; Zupkó, I. Investigation of the Antineoplastic Effects of 2-(4-Chlorophenyl)-13α-Estrone Sulfamate against the HPV16-Positive Human Invasive Cervical Carcinoma Cell Line SiHa. *Int J Mol Sci* **2023**, *24*, 6625, doi:10.3390/ijms24076625.

95. Čermák, V.; Dostál, V.; Jelínek, M.; Libusová, L.; Kovář, J.; Rösel, D.; Brábek, J. Microtubule-Targeting Agents and Their Impact on Cancer Treatment. *Eur J Cell Biol* **2020**, *99*, 151075, doi:10.1016/j.ejcb.2020.151075.

9. Acknowledgements

ANNEX

I.

Article

Antiproliferative and Antimetastatic Properties of 16-Azidomethyl Substituted 3-*O*-Benzyl Estrone Analogs [†]

Seyyed Ashkan Senobar Tahaei [1], Ágnes Kulmány [1], Renáta Minorics [1], Anita Kiss [2], Zoltán Szabó [3], Péter Germán [1], Gábor J. Szebeni [4], Nikolett Gémes [4], Erzsébet Mernyák [2,*] and István Zupkó [1,5,*]

[1] Institute of Pharmacodynamics and Biopharmacy, University of Szeged, H-6720 Szeged, Hungary
[2] Department of Inorganic, Organic and Analytical Chemistry, University of Szeged, H-6720 Szeged, Hungary
[3] Department of Medicinal Chemistry, University of Szeged, H-6720 Szeged, Hungary
[4] Laboratory of Functional Genomics, Biological Research Centre, H-6726 Szeged, Hungary
[5] Interdisciplinary Centre of Natural Products, University of Szeged, H-6720 Szeged, Hungary
[*] Correspondence: bobe@chem.u-szeged.hu (E.M.); zupko.istvan@szte.hu (I.Z.)
[†] Dedicated to the memory of Professor Gyula Schneider.

Abstract: Four diastereomers of 16-azidomethyl substituted 3-*O*-benzyl estradiol (**1–4**) and their two estrone analogs (**16AABE** and **16BABE**) were tested for their antiproliferative properties against human gynecological cancer cell lines. The estrones were selected for additional experiments based on their outstanding cell growth-inhibiting activities. Both compounds increased hypodiploid populations of breast cancer cells, and **16AABE** elicited cell cycle disturbance as evidenced by flow cytometry. The two analogs substantially increased the rate of tubulin polymerization in vitro. **16AABE** and **16BABE** inhibited breast cancer cells' migration and invasive ability, as evidenced by wound healing and Boyden chamber assays. Since both estrone analogs exerted remarkable estrogenic activities, as documented by a luciferase reporter gene assay, they can be considered as promising drug candidates for hormone-independent malignancies.

Keywords: estrone analogs; antiproliferative effect; metastasis; apoptosis; tubulin polymerization; breast cancer

1. Introduction

Cancer is prominent cause of death worldwide, with mortality rates comparable to those of stroke and coronary heart disease. According to the latest update from the International Agency for Research on Cancer (IARC) database, 19.3 million new cancer cases and almost 10 million cancer-related deaths occurred globally in 2020. Moreover, the global cancer burden is expected to reach 28.4 million cases by 2040, corresponding to a 47% rise in all cancer cases. Lung cancer is the leading cause of cancer death, responsible for 18% of tumor-related mortality, followed by colorectal (9.4%), liver (8.3%), stomach (7.7%), and female breast (6.9%) cancers. Concerning the incidence of different female tumors, breast carcinomas are the most common, accounting for 24.5% of all new cases. Altogether, 38.9% of new cancer cases in females involve gynecological malignancies [1]. The 2.26 million breast cancer cases diagnosed in 2020 show unequal geographical distribution, with the highest age-standardized incidence rate in Europe (69.7/100,000) and the lowest in South-East Asia (28.3/100,000). A statistically significant inverse correlation was observed between the mortality-to-incidence ratio (MIR) and the human development index (HDI), indicating poorer prognosis for patients living in less developed regions of the world [2]. All these epidemiological findings suggest that the prevention and treatment of female breast cancers are not yet resolved, despite the impressive therapeutic progress evidenced in past decades.

Substantial improvement of the global cancer burden is impossible without innovative therapeutic options, including original drugs. Studying compounds with steroidal skeleton

as potential anticancer agents has a long history. Over the past few decades, several new steroids, such as cyproterone, finasteride, exemestane and fulvestrant, have been integrated into clinical practice. A feasible strategy for developing novel drug candidates involves the chemical modification of endogenous molecules to produce semi-synthetic analogs with diverse biological activities [3].

The initial application of steroid-based compounds in the field of anticancer therapy emerged from the utilization of diverse botanical extracts. Evidence suggests that steroid-like triterpenes, including betulinic acid, oleanolic acid, and related derivatives, exhibit potent proapoptotic and antimigratory effects against numerous human cancer cell lines [4–10]. Many estrane-based compounds modified in rings A or D have been investigated recently, demonstrating that triazolyl estranes exert promising anticancer actions [11,12]. Studies have also demonstrated that numerous core-modified estradiol analogs exhibit considerable antiproliferative activity against human cancer cell lines derived from gynecological malignancies [13]. The position, specific nature, size and polarity of the substituents newly introduced into the molecule have been shown to substantially impact the anticancer properties of the designed derivatives. The antiproliferative mechanism of certain core-modified estrones is based on their direct effects on the tubule-microtubule system, resulting in disturbed tubulin polymerization rates [11,14,15].

We have recently reported on certain 16,17-functionalized 3-methoxy or 3-benzyloxy estrone derivatives behaving as potent antiproliferative compounds [16,17]. The substitution pattern of ring D, and the nature of the protecting group at C-3-*O* was demonstrated to influence the cell growth-inhibitory potential of these compounds markedly. Overall, 3-benzyl ethers were found to be more potent [16]. The substituents' nature and orientation affected the antitumoral behavior of these previously tested agents [17].

Based on these promising findings regarding the antiproliferative activities of 16,17-functionalized estrone 3-benzyl ethers, in the present study we aimed to assess the antiproliferative, antimetastatic and anticancer properties of these novel substituted steroidal compounds, including four 16-azidomethyl-17-hydroxy derivatives (**1–4**) and their 17-keto counterparts (**16AABE** and **16BABE**, Figure 1).
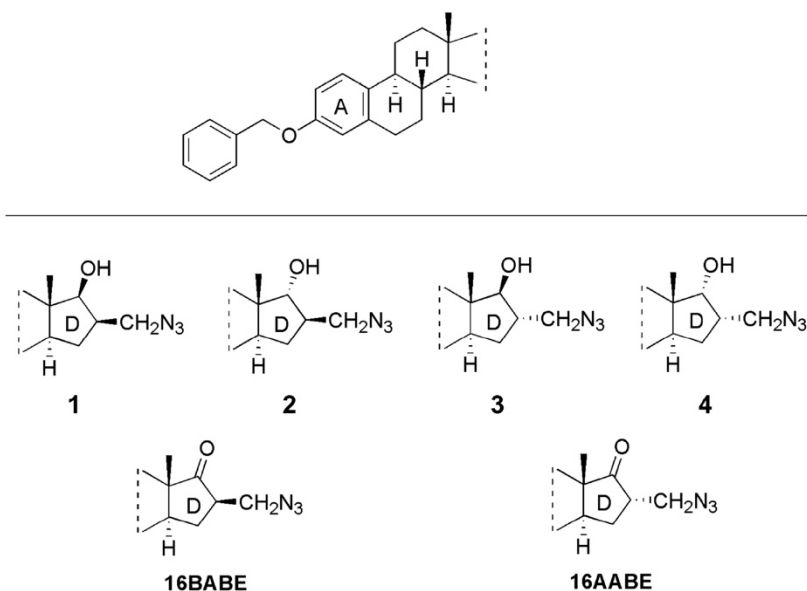

Figure 1. Structures of the tested starting compounds (**1–4**) and the newly synthesized agents 16β-azidomethyl-3-*O*-benzyl estrone (**16BABE**) and 16α-azidomethyl-3-*O*-benzyl estrone (**16AABE**).

2. Results

2.1. Chemistry

Compounds **16AABE** and **16BABE** were synthesized from their 17-hydroxy precursors (1 and 3, Scheme 1). The starting compounds were subjected to oxidation using the Jones reagent. The reactions furnished the products **16AABE** and **16BABE** in high yields. The structures of 17-keto compounds were deduced from ^{1}H and ^{13}C NMR assessments.
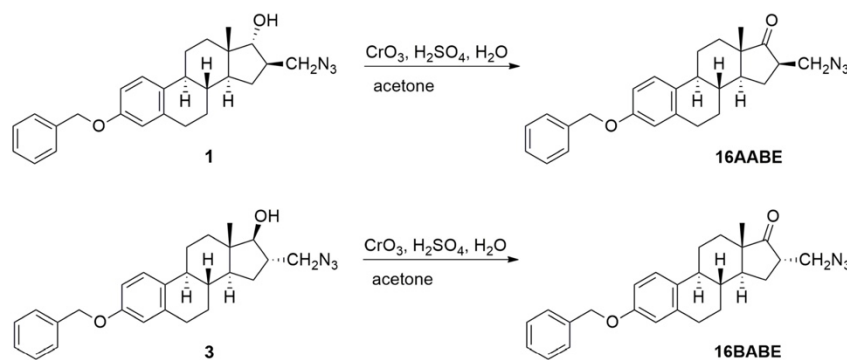
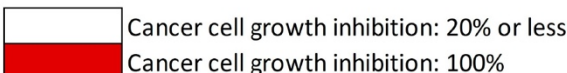**Scheme 1.** Syntheses of **16BABE** and **16AABE**.

2.2. Antiproliferative Assay

The antiproliferative capacities of the prepared compounds were determined by employing the MTT assay against a panel of human adherent cancer cell lines isolated from breast (MCF-7 and MDA-MB-231) or cervical (HeLa and SiHa) tumors. All compounds were tested at two concentrations (10 and 30 µM). When >50% of antiproliferative capacity was obtained at 10 µM, the assays were repeated with a broader concentration range (0.1–30 µM), and IC$_{50}$ values were calculated (Figure 2, Supplementary Table S1, Supplementary Figure S1). Starting molecules **1–4** exerted negligible action at 10 µM, but substantial cell growth inhibition was observed at the higher concentration (30 µM). On the other hand, the 17-keto analogs (**16AABE** and **16BABE**) elicited over 90% inhibition even at the lower concentration, and their calculated IC$_{50}$ values were lower than that of the reference agent cisplatin. MTT assays were performed against the noncancerous fibroblast cell line NIH/3T3 to obtain preliminary data on cancer selectivity of **16AABE** and **16BABE**. The fibroblast cells proved to be less sensitive, with calculated IC$_{50}$ values >10 µM. The ratios of IC$_{50}$ values obtained against cancer cells and fibroblasts were in the range of 0.2 and 0.5, indicating substantial cancer selectivity of these two compounds (Table 1).

Table 1. Tumor selectivity indices of **16AABE** and **16BABE** expressed as the ratio of IC$_{50}$ values obtained against cancer cells and fibroblasts.

Cancer Cell Line	$\dfrac{\text{IC}_{50} \text{ of Cancer Cell Line (µM)}}{\text{IC}_{50} \text{ of NIH/3T3 (µM)}}$	
	16AABE	**16BABE**
HeLa	0.369	0.243
SiHa	0.302	0.203
MCF-7	0.230	0.166
MDA-MB-231	0.347	0.429

Compound	Conc.	HeLa	SiHa	MDA-MB -231	MCF-7	NIH/3T3
1	10 µM					n.d.
	30 µM					
2	10 µM					n.d.
	30 µM					
3	10 µM					n.d.
	30 µM					
4	10 µM					n.d.
	30 µM					
16AABE	10 µM					
	30 µM					
16BABE	10 µM					
	30 µM					
cisplatin*	10 µM					
	30 µM					

Cancer cell growth inhibition: 20% or less

Cancer cell growth inhibition: 100%

Figure 2. Antiproliferative properties of the investigated molecules. Inhibition values <20% are considered negligible and are not given numerically. n.d.: not determined. *: data are from refererence [17]. Numeric results with calculated IC_{50} values are presented in Supplementary Table S1.

2.3. Propidium Iodide-Based Cell Cycle Analysis

16AABE and **16BABE** were subjected to propidium iodide-based cell cycle analysis by flow cytometry to elucidate their mechanism of action. MDA-MB-231 cells were treated with various concentrations of the test agents for 24 h, and DNA content of the cells was determined. **16AABE** induced a moderate but significant increase in the hypodiploid (subG1) cell population at 1 µM (Figures 3 and 4). At 2 µM, which approximately equals the IC_{50} value for this agent, a more profound cell cycle disturbance was observed with a pronounced increase in the subG1 and G2/M populations at the expense of G1 and S phases. Conversely, **16BABE** induced a minor but significant accumulation of subG1 cells at 8 µM, a concentration roughly equaling its IC_{50}, indicating the proapoptotic activity of this compound (Figure 3).

2.4. Tubulin Polymerization Assay

The impact of **16AABE** and **16BABE** on microtubule polymerization was assessed using a cell-free system with a photometric kinetic determination. Concentrations of the test compounds were selected based on their IC_{50} values, as recommended by the kit's manufacturer. Both compounds exhibited a stimulating effect on tubulin polymerization compared with control. Notably, the calculated maximum rates of tubulin polymerization (Vmax) were significantly higher than those observed for the control (Figure 5). Additionally, the Vmax values for the test compounds were higher than that for the reference agent paclitaxel (PAC, 10 µM), indicating their profound activity on tubulin polymerization.
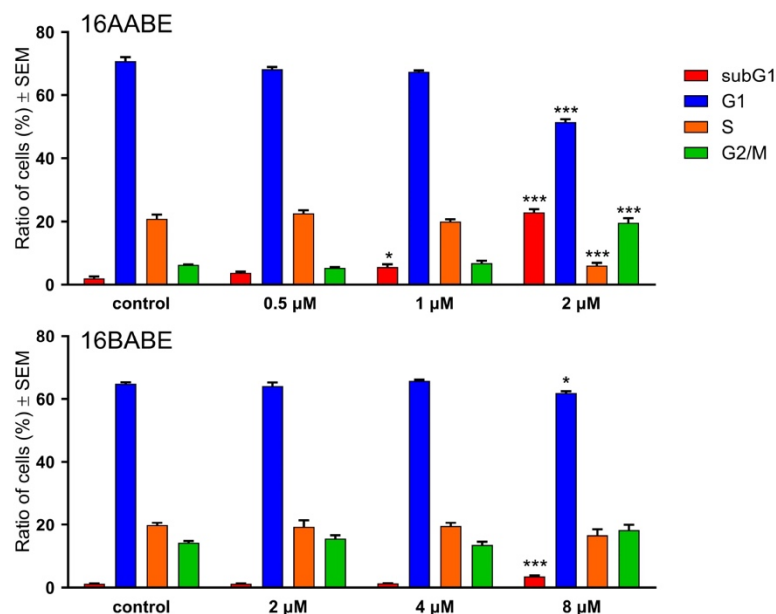
Figure 3. Effects of **16AABE** (upper panel) and **16BABE** (lower panel) on cell cycle distribution of MDA-MB-231 cells treated with the indicated concentrations for 24 h. * and *** indicate significant differences at $p < 0.05$ and $p < 0.001$, respectively. Data are from three independent experiments performed in triplicate.
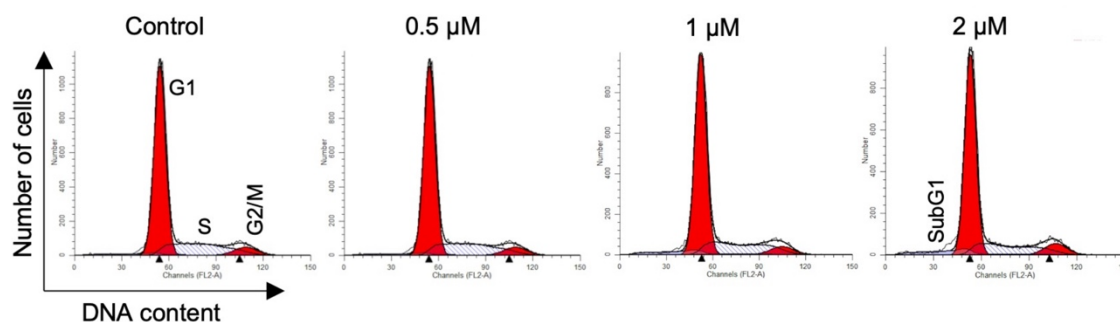
Figure 4. Representative histograms for MDA-MB-231 cells treated with **16AABE**. Histograms were generated using the ModFit LT 3.3.11 software.

2.5. Wound Healing Assay

To investigate the antimigratory activity of the test compounds, we conducted a wound-healing assay using the MCF-7 breast cancer cell line. Using an in vitro model of wound closure, a wound was created by removing silicone inserts from a cell-covered chamber, followed by incubating the cells in a minimal serum-containing (2%) medium for 0, 24, and 48 h. Microscope image analysis was performed to measure the reduction in cell-free areas, serving as an indicator of wound closure. Our findings demonstrated a significant decrease in the migratory capacity of cancer cells (Figures 6 and 7). Notably, both compounds exhibited remarkable antimigratory effects at subantiproliferative concentrations (1.5 µM), with **16BABE** demonstrating a more pronounced action after 24 h of incubation.

56
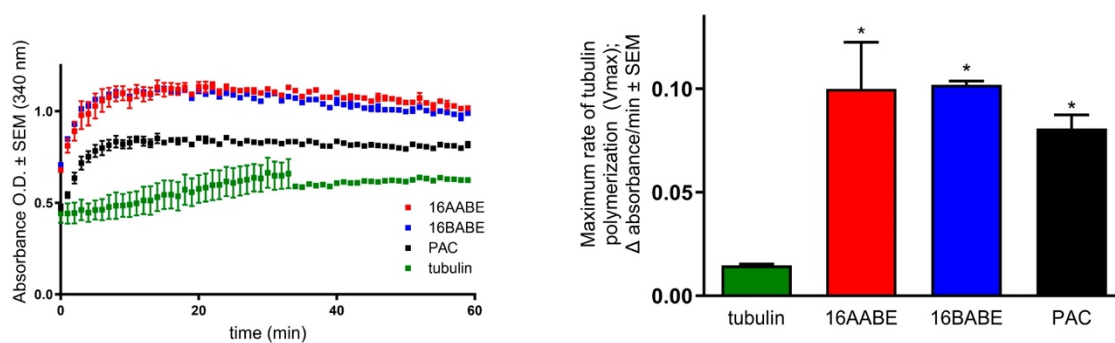
Figure 5. Direct effects of **16AABE** and **16BABE** (500 μM for both) on tubulin polymerization. Left panel: recorded kinetic curves; paclitaxel (10 μM PAC) was included as a reference agent. Right panel: calculated maximum values for the rate of tubulin polymerization. * indicates significance at $p < 0.05$ compared with untreated control. Data are from two independent experiments performed in duplicate.
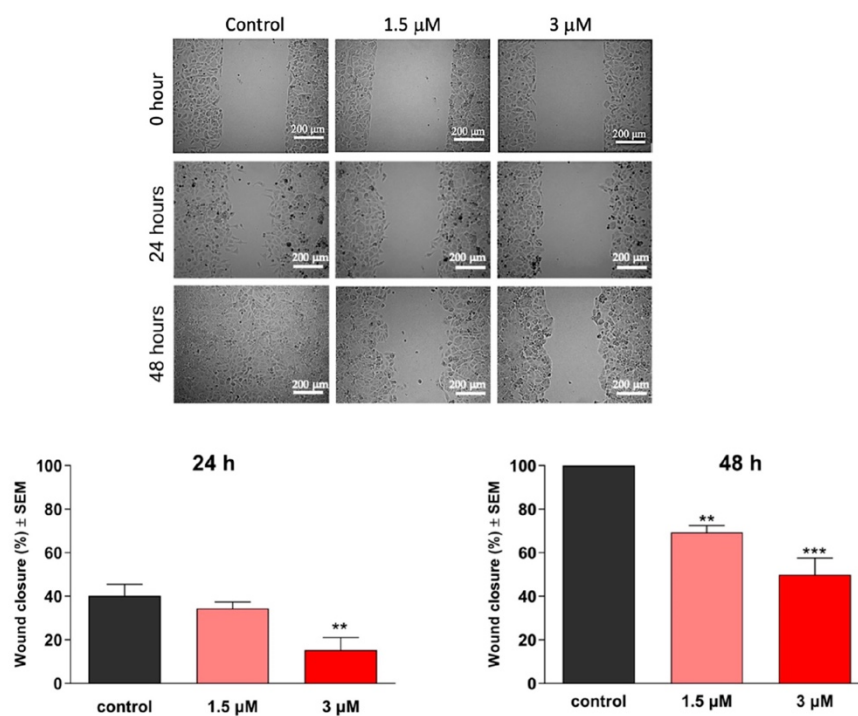
Figure 6. Effects of **16AABE** on the migration of MCF-7 cells. Upper panels: representative images taken at 24 or 48 h post-treatment with **16AABE**. Lower panels: calculated wound closure values determined at 24 or 48 h post-treatment. ** and *** indicate significance at $p < 0.01$ and $p < 0.001$, respectively. Data are based on 4 independent experiments, all performed in triplicate.
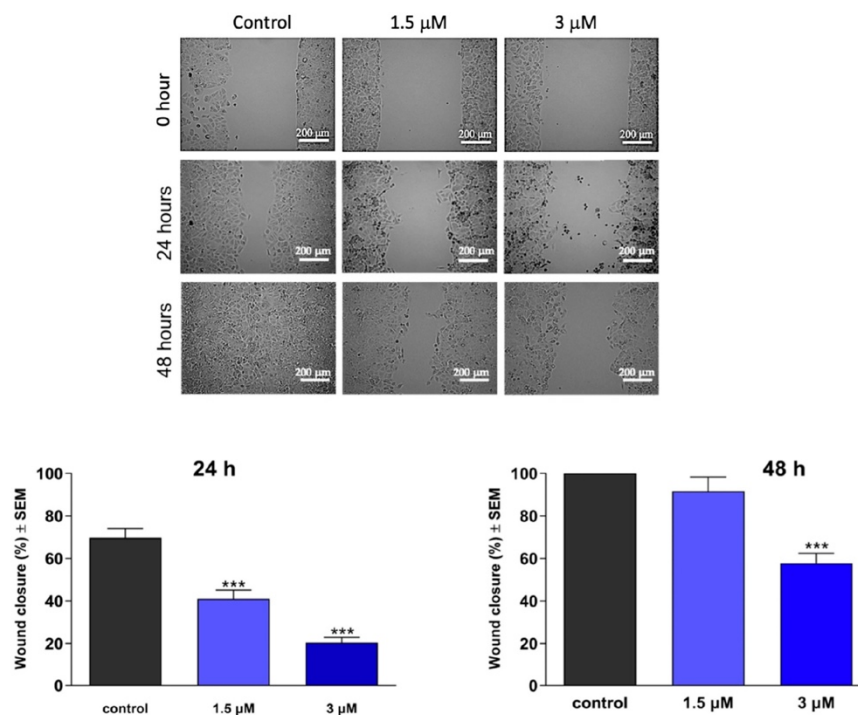
Figure 7. Effects of **16BABE** on the migration of MCF-7 cells. Upper panels: representative images taken at 24 or 48 h post-treatment with **16BABE**. Lower panels: calculated wound closure values determined at 24 or 48 h post-treatment. *** indicates significance at $p < 0.001$. Data are based on 4 independent experiments, all performed in triplicate.

2.6. Boyden Chamber Assay

As the invasive capacity of cancer cells plays a pivotal role in metastatic behavior, it is crucial to assess the antimetastatic potential of any promising anticancer agents, in addition to characterizing their impact on cell migration. Boyden chambers with Matrigel Matrix-coated membranes (pore diameter: 8.0 μm) were employed to evaluate invasiveness, as they permit the passage of invasive cells while impeding the migration of non-invading cells. Remarkably, the test compounds hindered the invasion of MDA-MB-231 cells efficiently, even at low concentrations of 0.5 or 1 μM at 24 h post-treatment (Figures 8 and 9). Moreover, both compounds exhibited a significant decrease in invading cells after 48 h of treatment, supporting their remarkable anti-invasive potential.

2.7. Estrogenic Activities of the Test Compounds

Since **16AABE** and **16BABE** are structurally closely related to the natural estrogen 17β-estradiol, their hormonal activities are considered crucial elements of their pharmacological profile. A T47D breast cancer cell line transfected with an estrogen-responsive luciferase reporter gene was utilized to clarify the estrogenic activity of the test compounds (Figure 10). Both agents were found to exert estrogenic activity at concentrations several orders of magnitude higher than the reference agent 17β-estradiol. The calculated concentrations eliciting 50% of maximum estrogenic stimulation were approximately 5.5 nM and 178 nM, respectively. These results indicate that the tested estrone analogs possess considerable hormonal activity at their antiproliferative or antimetastatic concentrations.

Figure 8. Effects of **16AABE** on the invasion capacity of MBA-MD-231 cells. Upper panels: representative images taken at 24 or 48 h post-treatment with **16AABE**. Lower panels: **16AABE** significantly reduced invasion of MDA-MB-231 cells at 24 h and 48 h post-treatment. Data are based on at least 4 independent experiments performed in duplicate. *** and **** indicate significance at $p < 0.001$ and $p < 0.0001$, respectively.

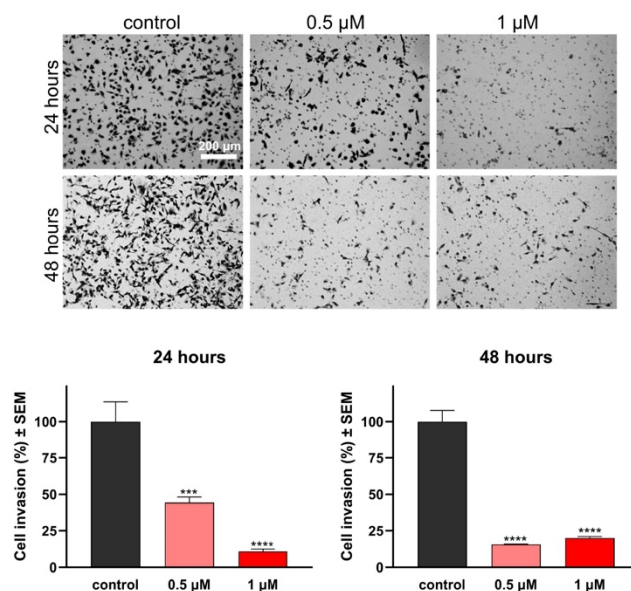**Figure 9.** Effects of **16BABE** on the invasion capacity of MBA-MD-231 cells. Upper panels: representative images taken at 24 or 48 h post-treatment with **16BABE**. Lower panels: **16BABE** significantly reduced the invasion of MDA-MB-231 cells at 24 h and 48 h post-treatment. Data are based on at least 4 independent experiments performed in duplicate. *** and **** indicate significance at $p < 0.001$ and $p < 0.0001$, respectively.
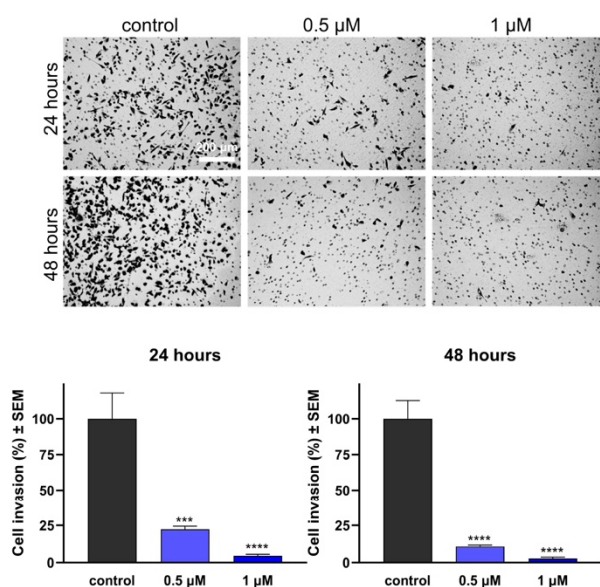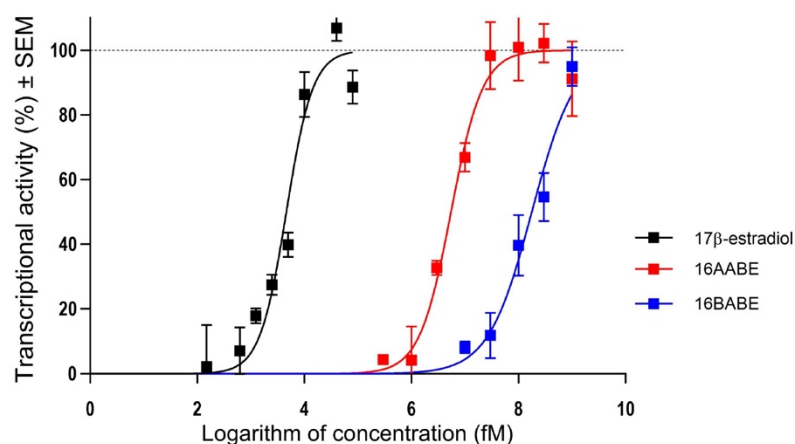
Figure 10. Estrogenic effects of **16AABE** and **16BABE** expressed as the intensity of the estrogen-responsive luciferase in transfected T47D breast cancer cell line. Data are based on 3 independent experiments performed in triplicate.

3. Discussion

Breast cancer is the most frequent malignancy in females globally. Based on crucial molecular markers, including estrogen and progestin receptors and human epidermal growth factor receptor 2 (HER2), the disease entity is classified into major subtypes: hormone receptor (HR) positive, HER2-positive, and triple-negative breast cancers (TNBC). TNBC accounts for approximately 15–20% of all cases, and its prevalence seems to be higher in younger patients, below 40 years of age [18,19]. TNBC exhibits aggressive behavior compared with other subtypes, and has a poorer prognosis. Due to the lack of targeted pharmacological interventions, current treatment of TNBC is limited to traditional cytotoxic agents [20].

Although estrogens, including the natural hormone 17β-estradiol, are generally considered to promote cell growth, several estrane-based molecules have been identified as potent anticancer drug candidates [13].

The 16-substituted triazolyl estranes represent a class of compounds with a unique structural framework combining a triazole ring with an estrane scaffold. The design and synthesis of these compounds involve click chemistry and structure-activity relationship studies to optimize their pharmacological profiles. Continued research and optimization of 16-substituted triazolyl estranes hold promise for developing novel therapeutics across multiple disease areas [11].

Our current study has focused on investigating the antiproliferative properties of four 16-azidomethyl estradiol analogs (**1–4**) previously utilized as intermediaries in synthesizing 16-triazolyl estranes [17]. Our screens for antiproliferative activity were extended to cover two estrone congeners (**16AABE** and **16BABE**), and compounds with a 17-keto function were found to be more active than the reference agent cisplatin. Moreover, the ratios of IC$_{50}$ values obtained against cancer cells and NIH/3T3 fibroblasts were below 1 (within the range of 0.166 and 0.429), indicating reliable cancer selectivity. At the same time, 17-hydroxy analogs exhibited modest actions only. According to the calculated IC$_{50}$ values, the stereochemical difference, i.e., the configuration of the 16-azidomethyl group, is not a crucial factor in the activity of these compounds. Based on these findings, the two estrone analogs were subjected to additional investigations to characterize their anticancer activities in detail.

Cell cycle analysis generally provides valuable insights into the mechanisms responsible for disturbing cell proliferation. Both selected compounds, **16AABE** and **16BABE** induced cell cycle disturbance in MDA-MB-231 TNBC cells. Treatment with **16AABE** resulted in a concentration-dependent increase in the hypodiploid (subG1) population

after 24 h of incubation. This action was detected at concentrations below the IC_{50} (1 and 2 μM), indicating the proapoptotic potency of this compound [21]. Additionally, profound accumulation of cells in the G2/M phase at the expense of the G1 and S populations was observed. On the other hand, **16BABE** elicited a detectable change in cell cycle distribution at its IC_{50} only (8 μM), and this action was limited to a modest increase in the subG1 and a decrease in the G1 cell population.

Based on these cell cycle disturbances, investigations into the effects on tubulin polymerization seemed rational. Microtubules, these highly dynamic filamentous proteins within the cytoskeleton, are considered significant targets for anticancer interventions [22]. Both compounds were found to induce a considerable increase in tubulin polymerization rate at a concentration of 500 μM, indicating their ability to enhance microtubule assembly and stability. These effects were comparable or even superior to that of the positive control paclitaxel, highlighting that direct action on tubulin seems to be a crucial component of our test compounds' pharmacological profile.

According to epidemiological data, approximately 90% of cancer-related deaths can be attributed to metastases [23]. This complex sequence of events encompasses several stages, including the local migration and invasion of tumor cells into neighboring tissues, penetration into the vascular system, survival, and exit from the circulatory system, followed by proliferation in distant organs, resulting in the establishment of new colonies [24]. Epidemiological evidence highlights the significant prevalence of invasive cervical cancer, ranking the fourth most frequent female malignancy after breast, colon, and lung cancers globally. Metastases of cervical carcinomas occur through either the hematogenous or lymphatic pathways. Patients with hematogenous metastases generally exhibit lower survival rates than those with lymphatic metastases [25–28]. These epidemiological characteristics illustrate the importance of developing effective antimetastatic compounds as potential drug candidates to hinder these tendencies.

Both **16AABE** and **16BABE** exhibited significant inhibitory effects on the migration of MDA-MB-231 cells. Both compounds demonstrated time- and concentration-dependent inhibition of cell migration as evidenced by the wound healing assay. Moreover, this antimigratory action was detected at a concentration of 1.5 μM, much lower than the IC_{50} values for cell growth inhibition in any cell lines tested. Based on these findings, the antimigratory properties of the test compounds may be explained by a separate pharmacological mechanism, rather than a consequence of cell growth inhibition.

A Boyden chamber assay was employed to evaluate the anti-invasive properties of our estrone analogs. After 24 h of treatment, both compounds demonstrated highly significant inhibition of breast cancer cell invasion at concentrations of 0.5 μM and 1 μM. Their actions became even more pronounced after 48 h of incubation. The exact characterization of the mechanism of their antimetastatic activities is beyond the scope of this study. However, in a previous study we investigated a set of 3-*O*-sulfamoyl-13α-estrone derivatives, and their pharmacological profile showed features similar to these currently tested compounds [29]. In that series, molecular docking studies were performed for three 13α-estrones to elucidate their binding properties to β-tubulin, and their binding affinity was found to correlate with their positive action on tubulin polymerization. Based on these findings, β-tubulin can be suggested as the probable site of action for **16AABE** and **16BABE**.

Since the role of microtubules is not limited to constructing the mitotic spindle, a tubulin disruptor may exert additional activities besides the expected antimitotic action. As tubulin dynamics are deeply involved in the mobility of cancer cells, pharmacological interventions affecting tubulin polymerization may influence metastatic potency, independently of the direct cytotoxicity of a given agent [30].

Finally, the estrane skeleton justified the characterization of the estrogenic activity of the tested analogs. Our findings indicate that **16AABE** and **16BABE** exhibit substantial hormonal activity at concentrations required for the antiproliferative and antimetastatic actions. Since a drug with estrogenic effect may promote the proliferation of estrogen sensitive cancer cells, this characteristic seems to be disadvantageous in most gynecological

cancers. However, in a subclass of hormone-independent malignancies including triple-negative breast cancer, the hormonal agonist action may not limit the usability of such an agent. Therefore, our currently presented estrone analogs can be considered as innovative drug candidates for such hormone-neutral cancerous disorders.

4. Materials and Methods

4.1. Chemistry

Melting points (Mp) were determined with a Kofler hot-stage apparatus and were uncorrected. Elemental analyses were performed with a PerkinElmer CHN analyzer model 2400 (PerkinElmer, Waltham, MA, USA). Thin-layer chromatography involved silica gel 60 F254; layer thickness 0.2 mm (Merck, Budapest, Hungary); eluent (ss): 20% ethyl acetate/80% hexane; detection with I_2 or UV (365 nm) after spraying with 5% phospho-molybdic acid in 50% aqueous phosphoric acid and heating at 100–120 °C for 10 min. Flash chromatography involved: silica gel 60, 40–63 μm (Merck). ^{1}H NMR spectra were recorded in CDCl$_3$ solution with a Bruker DRX-500 instrument (Bruker, Billerica, MA, USA) at 500 MHz, with Me$_4$Si as the internal standard. ^{13}C NMR spectra were recorded with the same instrument at 125 MHz under the same conditions (Supplementary Figures S2 and S3). Mass spectrometry: full scan mass spectra of the compounds were acquired in the range of 50 to 1000 *m/z* with a Finnigan TSQ-7000 triple quadrupole mass spectrometer (Finnigan-MAT, San Jose, CA, USA) equipped with a Finnigan electrospray ionization source. Analyses were performed in positive ion mode using flow injection mass spectrometry with a mobile phase of 50% aqueous acetonitrile containing 0.1% (*v/v*) formic acid. The flow rate was 0.3 mL/min. Five μL aliquot of the samples were loaded into the flow. The ESI capillary was adjusted to 4.5 kV and N$_2$ was used as a nebulizer gas.

The general procedure for the synthesis of 16β-azidomethyl-3-benzyloxyestra-1,3,5(10)-trien-17-on (**16BABE**) and 16α-azidomethyl-3-benzyloxyestra-1,3,5(10)-trien-17-on (**16AABE**) was as follows.

Compound **1** or **3** (417 mg, 1.00 mmol) was dissolved in acetone (5 mL), then cooled in an ice-water bath, and Jones reagent (0.4 mL, 8 N) was added in five portions. The reaction mixture was allowed to stand at room temperature for 1 h, then it was diluted with water and extracted with ethyl acetate. The combined organic phases were washed with water until neutral and dried over sodium sulfate, and the crude product was subjected to column chromatography with dichloromethane/hexane = 8/2 as eluent.

Compound **16BABE** was obtained as a white solid (382 mg, 92%). Mp 86–88 °C, Rf = 0.63. Anal. calcd. for C$_{26}$H$_{29}$N$_3$O$_2$: C, 75,15; H, 7.03. Found: C, 75, 27; H, 7.07. ^{1}H NMR (500 MHz, CDCl$_3$) δ ppm: 0.90 (m, 1H); 0.92 (s, 3H, 13-CH$_3$); 1.27–1.63 (overlapping multiplets with hexanes solvent peaks, 16H); 1.98–2.08 (overlapping multiplets, 3H); 2.22–2.32 (overlapping multiplets, 2H); 2.40 (m, 1H); 2.90 (m, 2H, 6-H$_2$); 3.62 (m, 2H, 16a-H$_2$); 5.04 (s, 2H, OCH$_2$); 6.74 (d, 1H, J = 2.5 Hz, 4-H); 6.79 (dd, 1H, J = 8.5 Hz, J = 2.6 Hz, 2-H); 7.20 (d, 1H, J = 8.6 Hz, 1-H); 7.32 (t, 1H, J = 7.7 Hz, 4′-H); 7.39 (t, 2H, J = 7.7 Hz, 3′- and 5′-H); 7.43 (d, 2H, J = 7.7 Hz, 2′- and 6′-H). ^{13}C NMR (CDCl$_3$) δ ppm: 13.4 (C-18); 25.8 (CH$_2$); 26.3 (CH$_2$); 26.7 (CH$_2$); 29.6 (CH$_2$); 31.9 (CH$_2$); 37.7 (CH); 44.1 (CH); 48.3 (C-13); 48.9 (CH); 49.4 (CH); 51.6 (C-16a); 69.9 (OCH$_2$); 112.4 (CH); 114.9 (CH); 126.2 (C-1); 127.4 (2C, 2× CH); 127.8 (CH); 128.5 (2C, 2× CH); 132.1 (C-10); 137.2 (C); 137.7 (C); 156.9 (C-3); 219.0 (C=O). MS *m/z* (%) 416 (100, [M+H]$^+$).

Compound **16AABE** was obtained as a white solid (374 mg, 90%). Mp 80–82 °C, Rf = 0.63. Anal. calcd. for C$_{26}$H$_{29}$N$_3$O$_2$: C, 75, 15; H, 7.03. Found: C, 75, 22; H, 7.09. ^{1}H NMR (500 MHz, CDCl$_3$) δ ppm: 0.88 (m, 1H); 0.97 (s, 3H, 13-CH$_3$); 1.26–1.56 (overlapping multiplets with hexanes solvent peaks, 18H); 1.91–2.00 (overlapping multiplets, 4H); 2.27 (m, 1H); 2.39 (m, 1H); 2.75 (m, 1H); 2.90 (m, 2H, 6-H$_2$); 3.51–3.62 (overlapping multiplets, 2H, 16a-H$_2$); 5.05 (s, 2H, OCH$_2$); 6.74 (d, 1H, J = 2.5 Hz, 4-H); 6.79 (dd, 1H, J = 8.5 Hz, J = 2.6 Hz, 2-H); 7.19 (d, 1H, J = 8.6 Hz, 1-H); 7.32 (t, 1H, J = 7.7 Hz, 4′-H); 7.38 (t, 2H, J = 7.7 Hz, 3′- and 5′-H); 7.43 (d, 2H, J = 7.7 Hz, 2′- and 6′-H). ^{13}C NMR (CDCl$_3$) δ ppm: 14.4 (C-18); 25.8 (CH$_2$); 26.0 (CH$_2$); 26.4 (CH$_2$); 29.6 (CH$_2$); 31.4 (CH$_2$); 38.3 (CH);

43.9 (CH); 44.4 (C-13); 48.2 (CH); 48.6 (C-13); 51.8 (C-16a); 70.0 (OCH$_2$); 112.4 (CH); 114.9 (CH); 126.3 (C-1); 127.4 (2C, 2× CH); 127.9 (CH); 128.5 (2C, 2× CH); 132.2 (C-10); 137.2 (C); 137.8 (C); 156.9 (C-3); 218.5 (C=O). MS *m/z* (%) 416 (100, [M+H]$^+$).

4.2. Cell CUlture and CHemicals

The utilized cell lines (HeLa, MDA-MB-231, MCF-7, and NIH/3T3) were obtained from ECACC (European Collection of Cell Cultures, Salisbury, UK), except for SiHa cells which were obtained from ATCC (American Tissue Culture Collection, Manassas, VA, USA). All cell lines were cultured in Eagle's Minimum Essential Medium (EMEM) at 37 °C in a humidified atmosphere with 5% carbon dioxide. The medium was supplemented with 10% fetal bovine serum (FBS), 1% non-essential amino acid solution, and 1% penicillin, streptomycin, and amphotericin B mixture. All cell culture mediums and supplements were obtained from Lonza Group Ltd. (Basel, Switzerland). Chemicals for the described in vitro experiments were purchased from Merck Ltd. (Budapest, Hungary) unless stated otherwise.

4.3. Determination of Antiproliferative Activity (MTT Assay)

The antiproliferative activity of the presented compounds were evaluated against a panel of human gynecological cancer cell lines. MCF-7 and MDA-MB-231 cell lines were derived from breast cancers, while HeLa and SiHa cell lines originated from cervical cancers of different pathological backgrounds. Non-cancerous human fibroblast cells (NIH/3T3) were used exclusively to assess cancer selectivity of the two azidomethyl compounds.

Cancer cells were seeded onto a 96-well microplate for the proliferation assay at a density of 5000 cells/well. After 24 h of incubation, 200 μL of new medium containing the test compounds at 10 or 30 μM concentrations was added.

Following incubation for 72 h at 37 °C in a humidified atmosphere containing 5% CO$_2$, cell viability was assessed by adding 20 μL of 5 mg/mL 3-(4,5-dimethylthiazol-2-yl)-2,5-diphenyltetrazolium bromide (MTT) solution. After 4 h of incubation, the yellow MTT solution was converted to violet crystals by mitochondrial reductases in viable cells. Subsequently, the medium was removed, and the formazan crystals were dissolved in 100 μL of DMSO with shaking at 37 °C for 60 min.

Absorbance of the reduced MTT solution was measured at 545 nm using a microplate reader, with untreated cells serving as the negative control [31]. In the case of active compounds (i.e., >50% cell growth inhibition at 10 μM), the assay was repeated with a series of dilutions, and sigmoidal dose–response curves were fitted to the obtained data. The IC$_{50}$ values, representing the concentration at which cell proliferation was reduced by 50% compared with the untreated control, were calculated using GraphPad Prism 5 (GraphPad Software, San Diego, CA, USA). Each in vitro experiment was conducted on two microplates with a minimum of five parallel wells. Stock solutions of the test substances (10 mM) were prepared in DMSO, with the highest DMSO concentration in the medium not exceeding 0.3%, which did not significantly affect cell proliferation. Cisplatin was used as a reference agent.

4.4. Propidium Iodide-Based Cell Cycle Analysis

Cell cycle analysis was conducted to investigate the mechanism of action of azidomethyl compounds in human breast cancer cell lines. Specifically, MDA-MB-231 cells were seeded onto 24-well plates at a density of 80,000 cells per well. The cells were treated with two concentrations of **16AABE** (0.5 or 1 μM) and **16BABE** (2 or 4 μM), respectively, for 24 h.

After treatment, the cells were washed with phosphate-buffered saline (PBS) and harvested using trypsin. The harvested cells were combined with the supernatants and PBS from the washing process. Subsequently, centrifugation at 1700 rpm for 5 min at room temperature was performed, followed by resuspending the cell pellets in a DNA staining solution. The DNA staining solution consisted of 10 μg/mL propidium iodide (PI), 0.1%

Triton-X, 10 µg/mL RNase A, and 0.1% sodium citrate dissolved in PBS. The resuspended cells were then incubated in dark at room temperature for 30 min.

At least 20,000 events per sample were analyzed using a FACSCalibur (BD Biosciences, Franklin Lakes, NJ, USA) flow cytometer to assess the DNA content. Data obtained were analyzed using the ModFit LT 3.3.11 software (Verity Software House, Topsham, ME, USA). Untreated cells served as the control, and the hypodiploid (subG1) phase indicated the apoptotic cell population [21].

4.5. Tubulin Polymerization Assay

Following the manufacturer's instructions, a tubulin polymerization assay kit (Cytoskeleton Inc., Denver, CO, USA) was employed to assess cell-independent direct effects of **16AABE** and **16BABE** on tubulin polymerization in vitro. Initially, 10 µL of a 500 µM solution of the desired compound was added to a UV-transparent microplate prewarmed to 37 °C. Positive control samples containing 10 µL of 10 µM paclitaxel, as well as untreated controls with general tubulin buffer (80 mM PIPES pH 6.9, 2 mM $MgCl_2$, 0.5 mM EGTA) were also prepared. Next, 100 µL of a 3.0 mg/mL tubulin solution dissolved in polymerization buffer (80 mM PIPES pH 6.9, 2 mM $MgCl_2$, 0.5 mM EGTA, 1 mM GTP, 10.2% glycerol) was added to each sample present in separate wells of a 96-well plate. The plate was immediately placed in an ultraviolet spectrophotometer (SPECTROstarNano, BMG Labtech, Ortenberg, Germany) prewarmed to 37 °C. A 60-min kinetic reaction was initiated, during which the absorbance was measured at 340 nm every minute to evaluate the effects of the test compounds. The tubulin polymerization curve was constructed by plotting the optical density against time. Maximum reaction rate (Vmax; Δabsorbance/min) was calculated based on the highest difference in absorbance observed over three consecutive time points on the kinetic curve.

4.6. Migration Assay

As previously described, MCF-7 cell suspension was prepared in a supplemented EMEM. The cells were then seeded onto 12-well plates using specialized silicone inserts (Ibidi GmbH, Grafelfing, Germany) at a concentration of 25,000 cells per well. The silicone inserts were gently removed after an overnight incubation, and the cells were washed with PBS. Subsequently, the cells were subjected to a wound healing assay by treating them with low concentrations of the test compounds (1.5 and 3 µM) prepared in EMEM medium with reduced serum content (2% FBS).

Antimigratory effect of the test compounds was assessed by measuring the size of cell-free areas. Images of the cell monolayer were captured at 0, 24, and 48 h using the QCapture Pro 6.0 software. Based on the captured images, the size of cell-free areas was determined using the ImageJ 1.53e software (National Institutes of Health, Bethesda, MD, USA).

4.7. Invasion Assay

To assess the impact of our test compounds on the invasion capacity of malignant MDA-MB-231 cells, we employed Boyden chambers equipped with a reconstituted membrane that mimics the basement membrane (BD Biosciences, Bedford, MA, USA). Treated cells were carefully pipetted onto the hydrated membranes in the upper chamber. In the lower chamber, EMEM supplemented with 10% FBS served as a chemoattractant. After a 24 h incubation period, the supernatants were removed, and non-invading cells on the upper side of the membrane were gently wiped using a cotton swab. The membrane was then rinsed twice with PBS and fixed with ice-cold 96% ethanol. Subsequently, invading cells were stained with 1% crystal violet dye solution for 30 min in the dark at room temperature. Multiple images (at least three per insert) were captured using a Nikon Eclipse TS100 microscope (Nikon Instruments Europe, Amstelveen, The Netherlands). Finally, invading cells were quantified and compared with untreated control samples.

4.8. Determination of Estrogenic Activity

T47D human breast adenocarcinoma cells expressing endogenous estrogen receptor (ERα), modified with an estrogen-responsive luciferase (Luc) reporter gene (T47D-KBluc, obtained from ATCC, Manassas, VA, USA) were used to assess the estrogenic activity of **16AABE** and **16BABE** [32]. Cells were maintained in phenol red-free MEM with 2 mM L-glutamine, 1 g/L glucose, 10% FBS and penicillin–streptomycin antibiotics. Before testing the compounds' effect, cells were maintained in the medium described above, supplemented with 10% charcoal dextran-treated FBS for at least six days. Cells were seeded onto a 96-well white flat bottom plate (Greiner Bio-One, Mosonmagyaróvár, Hungary) at a density of 50,000 per well in 200 μL of the medium above, and were allowed to attach for 72 h. Then the indicated concentrations of the test compounds or the reference agent 17β-estradiol were added (less than 0.1% DMSO in the final concentration). Plates were incubated at 37 °C in a humidified 5% CO_2 incubator before measuring luciferase activity. After 24 h of incubation, the dosing media was removed entirely, and 30 μL of One-Glo firefly luciferase reagent (Promega, Madison, WI, USA) per well was added to the plate, followed by incubation for 3 min at room temperature according to the manufacturer's protocol, and then the luminescence signal was quantified (FLUOstar Optima, BMG Labtech, Ortenberg, Germany).

4.9. Statistical Analysis

Statistical data analysis was conducted using the GraphPad Prism 5 software (GraphPad, San Diego, CA, USA). One-way analysis of variance (ANOVA) was employed, followed by the Dunnett post-test, to assess the significance of the observed differences. Data are expressed as mean values ± standard error of the mean (SEM).

5. Conclusions

In conclusion, our findings provide compelling experimental evidence to support the relevance of 16-azidomethyl-estrone analogs as potential drug candidates with anticancer properties. The observed tumor-selective antiproliferative and antimetastatic effects, combined with their ability to induce cell cycle disturbances and exhibit tumor selectivity, highlight the promising prospects of these compounds as innovative anticancer agents. Furthermore, their potent antimigratory and anti-invasive properties are exerted below their growth-inhibitory concentrations. The tested compounds substantially increased the polymerization of tubulin, which may be the basis of their actions. Since **16AABE** and **16BABE** possess estrogenic activity, their further development seems rational for treating hormone-independent malignancies.

References

1. Sung, H.; Ferlay, J.; Siegel, R.L.; Laversanne, M.; Soerjomataram, I.; Jemal, A.; Bray, F. Global Cancer Statistics 2020: GLOBOCAN Estimates of Incidence and Mortality Worldwide for 36 Cancers in 185 Countries. *CA Cancer J. Clin.* **2021**, *71*, 209–249. [CrossRef] [PubMed]
2. Azadnajafabad, S.; Saeedi Moghaddam, S.; Mohammadi, E.; Delazar, S.; Rashedi, S.; Baradaran, H.R.; Mansourian, M. Patterns of better breast cancer care in countries with higher human development index and healthcare expenditure: Insights from GLOBOCAN 2020. *Front. Public Health* **2023**, *11*, 1137286. [CrossRef] [PubMed]
3. Newman, D.J.; Cragg, G.M. Natural Products as Sources of New Drugs over the Nearly Four Decades from 01/1981 to 09/2019. *J. Nat. Prod.* **2020**, *83*, 770–803. [CrossRef] [PubMed]
4. AlQathama, A.; Shao, L.; Bader, A.; Khondkar, P.; Gibbons, S.; Prieto, J.M. Differential Antiproliferative and Anti-Migratory Activities of Ursolic Acid, 3-*O*-Acetylursolic Acid and Their Combination Treatments with Quercetin on Melanoma Cells. *Biomolecules* **2020**, *10*, 894. [CrossRef]
5. Bednarczyk-Cwynar, B.; Ruszkowski, P.; Bobkiewicz-Kozlowska, T.; Zaprutko, L. Oleanolic Acid A-lactams Inhibit the Growth of HeLa, KB, MCF-7 and Hep-G2 Cancer Cell Lines at Micromolar Concentrations. *Anticancer Agents Med. Chem.* **2016**, *16*, 579–592. [CrossRef]
6. Gheorgheosu, D.; Duicu, O.; Dehelean, C.; Soica, C.; Muntean, D. Betulinic acid as a potent and complex antitumor phytochemical: A minireview. *Anticancer Agents Med. Chem.* **2014**, *14*, 936–945. [CrossRef]
7. Liu, J.; Wu, N.; Ma, L.N.; Zhong, J.T.; Liu, G.; Zheng, L.H.; Lin, X.K. p38 MAPK signaling mediates mitochondrial apoptosis in cancer cells induced by oleanolic acid. *Asian Pac. J. Cancer Prev.* **2014**, *15*, 4519–4525. [CrossRef]
8. Sun, H.; Lv, C.; Yang, L.; Wang, Y.; Zhang, Q.; Yu, S.; Kong, H.; Wang, M.; Xie, J.; Zhang, C.; et al. Solanine induces mitochondria-mediated apoptosis in human pancreatic cancer cells. *BioMed Res. Int.* **2014**, *2014*, 805926. [CrossRef]
9. Wu, J.; Yang, C.; Guo, C.; Li, X.; Yang, N.; Zhao, L.; Hang, H.; Liu, S.; Chu, P.; Sun, Z.; et al. SZC015, a synthetic oleanolic acid derivative, induces both apoptosis and autophagy in MCF-7 breast cancer cells. *Chem. Biol. Interact.* **2016**, *244*, 94–104. [CrossRef]
10. Yang, S.J.; Liu, M.C.; Xiang, H.M.; Zhao, Q.; Xue, W.; Yang, S. Synthesis and in vitro antitumor evaluation of betulin acid ester derivatives as novel apoptosis inducers. *Eur. J. Med. Chem.* **2015**, *102*, 249–255. [CrossRef]
11. Mernyák, E.; Kovács, I.; Minorics, R.; Sere, P.; Czégány, D.; Sinka, I.; Wölfling, J.; Schneider, G.; Újfaludi, Z.; Boros, I.; et al. Synthesis of trans-16-triazolyl-13α-methyl-17-estradiol diastereomers and the effects of structural modifications on their in vitro antiproliferative activities. *J. Steroid Biochem. Mol. Biol.* **2015**, *150*, 123–134. [CrossRef]
12. Agarwal, D.S.; Sakhuja, R.; Beteck, R.M.; Legoabe, L.J. Steroid-triazole conjugates: A brief overview of synthesis and their application as anticancer agents. *Steroids* **2023**, *197*, 109258. [CrossRef]
13. Gomes, A.R.; Pires, A.S.; Roleira, F.M.F.; Tavares-da-Silva, E.J. The structural diversity and biological activity of steroid oximes. *Molecules* **2023**, *28*, 1690. [CrossRef] [PubMed]
14. Jurášek, M.; Černohorská, M.; Řehulka, J.; Spiwok, V.; Sulimenko, T.; Dráberová, E.; Darmostuk, M.; Gurská, S.; Frydrych, I.; Buriánová, R.; et al. Estradiol dimer inhibits tubulin polymerization and microtubule dynamics. *J. Steroid Biochem. Mol. Biol.* **2018**, *183*, 68–79. [CrossRef]
15. Jójárt, R.; Senobar Tahaei, S.A.; Trungel-Nagy, P.; Kele, Z.; Minorics, R.; Paragi, G.; Zupkó, I.; Mernyák, E. Synthesis and evaluation of anticancer activities of 2- or 4-substituted 3-(*N*-benzyltriazolylmethyl)-13α-oestrone derivatives. *J. Enzym. Inhib. Med. Chem.* **2021**, *36*, 58–67. [CrossRef] [PubMed]
16. Kiss, A.; Mernyak, E.; Wolfling, J.; Sinka, I.; Zupko, I.; Schneider, G. Stereoselective synthesis of the four 16-hydroxymethyl-3-methoxy- and 16-hydroxymethyl-3-benzyloxy-13α-estra-1,3,5(10)-trien-17-ol isomers and their antiproliferative activities. *Steroids* **2018**, *134*, 67–77. [CrossRef] [PubMed]
17. Kiss, A.; Wölfling, J.; Mernyák, E.; Frank, É.; Benke, Z.; Senobar Tahaei, S.A.; Zupkó, I.; Mahó, S.; Schneider, G. Stereocontrolled synthesis of the four possible 3-methoxy and 3-benzyloxy-16-triazolyl-methyl-estra-17-ol hybrids and their antiproliferative activities. *Steroids* **2019**, *152*, 108500. [CrossRef] [PubMed]
18. Sharma, J.D.; Khanna, S.; Ramchandani, S.; Kakoti, L.M.; Baruah, A.; Mamidala, V. Prevalence of Molecular Subtypes of Breast Carcinoma and Its Comparison between Two Different Age Groups: A Retrospective Study from a Tertiary Care Center of Northeast India. *South Asian J. Cancer* **2021**, *10*, 220–224. [CrossRef]
19. Li, Y.; Zhang, H.; Merkher, Y.; Chen, L.; Liu, N.; Leonov, S.; Chen, Y. Recent advances in therapeutic strategies for triple-negative breast cancer. *J. Hematol. Oncol.* **2022**, *15*, 121. [CrossRef]
20. Derakhshan, F.; Reis-Filho, J.S. Pathogenesis of Triple-Negative Breast Cancer. *Annu. Rev. Pathol.* **2022**, *17*, 181–204. [CrossRef]
21. Vermes, I.; Haanen, C.; Reutelingsperger, C. Flow cytometry of apoptotic cell death. *J. Immunol. Methods* **2000**, *243*, 167–190. [CrossRef] [PubMed]

22. Dumontet, C.; Jordan, M.A. Microtubule-binding agents: A dynamic field of cancer therapeutics. *Nat. Rev. Drug Discov.* **2010**, *9*, 790–803. [CrossRef] [PubMed]
23. Mehlen, P.; Puisieux, A. Metastasis: A question of life or death. *Nat. Rev. Cancer* **2006**, *6*, 449–458. [CrossRef] [PubMed]
24. Eger, A.; Mikulits, W. Models of epithelial–mesenchymal transition. *Drug Discov. Today Dis. Model.* **2005**, *2*, 57–63. [CrossRef]
25. Bhatla, N.; Berek, J.S.; Cuello Fredes, M.; Denny, L.A.; Grenman, S.; Karunaratne, K.; Kehoe, S.T.; Konishi, I.; Olawaiye, A.B.; Prat, J.; et al. Revised FIGO staging for carcinoma of the cervix uteri. *Int. J. Gynaecol. Obstet.* **2019**, *145*, 129–135. [CrossRef]
26. Franco, E.L.; Schlecht, N.F.; Saslow, D. The epidemiology of cervical cancer. *Cancer J.* **2003**, *9*, 348–359. [CrossRef]
27. Stolnicu, S.; Hoang, L.; Soslow, R.A. Recent advances in invasive adenocarcinoma of the cervix. *Virchows Arch.* **2019**, *475*, 537–549. [CrossRef]
28. Vandeperre, A.; Van Limbergen, E.; Leunen, K.; Moerman, P.; Amant, F.; Vergote, I. Para-aortic lymph node metastases in locally advanced cervical cancer: Comparison between surgical staging and imaging. *Gynecol. Oncol.* **2015**, *138*, 299–303. [CrossRef]
29. Ali, H.; Traj, P.; Szebeni, G.J.; Gémes, N.; Resch, V.; Paragi, G.; Mernyák, E.; Minorics, R.; Zupkó, I. Investigation of the antineoplastic effects of 2-(4-Chlorophenyl)-13α-estrone sulfamate against the HPV16-positive human invasive cervical carcinoma cell line SiHa. *Int. J. Mol. Sci.* **2023**, *24*, 6625. [CrossRef]
30. Cermak, V.; Dostal, V.; Jelinek, M.; Libusova, L.; Kovar, J.; Rosel, D.; Brabek, J. Microtubule-targeting agents and their impact on cancer treatment. *Eur. J. Cell Biol.* **2020**, *99*, 151075. [CrossRef]
31. Mosmann, T. Rapid colorimetric assay for cellular growth and survival: Application to proliferation and cytotoxicity assays. *J. Immunol. Methods* **1983**, *65*, 55–63. [CrossRef] [PubMed]
32. Wilson, V.S.; Bobseine, K.; Gray, L.E., Jr. Development and characterization of a cell line that stably expresses an estrogen-responsive luciferase reporter for the detection of estrogen receptor agonist and antagonists. *Toxicol. Sci.* **2004**, *81*, 69–77. [CrossRef] [PubMed]

II.

Taylor & Francis
Taylor & Francis Group

RESEARCH PAPER

OPEN ACCESS | Check for updates

Synthesis and evaluation of anticancer activities of 2- or 4-substituted 3-(*N*-benzyltriazolylmethyl)-13α-oestrone derivatives

Rebeka Jójárt[a]*, Seyyed Ashkan Senobar Tahaei[b]*, Péter Trungel-Nagy[a], Zoltán Kele[c], Renáta Minorics[b], Gábor Paragi[d], István Zupkó[b] and Erzsébet Mernyák[a]

[a]Department of Organic Chemistry, University of Szeged, Szeged, Hungary; [b]Department of Pharmacodynamics and Biopharmacy, University of Szeged, Szeged, Hungary; [c]Department of Medicinal Chemistry, University of Szeged, Szeged, Hungary; [d]MTA-SZTE Biomimetic Systems Research Group, University of Szeged, Szeged, Hungary

ABSTRACT

2- or 4-Substituted 3-*N*-benzyltriazolylmethyl-13α-oestrone derivatives were synthesised via bromination of ring A and subsequent microwave-assisted, Pd-catalysed C(sp^2)–P couplings. The antiproliferative activities of the newly synthesised brominated and phosphonated compounds against a panel of human cancer cell lines (A2780, MCF-7, MDA-MB 231) were investigated by means of MTT assays. The most potent compound, the 3-*N*-benzyltriazolylmethyl-4-bromo-13α-oestrone derivative exerted substantial selective cell growth-inhibitory activity against A2780 cell line with a submicromolar IC$_{50}$ value. Computational calculations reveal strong interactions of the 4-bromo derivative with both colchicine and taxoid binding sites of tubulin. Disturbance of tubulin function has been confirmed by photometric polymerisation assay.

1. Introduction

The development of anticancer agents is often based on synthetic modifications of endogenous compounds[1]. However, this approach might be limited by the retained original biological activity of the biomolecule. This happens in the case of antiproliferative drug candidates based on sex hormones. Certain oestrone derivatives efficiently suppress the growth of different tumour cells, but their retained oestrogenic behaviour limits their application. Nevertheless, directed chemical modifications of the estrane core may lead to the reduction of oestrogenic action. The inversion of configuration at C-13 or opening of ring D results in core-modified oestrone derivatives with complete loss of oestrogenic activity[2–5]. Accordingly, 13α-oestrone and D-secoestrone are promising scaffolds for the development of antitumoral oestrone derivatives lacking hormonal side effects. Literature reveals certain potent anticancer oestrone derivatives, but their mechanism of action is often unclarified[1]. There exist candidates acting via inhibition of oestrogen biosynthesis; however, the majority of this compound group target other objects, including transporter proteins or tubulin. Microtubules (MTs) consist of α- and β-tubulin heterodimers that play key role in cell division[6]. Drugs that interfere with tubulin polymerisation/depolymerisation dynamics might lead to suppression of the cell growth[7–9]. Drugs that target the MT might be divided into two groups. MT destabilising agents (MDAs) prevent polymerisation of tubulin and promote depolymerisation, whereas MT stabilising agents (MSAs) promote polymerisation of tubulin and stabilise the polymer, preventing depolymerisation. There exist six binding sites on tubulin polymer[7,10,11]. MSAs, in general, bind reversibly to the taxoid binding site. Several antitubulin agents targeting vinca alkaloid or taxane sites (TBS) have been approved by Food and Drug Administration (FDA), but their application is limited due to their inefficiency against multidrug resistant (MDR) cells. On the other hand, colchicine site-binding candidates (CBS) are often still active against MDR cells, too. Combrestatin A-4 (CA-4) is a colchicine site-binding nanomolar antitubulin agent, arresting the cells in metaphase. Moreover, it is assigned as a potent vascular disrupting agent. It is of note that certain CA-4 derivatives are in clinical trials as chemotherapeutic agents. X-ray crystal structures of tubulin show that there are three zones and a bridge in this binding site. The typical colchicine site-binding agent consists of two aryl rings and a bridge, which determine the relative orientation of the rings[11]. According to literature reports, replacement of methoxy groups with halogens and introduction of a triazole or tetrazole ring instead of an ethylene bridge might be a powerful strategy in the development of more effective antitubulin CA-4 derivatives (Figure 1)[12]. The triazole heterocycle is widely used in drug development according to its favourable characteristics. It might enhance the stability against metabolic degradation and the H-bonding ability. Additionally, this heterocyclic ring is an excellent mimetic of a peptide bond[13].

We have recently synthesised steroidal triazoles via the transformation of the phenolic OH group of the core-modified D-secoestrone scaffold[14]. 13α and 13β epimers of D-seco derivatives

Figure 1. Structures of combrestatin A-4 and its tetrazolyl derivative.

were used as starting compounds. The triazole moiety was introduced onto C-3-O via CuAAC reaction of 3-(prop-2-inyloxy) derivatives with benzyl azides. The evaluation of cell growth-inhibitory properties of 3-[(1-benzyl-1,2,3-triazol-4-yl)methoxy]-D-secoestrones against certain cervical, breast, and ovarian cancer cells was carried out. The determination of structure–activity relationship revealed that the antiproliferative effect greatly depends on both the orientation of the angular methyl group and the nature and size of the *para* substituent of the benzyl group. 13β Derivatives seemed to be generally more active, but a 13α compound displayed a substantial effect. The most potent compound displayed an IC$_{50}$ value in the low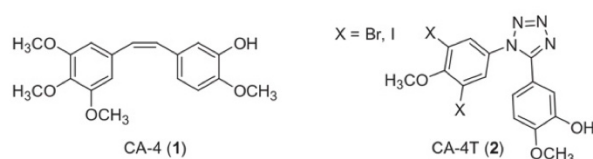 micromolar range. It was proved that the presence of the phenolic OH group is disadvantageous concerning the desired antiproliferative activity, but the introduction of a benzyl or, in particular, a 1-benzyl-1,2,3-triazol-4-yl moiety onto C-3-O leads to marked activity improvements. D-Secoestrone triazole **3** (Figure 2) was subjected to additional biological investigations in order to shed light on its mechanism of action[15]. The immunocytochemical flow cytometric analysis alluded to a cell cycle arrest at G2/M in HeLa cells with cell accumulation in the M phase. It was proved by an *in vitro* tubulin polymerisation assay that compound **3** significantly increases the maximum rate of microtubule formation. The antimigratory experiment showed that this triazole (**3**) inhibits the migration and invasion of HeLa cells. Based on these encouraging results, the 1-benzyl-1,2,3-triazol-4-yl moiety was introduced onto C-3-O of 13α-oestrone bearing an intact ring D[16]. Our concept was to improve the one-micromolar IC$_{50}$ value of the best D-secoestrone triazole by synthesising new compounds bearing the same structural element at C-3-O, but on the other promising, hormonally inactive 13α-oestrone scaffold. The most potent compound (**4a**) was that without any additional *para* substituent with IC$_{50}$ values in the submicromolar range. These results highlight the importance of 13α-oestrone as a scaffold and the 3-*N*-benzyltriazolylmethyl moiety as a key element in the development of potent oestrone-based antiproliferative agents lacking oestrogenic action.

In recent years, we turned our attention on the synthesis of novel 2- or 4-substituted 13α-oestrone derivatives. First ring A halogenations and then Pd-catalysed C–P cross-coupling reactions were carried out[17,18]. Hirao reaction is widely used for the synthesis of arylphosphonates from aryl halides[19]. Variations of the reaction have been described under traditional thermal conditions or microwave-irradiation[20–22]. Dialkyl phosphites are usually used as the reagents, Pd(PPh$_3$)$_4$ as the catalyst and Et$_3$N as the base. Our certain novel halo and phosphono 13α-oestrone derivatives displayed outstanding inhibitory activities against enzymes (steroid sulfatase, STS and 17β-hydroxysteroid dehydrogenase 1, 17β-HSD1) involved in oestrogen biosynthesis. Concerning oestrogen-dependent diseases, the suppression of local oestrogen production might serve as an effective therapy. This strategy might be intensified by the inhibition of polypeptides transporting organic anions (OATPs), which are able to transport oestrone-3-sulfate (E1S) into cells[23,24]. The desulphation of E1S and the stereospecific reduction of E1 result in E2 with a marked cell proliferative potential. Certain OATPs, known as E1S transporters, are overexpressed, among others, in breast and ovarian tumours. It is

of note that both 2-bromo- and 4-bromo-13α-oestrone derivatives (**5** and **6**, Figure 3), synthesised recently, exerted outstanding 17β-HSD1 inhibition (IC$_{50}$ = $\sim$ 1 μM). Compound **6**, however, displayed dual STS and 17β-HSD1 inhibition. Additionally, 3-hydroxy-2-phosphonate **7** proved to be dual 17β-HSD1 and OATP2B1 inhibitor with IC$_{50}$ values of 1–2 μM, whereas its 3-benzyloxy counterpart (**8**) exhibited selective OATP2B1 inhibition with IC$_{50}$ = 0.2 μM (Figure 3)[18].

Based on our above-mentioned structure–activity results obtained in antiproliferative, tubulin polymerisation and OATP2B1 transport assays, our aim in the present study was to combine the key structural elements (highlighted in blue, green, and red in Figures 2 and 3) to get potent antiproliferative compounds. Here we disclose the synthesis of 3-*N*-benzyltriazolylmethyl-13α-oestrone derivatives brominated or phosphonated at C-2 or C-4.

2. Results

2.1. Chemistry

The synthesis of 3-*N*-benzyltriazolylmethyl-13α-oestrone derivatives substituted at C-2 or C-4 was started with the propargylation of 13α-oestrone **9** (Scheme 1). The terminal alkyne function was introduced via our method established earlier[16] using propargyl bromide as the reagent. The resulting 3-(prop-2-inyloxy) compound (**10**) was subjected to CuAAC reaction with benzyl azides differing in their *para* substituent (R = H or *t*-Bu). The click reactions afforded the desired triazolyl derivatives (**4a** and **4b**) in high yields. The next transformation was the bromination of compounds **4a** and **4b**. Electrophilic substitutions were carried out with 1 equiv. of *N*-bromosuccinimide as a brominating agent. Halogenations occurred in *ortho* positions relative to the C-3-O function, yielding the two regioisomers in a ratio of **11**:**12** = 2:1. Bromo derivatives (**11a,b** or **12a,b**) were subjected to Pd-catalysed reactions with diethyl phosphite or diphenylphosphine oxide as coupling partners. Microwave-assisted Hirao couplings afforded new 2- or 4-phosphonated 3-*N*-benzyltriazolylmethyl-13α-oestrone derivatives (**13–15**) in excellent yields. The structures of the newly synthesised bromides and phosphonates (**11–15**) were deduced from ^{1}H and ^{13}C NMR spectra.

2.2. Antiproliferative activities

The new compounds (**11–15**) were evaluated for their cell growth-inhibitory action against an ovarian (A2780) and two breast (MCF-7 and MDA-MB-231) human adherent cancer cell lines. As a general tendency, ovarian cell line proved to be more sensitive for the tested agents than the utilised breast cancers. Certain newly synthesised derivatives exhibited substantial sub- or low-micromolar antiproliferative potentials (Table 1). Bromo derivatives (**11** and **12**) did not influence the growth of the tumour cells, except compound **12a**, which inhibited the proliferation of A2780 cells with a submicromolar IC$_{50}$ value. This test compound displayed substantially higher IC$_{50}$ values against the two other cell lines. Derivatives **13b** and **14a** proved to be the most potent in the phosphonate compound group with IC$_{50}$ values in the low micromolar range against all tested cell lines, which are comparable to those of reference agent cisplatin. Phosphonates exhibited a similar level of potency against MCF-7 and MDA-MB-231 cell lines. The only exception is compound **15 b**, which did not exert considerable growth inhibitory action against MDA-MB-231 cells. The cancer selectivity of compound **12a** was tested by means of the MTT assay using the non-cancerous mouse embryo fibroblast cell line NIH/3T3. The treatment with compound **12a** resulted in a
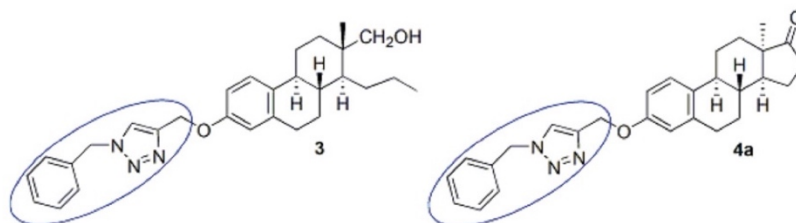
Figure 2. Structures of potent antiproliferative core-modified oestrone derivatives.
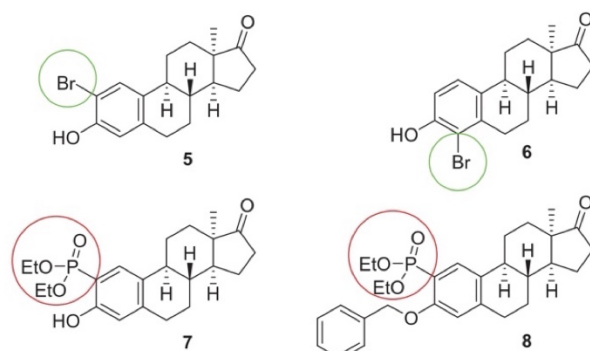

Figure 3. Structures of potent 17β-HSD1 and OATP2B1 inhibitors.

modest inhibition of cell growth (28.73 ± 1.26% and 37.94 ± 0.75% in 10 and 30 μM, respectively) indicating the cancer selective property of the determined antiproliferative action.

2.3. Tubulin polymerisation assay

Previously, D-secoestrone triazole (3) was proved to significantly increase maximum rate of tubulin polymerisation[15]. Based on structural similarity between compound 3 and the newly synthesised 12a owing the lowest IC$_{50}$ value against ovarian cancer cell line A2780, 12a was supposed to influence microtubule formation. To demonstrate our hypothesis, 12a was subjected to a cell-free, in vitro tubulin polymerisation assay in two different concentrations (125 and 250 μM). The calculated maximum rate of tubulin polymerisation was increased by our test compound which was significant when 12a was added in 250 μM concentration to the reaction mixture (Figure 4). Paclitaxel, the positive control agent recommended by the manufacturer, evoked a threefold increase in V_{max} (Figure 4).

2.4. Computational simulations

First, docking studies have been performed for the newly synthesised most potent antiproliferative compound 12a and for secosteroid 3 selected as a reference compound. Two potential binding sites, CBS and TBS, have been chosen on the tubulin polymer. MD investigations have been performed starting from the best docking poses of the compounds investigated. We found that the binding positions were stable for both compounds in both binding sites as they are presented by RMSD calculations for the ligands [see Figure S1(A–D) in Supplementary Materials]. Different MMGBSA binding energies collected in Table 2 clearly show that both compounds can bind to the regarded binding sites.

3. Discussion

3.1. Chemistry

The aim of the present work was to synthesise new 13α-oestrone derivatives as potent antiproliferative agents against human cancer cell lines of reproductive origin. Our strategy included the combination of structural elements of our promising antiproliferative or enzyme inhibitor compounds synthesised recently. Ring A was chosen as the subject for transformations and positions C-2, C-3, and C-4 were aimed to modify. Concerning the feasibility of the planned transformations, the order of the reaction steps seemed to be crucial. The activating behaviour of the phenolic OH group enables fast and effective bromination of the aromatic ring; however, the regio- and chemoselectivity is very low. To enhance the selectivity, first the 3-OH group was etherified. We have recently published that bromination of 3-O-methyl-13α-oestrone with 1 equiv. of NBS in dichloromethane results in a mixture of 2- and 4-bromo regioisomers in a ratio of 1:3[17]. Now we carried out the etherification of the phenolic OH group with a dual purpose: to get the two desired monobromo compounds regioselectively in the next step, and to introduce a terminal alkyne function onto C-3-O. We chose propargyl bromide as the reagent and performed the reaction under the conditions established earlier. The resulting phenolic ether (10) was suitable for the next bromination step, but the addition reactions on the terminal alkyne moiety had to be avoided. That is why we continued the sequence with the CuAAC reaction of the propargyl derivative (10) with two different benzyl azides (R = H or t-Bu). Azide reagents were selected based on the cell growth-inhibitory results of 3-N-benzyltriazolylmethyl-13α-oestrone derivatives synthesised and investigated earlier[16]. It has been established recently, that compound 4a displayed outstanding antiproliferative action against certain cancer cell lines; however, its para-t-Bu counterpart 4b did not influence cell growth markedly[16]. In this study, CuAAC reactions were performed using CuI as catalyst and PPh$_3$ as an accelerating phosphine ligand. The desired triazoles (4a and 4b) were formed in excellent yields. The CuAAC reactions were followed by the bromination of the 3-N-benzyltriazolylmethyl compounds (4a and 4b) with 1 equiv. of NBS in dichloromethane. Electrophilic brominations furnished the two ortho regioisomers in a ratio of 8:9 = 2:1 in high yields. Interestingly, regioselectivity of the bromination depends markedly on the nature and size of the C-3-O function. The difference in regioisomeric ratios compared to those of 3-O-Me derivatives might be explained by the steric hindrance of a more bulky 3-O substituent in 3-N-benzyltriazolylmethyl compounds 4a and 4b. In the last step, the 2- and 4-bromo regioisomers were subjected to Hirao couplings. In our earlier study, microwave-assisted conditions for the transformations of 2- and 4-bromo-3-O-mehyl and −3-O-benzyl derivatives involved 10 mol% Pd(PPh$_3$)$_4$ as a catalyst, 1.3 equiv. of phosphite or phosphine oxide, and 3 equiv. K$_2$CO$_3$ in toluene[18]. The reaction time and temperature depended on the nature of the 3-O
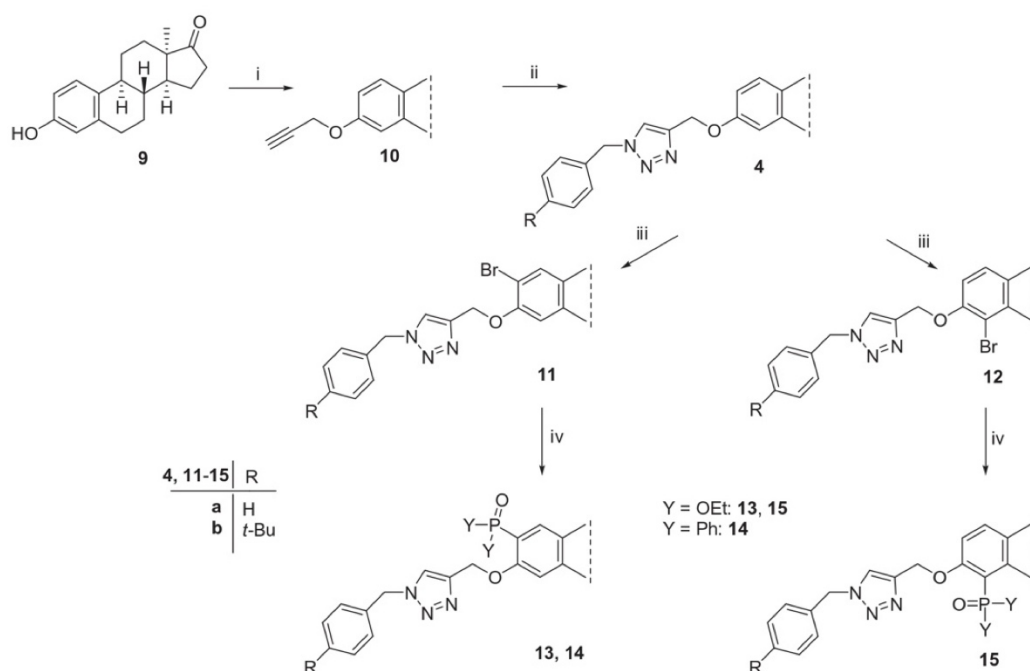
Scheme 1. Synthesis of 2-substituted 3-N-benzyltriazolylmethyl-13α-oestrone derivatives.

Table 1. Antiproliferative properties of the synthesised compounds

		Inhibition (%) ± SEM [calculated IC$_{50}$]^a		
Comp.	Conc. (µM)	A2780	MDA- MB-231	MCF-7
11a	10	44.87 ± 0.09	47.49 ± 1.21	29.06 ± 1.42
	30	52.00 ± 0.80 [21.51]	38.18 ± 2.78	36.49 ± 1.22
11b	10	30.18 ± 2.35	24.39 ± 2.20	–^{b}
	30	33.94 ± 2.70	23.92 ± 1.07	–
12a	10	93.16 ± 0.47	52.94 ± 1.32	41.98 ± 0.97
	30	95.43 ± 0.42 [0.55]	53.81 ± 2.43 [8.80]	52.50 ± 0.94 [12.69]
12b	10	46.93 ± 1.75	–	23.46 ± 1.03
	30	54.72 ± 0.70 [18.34]	–	29.19 ± 2.94
13a	10	29.53 ± 1.86	–	–
	30	90.85 ± 0.40 [13.52]	35.95 ± 3.17	43.54 ± 2.63
13b	10	95.61 ± 0.59	57.03 ± 2.58	73.99 ± 1.88
	30	99.73 ± 0.21 [2.95]	98.93 ± 0.20 [9.51]	95.52 ± 0.23 [6.59]
14a	10	95.97 ± 1.28	81.95 ± 2.49	66.93 ± 1.46
	30	98.06 ± 0.89 [4.87]	98.52 ± 0.10 [7.13]	92.52 ± 1.08 [8.38]
14b	10	85.52 ± 0.64	46.57 ± 1.21	77.87 ± 0.66
	30	95.82 ± 0.12 [5.07]	71.28 ± 1.23 [13.64]	90.69 ± 0.18 [7.16]
15a	10	79.93 ± 1.08	25.67 ± 1.76	42.44 ± 2.94
	30	99.50 ± 0.03 [5.91]	96.87 ± 0.28 [13.15]	91.04 ± 1.49 [11.39]
15b	10	46.25 ± 1.27	–	30.14 ± 1.53
	30	92.05 ± 0.86 [9.96]	34.79 ± 2.20	77.45 ± 1.56
Cisplatin		83.57 ± 1.21	67.51 ± 1.01	53.03 ± 2.29
		95.02 ± 0.28 [1.30]	87.75 ± 1.10 [3.70]	86.90 ± 1.24 [5.78]

^{a}Mean value from two independent measurements with five parallel wells; standard deviation <20%.
^{b}Inhibition values <20% are not presented.
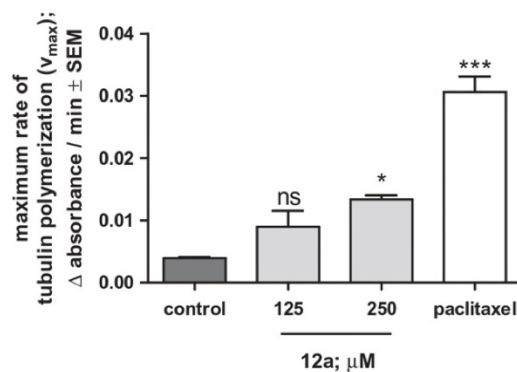
Figure 4. Effects of **12a** and 10 µM paclitaxel on the calculated maximum reaction rate (V_{max}) of *in vitro* microtubule formation. Control: untreated samples. The experiment was performed in two parallels and the measurements were repeated twice. Each bar denotes the mean ± SEM, $n = 4$. ns, * and ***indicate $p > 0.05$, $p < 0.05$ and $p < 0.001$, respectively, compared with the control values.

Table 2. MMGBSA binding energies (in kcal/mol) of compound **3** and **12a** in the CBS and TBS. Standard deviations of calculations are presented in parenthesis.

Compd.	CBS	TBS
3	−55.8 (8.3)	−58.8 (7.1)
12a	−63.3 (6.2)	−70.1 (6.5)

substituent. The transformations of 3-O-benzyl ethers required a more apolar solvent (toluene instead of acetonitrile) and harsher reaction conditions (150 °C, 30 min). Based on these experiences, we performed the present couplings in toluene at 150 °C, under microwave irradiation for 30 min. These conditions proved to be
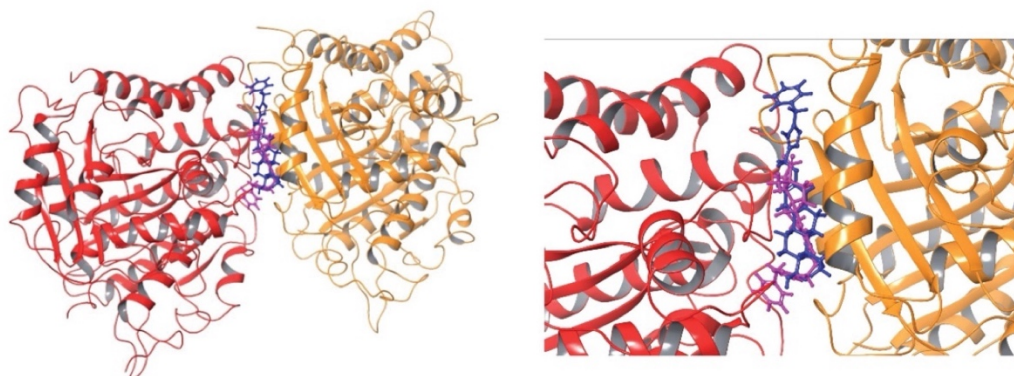
Figure 5. Best docking poses of compound **3** and **12a** in the CBS of tubulin dimer. The dark blue structure represents compound **3**, while purple marks compound **12a**.

excellent for the effective synthesis of the desired phosphonates (**13a,b**; **14a,b**, and **15a**), except for that of a 4-bromo derivative bearing a 4′-*t*-Bu substituent (**15b**). This coupling required longer irradiation (150 °C, 1 h), which might be attributed to steric factors.

3.2. Determination of the antiproliferative activities

We described earlier that triazole **4a** exerted outstanding inhibitory activities against A2780 and MCF-7 cell lines in the range of $IC_{50} = 0.5$–$0.6\,\mu M$. However, **4b**, its 4′-*t*-Bu counterpart did not have marked influence on the growth of the tested cell lines. Regarding the substantial difference in the antiproliferative potential of **4a** and **4b**, these two compounds have been selected for further transformations. Besides testing the newly synthesised compounds on A2780 (ovarian carcinoma) and MCF-7 (breast adenocarcinoma, expressing the oestrogen, progesterone, and androgen receptors), an additional cell line, the triple-negative breast carcinoma MDA-MB-231, was also included in our study. Based on the present results obtained for the phosphonates (Table 1), it can be stated, that this type of modification did not improve the high potency of parent compound **4a**. The cell growth-inhibitory potential of the phosphonates is far behind to that of unsubstituted **4a**. The low micromolar IC_{50} values of the phosphonates (**13b**, **14a,b**, and **15a**) reflect their moderate antiproliferative potential. Interestingly, phosphonates influenced the growth of A2780 cells most. Considering the two breast cancer cell lines with different receptorial status, no significant difference in growth-inhibitory activities have been observed. However, two compounds (**12a** and **14a**) proved to be more potent against the triple-negative MDA-MB-231 line. The presented pharmacological results are considered preliminary and, therefore, no conclusion can be made concerning the mechanism of the action. However, based on the comparison of the IC_{50} values obtained on the two breast cancer cell lines, a receptor-independent mechanism could be proposed. Results obtained for the 2-bromo compounds (**11a,b**) reveal that bromination at this position is disadvantageous concerning the antiproliferative potential against the tested cell lines. However, the other regioisomer without the 4′-*t*-Bu group (**12a**), proved to be highly potent with selective action against A2780 cells. The dependence of the cell growth-inhibitory potential on the regioisomerism is a very important structure–activity result.

Interestingly, the empirical rules established earlier proved to be valid for the bromo derivatives (**11a,b** and **12a,b**) as well. The presence of the 4′-*t*-Bu group on the newly introduced benzylic moiety was also detrimental.

The cancer selectivity of compound **12a** was tested by means of the MTT assay using the non-cancerous mouse embryo fibroblast cell line NIH/3T3. The growth inhibitory effect was found to be substantially lower than those against cancer cell lines. Since the inhibition of proliferation was less than 40% even at the highest concentration (30 μM), the IC_{50} value was not calculated but it is definitely above 30 μM. This kind of viability assay cannot be considered to be sufficient to declare a cancer-selective action. The huge difference in the determined antiproliferative properties may reflect a cell type-dependent action instead of a general toxic character indicating the relevance of the presented structure in lead-finding projects.

3.3. Tubulin polymerisation assay

Performing a 60-min-long tubulin polymerisation assay a direct effect of **12a** has been demonstrated on microtubule formation. The significant increase in V_{max} induced by our test compound is similar to the effects of other oestrone derivatives from D-secoalcohol[25] and D-secoestrone-triazole[15] series. However, another ring A substituted cytotoxic oestradiol analogue, 2-methoxyestradiol, has been reported to inhibit tubulin polymerisation[26]. This result is suitable for providing evidence about the final effect of our test compound on tubulin-microtubule system.

3.4. Computational simulations

We have demonstrated earlier that core-modified oestrone derivative **3** might be considered as an MSA. However, the majority of antitubulin oestrone derivatives described in literature belong to the MDA group, acting at the CBS of tubulin. From the comparison of the structures of the brominated combrestatine triazole **2** as an MDA and oestrone derivative **3**, it can be stated that they possess similar structural elements, such as the two aryl systems connected with a tetrazole or triazole bridge. It was shown by Beale et al. that the presence of bromines in compound **2** is advantageous concerning the antitubulin action. Interestingly, the two compounds belong to different MT targeting groups. Here we synthesised a new compound (**12a**) with structural similarity to both MT targeting agents **2** and **3**. Based on these structural
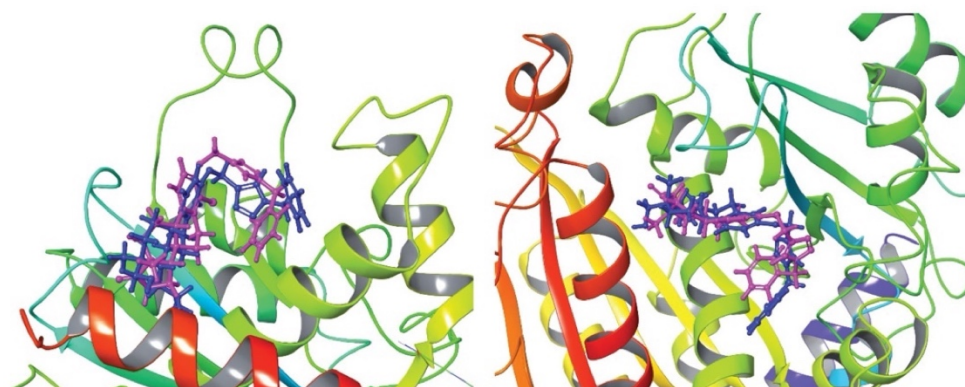
Figure 6. Best docking poses of compound **3** and **12a** in the TBS of tubulin monomer. The dark blue structure represents compound **3** while purple marks compound **12a**.

similarities and the substantial antiproliferative action of new derivative **12a**, here we performed computational studies to investigate the possible interaction of this compound with tubulin. Our selection, concerning the potential binding region of compound **12a** out of the known 6 possibilities[7,10] taking tubulin surface, was based on the following considerations. (i) Oestrone derivatives usually interact with tubulin at the CBS[11]. (ii) Ligands which promote polymerisation of tubulin usually bind to the TBS[7,8]. Because we did not have experimental evidence for the exact binding position of compound **12a**, both potential binding sites (CBS and TBS) were considered. Secosteroid **3** was selected as a reference compound and, altogether, four different complexes were investigated in the simulations. Molecular docking studies were performed first in order to get the best poses for the following MD calculations. In Figures 5 and 6, we represented the binding poses of ligands **3** and **12a** in CBS and TBS, respectively. The purple structure always represents compound **12a**, while secoestrone **3** is represented in dark blue. It is clear, that in the TBS both compounds **3** and **12a** adopted almost the same binding position, while in the CBS the estrane cores occupied a common region, but in a reverse manner. Consequently, the 3-*N*-benzyltriazolyl-methyl moiety oriented in an opposite way in the two cases.

Concerning binding preference order, SP docking score only helps to separate binding and non-binding molecules in a molecular pocket. However, it is not suitable to determine an accurate binding preference order; therefore, molecular dynamics (MD) calculations were performed. This allowed us to calculate binding energy at a more advanced level (MMGBSA method). Furthermore, calculations also provide information about the stability of the binding pose concerning the different ligand–protein complexes. It was established that the binding positions were stable in all four cases, even though the two compounds occupy the CBS in reversed manner (Table 2). Comparing binding energies at the same region, compound **12a** had always stronger interaction than compound **3**. Comparing binding energies at the different binding sites, compound **3** provided almost the same interaction energies in the two binding pockets, while compound **12a** had stronger interaction at the TBS. The strong interactions of compound **12a** indicate that the hormonally inactive 13α-estrane core with certain ring A modifications might be a suitable scaffold in the design of potent MT targeting agents. Concerning its possible dual binding (at CBS and at TBS), it might be a promising candidate in the development of antitubulin drugs targeting MDR cells, too.

4. Materials and methods

4.1. Chemistry

Melting points (Mp) were determined with a Kofler hot-stage apparatus and are uncorrected. Elemental analyses were performed with a Perkin-Elmer CHN analyser model 2400 (PerkinElmer, Waltham, MA). Thin-layer chromatography: silica gel 60 F254; layer thickness 0.2 mm (Merck); eluents (ss): A: 50% ethyl acetate/50% hexane, B: ethyl acetate, C: 2% methanol/98% ethyl acetate, detection with I_2 or UV (365 nm) after spraying with 5% phosphomolybdic acid in 50% aqueous phosphoric acid and heating at 100–120 °C for 10 min. Flash chromatography: silica gel 60, 40–63 μm (Merck, Kenilworth, NJ). Reactions under microwave irradiation were carried out with a CEM Corporation focussed microwave system, Model Discover SP. The maximum power of irradiation was 200 W. ^{1}H NMR spectra were recorded in DMSO-d_6, $CDCl_3$ solution with a Bruker DRX-500 instrument (Bruker, Billerica, MA) at 500 MHz, with Me_4Si as internal standard. ^{13}C NMR spectra were recorded with the same instrument at 125 MHz under the same conditions. Mass spectrometry: full scan mass spectra of the compounds were acquired in the range of 50–1000 m/z with a Finnigan TSQ-7000 triple quadrupole mass spectrometer (Finnigan-MAT, San Jose, CA) equipped with a Finnigan electrospray ionisation source. Analyses were performed in positive ion mode using flow injection mass spectrometry with a mobile phase of 50% aqueous acetonitrile containing 0.1 v/v% formic acid. The flow rate was 0.3 ml/min. Five μl aliquot of the samples were loaded into the flow. The ESI capillary was adjusted to 4.5 kV and N_2 was used as a nebuliser gas.

4.1.1. Synthesis of 3-(prop-2-inyloxy)-13α-estra-1,3,5(10)-triene (10)

3-Hydroxy-13α-estra-1,3,5(**10**)-trien-17-one (**1**, 540 mg, 2.0 mmol) was dissolved in acetone (15 ml), then propargyl bromide [0.34 ml (80 wt.% in toluene), 3.0 mmol], and K_2CO_3 (1.94 g, 14 mmol) were added. The reaction mixture was stirred at 70 °C for 24 h, the solvent was then evaporated off, and the residue was purified by flash chromatography with EtOAc/CH_2Cl_2 = 2/98 as eluent. Compound **7** was obtained as a white solid (610 mg, 98%), mp 133–134 °C, R_f = 0.70 (ss B); Anal calcd. for $C_{21}H_{24}O_2$: C, 81.78; H, 7.84. Found: C, 81.93; H, 7.64. ^{1}H NMR: δ ppm H 1.06 (s, 3H, H-18); 2.49 (s, 1H, C≡CH); 2.83 (m, 2H, H-6); 4.65 (s, 2H, OCH$_2$); 6.68 (s, 1H, H-4); 6.77 (d, $J = 8.5$ Hz, 1H, H-2); 7.19 (d, $J = 8.5$ Hz, 1H, H-1). Compound **7** is identical with the compound described in Ref. [16].

74

4.1.2. Synthesis of 3-[{1-benzyl-1H-1,2,3-triazol-4-yl}methoxy]- and 3-[{1-(4-tert-butylbenzyl)-1H-1,2,3-triazol-4-yl}methoxy]-13α-estra-1,3,5(10)-trien-17-one (4a and 4b)

To a stirred solution of 3-(prop-2-inyloxy)-13α-estra-1,3,5(10)-trien-17-one **7** (616 mg, 2.0 mmol) in toluene (8 ml), Ph₃P (52 mg, 0.2 mmol), CuI (19.0 mg, 0.1 mmol), DIPEA (1.04 ml, 6.0 mmol), and benzylazide or 4-*tert*-butyl-benzylazide (1 equiv.[16]) were added. The reaction mixtures were refluxed for 2 h, cooled to rt and evaporated *in vacuo*. The residues were purified by flash chromatography with EtOAc/CH₂Cl₂ = 5/95 as eluent. Compound **4a** was obtained as a white solid (862 mg, 97%), mp 164–165 °C, R_f = 0.35 (ss C); ¹H NMR: δ ppm 1.05 (s, 3H, H-18); 2.80 (m, 2H, H-6); 5.14 (s, 2H, OCH₂); 5.51 (s, 2H, NCH₂); 6.67 (s, 1H, H-4); 6.75 (dd, J = 8.5 Hz, J = 2.0 Hz, 1H, H-2); 7.16 (d, J = 8.5 Hz, 1H, H-1); 7.27 (m, 2H, H-2′, H-6′); 7.36 (m, 3H, H-3′, H-4′, H-5′); 7.50 (s, 1H, C=CH). Compound **4a** is identical with the compound described in Ref. [16].

Compound **4b** was obtained as a white solid (961 mg, 96%), mp 111–112 °C, R_f = 0.28 (ss C); ¹H NMR: δ ppm 1.05 (s, 3H, H-18); 1.31 (s, 3 × 3H, C(CH₃)3); 2.81 (m, 2H, H-6); 5.11 (s, 2H, OCH₂); 5.50 (s, 2H, NCH₂); 6.69 (s, 1H, H-4); 6.78 (m, 1H, H-2); 7.16–7.20 (overlapping multiplets, 3H, H-1, H-2′, H-6′); 7.39 (d, 2H, H-3′, H-5′); 7.55 (s, 1H, C=CH). Compound **4a** is identical with the compound described in Ref. [16].

4.1.3. General procedure for the bromination of triazoles 4a and 4b

Triazole **4a** or **4b** (442 mg or 498 mg, 1.00 mmol) was dissolved in dichloromethane (5 ml) and NBS (178 mg, 1.00 mmol) was added. The mixture was stirred at rt for 2.5 h, the solvent was then evaporated off and the crude product was purified by flash chromatography with EtOAc/hexane = 30/70 as eluent.

4.1.3.1. Synthesis of 3-[{1-benzyl-1H-1,2,3-triazol-4-yl}methoxy]-2-bromo-13α-estra-1,3,5(10)-trien-17-one (11a) and 3-[{1-benzyl-1H-1,2,3-triazol-4-yl}methoxy]-4-bromo-13α-estra-1,3,5(10)-trien-17-one (12a).

The first-eluting **12a** was obtained as a white solid (160 mg, 31%). Mp.: 188–190 °C. R_f = 0.66 (ss A). Anal calcd. for C₂₈H₃₀BrN₃O₂: C, 64.26; H, 5.81. Found: C, 64.34; H, 5.89. ¹H NMR (CDCl₃) δ ppm: 1.05 (s, 3H, H-18), 2.65 and 3.00 (2 × m, 2 × 1H, H-6), 5.24 (m, 2H, OCH₂), 5.52 (s, 2H, NCH₂), 6.87 (d, J = 8.6 Hz, 1H, H-2), 7.19 (d, J = 8.6, 1H, H-1), 7.27–7.28 (overlapping multiplets, 2H, H-2′ and H-6′), 7.34–7.37 (overlapping multiplets, 3H, H-3′, H-4′ and H-6′), 7.58 (s, 1H, C = CH). ¹³C NMR (CDCl₃) δ ppm: 21.0 (CH₂), 25.0 (C-18), 28.3 (CH₂), 28.4 (CH₂), 31.6 (CH₂), 31.9 (CH₂), 33.4 (CH₂), 40.6 (CH), 41.7 (CH), 49.0 (CH), 50.0 (C-13), 54.2 (NCH₂), 63.7 (OCH₂), 111.4 (C-2), 115.2 (C-4), 122.7 (C = CH), 125.5 (C-1), 128.0 (2 C, C-3′ and C-5′), 128.8 (C-4′), 129.1 (2 C, C-2′ and C-6′), 134.5 (C-1′), 134.9 (C-10), 137.9 (C-5), 144.7 (C = CH),152.6 (C-3), 221.4 (C-17). MS: [M + H]⁺ (79/81Br) 519 and 521.

The next-eluting **11a** was obtained as a white solid (319 mg, 61%). Mp.: 151–154 °C. R_f = 0.54 (ss A). Anal calcd. for C₂₈H₃₀BrN₃O₂: C, 64.26; H, 5.81. Found: 64.36; H, 5.88. ¹H NMR (CDCl₃) δ ppm: 1.05 (s, 3H, H-18), 2.70–2.82 (overlapping multiplets, 2H, H-6), 5.26 (m, 2H, OCH₂), 5.55 (s, 2H, NCH₂), 6.72 (s, 1H, H-4), 7.27–7.29 (overlapping multiplets, 2H, H-2′, and H-6′), 7.38–7.39 (overlapping multiplets, 3H, H-3′, H-4′, H-6′), 7.66 (s, 1H, C = CH). ¹³C NMR (CDCl₃) δ ppm: 20.9 (CH₂), 25.0 (C-18), 28.0 (CH₂), 28.2 (CH₂), 30.0 (CH₂), 31.9 (CH₂), 33.4 (CH₂), 41.1 (CH), 41.3 (CH), 49.1 (CH), 50.1 (C-13), 54.8 (NCH₂), 63.1 (OCH₂), 109.4 (C-2), 114.3 (C-4), 123.2 (C=CH), 128.2 (2 C, C-3′, and C-5′), 129.1 (C-4′), 129.2 (2 C, C-2′, and C-6′), 130.8 (C-1), 133.8 (C-10), 134.7 (C-1′), 137.6 (C-5),

144.1 (C=CH), 152.1 (C-3), 221.4 (C-17). MS m/z (%): MS: [M + H]⁺ (79/81Br) 519 and 521.

4.1.3.2. Synthesis of 2-bromo-3-[{1-(4-tert-butylbenzyl)-1H-1,2,3-triazol-4-yl}methoxy]-13α-estra-1,3,5(10)-trien-17-one (11b) and 4-bromo-3-[{1-(4-tert-butylbenzyl)-1H-1,2,3-triazol-4-yl}methoxy]-13α-estra-1,3,5(10)-trien-17-one (12b).

The first-eluting **12b** was obtained as a white solid (98 mg, 17%). Mp.: 178–180 °C. R_f = 0.71 (ss A). Anal calcd. for C₃₂H₃₈BrN₃O₂: C, 66.66; H, 6.64. Found: 66.73; H, 6.72. ¹H NMR (CDCl₃) δ ppm: 1.05 (s, 3H, H-18), 1.31 (s, 9H, 4′-C(CH₃)₃), 2.65 and 3.00 (2 × m, 2 × 1H, H-6), OCH₂), 5.49 (s, 2H, NCH₂), 6.87 (d, J = 8.7 Hz, H-2), 7.18 (d, J = 8.7 Hz, 1H, H-1), 7.20 (d, J = 8.4 Hz, 2H, H-2′, and H-6′), 7.38 (d, J = 8.4 Hz, 2H, H-3′, and H-5′), 7.58 (s, 1H, C=CH). ¹³C NMR (CDCl₃) δ ppm: 21.0 (CH₂), 25.0 (C-18), 28.3 (CH₂), 28.4 (CH₂), 31.2 (3 C, 4′-C(CH₃)₃), 31.6 (CH₂), 31.9 (CH₂), 33.4 (CH₂), 34.6 (4′-C(CH₃)₃), 40.6 (CH), 41.7 (CH), 49.0 (CH), 50.0 (C-13), 53.9 (NCH₂), 63.6 (OCH₂), 111.4 (C-2), 115.2 (C-4), 122.6 (C=CH), 125.5 (C-1), 126.0 (2 C, C-3′, and C-5′), 127.8 (2 C, C-2′, and C-6′), 131.5 (C-10), 134.9 (C-1′), 137.9 (C-5), 144.6 (C=CH), 151.9 and 152.6 (2 C, C-3, and C-4′), 221.4 (C-17). MS: [M + H]⁺ (79/81Br) 575 and 577. Continued elution yielded first a mixture of **12b** (80 mg, 14%) and **11b** (140 mg, 24%), and then compound **11b** (218 mg, 38%) as a white solid. Mp.: 148–150 °C. R_f = 0.62 (ss A). Anal calcd. for C₃₂H₃₈BrN₃O₂: C, 66.66; H, 6.64. Found: 64.72; H, 6.72. ¹H NMR (CDCl₃) δ ppm: 1.05 (s, 3H, H-18), 1.37 (s, 9H, 4′-C(CH₃)₃), 2.70–2.82 (overlapping multiplets 2H, H-6), 5.22 (m, 2H, OCH₂), 5.49 (s, 2H, NCH₂), 6.74 (s, 1H, H-4), 7.20 (d, J = 8.4 Hz, 2H, H-2′, and H-6′), 7.37–7.39 (overlapping multiplets, 3H, H-3′, H-5′, and H-1), 7.58 (s, 1H, C = CH). ¹³C NMR (CDCl₃) δ ppm: 20.9 (CH₂), 25.0 (C-18), 28.0 (CH₂), 28.2 (CH₂), 31.2 (4′-C(CH₃)₃), 31.9 (CH₂), 33.4 (C), 34.6 (4′-C(CH₃)₃), 41.1 (CH), 41.3 (CH), 49.1 (CH), 50.0 (C-13), 53.9 (NCH₂), 63.7 (OCH₂), 109.5 (C-2), 114.3 (C-4), 122.6 (C=CH), 126.0 (2 C, C-3′, and C-5′), 127.8 (2 C, C-2′, and C-6′), 130.7 (C-1), 131.4 (C-10), 134.4 (C-1′), 137.4 (C-5), 144.6 (C=CH), 151.9 and 152.4 (2 C, C-3, and C-4′), 221.3 (C-17). MS: [M + H]⁺ (79/81Br) 575 and 577.

4.1.4. General procedure for Hirao coupling of brominated triazoles (11a,b and 12a,b)

2- or 4-Bromo triazoles (**11a,b** or **12a,b**; 260 mg or 288 mg, 0.50 mmol), tetrakis(triphenylphosphine)palladium(0) (57.8 mg, 0.050 mmol, 10 mol%), potassium carbonate (104 mg, 0.75 mmol, 1.5 equiv.), diethyl phosphite (0.50 mmol, 69 mg) or diphenylphosphine oxide (0.50 mmol, 101 mg), and acetonitrile or toluene (5 ml) were added into a 10 ml Pyrex pressure vessel (CEM, Part #: 908035) with silicone cap (CEM, Part #: 909210). The mixture was irradiated in a CEM microwave reactor at 150 °C 30–60 min under stirring. The solvent was evaporated *in vacuo* and the residue was purified by flash chromatography.

4.1.4.1. Synthesis of (3-[{1-benzyl-1H-1,2,3-triazol-4-yl}methoxy]-13α-estra-1,3,5(10)-trien-17-on-2-yl)-diethylphosphonate.

The residue was purified by flash chromatography with MeOH/EtOAc = 2/98 as eluent. Compound **13a** was isolated as a white solid (84%). Mp.: 75–80 °C. R_f = 0.31 (ss B). Anal calcd. for C₃₂H₄₀N₃O₅P: C, 66.54; H, 6.98. Found: 66.62; H, 7.07. ¹H NMR (CDCl₃) δ ppm: 1.05 (s, 3H, H-18), 1.16 (t, J = 7.1 Hz, 6H, 2 × OCH₂CH₃), 2.85 (m, 2H, H-6), 3.93–4.03 (overlapping multiplets, 4H, 2 × OCH₂CH₃), 5.25 (m, 2H, OCH₂), 5.53 (s, 2H, NCH₂), 6.73 (d, J = 6.8 Hz, 1H, H-4), 7.27 (m. 2H, H-2′, and H-6′), 7.39 (overlapping multiplets, 3H, H-3′, H-4′and H-5′), 7.66 (d, J = 15.7 Hz, H-1), 7.83 (s, 1H, C=CH). ¹³C NMR

(CDCl$_3$) δ ppm: 16.3 (d, $J = 6.3$ Hz, 2 C: 2 × OCH$_2$CH$_3$), 20.9 (CH$_2$), 25.0 (C-18), 27.8 (CH$_2$), 28.2 (CH$_2$), 30.6 (CH$_2$), 31.8 (CH$_2$), 33.3 (CH$_2$), 41.2 (CH), 41.3 (CH), 49.1 (CH), 50.1 (C-13), 54.3 (NCH$_2$), 61.9 (2 C, 2 × OCH$_2$CH$_3$), 63.1 (OCH$_2$), 112.8 (d, $J = 9.9$ Hz, C-4), 114.1 (d, $J = 188.9$ Hz, C-2), 123.1 (C=CH), 128.1 (2 C, C-3′, and C-5′), 128.7 (C-4′), 129.1 (2 C, C-2′, and C-6′), 132.6 (d, $J = 13.8$ Hz, C-10), 132.8 (d, $J = 8.1$ Hz, C-1), 134.5 (C-1′), 144.0 (2 C, C-5, and C=CH), 157.4 (C-3), 221.4 (C-17). ^{31}P NMR δ ppm: 17.8. MS m/z (%): 578 (100, [M + H]$^+$).

4.1.4.2. Synthesis of (3-[{1–(4-tert-butylbenzyl)-1H-1,2,3-triazol-4-yl}methoxy]-13α-estra-1,3,5(10)-trien-17-on-2-yl)-diethylphosphonate.
The residue was purified by flash chromatography with MeOH/EtOAc = 2/98 as eluent. Compound **13b** was isolated as a colourless oil (83%). R$_f$=0.55 (ss B). Anal calcd. for C$_{36}$H$_{48}$N$_3$O$_5$P: C, 68.23; H, 7.63. Found: 68.31; H, 7.72. ^{1}H NMR (CDCl3) δ ppm: 1.05 (s, 3H, H-18), 1.15 (t, $J = 7.1$ Hz, 6H, 2 × OCH$_2$CH$_3$), 1.29 (s, 9H, 4′-C(CH$_3$)$_3$), 2.85 (m, 2H, H-6), 3.92–4.03 (overlapping multiplets, 4H, 2 × OCH$_2$CH$_3$), 5.23 (m, 2H, OCH$_2$), 5.48 (s, 2H, NCH$_2$), 6.73 (d, $J = 6.9$ Hz, 1H, H-4), 7.21 (d, $J = 8.4$ Hz, 2H, H-2′, and H-6′), 7.37 (d, $J = 8.4$ Hz, 2H, H-3′, and H-5′), 7.67 (d, $J = 15.7$ Hz, 1H, H-1), 7.77 (s, 1H, C=CH). ^{13}C NMR (CDCl$_3$) δ (ppm): 16.3 (d, $J = 6.6$ Hz, 2 C, 2 × OCH$_2$CH$_3$), 20.9 (CH$_2$), 25.0 (C-18), 27.8 (CH$_2$), 28.2 (CH$_2$), 30.6 (CH$_2$), 31.2 (3 C, 4′-C(CH$_3$)$_3$), 31.9 (CH$_2$), 33.3 (CH$_2$), 34.6 (4′-C(CH$_3$)$_3$), 41.2 (CH), 41.3 (CH), 49.1 (CH), 50.0 (C-13), 53.9 (NCH$_2$), 61.8 (2 C, 2 × OCH$_2$CH$_3$), 63.2 (OCH$_2$), 112.7 (d, $J = 9.8$ Hz, C-4), 114.1 (d, $J = 189.4$ Hz, C-2), 122.8 (C=CH), 125.9 (2 C, C-3′, and C-5′), 127.8 (2 C, C-2′, and C-6′), 131.6 (C-1′), 132.6 (d, $J = 14.1$ Hz, C-10), 132.9 (d, $J = 7.9$ Hz, C-1), 143.9 and 144.9 (2 C, C-5, and C=CH), 151.8 (C-4′), 157.5 (C-3), 221.3 (C-17). ^{31}P NMR δ ppm 17.8. MS m/z (%): 634 (100, [M + H]$^+$).

4.1.4.3. Synthesis of (3-[{1-benzyl-1H-1,2,3-triazol-4-yl}methoxy]-13α-estra-1,3,5(10)-trien-17-on-2-yl)diphenylphosphine oxide.
The residue was purified by flash chromatography with MeOH/EtOAc = 2/98 as eluent. Compound **14a** was isolated as a white solid (79%). Mp.: 117–120 °C. R$_f$=0.28 (ss C). Anal calcd. for C$_{40}$H$_{40}$N$_3$O$_3$P: C, 74.86; H, 6.28. Found: 74.93; H, 6.33. ^{1}H NMR (CDCl$_3$) δ ppm: 1.03 (s, 3H, H-18), 2.87 (m, 2H, H-6), 5.00 (m, 2H, OCH$_2$), 5.38 (s, 2H, NCH$_2$), 6.72–6.73 (overlapping multiplets, 2H), 7.15–7.17 (overlapping multiplets, 2H), 7.24–7.30 (m, 2H), 7.34–7.41 (overlapping multiplets, 6H), 7.55–7.63 (overlapping multiplets, 6H). ^{13}C NMR (CDCl$_3$) δ ppm: 20.9 (CH$_2$), 25.0 (C-18), 27.9 (CH$_2$), 28.1 (CH$_2$), 30.7 (CH$_2$), 31.8 (CH$_2$), 33.4 (CH$_2$), 41.3 (CH), 41.5 (CH), 49.2 (CH), 50.1 (C-13), 54.0 (NCH$_2$), 62.5 (OCH$_2$), 112.4 (d, $J = 6.9$ Hz, C-4), 117.6 (d, $J = 105.5$ Hz, C-2), 122.6 (C=CH), 127.9 (2 C, C-3′, and C-5′), 128.0–128.2 (overlapping multiplets, 4 C), 128.7 (C-4′), 129.1 (2 C, C-2′, and C-6′), 131.3 (m, 2 C, C-4″ and C-4‴), 131.6–131.8 (overlapping multiplets, 4 C), 132.6 (C), 132.9 (d, $J = 7.5$ Hz, C-1), 133.0 (C), 133.5 (C), 134.7 (C), 143.9 (C), 144.1 (C), 157.1 (C-3), 221.2 (C-17). ^{31}P NMR δ ppm: 27.2. MS m/z (%): 642 (100, [M + H]$^+$).

4.1.4.4. Synthesis of (3-[{1–(4-tert-butylbenzyl)-1H-1,2,3-triazol-4-yl}methoxy]-13α-estra-1,3,5(10)-trien-17-on-2-yl)diphenylphosphine oxide.
The residue was purified by flash chromatography with MeOH/EtOAc = 2/98 as an eluent. Compound **14b** was isolated as a white solid (73%). Mp.: 205–208 °C. R$_f$=0.42 (ss C). Anal calcd. for C$_{44}$H$_{48}$N$_3$O$_3$P: C, 75.73; H, 6.93. Found: 75.79; H, 6.99. ^{1}H NMR (CDCl$_3$) δ ppm: 1.03 (s, 3H, H-18), 1.31 (s, 9H, 4′-C(CH$_3$)$_3$), 2.87 (m, 2H, H-6), 5.00 (d, $J = 4.0$ Hz, 2H, OCH$_2$), 5.38 (s, 2H, NCH$_2$), 6.61 (s, 1H, C=CH), 6.71 (d, $J = 5.5$ Hz, 1H, H-4), 7.09 (d, 2H), 7.21 (m,

2H), 7.27 (m, 2H), 7.33–7.40 (overlapping multiplets, 4H), 7.54–7.62 (overlapping multiplets, 4H), 7.64 (d, $J = 14.2$ Hz, 1H, H-1). ^{13}C NMR (CDCl$_3$) δ ppm: 20.9 (CH$_2$), 25.0 (C-18), 27.9 (CH$_2$), 28.1 (CH$_2$), 30.7 (CH$_2$), 31.2 (3 C, 4′-C(CH$_3$)$_3$), 31.8 (CH$_2$), 33.4 (CH$_2$), 34.6 (4′-C(CH$_3$)$_3$), 41.3 (CH), 41.4 (CH), 49.1 (CH), 50.1 (C-13), 53.7 (NCH$_2$), 62.3 (OCH$_2$), 112.2 (d, $J = 7.1$ Hz, C-4), 117.5 (d, $J = 105.6$ Hz, C-2), 122.4 (C=CH), 125.9 (2 C, C-3′, and C-5′), 127.7 (2 C, C-2′, and C-6′), 127.9–128.1 (overlapping multiplets, 4 C), 131.2 and 131.3 (C-4″ and C-4‴), 131.6–131.8 (overlapping multiplets, 4 C), 131.6–134.0 (overlapping multiplets, 4 C), 132.9 (d, $J = 7.6$ Hz, C-1), 143.9 and 144.0 (C-5 and C=CH), 151.9 (C-4′), 156.9 (d, $J = 3.0$ Hz, C-3), 221.4 (C-17). ^{31}P NMR δ ppm: 26.9. MS m/z (%): 698 (100, [M + H]$^+$).

4.1.4.5. Synthesis of (3-[{1-benzyl-1H-1,2,3-triazol-4-yl}methoxy]-13α-estra-1,3,5(10)-trien-17-on-4-yl)-diethylphosphonate.
The residue was purified by flash chromatography with MeOH/EtOAc = 2/98 as an eluent. Compound **15a** was isolated as a white solid (72%). Mp.: 43–45 °C. R$_f$=0.45 (ss B). Anal calcd. for C$_{32}$H$_{40}$N$_3$O$_5$P: C, 66.54; H, 6.98. Found: C, 66.62; H, 7.07. ^{1}H NMR (CDCl$_3$) δ (ppm): 1.05 (s, 3H, H-18), 1.13 (t, $J = 7.2$ Hz, 6H, 2 × OCH$_2$CH$_3$), 3.26 (m, 2H, H-6), 3.88–4.01 (overlapping multiplets, 4H, 2 × OCH$_2$CH$_3$), 5.21 (d, $J = 3.8$ Hz, 2H, OCH$_2$), 5.53 (s, 2H, NCH$_2$), 6.87 (dd, $J = 6.7$ Hz, $J = 8.4$ Hz, 1H, H-2), 7.26–7.28 (m, 2H, H-2′, and H-6′), 7.33–7.38 (overlapping multiplets, 2H, H-3′, H-4′, H-5′, and H-1), 7.72 (s, 1H, C=CH). ^{13}C NMR (CDCl$_3$) δ (ppm): 16.2 (2 C, 2 × OCH$_2$CH$_3$), 20.9 (CH$_2$), 24.9 (C-18), 28.2 (CH$_2$), 29.3 (CH$_2$), 32.0 (CH$_2$), 33.3 (CH$_2$), 40.3 (CH), 41.7 (CH), 49.5 (CH), 50.1 (C-13), 54.2 (NCH$_2$), 61.3 (d, $J = 5.2$ Hz, OCH$_2$CH$_3$), 61.4 (d, $J = 5.2$ Hz, OCH$_2$CH$_3$), 63.7 (OCH$_2$), 110.9 (d, $J = 10.1$ Hz, C-2), 115.1 (d, $J = 182.0$ Hz, C-4), 122.8 (C=CH), 128.1 (2 C, C-3′, and C-5′), 128.7 (C-4′), 129.1 (2 C, C-2′, and C-6′), 131.5 (C-1), 134.4 (d, $J = 14.0$ Hz, C-10), 134.6 (C-1′), 144.8 (d, $J = 10.0$ Hz, C-5), 144.8 (C=CH), 145.0 (C), 159.0 (C-3), 221.6 (C-17). ^{31}P NMR δ (ppm): 18.2. MS m/z (%): 578 (100, [M + H]$^+$).

4.1.4.6. Synthesis of (3-[{1–(4-tert-butylbenzyl)-1H-1,2,3-triazol-4-yl}methoxy]-13α-estra-1,3,5(10)-trien-17-on-4-yl)-diethylphosphonate.
The residue was purified by flash chromatography with EtOAc as an eluent. Compound **15b** was obtained as a white solid (70%). Mp.: 54–59 °C. R$_f$=0.51 (ss B). Anal calcd. for C$_{36}$H$_{48}$N$_3$O$_5$P: C, 68.26; H, 7.63. Found: C, 68.34; H, 7.69. ^{1}H NMR (CDCl$_3$) δ (ppm) 1.05 (s, 3H, H-18), 1.11 (t, $J = 7.1$ Hz, 6H, 2 × OCH$_2$CH$_3$), 1.29 (s, 9H, 4′-C(CH$_3$)$_3$), 3.25 (m, 2H, H-6), 3.88–4.01 (overlapping multiplets, 4H, 2 × OCH$_2$CH$_3$), 5.20 (d, $J = 3.9$ Hz, 2H, OCH$_2$), 5.49 (s, 2H, NCH$_2$), 6.87 (dd, $J = 6.6$ Hz, $J = 8.6$ Hz, 1H, 2-H), 7.21 (d, $J = 8.2$ Hz, 2H, H-3′, and H-5′), 7.37 (overlapping multiplets, 3H, H-2′, H-6′, and H-1), 7.71 (s, 1H, C=CH). ^{13}C NMR (CDCl$_3$) δ (ppm): 16.2 (d, $J = 6.6$ Hz, 2 C, 2 × OCH$_2$CH$_3$), 20.9 (CH$_2$), 24.9 (C-18), 28.1 (CH$_2$), 28.6 (CH$_2$), 29.3 (CH$_2$), 31.2 (3 C, 4′-C(CH$_3$)$_3$), 31.9 (CH$_2$), 33.3 (CH$_2$), 34.6 (4′-C(CH$_3$)$_3$), 40.3 (CH), 41.7 (CH), 49.4 (CH), 50.1 (C-13), 53.9 (NCH$_2$), 61.2 (d, $J = 5.4$ Hz, OCH$_2$CH$_3$), 61.4 (d, $J = 5.4$ Hz, OCH$_2$CH$_3$), 63.6 (OCH$_2$), 110.8 (d, $J = 9.9$ Hz, C-2), 114.9 (d, $J = 182.5$ Hz, C-4), 122.7 (C=CH), 126.0 (2 C, C-3′, and C-5′), 127.9 (2 C, C-2′, and C-6′), 131.4 (d, $J = 1.8$ Hz, C-1), 131.5 (C-1′), 134.4 (d, $J = 14.4$ Hz, C-10), 144.7 and 144.8 (C=CH and C-5), 151.9 (C-4′), 158.9 (C-3), 221.6 (C-17). ^{31}P NMR δ (ppm): 18.2. MS m/z (%): 634 (100, [M + H]$^+$).

4.2. Determination of antiproliferative activities

The antiproliferative properties of the newly synthesised triazoles (**11a,b–15a,b**) were determined on a panel of human adherent cancer cell lines of gynaecological origin. MCF-7 and MDA-MB-231

were isolated from breast cancers differing in biochemical background, while A2780 cells were isolated from ovarian cancer. The cancer selectivity of compound **12a** was tested on the non-cancerous mouse embryo fibroblast cell line NIH/3T3. All cell lines were purchased from European Collection of Cell Cultures (ECCAC, Salisbury, UK). Cells were cultivated in minimal essential medium supplemented with 10% foetal bovine serum, 1% non-essential amino acids and an antibiotic–antimycotic mixture. All media and supplements were obtained from Lonza Group Ltd., Basel, Switzerland. Near-confluent cancer cells were seeded onto a 96-well microplate (5000 cells/well) and, after overnight standing, 200 μL new medium, containing the tested compounds at 10 and 30 μM, was added. After incubation for 72 h at 37 °C in humidified air containing 5% CO_2, the living cells were assayed by the addition of 20 μL of 5 mg/ml 3-(4,5-dimethylthiazol-2-yl)-2,5-diphenyl-tetrazolium bromide (MTT) solution. MTT was converted by intact mitochondrial reductase and precipitated as purple crystals during a 4-h contact period. The medium was next removed and the precipitated formazan crystals were dissolved in 100 μL of DMSO during a 60-min period of shaking at 37 °C.

Finally, the reduced MTT was assayed at 545 nm, using a microplate reader utilising wells with untreated cells serving as control[27]. In the case of the most active compounds (i.e. higher than 50% growth inhibition at 30 μM), the assays were repeated with a set of dilutions, sigmoidal dose–response curves were fitted to the determined data and the IC_{50} values (the concentration at which the extent of cell proliferation was half that of the untreated control) were calculated by means of GraphPad Prism 4.0 (GraphPad Software, San Diego, CA). All *in vitro* experiments were carried out on two microplates with at least five parallel wells. Stock solutions of the tested substances (10 mM) were prepared in DMSO. The highest DMSO content of the medium (0.3%) did not have any substantial effect on cell proliferation. Cisplatin (Ebewe Pharma GmbH, Unterach, Austria) was used as positive control.

4.3. Tubulin polymerisation assay

The effect of brominated triazole (**12a**) on tubulin polymerisation was tested with the HTS-Tubulin Polymerisation Assay Biochem Kit (Bio-Kasztel Ltd., Budapest, Hungary) according to the manufacturer's recommendations. Briefly, 10 μl of a 0.125 or 0.25 mM solution of the test compound (**12a**) was placed on a prewarmed (37 °C), UV-transparent microplate. About 10 μl 10 μM paclitaxel and 10 μl General Tubulin Buffer were used as positive and negative control, respectively. 100 μl 3.0 mg/ml tubulin in 80 mM PIPES pH 6.9, 2 mM $MgCl_2$, 0.5 mM EGTA, 1 mM GTP was added to each sample, and the microplate was immediately placed into a prewarmed (37 °C) UV-spectrophotometer (SpectoStarNano, BMG Labtech, Ortenberg, Germany) to start the recording reaction. A 60-min kinetic measurement protocol was applied to determine the absorbance of the reaction solution per minute at 340 nm. For the evaluation of the experimental data, the maximum reaction rate (V_{max}: Δabsorbance/min) was calculated. Moving averages of absorbances determined at three consecutive timepoints were calculated and the highest difference between two succeeding moving averages was taken as the V_{max} of the tested compound in the tubulin polymerisation reaction. Each sample was prepared in two parallels and the measurements were repeated twice. For statistical evaluation, V_{max} data were analysed by the one-way ANOVA test with the Newmann–Keuls post-test by using Prism 4.01 software (GraphPad Software, San Diego, CA).

4.4. Computational simulations

4.4.1. Docking studies

In all cases, the Glide package[28,29] of the Schrodinger suit[30] was applied for docking calculations. Dimer structure with a colchicine analogue was cut out from crystal structure (pdb id: 3HKC, www.rcsb.org[31]) for colchicine binding side studies, and a monomer unit in complex with taxol was taken from taxol-stabilized microtubule (pdb id: 5SYF).

The protein preparation wizard[32] was applied in the Maestro GUI[33] for the preparation of the downloaded rough crystal structures, and docking grids were prepared first. Each grid was centred to the original crystal ligand position, and default box size was applied. Following the grid generation, single precision (SP) docking was performed with enhanced ligand sampling. In the output, five poses were written out for each ligand.

4.4.2. Molecular dynamics calculations

The MD calculations were carried out with the Desmond[34,35] program of the Schrodinger suit. OPLS3e forcefield[36] in combination with SPC explicit water model was applied in physiological salt concentration. Orthorhombic box with 10 Å buffer size was set up, and single strand 250 ns long NPT MD running was performed at 310 K after the relaxation of the system. The Nose–Hoover[37] thermostat and Martyna–Tobias–Klein barostat were applied with default relaxation times. The MMGBSA interaction energies were determined by taking 250 snapshots periodically from the MD trajectories and the thermal_mmgbsa.py script of the Desmond program was applied to calculate the binding free energy of a ligand.

5. Conclusions

In conclusion, new ring A modified 13α-oestrone derivatives have been synthesised via directed combination of different structural elements. Certain new compounds displayed potent antiproliferative action against human reproductive cancer cell lines. 4-Bromo derivative **12a** exerted submicromolar cell growth-inhibitory action against A2780 cell line. Computational simulations reveal strong interactions of compound **12a** with colchicine and taxoid binding sites of tubulin. Direct effect of compound **12a** on microtubule formation was demonstrated via tubulin polymerisation assay.

Disclosure statement

No potential conflict of interest was reported by the author(s).

Funding

References

1. Gupta A, Kumar SB, Negi AS. Current status on development of steroids as anticancer agents. J Steroid Biochem Mol Biol 2013;137:242–70.
2. Butenandt A, Wolff A, Karlson P. Über Lumi-oestron. Chem Ber 1941;74:1308–12.
3. Yaremenko FG, Khvat AV. A new one-pot synthesis of 17-oxo-13α-steroids of the androstane series from their 13β-analogues. Mendeleev Commun 1994;187:187–8.
4. Ayan D, Roy J, Maltais R, Poirier D. Impact of estradiol structural modifications (18-methyl and/or 17-hydroxy inversion of configuration) on the *in vitro* and *in vivo* estrogenic activity. J Steroid Biochem Mol Biol 2011;127:324–30.
5. Schönecker B, Lange C, Kötteritzsch M, et al. Conformational design for 13α-steroids. J Org Chem 2000;65:5487–97.
6. Kaur R, Kaur G, Kaur Gill R, et al. Recent developments in tubulin polymerization inhibitors: an overview. Eur J Med Chem 2014;87:89–124.
7. Steinmetz MO, Prota AE. Microtubule-targeting agents: strategies to hijack the cytoskeleton. Trends Cell Biol 2018;28:776–92.
8. Naaz F, Haider MR, Shafi S, Yar MS. Anti-tubulin agents of natural origin: targeting taxol, vinca, and colchicine binding domains. Eur J Med Chem 2019;171:310–31.
9. Cao YN, Zheng LL, Wang D, et al. Recent advances in microtubule-stabilizing agents. Eur J Med Chem 2018;143:806–28.
10. Field JJ, Díaz JF, Miller JH. The binding sites of microtubule-stabilizing agents. Chem Biol 2013;20:301–15.
11. Li W, Sun H, Xu S, et al. Tubulin inhibitors targeting the colchicine binding site: a perspective of privileged structures. Future Med Chem 2017;9:1765–94.
12. Beale TM, Allwood DM, Bender A, et al. A-ring dihalogenation increases the cellular activity of combretastatin templated tetrazoles. ACS Med Chem Lett 2012;3:177–81.
13. Liang L, Astruc D. The copper(I)-catalyzed alkyne-azide cycloaddition (CuAAC) "click" reaction and its applications. An overview. Coord Chem Rev 2011;255:2933–45.
14. Szabó J, Jerkovics N, Schneider G, et al. Synthesis and in vitro antiproliferative evaluation of C-13 epimers of triazolyl-d-secoestrone alcohols: the first potent 13α-d-secoestrone derivative. Molecules 2016;21:611–24.
15. Bózsity N, Minorics R, Szabó J, et al. Mechanism of antiproliferative action of a new d-secoestrone-triazole derivative in cervical cancer cells and its effect on cancer cell motility. J Steroid Biochem Mol Biol 2017;165:247–57.
16. Szabó J, Pataki Z, Wölfling J, et al. Synthesis and biological evaluation of 13α-estrone derivatives as potential antiproliferative agents. Steroids 2016;113:14–21.
17. Bacsa I, Herman BE, Jójárt R, et al. Synthesis and structure-activity relationships of 2- and/or 4-halogenated 13β- and 13α-estrone derivatives as enzyme inhibitors of estrogen biosynthesis. J Enzyme Inhib Med Chem 2018;33:1271–82.
18. Jójárt R, Pécsy S, Keglevich G, et al. Pd-catalyzed microwave-assisted synthesis of phosphonated 13α-estrones as potential OATP2B1, 17β-HSD1 and/or STS inhibitors. Beilstein J Org Chem 2018;14:2838–45.
19. Hirao T, Masunaga T, Ohshiro Y, Agawa T. Stereoselective synthesis of vinylphosphonate. Tetrahedron Lett 1980;21:3595–8.
20. Keglevich G, Jablonkai E, László BB. A "green" variation of the Hirao reaction: the P-C coupling of diethyl phosphite, alkyl phenyl-H-phosphinates and secondary phosphine oxides with bromoarenes using a P-ligand-free Pd(OAc)$_2$ catalyst under micro-wave and solvent-free conditions. RSC Adv 2014;4:22808–16.
21. Dziuganowska ZA, Ślepokura K, Volle JN, et al. Structural analogues of Selfotel (CGS-19755). J Org Chem 2016;81:4947–54.
22. Keglevich G, Henyecz R, Mucsi Z, Kiss NZ. The palladium acetate-catalyzed microwave-assisted Hirao reaction without an added phosphorus ligand as a "green" protocol: a quantum chemical study on the mechanism. Adv Synth Catal 2017;359:4322–31.
23. Matsumoto J, Ariyoshi N, Sakakibara M, et al. Organic anion transporting polypeptide 2B1 expression correlates with uptake of estrone-3-sulfate and cell proliferation in estrogen receptor-positive breast cancer cells. Drug Metab Pharmacokinet 2015;30:133–41.
24. Banerjee N, Allen C, Bendayan R. Differential role of organic anion-transporting polypeptides in estrone-3-sulphate uptake by breast epithelial cells and breast cancer cells. J Pharmacol Exp Ther 2012;342:510–09.
25. Mernyák E, Szabó J, Bacsa I, et al. Syntheses and antiproliferative effects of D-homo- and D-secoestrones. Steroids 2014;87:128–36.
26. Peyrat J-F, Brion J-D, Alami M. Synthetic 2-methoxyestradiol derivatives: structure-activity relationships. Curr Med Chem 2012;19:4142–56.
27. Mosmann T. Rapid colorimetric assay for cellular growth and survival: application to proliferation and citotoxicity assays. J Immunol Methods 1983;65:55–63.
28. Friesner RA, Banks JL, Murphy RB, et al. Glide: a new approach for rapid, accurate docking and scoring. 1. Method and assessment of docking accuracy. J Med Chem 2004;47:1739–49.
29. Halgren TA, Murphy RB, Friesner RA, et al. Glide: a new approach for rapid, accurate docking and scoring. 2. Enrichment factors in database screening. J Med Chem 2004;47:1750–9.
30. Schrödinger Release 2019-4: Schrödinger, LLC, New York, NY, 2019.
31. Berman HM, Westbrook J, Feng Z, et al. The protein data bank. Protein Data Bank Nucleic Acids Res 2000;28:235–42.
32. Sastry GM, Adzhigirey M, Day T, et al. Protein and ligand preparation: parameters, protocols, and influence on virtual screening enrichments. J Comput Aid Mol Des 2013;27:221–34.
33. Schrödinger Release 2019-4: Maestro, Schrödinger, LLC, New York, NY; 2019.
34. Bowers KJ, Chow E, Xu H, et al. Scalable Algorithms for Molecular Dynamics Simulations on Commodity Clusters. *Proceedings of the ACM/IEEE Conference on Supercomputing (SC06)*, Tampa, FL, 2006, November 11–17.
35. Schrödinger Release 2019-4: Desmond Molecular Dynamics System, D. E. Shaw Research, New York, NY, 2019.
36. Harder E, Damm W, Maple J, et al. OPLS3: a force field providing broad coverage of drug-like small molecules and proteins. J Chem Theory Comput 2016;12:281–96.
37. Hoover WG. Canonical dynamics: equilibrium phase-space distributions. Phys Rev A 1985;31:1695–7.

III.
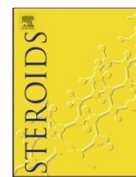
Stereocontrolled synthesis of the four possible 3-methoxy and 3-benzyloxy-16-triazolyl-methyl-estra-17-ol hybrids and their antiproliferative activities

Anita Kiss[a], János Wölfling[a], Erzsébet Mernyák[a], Éva Frank[a], Zsanett Benke[b], Seyyed Ashkan Senobar Tahaei[c], István Zupkó[c,d], Sándor Mahó[e], Gyula Schneider[a,*]

[a] Department of Organic Chemistry, University of Szeged, Dóm tér 8, H-6720 Szeged, Hungary
[b] Institute of Pharmaceutical Chemistry, University of Szeged, H-6720, Eötvös u. 6, H-6720 Szeged. Hungary
[c] Department of Pharmacodynamics and Biopharmacy, University of Szeged, Eötvös u. 6, H-6720 Szeged, Hungary
[d] Interdisciplinary Centre for Natural Products, University of Szeged, Eötvös u. 6, H-6720 Szeged, Hungary
[e] Chemical Works of Gedeon Richter Plc., Gyömrői út 19-21, H-1103 Budapest, Hungary

ABSTRACT

The four possible isomers of each of 3-methoxy- and 3-benzyloxyestra-1,3,5(10)-trien-17-ols (5–8 and 9–12) were converted through 16-p-tosyloxymethyl- or 16-bromomethyl derivatives into their 3-methoxy- and 3-benzyloxy-16-azidomethylestra(1,3,5(10)-triene derivatives (13–16 and 17–20). The regioselective Cu(I)-catalyzed 1,3-dipolar cycloaddition of these compounds with different terminal alkynes afforded novel 1,4-disubstituted diastereomers (21a–f, 22a–f, 23a–f, 24a–f and 25a–f, 26a–f, 27a–f, 28a-f). The antiproliferative activities of the structurally related triazoles were determined in vitro with the microculture tetrazolium assay on four malignant human cell lines of gynecological origin (Hela, SiHa, MCF-7 and MDA-MB-231).

1. Introduction

Among the hybrid natural products, hybrids of steroid frameworks have attracted great attention due to significant biological properties and numerous therapeutic effects of the basic compound. Steroids have become ideal synthons for the development of diverse conjugates due to their rigid framework and potential for varying levels of functionalization, broad biological activity profile and their ability to penetrate the cell membranes and bind to specific hormonal receptors [1–3].

The place, length and orientation of the linkers between the two parts of the hybrids stems unequivocally from the method of their synthesis. The literature provides a large number of methods to introduce the linker onto the sterane skeleton. The effect of the length and character of the linker are very often discussed [4]. However, only limited information is available with respect to the steric effect of the linkers on biological properties. As concerns the 16-substituted estrogenes, usually the 16α-substituted-17β-hydroxy compounds have been studied. The biological activity has generally not been studied for the whole isomer series [5].

In the 16-substituted 17-hydroxysteroids, the two chiral centres permit four stereochemical modifications. Since availability of the complete series of isomers would permit a number of interesting comparative examinations.

We have previously reported the preparation and configurational assignment of the four possible isomers of the 3-methoxy- and 3-benzyloxy-16-hydroxymethyl-estra-1,3,5(10)-trien-17-ol derivatives (5a–8a and 9a–12a) [6–8]. Treatment of 3-methoxy- and 3-benzyloxyestra-1,3,5(10)-trien-17-ones (1 and 3) with NaOMe and ethyl formate gave 3-methoxy- and 3-benzyloxy-16-hydroxymethylidene-estra-1,3,5(10)-trien-17 ones (2 and 4). The C-16 formyl compounds were reduced with KBH₄ in methanol yielding a mixture of three (5a–7a and 9a–11a) of the four possible isomers of each of the 3-methoxy- and 3-benzyloxy-16-hydroxymethylestra-1,3,5(10)-trien-17-ol isomers in a ratio of 50:45:5 in 94% yield [6,8]. The fourth isomers (8a and 12a) were prepared from 16α-acetoxymethyl-17β-toluenesulfonate mixed esters 6d and 10d, respectively, by neighbouring group participation during solvolysis in aqueous AcOH. The structures of the isomers were confirmed unambiguously by their IR, ^{1}H and ^{13}C NMR spectra (Scheme 1) [7,8]. (Scheme 1)

The four 3-methoxy- and 3-benzyloxy-estra-1,3,5(10)-trien-17-ol isomers (5a–8a and 9a–12a) are suitable starting materials to prepare 16-triazolyl-methyl derivatives. Triazoles are attractive units because of their stability against metabolic degradation and their ability to form hydrogen bonds. The Cu(I)-catalysed azide–alkyne cycloaddition (CuAAC) is a facile method of wide applicability for the introduction of a triazole moiety into natural products [9]. In these compounds the
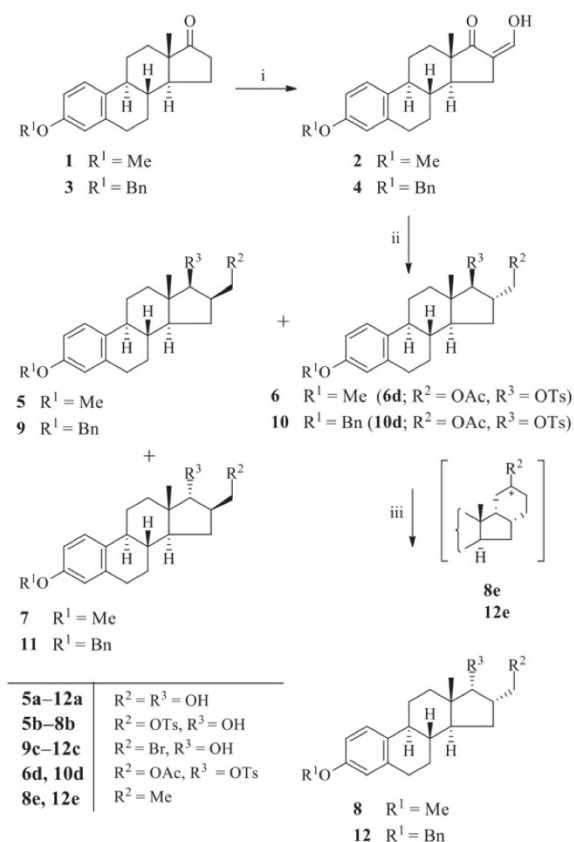
---

* Corresponding author.
    E-mail address: schneider@chem.u-szeged.hu (G. Schneider).

Scheme 1. Reagents and conditions: (i) NaOMe, HCOOEt, anhydrous toluene, 50 °C; (ii) KBH₄, MeOH; (iii) KOAc, CH₃COOH, NaOMe/MeOH.

triazole heterocycles and their substituted derivatives are connected through a methylene linker to the sterane skeleton. The 16-*p*-tolylsulfonyloxymethyl ester [5,6] and 16-bromomethyl derivatives [10] of the 16-hydroxymethyl starting materials were used for substitution reaction with NaN₃ in *N,N*-dimethylformamide to have the desired 3-methoxy- and 3-benzyloxy-16-azidomethylestra-1,3,5(10)-trien-17-ols (13–16 and 17–20). From these azido compounds several D-ring-substituted estrane derivatives containing a 1,2,3-triazole ring were synthesized by the reaction of 13–16 and 17–20 with various terminal alkynes through the use of the "click" chemistry approach to deliver compounds 21a–e, 22a–e, 23a–e, 24a–e, 25a–e, 26a–e, 27a–e and 28a–e.

2. Experimental

2.1. General

Melting points (Mp) were determined on a Kofler block and are uncorrected. Specific rotations were measured in CHCl₃ (*c* 1) at 20 °C with a POLAMAT-A (Zeiss-Jena) polarimeter and are given in units of 10^{-1} deg cm² g⁻¹. Elementary analysis data were determined with a Perkin-Elmer CHN analyzer model 2400. The reactions were monitored by TLC on Kieselgel-G (Merck Si 254F) layers (0.25 mm thick); solvent systems (ss): (A) diisopropyl ether, (B) acetone/toluene/hexane (30:35:35 v/v). The spots were detected by spraying with 5% phosphomolybdic acid in 50% aqueous phosphoric acid. The R_f values were determined for the spots observed by illumination at 254 and 365 nm. Flash chromatography: silica gel 60, 40–63 μm. All solvents were

distilled prior to use. NMR spectra were recorded on a Bruker DRX 500 and Bruker Ascend 500 instrument at 500 (¹H NMR) or 125 MHz (¹³C NMR). Chemical shifts are reported in ppm (δ scale) and coupling constants (*J*) in Hertz. For the determination of multiplicities, the *J*-MOD pulse sequence was used.

2.2. 3-Methoxy- and 3-benzyloxy-16-azidomethylestra-1,3,5(10)-trienes (13–16 and 17–20)

2.2.1. General procedure

Compounds 5b–8b [5,6] (470 mg, 1 mmol) or 9c–12c [8] (455 mg, 1 mmol) were dissolved in *N,N*-dimethylformamide (25 ml) and then NaN₃ (260 mg) was added. The mixture was stirred for 6 h at 80 °C, then poured into water (50 ml). The precipitate separating out was filtered off and subjected to chromatographic separation with CH₂Cl₂/hexane in different ratios.

2.2.2. 3-Methoxy-16β-azidomethyl-estra-1,3,5(10)-trien-17β-ol (13)

Compound 5b (470 mg, 1 mmol) was used for the synthesis as described in Section 2.2. The crude product was chromatographed on silica gel with CH₂Cl₂/hexane (1:3 v/v) to yield pure 13 (318 mg, 93%). Mp 134–135 °C; R_f = 0.65 (ss A); $[\alpha]_D^{20}$ = + 80 (*c* 1 in CHCl₃). (Found C, 70.23; H, 8.05. C₂₀H₂₇N₃O₂ (341.45) requires C, 70.35; H, 7.97%). ¹H NMR (δ, ppm, CDCl₃): 0.82 (s, 3H, 18-H₃), 2.87 (m, 2H, 6-H₂), 3.32 (dd, 1H, *J* = 12.5 Hz, *J* = 7.5 Hz, 16a-H₂), 3.61 (dd, 1H, *J* = 12.5 Hz, *J* = 7.5 Hz, 16a-H₂), 3.78 (s, 3H, 3-OCH₃), 3.87 (d, 1H, *J* = 10.0 Hz, 17-H), 6.64 (d, 1H, *J* = 2.5 Hz, 4-H), 6.72 (dd, 1H, *J* = 8.5 Hz, *J* = 2.5 Hz, 2-H), 7.20 (d, 1H, *J* = 8.5 Hz, 1-H). ¹³C NMR (δ, ppm, CDCl₃): 12.2 (C-18), 26.3, 27.5, 29.7, 30.4, 37.7, 38.2, 40.2, 44.0, 44.3 (C-13), 49.0, 53.4 (C-16a), 55.2 (3-OCH₃), 81.5 (C-17), 111.6 (C-2), 113.9 (C-4), 126.2 (C-1), 132.5 (C-10), 137.9 (C-5), 157.7 (C-3).

2.2.3. 3-Methoxy-16α-azidomethylestra-1,3,5(10)-trien-17β-ol (14)

Compound 6b (470 mg, 1 mmol) was used for the synthesis as described in Section 2.2. The crude product was chromatographed on silica gel with CH₂Cl₂/hexane (1:3 v/v) to yield pure 14 (287 mg, 84%). Mp 85–86 °C; R_f = 0.62 (ss A); $[\alpha]_D^{20}$ = + 48 (*c* 1 in CHCl₃). (Found C, 70.42; H, 7.65. C₂₀H₂₇N₃O₂ (341.45) requires C, 70.35; H, 7.97%). ¹H NMR (δ, ppm, CDCl₃): 0.84 (s, 3H, 18-H₃), 2.86 (m, 2H, 6-H₂), 3.43 (d, 1H, *J* = 7.5 Hz, 17-H), 3.48 (dd, 2H, *J* = 6.5 Hz, *J* = 3.5 Hz, 16a-H₂), 3.78 (s, 3H, 3-OCH₃), 6.63 (s, 1H, 4-H), 6.72 (dd, 1H, *J* = 6.5 Hz, *J* = 2.0 Hz, 2-H), 7.20 (d, 1H, *J* = 8.5 Hz, 1-H). ¹³C NMR (δ, ppm, CDCl₃): 11.8 (C-18), 26.1, 27.2, 28.0, 29.7, 36.6, 38.5, 43.6, 43.9, 44.2 (C-13), 48.5, 55.2 (3-OCH₃), 55.6 (C-16a), 85.1 (C-17), 111.5 (C-2), 113.8 (C-4), 126.3 (C-1), 132.4 (C-10), 137.8 (C-5), 157.5 (C-3).

2.2.4. 3-Methoxy-16β-azidomethylestra-1,3,5(10)-trien-17α-ol (15)

Compound 7b (470 mg, 1 mmol) were used for the synthesis as described in Section 2.2. The crude porduct was chromatograped on silica gel with CH₂Cl₂/hexane (1:3 v/v) to yield pure 15 (275 mg, 80%). Mp 96–98; °C; R_f = 0.60 (ss A); $[\alpha]_D^{20}$ = + 68 (*c* 1 in CHCl₃). (Found C, 70.26; H, 8.15. C₂₀H₂₇N₃O₂ (341.45) requires C, 70.35; H, 7.97%). ¹H NMR (δ, ppm, CDCl₃): 0.76 (s, 3H, 18-H₃), 2.86 (m, 2H, 6-H₂), 3.43 (dd, 2H, *J* = 7.5 Hz, *J* = 3.0 Hz, 16a-H₂), 3.61 (s, 1H, 17-H), 3.78 (s, 3H, 3-OCH₃), 6.64 (d, 1H, *J* = 2.5 Hz, 4-H), 6.72 (dd, 1H, *J* = 8.5 Hz, *J* = 2.5 Hz, 2-H), 7.22 (d, 1H, *J* = 8.5 Hz, 1-H). ¹³C NMR (δ, ppm, CDCl₃): 17.7 (C-18), 25.9, 27.9, 29.8, 30.3, 31.9, 38.6, 43.3, 45.0 (C-13), 48.9, 55.2 (3-OCH₃), 55.6 (C-16a), 83.0 (C-17), 111.5 (C-2), 113.8 (C-4), 126.3 (C-1), 132.4 (C-10), 137.9 (C-5), 157.5 (C-3).

2.2.5. 3-Methoxy-16α-azidomethylestra-1,3,5(10)-trien-17α-ol (16)

Compound 8b (470 mg, 1 mmol) was used for the synthesis as described in Section 2.2. The crude product was chromatographed on silica gel with CH₂Cl₂/hexane (1:3 v/v) to yield pure 16 (283 mg, 86%). Mp 118–120 °C; R_f = 0.65 (ss A); $[\alpha]_D^{20}$ = + 34 (*c* 1 in CHCl₃). (Found C, 70.55; H, 7.78. C₂₀H₂₇N₃O₂ (341.45) requires C, 70.35; H, 7.97%).

^{1}H NMR (δ, ppm, CDCl$_3$): 0.80 (s, 3H, 18-H$_3$), 2.87 (m, 2H, 6-H$_2$), 3.35 (dd, 1H, J = 12.0 Hz, J = 6.0 Hz, 16a-H$_2$), 3.53 (dd, 1H, J = 12.0 Hz, J = 9.5 Hz, 16a-H$_2$), 3.78 (s, 3H, 3-OCH$_3$), 3.84 (d, 1H, J = 6.0 Hz, 17-H), 6.63 (d, 1H, J = 2.5 Hz, 4-H), 6.72 (dd, 1H, J = 8.5 Hz, 2-H), 7.21 (d, 1H, J = 8.5 Hz, 1-H). ^{13}C NMR (δ, ppm, CDCl$_3$): 17.3 (C-18), 26.1, 28.0, 29.2, 31.3, 39.1, 40.5, 43.6, 46.4 (C-13), 47.0, 52.4 (C-16a), 55.2 (3-OCH$_3$), 79.9 (C-17), 111.6 (C-2), 114.0 (C-4), 126.3 (C-1), 132.7 (C-10), 137.9 (C-5), 157.6 (C-3).

2.2.6. 3-Benzyloxy-16β-azidomethylestra-1,3,5(10)-trien-17β-ol (17)

Compound **9c** (455 mg, 1 mmol) was used for the synthesis as described in Section 2.2. The crude product was chromatographed on silica gel with CH$_2$Cl$_2$/hexane (1:1 v/v) to yield pure **17** (250 mg, 59%). Mp 115–117 °C; R_f = 0.45 (ss A). (Found C, 74.55; H, 7.64. C$_{26}$H$_{31}$N$_3$O$_2$ (417.54) requires C, 74.79; H, 7.48%). ^{1}H NMR (δ, ppm, CDCl$_3$): 0.82 (s, 3H, 18-H$_3$), 2.86 (m, 2H, 6-H$_2$), 3.33 (dd, 1H, J = 12.0 Hz, J = 7.5 Hz, 16a-H$_2$), 3.60 (dd, 1H, J = 12.5 Hz, J = 7.5 Hz, 16a-H$_2$), 3.87 (d, 1H, J = 9.5 Hz, 17-H), 5.04 (s, 2H, Bn-H$_2$), 6.73 (s, 1H, 4-H), 6.79 (d, 1H, J = 8.0 Hz, J = 2.0 Hz, 2-H), 7.21 (d, 1H, J = 8.0 Hz, 1-H), 7.32 (t, 1H, J = 7.5 Hz, 4′-H), 7.39 (t, 2H, J = 7.5 Hz, 3′-H and 5′-H), 7.44 (d, 2H, J = 7.5 Hz, 2′-H and 6′-H). ^{13}C NMR (δ, ppm, CDCl$_3$): 12.2 (C-18), 26.2, 27.5, 29.7, 30.3, 37.6, 38.1, 40.1, 43.9, 44.2 (C-13), 48.8 (C-16), 53.3 (C-16a), 69.9 (Bn-CH$_2$), 81.5 (C-17), 112.3 (C-2), 114.8 (C-4), 126.3 (C-1), 127.3 (C-2′ and C-6′), 127.8 (C-4′), 128.5 (C-3′ and C-5′), 132.7 (C-10), 137.3 (C-1′), 137.9 (C-5), 156.8 (C-3).

2.2.7. 3-Benzyloxy-16α-azidomethylestra-1,3,5(10)-trien-17β-ol (18)

Compound **10c** (455 mg, 1 mmol) was used for the synthesis as described in Section 2.2. The crude product was chromatographed on silica gel with CH$_2$Cl$_2$/hexane (3:1 v/v) to yield pure **18** (254 mg, 61%). Mp 75–77 °C; R_f = 0.40 (ss A). (Found C, 74.87; H, 7.32. C$_{26}$H$_{31}$N$_3$O$_2$ (417.54) requires C, 74.79; H, 7.48%). ^{1}H NMR (δ, ppm, CDCl$_3$): 0.84 (s, 3H, 18-H$_3$), 2.85 (m, 2H, 6-H$_2$), 3.44 (t, 1H, J = 8.0 Hz, 17-H), 3.48 (m, 2H, 16a-H$_2$), 5.04 (s, 2H, Bn-H$_2$), 6.73 (s, 1H, 4-H), 6.79 (d, 1H, J = 8.5 Hz, 2-H), 7.21 (d, 1H, J = 8.5 Hz, 1-H), 7.32 (t, 1H, J = 7.0 Hz, 4′-H), 7.39 (t, 2H, J = 7.0 Hz, 3′- and 5′-H), 7.44 (d, 2H, J = 7.0 Hz, 2′- and 6′-H). ^{13}C NMR (δ, ppm, CDCl$_3$): 11.8 (C-18), 26.1, 27.2, 27.9, 29.7, 36.6, 38.5, 43.6, 43.9, 44.2 (C-13), 48.6 (C-16), 55.6 (C-16a), 69.9 (Bn-CH$_2$), 85.1 (C-17), 112.3 (C-2), 114.8 (C-4), 126.3 (C-1), 127.4 (C-2′ and -6′), 127.8 (C-4′), 128.5 (C-3′ and -5′), 132.7 (C-10), 137.3 (C-1′), 137.9 (C-5), 156.8 (C-3).

2.2.8. 3-Benzyloxy-16β-azidomethyl-estra-1,3,5(10)-trien-17α-ol (19)

Copound **11c** (455 mg, 1 mmol) was used for the synthesis as described in Section 2.2. The crude product was chromatographed on silica gel with CH$_2$Cl$_2$/hexane (3:1 v/v) to yield pure **19** (23. mg, 40%). Mp. 134–136 °C. R_f = 0.38 (ss A). (Found C, 74.92; H, 7.37. C$_{26}$H$_{31}$N$_3$O$_2$ (417.54) requires C, 74.79; H, 7.48%). ^{1}H NMR (δ, ppm, CDCl$_3$): 0.84 (s, 3H, 18-H$_3$), 2.85 (m, 2H, 6-H$_2$), 3.43 (d, 2H, J = 8.0 Hz, 17-H), 3.48 (t, 2H, J = 6.5 Hz, 16a-H$_2$), 5.04 (s, 2H, Bn-H$_2$), 6.73 (s, 1H, 4-H), 6.79 (d, 1H, J = 8.0 Hz, 2-H), 7.22 (d, 1H, J = 8.0 Hz 1-H), 7.33 (d, 1H, J = 7.0 Hz, 4′-H), 7.39 (t, 2H, J = 7.0 Hz, 3′- and 5′-H), 7.44 (d, 2H, J = 7.0 Hz, 2′- and 6′-H). ^{13}C NMR (δ, ppm, CDCl$_3$): 11.8 (C-18), 26.1, 27.2, 28.0, 29.7, 36.6, 38.4, 43.5, 43.9, 44.1 (C-13), 48.5 (C-16), 55.6 (C-16a), 69.9 (Bn-CH$_2$), 85.1 (C-17), 112.3 (C-2), 114.8 (C-4), 126.3 (C-1), 127.4 (C-2′ and -6′), 127.8 (C-4′), 128.5 (C-3′ and -5′), 132.7 (C-10), 137.3 (C-1′), 137.9 (C-5), 156.7 (C-3).

2.2.9. 3-Benzyloxy-16α-azidomethyl-estra-1,3,5(10)-trien-17α-ol (20)

Compound **12c** (455 mg, 1 mmol) was used for the synthesis as described in Section 2.2. The crude was chromatographed on silica gel with CH$_2$Cl$_2$/hexane (1:1 v/v) to yield pure **20** (330 mg, 79%). Mp 90–92 °C. R_f = 0.45 (ss A). (Found C, 74.68; H, 7.55. C$_{26}$H$_{31}$N$_3$O$_2$ (417.54) requires C, 74.79; H, 7.48%). ^{1}H NMR (δ, ppm, CDCl$_3$): 0.79 (s, 3H, 18-H$_3$), 2.71 (m, 2H, 6-H$_2$), 3.35 (dd, 1H, J = 12.0 Hz, J = 6.5 Hz, 16a-H$_2$), 3.52 (dd, 1H, J = 12.0 Hz, J = 6.5 Hz, 16a-H$_2$), 3.84 (d, 1H, J = 5.0 Hz, 17-H), 5.04 (s, 2H, Bn-H$_2$), 6.73 (s, 1H, 4-H), 6.79 (dd, 1H, J = 8.5 Hz, J = 2.5 Hz, 2-H), 7.22 (d, 1H, J = 8.5 Hz, 1-H), 7.33 (t, 1H, J = 7.5 Hz, 4′-H), 7.39 (t, 2H, J = 7.5 Hz, 3′- and 5′-H), 7.44 (d, 2H, J = 7.5 Hz, 2′- and 6′-H). ^{13}C NMR (δ, ppm, CDCl$_3$): 17.2 (C-18), 26.0, 27.9, 29.0, 29.7, 31.2, 38.9, 40.4, 43.5, 46.3 (C-13), 46.8 (C-16), 52.2 (C-16a), 69.9 (Bn-CH$_2$), 79.7 (C-17), 112.3 (C-2), 114.8 (C-4), 126.3 (C-1), 127.4 (C-2′ and -6′), 127.8 (C-4′), 128.5 (C-3′ and -5′), 132.8 (C-10), 137.3 (C-1′), 138.0 (C-5), 156.7 (C-3).

2.3. General procedure for the synthesis of triazoles (21a–e, 22a–e, 23a–e, 24a–e, 25a–e, 26a–e, 27a–e, and 28a–e)

3-Methoxy-16-azidomethylestra-1,3,5(10)-trien-17-ol isomers (**13–16**) (342 mg, 1 mmol) or 3-benzyloxy-16-azidomethylestra-1,3,5(10)-trien-17-ol isomers (**17–20**) 418 mg, 1 mmol) were dissolved in CH$_2$Cl$_2$ (20 ml), then CuI (19 mg, 0.10 mmol), Et$_3$N (0.2 ml, 2 mmol) and the appropriate terminal alkynes (2 mmol) were added. The mixtures were stirred under reflux for 24 h, then diluted with water (30 ml) and extracted with CH$_2$Cl$_2$ (2 × 30 ml). The combined organic phases were dried over Na$_2$SO$_4$ and evaporated *in vacuo*. The crude products were purified by flash chromatography using CH$_2$Cl$_2$/ethyl acetate in different ratios.

2.3.1. 3-Methoxy-16β-(4′-cyclopropyl-1′H-1′,2′,3′-triazol-1′-yl) methylestra-1,3,5(10)-trien-17β-ol (21a)

Compound **13** (342 mg, 1 mmol) and cyclopropylacetylene (2 mmol, 0.22 ml) were used for the synthesis as described in Section 2.3. The crude product was chromatographed on silica gel with CH$_2$Cl$_2$/hexane (3:1 v/v) to yield pure **21a** (210 mg, 51%) as a white solid. Mp: 189–191 °C; R_f = 0.44 (ss B). (Found C, 73.84; H, 7.98. C$_{25}$H$_{33}$N$_3$O$_2$ (407.55) requires C, 73.68; H, 8.16%). ^{1}H NMR (δ, ppm, CDCl$_3$): 0.80 (s, 3H, 18-H$_3$), 0.83 (s, 2H, cyclopropyl-H$_2$), 0.94 (s, 2H, cyclopropyl-H$_2$), 2.72 (d, 1H, J = 7.0 Hz, 1″-H), 2.84 (m, 2H, 6-H$_2$), 3.77 (s, 3H, 3-OCH$_3$), 3.93 (d, 1H, J = 9.5 Hz, 17-H), 4.21 (dd, 1H, J = 13.0 Hz, J = 6.0 Hz, 16a-H$_2$), 4.62 (t, 1H, J = 8.0 Hz, 16a-H$_2$), 6.62 (s, 1H, 4-H), 6.71 (d, 1H, J = 8.5 Hz, 2-H), 7.20 (d, 1H, J = 8.5 Hz, 1-H), 7.29 (s, 1H, 5′-H). ^{13}C NMR (δ, ppm, CDCl$_3$): 6.7 (C-1″), 7.68 (C-2″ and -3″),12.3 (C-18), 26.2, 27.4, 29.7, 30.8, 37.5, 38.0, 41.4, 43.8, 44.3 (C-16a), 48.7, 51.7 (C-13), 55.2 (3-OCH$_3$), 80.7 (C-17), 111.5 (C-2), 113.8 (C-4), 126.3 (C-1), 132.4 (C-10), 137.8 (C-5), 157.5 (C-3).

2.3.2. 3-Methoxy-16β-(4′-cyclopentyl-1′H-1′,2′,3′-triazol-1′-yl) methylestra-1,3,5(10)-trien-17β-ol (21b)

Compound **13** (342 mg, 1 mmol) and cyclopentylacetylene (2 mmol, 0.22 ml) were used for the synthesis as described in Section 2.3. The crude product was chromatographed on silica gel with CH$_2$Cl$_2$ to yield pure **21b** (370 mg, 85%) as a white solid. Mp: 191–192 °C; R_f = 0.46 (ss B). (Found C, 74.62; H, 8.42. C$_{27}$H$_{37}$N$_3$O$_2$ (435.60) requires C, 74.45; H, 8.56%). ^{1}H NMR (δ, ppm, CDCl$_3$): 0.79 (s, 3H, 18-H$_3$), 2.85 (m, 2H, 6-H$_2$), 3.19 (s, 1H, 1″-H), 3.77 (s, 3H, 3-OCH$_3$), 3.94 (d, 1H, J = 9.5 Hz, 17-H), 4.24 (d, 1H, J = 8.0 Hz, 16a-H$_2$), 4.65 (s, 1H, 16a-H$_2$), 6.62 (s, 1H, 4-H), 6.71 (d, 1H, J = 8.5 Hz, 2-H), 7.20 (d, 1H, J = 8.5 Hz, 1-H), 7.34 (s, 1H, 5′-H). ^{13}C NMR (δ, ppm, CDCl$_3$): 12.3 (C-18), 25.1 (C-3″ and -4″), 26.2, 27.4, 29.7 (C-2″ and 5″), 30.8, 33.2, 36.7, 37.5, 38.0, 42.4 (C-16a), 43.8, 44.3 (C-13), 48.7, 51.8, 55.2 (3-OCH$_3$), 62.1 (C-16), 80.7 (C-17), 111.5 (C-2), 113.7 (C-4), 126.3 (C-1), 132.4 (C-10), 137.8 (C-5), 157.4 (C-3).

2.3.3. 3-Methoxy-16β-(4′-cyclohexyl-1′H-1′,2′,3′-triazol-1′-yl) methylestra-1,3,5(10)-trien-17β-ol (21c)

Compound **13** (342 mg, 1 mmol) and cyclohexylacetylene (2 mmol, 0.22 ml) were used for the synthesis as described in Section 2.3. The crude product was chromatographed on silica gel with ethyl acetate/CH$_2$Cl$_2$ (1:99 v/v) to yield pure **21c** (370 mg, 82%) as a white solid. Mp: 189–190 °C; R_f = 0,40 (ss B). (Found C, 74.92; H, 8.55. C$_{28}$H$_{41}$N$_3$O$_2$ (449.63) requires C, 74.80; H, 8.74%). ^{1}H NMR (δ, ppm, CDCl$_3$): 0.79

(s, 3H, 18-H₃), 2.84 (m, 2H, 6-H₂), 3.77 (s, 3H, 3-OCH₃), 3.94 (d, 1H, J = 9.5 Hz, 17-H), 4.24 (m, 1H, 16a-H₂), 4.65 (m, 1H, 16a-H₂), 6.62 (s, 1H, 4-H), 6.71 (d, 1H, J = 8.5 Hz, 2-H), 7.20 (d, 1H, J = 8.5 Hz, 1-H), 7.32 (s, 1H, 5′-H). ¹³C NMR (δ, ppm, CDCl₃): 12.3 (C-18), 26.0, 26.1 (C-2″ and -6″), 26.2, 27.4, 29.7, 30.8, 33.0, 37.5, 38.0, 41.4 (C-1″), 43.8, 44.3 (C-13), 48.3, 55.2 (3-OCH₃), 62.1, 80.7 (C-17), 111.5 (C-2), 113.7 (C-4), 126.3 (C-1), 132.4 (C-10), 137.8 (C-5), 157.4 (C-3).

2.3.4. 3-Methoxy-16β-(4′-phenyl-1′H-1′,2′,3′-triazol-1′-yl)methylestra-1,3,5(10)-trien-17β-ol (21d)

Compound **13** (342 mg, 1 mmol) and phenylacetylene (2 mmol, 0.22 ml) were used for the synthesis as described in Section 2.3. The crude product was chromatographed on silica gel with ethyl acetate/CH₂Cl₂ (1:99 v/v) to yield pure **21d** (368 mg, 83%) as a white solid. Mp: 232–234 °C; R_f = 0.35. (Found C, 75.98; H, 7.36. C₂₈H₃₃N₃O₂ (443.58) requires C, 75.81; H, 7.50%). ¹H NMR (δ, ppm, CDCl₃): 0.79 (s, 3H, 18-H₃), 2.73 (m, 2H, 6-H₂), 3.68 (s, 3H, 3-OCH₃), 3.79 (d, 1H, J = 10.0 Hz, 17-H), 4.20 (t, 1H, J = 13.5 Hz, 16a-H₂), 4.63 (dd, 1H, J = 13.5 Hz, J = 4.5 Hz, 16a-H₂), 6.59 (s, 1H, 4-H), 6.67 (d, 1H, J = 8.5 Hz, 2-H), 7.16 (d, 1H, J = 8.5 Hz, 1-H), 7.32 (t, 1H, J = 7.5 Hz, 4″-H), 7.44 (t, 2H, J = 7.5 Hz, 3″- and 5″-H), 7.85 (d, 2H, J = 7.5 Hz, 2″- and 6″-H), 8.60 (s, 1H, 5′-H). ¹³C NMR (δ, ppm, CDCl₃): 12.4 (C-18), 25.8, 26.9, 29.1, 30.0, 36.9, 37.8, 40.4, 43.3, 43.7 (C-13), 47.8, 52.3 (C-16a), 54.8 (3-OCH₃), 79.5 (C-17), 111.4 (C-2), 113.3 (C-4), 121.5 (C-5′), 124.5 (C-2″ and -6″), 126.0 (C-1), 127.6 (C-4″), 127.8 (C-3″ and -5″), 130.9 (C-1″), 132.0 (C-10), 137.3 (C-5), 146.0 (C-4′), 156.9 (C-3).

2.3.5. 3-Methoxy-16β-(4′-nitro-benzoyloxymethyl-1′H-1′,2,′3′-triazol-1′-yl)methylestra-1,3,5(10)-trien-17β-ol (21e)

Compound **13** (342 mg, 1 mmol) and propargyl 4-nitrobenzoate (2 mmol, 410 mg) were used for the synthesis as described in Section 2.3. The crude product was chromatographed on silica gel with ethyl acetate/CH₂Cl₂ (5:95 v/v) to yield pure **21e** (475 mg, 86%) as a yellow solid. Mp: 134–135.5 °C; R_f = 30 (ss B). (Found C, 66.12; H, 6.08. C₃₀H₃₄N₄O₆ (546.61) requires C, 65.92; H, 6.27%). ¹H NMR (δ, ppm, CDCl₃): 0.73 (s, 3H, 18-H₃), 2.70 (m, 2H, 6-H₂), 3.66 (s, 3H, 3-OCH₃), 4.18 (dd, 1H, J = 13.5 Hz, J = 11.5 Hz, 16a-H2), 4.58 (dd, 1H, J = 13.5 Hz, J = 4.5 Hz, 16a-H₂), 5.02 (d, 1H, J = 4.5 Hz, 17-H), 5.44 (s, 2H, 4′-H₂), 6.55 (d, 1H, J = 1.5 Hz, 4-H), 6.63 (dd, 1H, J = 8.5 Hz, J = 2.0 Hz, 2-H), 7.12 (d, 1H, J = 8.5 Hz, 1-H), 8.16 (d, 2H, J = 8.5 Hz, 3″- and 5″-H), 8.31 (t, 3H, J = 8.5 Hz, 2″- and 6″-H, 5′-H). ¹³C NMR (δ, ppm, CDCl₃): 12.3 (C-18), 25.8, 26.9, 29.1, 30.0, 36.9, 37.8, 40.4, 43.3, 43.7 (C-13), 47.8, 52.2 (C-16a), 54.7 (3-OCH₃), 58.7 (4′-CH₂), 79.5 (C-17), 111.3 (C-2), 113.3 (C-4), 123.8 (C-2″ and -6″), 125.1 (C-5′), 126.0 (C-1), 130.6 (C-3″ and -5″), 131.9 (C-10), 134.7 (C-1″), 137.2 (C-5), 141.0 (C-4″), 150.2 (C-4′), 156.9 (C-3), 163.9 (C=O).

2.3.6. 3-Methoxy-16β-(4′-hydroxymethyl-1′H-1′,2′,3′-triazol-1′-yl)methylestra-1,3,5(10)-trien-17β-ol (21f)

Compound **13** (274 mg, 0.5 mmol) was dissolved in methanol (10 ml) containing NaOCH₃ (14 mg, 0.25 mmol), and the solution was allowed to stand for 24 h. It was then diluted with water, and the precipitate separating out was filtered off and recrystallized from a mixture of ethyl acetate/hexane to afford **21f** (171 mg, 86%) as a white crystalline material. Mp: 194–195 °C; R_f = 0.25 (ss B). (Found C, 69.23; H, 8.04. C₂₃H₃₁N₃O₃ (397.51) requires C, 69.49; H, 7.86%). ¹H NMR (δ, ppm, DMSO-d_6): 0.76 (s, 3H, 18-H₃), 2.71 (m, 2H, 6-H₂), 3.68 (s, 3H, 3-OCH₃), 3.76 (d, 1H, J = 5.5 Hz, 17-H), 4.14 (t, 1H, J = 12.5 Hz, 16a-H₂), 4.49 (m, 3H, 4′-H₂ and 16a-H₂), 5.03 (d, 1H, J = 3.5 Hz, 17-OH), 5.15 (brs, 1H, CH₂-OH), 6.59 (s, 1H, 4-H), 6.66 (d, 1H, J = 8.5 Hz, 2-H), 7.16 (d, 1H, J = 8.5 Hz, 1-H), 7.99 (s, 1H, 5′-H). ¹³C NMR (δ, ppm, DMSO-d_6): 12.4 (C-18), 25.9, 26.9, 29.2, 30.0, 36.9, 37.9, 40.5, 43.4, 43.8 (C-13), 47.8, 52.0 (C-16a), 54.8 (3-OCH₃), 55.0 (4′-CH₂), 79.5 (C-17), 111.4 (C-2), 113.4 (C-4), 122.8 (C-5′), 126.1 (C-1), 132.0 (C-10), 137.3 (C-5), 147.6 (C-4′), 157.0 (C-3).

2.3.7. 3-Methoxy-16a-(4′-cyclopropyl-1′H-1′,2′,3′-triazol-1′-yl)methylestra-1,3,5(10)-trien-17β-ol (22a)

Compound **14** (342 mg, 1 mmol) and cyclopropylacetylene (2 mmol, 0.22 ml) were used for the synthesis as described in Section 2.3. The crude product was chromatographed on silica gel with ethyl acetate/CH₂Cl₂ (5:95 v/v) to yield pure **22a** (261 mg, 64%) as a white solid. Mp: 67–69 °C; R_f = 0.35 (ss B). (Found C, 73.55; H, 7.98. C₂₅H₃₃N₃O₂ (407.55) requires C, 73.68; H, 8.16%). ¹H NMR (δ, ppm, CDCl₃): 0.82 (m, 5H, 18-H₃ and cyclopropyl-H₂), 0.95 (m, 2H, cyclopropyl-H₂), 2.83 (m, 2H, 6-H₂), 3.53 (d, 1H, J = 7.5 Hz, 17-H), 3.77 (s, 3H, 3-OCH₃), 4.35 (t, 1H, J = 7.5 Hz, 16a-H₂), 4.44 (dd, 1H, J = 13.5 Hz, J = 7.5 Hz, 16a-H₂), 6.62 (d, 1H, J = 2.0 Hz, 4-H), 6.70 (dd, 1H, J = 8.5 Hz, J = 2.0 Hz, 2-H), 7.18 (d, 1H, J = 8.5 Hz, 1-H). ¹³C NMR (δ, ppm, CDCl₃): 6.7 (C-1″), 7.7 (C-2″ and -3″), 11.8 (C-18), 26.1, 27.2, 28.2, 29.7, 36.6, 38.4, 43.9, 44.3, 44,3 (C-16a), 48.3, 54.5 (C-13), 62.1 (3-OCH₃), 85.1 (C-17), 111.5 (C-2), 113.8 (C-4), 126.2 (C-1), 132.3 (C-10), 137.8 (C-5), 157.4 (C-3).

2.3.8. 3-Methoxy-16a-(4′-cyclopentyl-1′H-1′,2′,3′-triazol-1′-yl)methylestra-1,3,5(10)-trien-17β-ol (22b)

Compound **14** (342 mg, 1 mmol) and cyclopentylacetylene (2 mmol, 0.22 ml) were used for the synthesis as described in Section 2.3. The crude product was chromatographed on silica gel with ethyl acetate/CH₂Cl₂ (5:95 v/v) to yield pure **22b** (290 mg, 66%) as a white solid. Mp: 163–165 °C; R_f = 0.32 (ss B). (Found C, 74.63; H, 8.41. C₂₇H₃₇N₃O₂ (435.60) requires C, 74.45; H, 8.56%). ¹H NMR (δ, ppm, CDCl₃): 0.83 (s, 3H, 18-H₃), 1.68 (s, 4H, 3″- and 4″-H₂), 2.83 (m, 2H, 6-H₂), 3.19 (m, 1H, 1″-H), 3.56 (d, 1H, J = 7.0 Hz, 17-H), 3.77 (s, 3H, 3-OCH₃), 4.43 (m, 2H, 16a-H₂), 6.62 (s, 1H, 4-H), 6.70 (d, 1H, J = 8.5 Hz, 2-H), 7.19 (d, 1H, J = 8.5 Hz, 1-H), 7.35 (s, 1H, 5′-H). ¹³C NMR (δ, ppm, CDCl₃): 11.9 (C-18), 25.1 (C-3″ and -4″), 26.1, 27.2, 28.3, 29.7 (C-2″ and -5″), 33.2, 36.6, 38.4, 43.9, 44.2, 44.3 (C-13), 48.4, 55.2 (3-OCH₃), 62.1 (C-16a), 85.3 (C-17), 111.5 (C-2), 113.8 (C-4), 126.3 (C-1), 132.3 (C-10), 137.8 (C-5), 157.5 (C-3).

2.3.9. 3-Methoxy-16a-(4′-cyclohexyl-1′H-1′,2′,3′-triazol-1′-yl)methylestra-1,3,5(10)-trien-17β-ol (22c)

Compound **14** (342 mg, 1 mmol) and cyclohexylacetylene (2 mmol, 0.22 ml) were used for the synthesis as described in Section 2.3. The crude product was chromatographed on silica gel with ethyl acetate/CH₂Cl₂ (5:95 v/v) to yield pure **22c** (345 mg, 76%) as a white solid. Mp: 80–82 °C; R_f = 0.34 (ss B). (Found 74.96; H, 8.54. C₂₈H₄₁N₃O₂ (449.63) requires C, 74.80; H, 8.74%). ¹H NMR (δ, ppm, CDCl₃): 0.83 (s, 3H, 18-H₃), 2.83 (m, 2H, 6-H₂), 3.55 (s, 1H, 17-H), 3.77 (s, 3H, 3-OCH₃), 4.46 (s, 2H, 16a-H₂), 6.62 (d, 1H, J = 2.0 Hz, 4-H), 6.70 (dd, 1H, J = 8.5 Hz, J = 2.0 Hz, 2-H), 7.19 (d, 1H, J = 8.5 Hz, 1-H). ¹³C NMR (δ, ppm, CDCl₃): 11.9 (C-18), 26.0 and 26.1 (C-2″ and -6″, C-3″ and -5″), 27.2, 28.3, 29.7, 36.6, 38.4, 43.9, 44.3 (C-13), 48.4, 55.2 (3-OCH₃), 62.1 (C-1″), 62.1 (C-16a), 85.2 (C-17), 111.5 (C-2), 113.8 (C-4), 126.2 (C-1), 132.3 (C-10), 137.8 (C-5), 157.4 (C-3).

2.3.10. 3-Methoxy-16a-(4′-phenyl-1′H-1′,2′,3′-triazol-1′-yl)methylestra-1,3,5(10)-trien-17β-ol (22d)

Compound **14** (342 mg, 1 mmol) and phenylacetylene (2 mmol, 0.22 ml) were used for the synthesis as described in Section 2.3. The crude product was chromatographed on silica gel ethyl acetate/CH₂Cl₂ (5:95 v/v) to yield pure **22d** (368 mg, 82%) as a white solid. Mp: 204–205 °C; R_f = 0.38 (ss B). (Found C, 75.63; H, 7.72. C₂₈H₃₃N₃O₂ (443.58) requires C, 75.81; H, 7.50%). ¹H NMR (δ, ppm, DMSO-d_6): 0.73 (s, 3H, 18-H₃), 2.73 (m, 2H, 6-H₂), 3.67 (s, 3H, 3-OCH₃), 4.36 (t, 1H, J = 13.5 Hz, 16a-H₂), 4.54 (dd, 1H, J = 13.5 Hz, J = 4.0 Hz, 16a-H₂), 4.91 (d, 1H, J = 4.0 Hz, 17-H), 6.58 (s, 1H, 4-H), 6.67 (d, 1H, J = 8.5 Hz, 2-H), 7.15 (d, 1H, J = 8.5 Hz, 1-H), 7.32 (t, 1H, J = 7.0 Hz, 4″-H), 7.44 (t, 2H, J = 7.0 Hz, 3″- and 5″-H), 7.86 (d, 2H, J = 7.0 Hz, 2″- and 6″-H), 8.61 (s, 1H, 5′-H). ¹³C NMR (δ, ppm, DMSO-d_6): 11.8 (C-18), 25.8, 26.7, 27.3, 29.1, 36.3, 38.1, 43.4, 43.5, 43.8, 47.5, 53.5 (C-

4

13), 54.8 (3-OCH$_3$), 83.1 (C-17), 111.4 (C-2), 113.3 (C-4), 121.4 (C-5′), 125.0 (C-2″ and -6″), 126.0 (C-1), 127.6 (C-4″), 128.8 (C-3″ and -5″), 130.8 (C-1″), 132.0 (C-10), 137.3 (C-5), 146.1 (C-4′), 156.9 (C-3).

2.3.11. 3-Methoxy-16α-[4′(4″-nitro-benzoyloxymethyl)-1′H-1′,2′,3′-triazol-1′-yl]methylestra-1,3,5(10)-trien-17β-ol (22e)

Compound **14** (342 mg, 1 mmol) and propargyl 4-nitrobenzoate (2 mmol, 410 mg) were used for the synthesis as described in Section 2.3. The crude product was chromatographed on silica gel with ethyl acetate/CH$_2$Cl$_2$ (5:95 v/v) to yield pure **22e** (445 mg, 81%) as a yellow solid. Mp: 86–88 °C; R_f = 0.28 (ss B). (Found C, 66.08; H, 6.43. C$_{30}$H$_{34}$N$_4$O$_6$ (546.61) requires C, 65.92; H, 6.27%). ^{1}H NMR (δ, ppm, DMSO-d_6): 0.69 (s, 3H, 18-H$_3$), 2.68 (m, 2H, 6-H$_2$), 3.57 (s, 3H, 3-OCH$_3$), 4.38 (dd, 1H, J = 13.5 Hz, J = 9.0 Hz, 16a-H$_2$), 4.52 (dd, 1H, J = 13.5 Hz, J = 4.5 Hz, 16a-H$_2$), 4.86 (d, 1H, J = 4.5 Hz, 17-H), 5.46 (s, 2H, 4′-H$_2$), 6.55 (d, 1H, J = 1.5 Hz, 4-H), 6.63 (dd, 1H, J = 8.5 Hz, 2-H), 7.10 (d, 1H, J = 8.5 Hz, 1-H), 8.16 (d, 2H, J = 8.5 Hz, 3″- and 5″-H), 8.28 (d, 2H, J = 8.5 Hz, 2″- and 6″-H), 8.31 (s, 1H, 5′-H). ^{13}C NMR (δ, ppm, DMSO-d_6): 11.7 (C-18), 25.7, 26.6, 27.1, 29.0, 36.4, 38.0, 43.3, 43.4 (C-13), 43.7, 47.7, 53.1 (C-16a), 54.7 (3-OCH$_3$), 58.6 (4″-CH$_2$), 82.8 (C-17), 111.3 (C-2), 113.3 (C-4), 123.8 (C-2″ and -6″), 125.2 (C-5′), 125.9 (C-1), 130.6 (C-3″ and -5″), 131.8 (C-10), 134.7 (C-1′), 137.2 (C-5), 141.1 (C-4″), 150.2 (C-4′), 156.9 (C-3), 163.9 (C=O).

2.3.12. 3-Methoxy-16α-(4′-hydroxymethyl-1′H-1′,2′3′-triazol-1′-yl)methylestra-1,3,5(10)-trien-17β-ol (22f)

Compound **22e** (274 mg, 0.5 mmol) was dissolved in methanol (10 ml) containing NaOCH$_3$ (14 mg, 0.25 mmol), and the solution was allowed to stand for 24 h. It was then diluted with water, and the precipitate separating out was filtered off and recrystallized from a mixture of ethyl acetate/hexane to afford **22f** (175 mg, 88%) as a white crystalline product. Mp: 98–100 °C; R_f = 0.28 (ss B). (Found C, 69.74; H, 7.72. C$_{23}$H$_{31}$N$_3$O$_3$ (397.51) requires C, 69.49; H, 7.86%). ^{1}H NMR (δ, ppm, CDCl$_3$): 0.81 (s, 3H, 18-H$_3$), 2.82 (m, 2H, 6-H$_2$), 3.50 (d, 1H, J = 7.0 Hz, 17-H), 3.76 (s, 3H, 3-OCH$_3$), 4.42 (d, 2H, J = 7.0 Hz, 16a-H$_2$), 4.71 (s, 2H, 4′-H$_2$), 6.61 (s, 1H, 4-H), 6.69 (d, 1H, J = 8.5 Hz, 2-H), 7.17 (d, 1H, J = 8.5 Hz, 1-H), 7.68 (s, 1H, 5′-H). ^{13}C NMR (δ, ppm, CDCl$_3$): 11.9 (C-18), 26.1, 27.2, 28.2, 29.6, 36.5, 38.4, 43.8, 44.0, 44.4 (C-13), 48.2, 54.6 (C-16a), 55.2 (3-OCH$_3$), 56.0 (4′-CH$_2$), 85.1 (C-17), 111.5 (C-2), 113.8 (C-4), 126.3 (C-1), 132.3 (C-10), 137.8 (C-5), 157.4 (C-3).

2.3.13. 3-Methoxy-16α-(4′-cyclopropyl-1′H-1′,2′,3′-triazol-1′-yl)methylestra-1,3,5(10)-trien-17β-ol (23a)

Compound **15** (342 mg, 1 mmol) and cyclopropylacetylene (2 mmol, 0.22 ml) were used for the synthesis as described in Section 2.3. The crude product was chromatographed on silica gel with ethyl acetate/CH$_2$Cl$_2$ (1:99 v/v) to yield pure **23a** (261 mg, 64%) as a white solid. Mp: 67–69 °C; R_f = 0.32 (ss B). (Found C, 73.85; H, 8.32. C$_{25}$H$_{33}$N$_3$O$_2$ (407.55) requires C, 73.68; H, 8.16%). ^{1}H NMR (δ, ppm, CDCl$_3$): 0.82 (m, 5H, 18-H$_3$ and cyclopropyl-H$_2$), 0.95 (m, 2H, cyclopropyl-H$_2$), 2.83 (m, 2H, 6-H$_2$), 3.53 (d, 1H, J = 7.5 Hz, 17-H), 3.77 (s, 3H, 3-OCH$_3$), 4.35 (t, 1H, J = 7.5 Hz, 16a-H$_2$), 4.44 (dd, 1H, J = 13.5 Hz, J = 7.5 Hz, 16a-H$_2$), 6.62 (d, 1H, J = 2.0 Hz, 4-H), 6.70 (dd, 1H, J = 8.5 Hz, J = 2.0 Hz, 2-H), 7.18 (d, 1H, J = 8.5 Hz, 1-H). ^{13}C NMR (δ, ppm, CDCl$_3$): 6.7 (C-1″), 7.7 (C-2″ and -3″), 11.8 (C-18), 26.1, 27.2, 28.2, 29.7, 36.6, 38.4, 43.9, 44.3, 44,3 (C-16a), 48.3, 54.5 (C-13), 62.1 (3-OCH$_3$), 85.1 (C-17), 111.5 (C-2), 113.8 (C-4), 126.2 (C-1), 132.3 (C-10), 137.8 (C-5), 157.4 (C-3).

2.3.14. 3-Methoxy-16β-(4′-cyclopentyl-1′H-1′,2′,3′-triazol-1-yl)methylestra-1,3,5(10)-trien-17α-ol (23b)

Compound **15** (342 mg, 1 mmol) and cyclopentylacetylene (2 mmol, 0.22 ml) were used for the synthesis as described in Section 2.3. The crude product was chromatographed on silica gel with ethyl acetate/CH$_2$Cl$_2$ (1:99 v/v) to yield pure **23b** (380 mg, 87%) as yellow

crystalline material. Mp: 67–68 °C; R_f = 0.36 (ss B). (Found C, 74.28; H, 8.47. C$_{27}$H$_{37}$N$_3$O$_2$ (435.60) requires C, 74.45; H, 8.56%). ^{1}H NMR (δ, ppm, CDCl$_3$): 0.75 (s, 3H, 18-H$_3$), 2.85 (m, 2H, 6-H$_2$), 3.68 (s, 1H, 17-H), 3.77 (s, 3H, 3-OCH$_3$), 4.44 (d, 2H, J = 15.0 Hz, 16a-H$_2$), 6.62 (s, 1H, 4-H), 6.70 (d, 1H, J = 8.5 Hz, 2-H), 7.20 (t, 1H, J = 8.5 Hz, 1-H). ^{13}C NMR (δ, ppm, CDCl$_3$): 17.9 (C-18), 25.1 (C-3″ and -4″), 25.9, 26.1, 27.2, 28.0, 29.7, 30.4, 31.8, 36.6 (C-16a), 38.5, 43.3, 43.8, 45.1 (C-13), 48.9, 55.2 (3-OCH$_3$), 62.1 (C-1″), 82.6 (C-17), 111.5 (C-2), 113.7 (C-4), 113.8 (C-5′), 126.2 (C-1), 132.1 (C-10), 137.8 (C-5), 137.8 (C-4′), 157.4 (C-3).

2.3.15. 3-Methoxy-16β-(4′-cyclohexyl-1′H-1′,2′,3′-triazol-1′-yl)methyestra-1,3,5(10)-trien-17α-ol (23c)

Compound **15** (342, 1 mmol) and cyclohexylacetylene (2 mmol, 0.22 ml) were used for the synthesis as described in Section 2.3. The crude product was chromatographed on silica gel with ethyl acetate/CH$_2$Cl$_2$ (5:95 v/v) to yield pure **23c** (306 mg, 68%) as a white solid. Mp: 90–92 °C; R_f = 0.37 (ss B). (Found C, 74.95; H, 8.83. C$_{28}$H$_{41}$N$_3$O$_2$ (449.63) requires C, 74.80; H, 8.74%). ^{1}H NMR (δ, ppm, CDCl$_3$): 0.75 (s, 3H, 18-H$_3$), 2.84 (m, 2H, 6-H$_2$), 3.67 (d, 1H, J = 1.0 Hz, 17-H), 3.77 (S, 3H, 3-OCH$_3$), 4.43 (m, 1H, 16a-H$_2$), 6.62 (d, 1H, J = 2.5 Hz, 4-H), 6.71 (dd, 1H, J = 8.5 Hz, J = 2.5 Hz, 2-H), 7.20 (t, 1H, J = 8.5 Hz, 1-H), 7.35 (s, 1H, 5′-H). ^{13}C NMR (δ, ppm, CDCl$_3$): 17.9 (C-18), 25.9, 26.0, 26.1 (C-2″ and -6″), 28.0, 29.7, 30.4, 31.8, 33.0, 35.2 (C-1″), 36.6, 38.5, 43.3, 45.1 (C-13), 48.9, 49.1, 54.3 (C-16a), 55.2 (3-OCH$_3$), 82.6 (C-1), 132.4 (C-10), 137.8 (C-5), 153.7 (C-4′), 157.7 (C-3).

2.3.16. 3-Methoxy-16β-(4′-phenyl-1′H-1′,2′,3′-triazol-1′-yl)methy-estra-1,3,5(10)-trien-17α-ol (23d)

Compound **15** (342 mg, 1 mmol) and phenylacetylene (2 mmol, 0.22 ml) were used for the synthesis as described in Section 2.3. The crude product was chromatographed on silica gel with ethyl acetate/CH$_2$Cl$_2$ (2.5:97.5 v/v) to yield pure **23d** (299 mg, 67%) as white crystals. Mp: 173–174 °C; R_f = 0.34 (ss B). (Found C 75.98; H, 7.33. C$_{28}$H$_{33}$N$_3$O$_2$ (443.58) requires C, 75.81; H, 7.50%). ^{1}H NMR (δ, ppm, CDCl$_3$): 0.79 (s, 3H, 18-H$_3$), 2.85 (m, 2H, 6-H$_2$), 3.71 (d, 1H J = 1.5 Hz, 17-H), 3.78 (s, 3H, 3-OCH$_3$), 4.46 (dd, 1H, J = 13.5 Hz, J = 8.0 Hz, 16a-H$_2$), 4.55 (dd, 1H, J = 13.5 Hz, J = 8.0 Hz, 16a-H$_2$), 6.63 (d, 1H, J = 2.0 Hz, 4-H), 6.72 (dd, 1H, J = 8.5 Hz, J = 2.5 Hz, 2-H), 7.21 (d, 1H, J = 8.5 Hz, 1-H), 7.27 (t, 1H J = 7.5 Hz, 4″-H), 7.42 (t, 2H, J = 7.5 Hz, 3″- and 5″-H), 7.83 (d, 2H, J = 7.5 Hz, 2″- and 6″-H), 7.87 (s, 1H, 5′-H). ^{13}C NMR (δ, ppm, CDCl$_3$): 17.9 (C-18), 25.9, 27.9, 29.7, 30.4, 31.8, 38.5, 43.3, 45.1, (C-13), 48.8, 49.1, 54.5 (C-16a), 55.2 (3-OCH$_3$), 82.5 (C-17), 111.5 (C-2), 113.7 (C-4), 119.6 (C-5′), 125.7 (C-2″ and -6″), 126.3 (C-1), 128.1 (C-4″), 128.8 (C-3″ and -5″), 130.5 (C-1″), 132.4 (C-10), 137.8 (C-5), 147.8 (C-4′), 157.4 (C-3).

2.3.17. 3-Methoxy-16β-[4′(4″-nitro-benzoyloxymethyl)-1′H-1′,2′,3′-triazol-1′-yl]methylestra-1,3,5(10)-trien-17α-ol (23e)

Compound **15** (342, 1 mmol) and propargyl 4-nitro benzoate (2 mmol, 410 mg) were used for the synthesis as described in Section 2.3. The crude product was chromatographed on silica gel with ethyl acetate/CH$_2$Cl$_2$ (5:95 v/v) to yield pure **23e** (370 mg, 67%) as a yellow crystalline material. Mp: 62–63 °C; R_f = 0.38 (ss B). (Found C, 66.14; H, 6.42. C$_{30}$H$_{34}$N$_4$O$_6$ (546.61) requires C, 65.92; H, 6.27%). ^{1}H NMR (δ, ppm, DMSO-d_6): 0.65 (s,3H, 18-H$_3$), 2.74 (m,2H, 6-H$_2$), 3.68 (s, 3H, 3-OCH$_3$), 4.41 (dd, 1H, J = 13.0 Hz, J = 8.5 Hz, 16a-H$_2$), 4.56 (dd, 1H, J = 13.0 Hz, J = 8.5 Hz, 16a-H$_2$), 4.63 (d, 1H, J = 4.5 Hz, 17-H), 6.58 (s, 1H, 4-H), 6.66 (d, 1H, J = 8.5 Hz, 2-H), 7.16 (d, 1H, J = 8.5 Hz, 1-H), 8.19 (d, 2H, J = 8.5 Hz, 3″- and 5″-H), 8.34 (d, 2H, J = 8.5 Hz, 2″- and 6″-H). ^{13}C NMR (δ, ppm, DMSO-d_6): 17.5 (C-18), 25.6, 27.5, 29.6, 31.8, 38.2, 43.0, 44.5, 47.9 (C-13), 48.2, 49.1, 53.6 (C-16a), 54.8 (3-OCH$_3$), 58.7 (4′-CH$_2$), 80.8 (C-17), 111.3 (C-2), 113.3 (C-4), 123.8 (C-1), 126.1 (C-5′), 130.6 (C-2″ and -6″), 131.9 (C-3″ and -5″), 133.0 (C-10), 134.7 (C-1″), 137.3 (C-5), 141.4 (C-4″), 150.2 (C-4′), 156.9 (C-3), 163.9 (C=O).

5

2.3.18. 3-Methoxy-16β-(4′-hydroxymethyl-1′H-1′,2′3′-triazol-1′-yl) methylestra-1,3,5(10)-trien-17α-ol (23f)

Compound **23e** (274 mg, 0.5 mmol) was dissolved in methanol (10 ml) containing NaOCH$_3$ (14 mg, 0.25 mmol), and the solution was allowed to stand for 24 h. It was then diluted with water, and the precipitate separating out was filtered off, dissolved in dichloromethane and washed with water. The organic phase was dried over Na$_2$SO$_4$, and evaporated *in vacuo* to afford **23f** (183 mg, 92%) as oil. R_f = 0.26 (ss B). (Found C, 69.28; H, 7.95. C$_{23}$H$_{31}$N$_3$O$_3$ (397.51) requires C, 69.49; H, 7.86%). ^{1}H NMR (δ, ppm, CDCl$_3$): 0.78 (s, 3H, 18-H$_3$), 2.85 (m, 2H, 6-H$_2$), 3.65 (s, 1H, 17-H), 3.77 (s, 3H, 3-OCH$_3$), 4.46 (m, 2H, 16a-H$_2$), 4.78 (s, 2H, 4′-H$_2$), 6.62 (d, 1H, J = 2.0 Hz, 4-H), 6.72 (dd, 1H, J = 8.5 Hz, J = 2.5 Hz, 2-H), 7.19 (d, 1H, J = 8.5 Hz, 1-H). ^{13}C NMR (δ, ppm, CDCl$_3$): 17.9 (C-18), 25.9, 27.9, 29.7, 30.3, 31.8, 38.5, 43.3, 45.2 (C-13), 48.8, 49.2, 54.6 (C-16a), 55.2 (3-OCH$_3$), 56.1 (4′-CH$_2$), 82.1 (C-17), 111.5 (C-2), 113.7 (C-4), 123.5 (C-5′), 126.3 (C-1), 132.4 (C-10), 137.8 (C-5), 157.4 (C-3).

2.3.19. 3-Methoxy-16a-(4′-cyclopropyl-1′H-1′,2′,3′-triazol-1′-yl) methylestra-1,3,5(10)-trien-17α-ol (24a)

Compound **16** (342 mg, 1 mmol) and cyclopropylacetylene (2 mmol, 0.22 ml) were used for the synthesis as described in Section 2.3. The crude product was chromatographed on silica gel with ethyl acetate/CH$_2$Cl$_2$ (2.5:97.5 v/v) to yield pure **24a** (310 mg, 76%) as a white solid. Mp: 165–166 °C; R_f = 0.40 (ss B). (Found C, 73.85; H, 8.34. C$_{25}$H$_{33}$N$_3$O$_2$ (407.55) requires C, 73.68; H, 8.16%). ^{1}H NMR (δ, ppm, CDCl$_3$): 0.74 (s, 3H, 18-H$_3$), 0.85 and 0.96 (2 × m, 4H, 2″- and 3″-H$_2$), 2.85 (m, 2H, 6-H$_2$), 3.63 (d, 1H, J = 5.0 Hz, 17-H), 3.77 (s, 3H, 3-OCH$_3$), 4.28 (dd, 1H, J = 13.0 Hz, J = 5.0 Hz, 16a-H$_2$), 4.59 (t, 1H, J = 12.0 Hz, 16a-H$_2$), 6.63 (d, 1H, J = 2.0 Hz, 4-H), 6.71 (dd, 1H, J = 8.5 Hz, J = 2.5 Hz, 2-H), 7.22 (d, 1H, J = 8.5 Hz, 1-H). ^{13}C NMR (δ, ppm, CDCl$_3$): 6.6 (C-1″), 7.7 and 7.8 (C-2″ and -3″), 17.1 (C-18), 26.0, 28.0, 28.9, 29.8, 31.2, 38.9, 42.3, 46.3 (C-16a), 47.0, 50.5 (C-13), 55.2 (3-OCH$_3$), 78.8 (C-17), 111.4 (C-2), 113.7 (C-4), 120.6 (C-5′), 126.3 (C-1), 132.5 (C-10), 137.9 (C-5), 149.8 (C-4′), 157.4 (C-3).

2.3.20. 3-Methoxy-16a-(4′-cyclopentyl-1′H-1′,2′,3′-triazol-1′-yl)methyl-estra-1,3,5(10)-trien-17α-ol (24b)

Compound **16** (342 mg, 1 mmol) and cyclopentylacetylene (2 mmol, 0.22 ml) were used for the synthesis as described in Section 2.3. The crude product was chromatographed on silica gel with ethyl acetate/CH$_2$Cl$_2$ (1:99 v/v) to yield pure **24b** (383 mg, 88%) as yellow crystalline product. Mp: 171–173 °C; R_f = 0.42 (ss B). (Found C, 74.67; H, 8.72. C$_{27}$H$_{37}$N$_3$O$_2$ (435.60) requires C, 74.45; H, 8.56%). ^{1}H NMR (δ, ppm, CDCl$_3$): 075 (s, 3H, 18-H$_3$), 1.25 (s, 8H, 2″-, 3″-, 4″- and 5″-H$_2$), 2.86 (m, 2H, 6-H$_2$), 3.18 (m, 1H, 1″-H), 3.64 (d, 1H, J = 5.0 Hz, 17-H), 3.77 (s, 3H, 3-OCH$_3$), 4.29 (dd, 1H, J = 13.5 Hz, J = 5.5 Hz, 16a-H$_2$), 4.62 (dd, 1H, J = 13.5 Hz, J = 11.5 Hz, 16a-H$_2$), 6.63 (d, 1H, J = 2.0 Hz, 4-H), 6.71 (dd, 1H, J = 8.5 Hz, J = 2.0 Hz, 2-H), 7.22 (d, 1H, J = 8.5 Hz, 1-H), 7.36 (s, 1H, 5′-H). ^{13}C NMR (δ, ppm, CDCl$_3$): 17.2 (C-18), 25.1 (C-3″ and -4″), 26.0, 28.0, 29.0, 29.7, 29.9, 31.2, 33.2, 36.7, 38.9, 42.4, 43.5, 46.3 (C-13), 47.0 (C-1″), 50.5 (C-16a), 55.2 (3-OCH$_3$), 78.8 (C-17), 111.4 (C-2), 113.8 (C-4), 120.6 (C-5′), 126.3 (C-1), 132.6 (C-10), 137.9 (C-5), 152.3 (C-4′), 157.4 (C-3).

2.3.21. 3-Methoxy-16a-(4′-cyclohexyl-1′H-1′,2′,3′-triazol-1′-yl) methylestra-1,3,5(10)-trien-17α-ol (24c)

Compound **16** (342 mg, 1 mmol) and cyclohexylacetylene (2 mmol, 0.22 ml) were used for the synthesis as described in Section 2.3. The crude product was chromatographed on silica gel with ethyl acetate/CH$_2$Cl$_2$ (1:99 v/v) to yield pure **24c** (162 mg, 36%) as yellow crystals. Mp: 208–210 °C; R_f = 0.42 (ss B). (Found C, 74.97; H, 8.56. C$_{28}$H$_{41}$N$_3$O$_2$ (449.63) requires C, 74.80; H, 8.74%). ^{1}H NMR (δ, ppm, CDCl$_3$): 0.75 (s, 3H, 18-H$_3$), 1.26 (s, 8H, 2″-, 3″-, 5″- and 6″-H$_2$), 2.88 (m, 2H, 6-H$_2$), 2.90 (m, 2H, 4″-H$_2$), 3.64 (d, 1H, J = 5.0 Hz, 17-H), 3.77 (s, 3H, 3-OCH$_3$), 4.29 (dd, 1H, J = 13.5 Hz, J = 5.0 Hz, 16a-H$_2$), 4.62

2.3.22. 3-Methoxy-16a-(4′-phenyl-1′H-1′,2′,3′-triazol-1′-yl)methylestra-1,3,5(10)-trien-17α-ol (24d)

Compound **16** 342 mg, 1 mmol) and phenylacetylene (2 mmol, 0.22 ml) were used for the synthesis as described in Section 2.3. The crude product was chromatographed on silica gel with CH$_2$Cl$_2$ yield pure **24d** (394 mg, 89%) as white solid. Mp: 189.5–191 °C; R_f = 0.46 (ss B). (Found C, 75.65; H, 7.67. C$_{28}$H$_{33}$N$_3$O$_2$ (443.58) requires C, 75.81; H, 7.50%). ^{1}H NMR (δ, ppm, CDCl$_3$): 0.75 (s, 3H, 18-H$_3$), 2.86 (m, 2H, 6-H$_2$), 3.68 (d, 1H, J = 5.0 Hz, 17-H), 3.78 (s, 3H, 3-OCH$_3$), 4.41 (dd, 1H, J = 13.5 Hz, J = 6.0 Hz, 16a-H$_2$), 4.69 (dd, 1H, J = 14.5 Hz, J = 10.5 Hz, 16a-H$_2$), 6.64 (d, 1H, J = 2.0 Hz, 4-H), 6.72 (dd, 1H, J = 8.5 Hz, J = 2.5 Hz, 2-H), 7.22 (d, 1H, J = 8.5 Hz, 1-H), 7.34 (t, 1H, J = 7.5 Hz, 4″-H), 7.43 (t, 2H, J = 7.5 Hz, 3″- and 5″-H), 7.83 (d, 2H, J = 7.5 Hz, 2″- and 6″-H), 7.88 (s, 1H, 5′-H). ^{13}C NMR (δ, ppm, CDCl$_3$): 17.1 (C-18), 26.0, 28.0, 29.8, 31.2, 38.9, 42.3, 43.5, 46.4 (C-13), 47.0, 50.7, 55.2 (3-OCH$_3$), 78.8 (C-17), 111.5 (C-2), 113.8 (C-4), 120.6 (C-5′), 125.6 (C-2″ and -6″), 126.3 (C-1), 128.1 (C-4″), 128.8 (C-3″ and -5″), 130.5 (C-1″), 132.5 (C-10), 137.9 (C-5), 147.3 (C-4′), 157.4 (C-3).

2.3.23. 3-Methoxy-16a-[4′-(4″nitrobenzoyloxymethyl)-1′H-1′,2′,3′-triazol-1′-yl]methylestra-1,3,5(10)-trien-17α-ol (24e)

Compound **16** (342, 1 mmol) and propargyl 4-nitrobenzoate (2 mmol, 210 mg) were used for the synthesis as described in Section 2.3. The crude product was chromatographed on silica gel with CH$_2$Cl$_2$/hexane (1:3, v/v) to yield pure (344 mg, 63%) as yellow crystals. Mp: 64 °C; R_f = 0.45 (ss B). (Found, C, 66.14; H, 6.05. C$_{30}$H$_{34}$N$_4$O$_6$ (546.61) requires C, 65.92; H, 6.27%). ^{1}H NMR (δ, ppm, CDCl$_3$): 0.75 (s, 3H, 18-H$_3$), 2.84 (m, 2H, 6-H$_2$), 3.66 (d, 1H, J = 4.5 Hz, 17-H), 3.77 (s, 3H, 3-OCH$_3$), 4.40 (dd, 1H, J = 13.5 Hz, J = 5.5 Hz, 16a-H$_2$), 4.66 (t, 1H, J = 13.5 Hz, 16a-H$_2$), 5.53 (s, 2H, 4′-H$_2$), 6.62 (t, 1H, J = 2.0 Hz, 4-H), 6.71 (dd, 1H, J = 8.5 Hz, J = 2.5 Hz, 2-H), 7.20 (d, 1H, J = 8.5 Hz, 1-H), 7.85 (s, 1H, 5′-H), 8.22 (d, 2H, J = 9.0 Hz, 3″- and 5″-H), 8.72 (d, 2H, J = 9.0 Hz, 2″- and 6″-H). ^{13}C NMR (δ, ppm, CDCl$_3$): 17.1 (C-18), 22.7, 25.9, 28.0, 29.0, 29.8, 31.2, 38.9, 42.0, 43.5, 46.4 (C-13), 47.0 (4′-CH2), 78.8 (C-17), 111.5 (C-2), 113.8 (C-4), 114.0 (C-1′), 123.5 (C-2″ and -6″) 126.3 (C-5′), 130.9 (C-3″ and -5″), 135.0 (C-10), 137.8 (C-5), 141.5 (C-4″), 150.6 (C-4′), 157.5 (C-3), 164.6 (C=O).

2.3.24. 3-Methoxy-16a-(4′-hydroxymethyl-1′H-1′,2′,3′-triazol-1′-yl) methylestra-1,3,5(10)-trien-17α-ol (24f)

Compound **24e** (274 mg, 0.5 mmol) was dissolved in methanol (10 ml) containing NaOCH$_3$ (14 mg, 0.25 mmol), and the solution was allowed to stand for 24 h. It was then diluted with water, and the precipitate separating out was filtered off and recrystallized from a mixture of acetone/hexane to afford **24f** (187 mg, 94%) as a white crystalline product. Mp: 149–150 °C; R_f = 0.25 (ss B). (Found C, 69.55; H, 7.95. C$_{23}$H$_{31}$N$_3$O$_3$ (397.51) requires C, 69.49; H, 7.86%). ^{1}H NMR (δ, ppm, CDCl$_3$): 0.74 (s, 3H, 18-H$_3$), 2.85 (m, 2H, 6-H$_2$), 3.62 (d, 1H, J = 4.0 Hz, 17-H), 3.77 (s, 3H, 3-OCH$_3$), 4.39 (m, 1H, 16a-H$_2$), 4.64 (m, 1H, 16a-H$_2$), 6.63 (s, 1H, 4-H), 6.71 (d, 1H, J = 8.5 Hz, 2-H), 7.21 (d, 1H, J = 8.5 Hz, 1-H), 7.77 (s, 1H, 5′-H). ^{13}C NMR (δ, ppm, CDCl$_3$): 11.9 (C-18), 26.0, 28.0, 28.9, 31.3, 31.9, 33.8 (C-13), 38.9, 41.9, 43.5, 46.4 (4′-CH$_2$), 46.9, 51.0 (C-16a), 55.2 (3-OCH$_3$), 78.6 (C-17), 111.5 (C-2), 113.8 (C-4), 123.4 (C-5′), 126.3 (C-1), 132.5 (C-10), 137.8 (C-5), 157.4 (C-3).

2.3.25. 3-Benzyloxy-16β-(4′-cyclopropyl-1′H-1′,2′,3′-triazol-1′-yl) methylestra-1,3,5(10)-trien-17β-ol (25a)

Compound **17** (420 mg, 1 mmol) and cyclopropylacetylene (2 mmol, 0.22 ml) were used for the synthesis as described in Section 2.3. The crude product was chromatographed on silica gel with ethyl acetate/CH$_2$Cl$_2$ (1:99 v/v) to yield pure **25a** (394 mg, 84%) as a white solid. Mp: 278–280 °C; R_f = 0.35 (ss B). (Found C, 77.16; H, 7.62. C$_{31}$H$_{37}$N$_3$O$_2$ (483.64) requires C, 76.98; H, 7.71%). ^{1}H NMR (δ, ppm, CDCl$_3$): 0.80 (s, 3H, 18-H$_3$), 0.86 and 0.97 (2 × m, 2 × 2H, 2″- and 3″-H), 2.83 (m, 2H, 6-H$_2$), 3.93 (d, J = 9.5 Hz, 1H, 17-H), 4.21 (m, 1H, 16a-H$_2$), 4.64 (m, 1H, 16a-H$_2$), 5.03 (s, 2H, Bn-H$_2$), 6.71 (s, 1H, 4-H), 6.78 (d, 1H, J = 8.5 Hz, 2-H), 7.20 (d, 1H, J = 8.5 Hz, 1-H), 7.31 (t, 1H, J = 7.0 Hz, 4′-H), 7.38 (t, 2H, J = 7.0 Hz, 3′- and 5′-H), 7.43 (d, 2H, J = 7.0 Hz, 2′- and 6′-H). ^{13}C NMR (δ, ppm, CDCl$_3$): 7.8 (C-2″ and -3″), 12.3 (C-18), 26.2, 27.4, 29.7, 30.8, 37.5, 38.0, 41.4, 43.9, 44.3 (C-13), 48.7 (C-16), 67.8 (C-16a), 69.9 (Bn-CH$_2$), 80.7 (C-17), 112.3 (C-2), 114.8 (C-4), 126.3 (C-1), 127.4 (C-2′ and -6′), 127.8 (C-4′), 128.5 (C-3′ and C-5′), 132.7 (C-10), 137.3 (C-1′), 137.8 (C-5), 156.8 (C-3).

2.3.26. 3-Benzyloxy-16β-(4′-cyclopentyl-1′H-1′,2′,3′-triazol-1′-yl) methylestra-1,3,5(10)-trien-17β-ol (25b)

Compound **17** (420 mg, 1 mmol) and cyclopentylacetylene (2 mol, 0.22 ml) were used for the synthesis as described in Section 2.3. The crude product was chromatographed on silica gel with ethyl acetate/CH$_2$Cl$_2$ (1:99 v/v) to yield pure **25b** (350 mg, 68%) as a white solid. Mp: 288–290 °C; R_f = 0.38 (ss B). Found C, 77.58; H, 7.92. C$_{33}$H$_{41}$N$_3$O$_2$ (511.70) requires C, 77.46; H, 8.08%). ^{1}H NMR (δ, ppm, CDCl$_3$): 0.79 (s, 3H, 18-H$_3$), 2.75 (s, 1H, 1″-H), 2.83 (m, 2H, 6-H$_2$), 3.94 (d, 1H, J = 9.5 Hz, 17-H), 4.24 (m, 1H, 16-H$_2$), 4.67 (m, 1H, 16-H$_2$), 5.03 (s., 2H, Bn-H$_2$), 6.71 (s, 1H, 4-H), 6.78 (d, 1H, J = 8.5 Hz, 2-H), 7.19 (d, 1H, J = 8.5 Hz, 1-H), 7.31 (t, 1H, J = 7.5 Hz, 4′-H), 7.38 (t, 2H, J = 7.5 Hz, 3′- and 5′-H), 7.42 (d, 2H, J = 7.5 Hz, 2′- and 6′-H). ^{13}C NMR (δ, ppm, CDCl$_3$): 12.3 (C-18), 25.1 (C-3″ and -4″), 26.2, 27.5, 29.7, 30.8, 34.3 (C-2″ and -5″), 37.5, 38.0, 41.4, 43.9, 44.3 (C-13), 48.7 (C-16), 62.1 (16a-CH$_2$), 69.9 (Bn-CH$_2$), 80.7 (C-17), 112.3 (C-2), 114.8 (C-4), 126.3 (C-1), 127.4 (C-2′ and -6′), 127.8 (C-4′), 128.5 (C-3′ and -5′), 132.7 (C-10), 137.3 (C-1′), 137.8 (C-5), 156.8 (C-3).

2.3.27. 3-Benzyloxy-16β-(4′-cyclohexyl-1′H-1′,2′,3′-triazol-1′-yl) methylestra-1,3,5(10)-trien-17β-ol (25c)

Compound **17** (420 mg, 1 mmol) and cyclohexylacetylene (2 mmol, 0.22 ml) were used for the synthesis as described in Section 2.3. The crude product was chromatographed on silica gel with ethyl acetate/CH$_2$Cl$_2$ (1:99, v/v) to yield pure **25c** (146 mg, 28%) as a white solid. Mp: 214–216 °C; R_f = 0.38 (ss B). (Found C, 77.43; H, 8.36. C$_{34}$H$_{43}$N$_3$O$_2$ (525.72) requires C, 77.68; H, 8.24%). ^{1}H NMR (δ, ppm, CDCl$_3$): 0.79 (s, 3H, 18-H$_3$), 2.79 (m, 4H, 3″- and 5″-H), 3.94 (d, J = 9.5 Hz, 1H, 17-H), 4.25 (m, 1H, 16a-H$_2$), 4.67 (m, 1H, 16a-H$_2$), 5.03 (s, 2H, Bn-H$_2$), 6.71 (s, 1H, 4-H), 6.78 (d, 1H, J = 8.5 Hz, 2-H), 7.19 (d, 1H, J = 8.5 Hz, 1-H), 7.32 (d, 1H, J = 7.0 Hz, 4′-H), 7.38 (t, 2H, J = 7.0 Hz, 3′- and 5′-H), 7.42 (d, 2H, J = 7 Hz, 2′- and 6′-H). ^{13}C NMR (δ, ppm, CDCl$_3$): 12.3 (C-18), 26.0 (C-4″), 26.1 (C-3″ and -5″), 26.2, 27.5, 29.7, 30.8 (C-2″ and -6″), 33.0 (C-1″), 37.5, 38.0, 41.4, 43.9, 44.3 (C-13), 48.7 (C-16), 62.1 (C-16a), 69.9 (Bn-CH$_2$), 80.7 (C-17), 112.3 (C-2), 114.8 (C-4), 126.3 (C-1), 127.4 (C-2′ and -6′), 127.8 (C-4′), 128.5 (C-3′ and -5′), 132.7 (C-10), 137.3 (C-1′), 137.8 (C-5), 157.8 (C-3).

2.3.28. 3-Benzyloxy-16β-(4′-phenyl-1′H-1′,2′,3′-triazol-1′-yl) methylestra-1,3,5(10)-trien-17β-ol (25d)

Compound **17** (420 mg, 1 mmol) and phenylacetylene (2 mmol, 0.22 ml) were used for the synthesis as described in Section 2.3. The crude product was chromatographed on silica gel with ethyl acetate/CH$_2$Cl$_2$ (5:95 v/v) to yield pure **25d** (391 mg, 75%) as a white solid. Mp: 202–204 °C; R_f = 0.45 (ss B). (Found C, 78.73; H, 6.98. C$_{34}$H$_{37}$N$_3$O$_2$ (519.68) requires C, 78.58; H, 7.18%). ^{1}H NMR (δ, ppm,

C$_6$D$_6$): 0.68 (s, 3H, 18-H$_3$), 2.69 (m, 2H, 6-H$_2$), 3.43 (dd, J = 9.5 Hz, J = 4 Hz, 1H, 17-H), 3.77 (dd, 1H, J = 13.5 Hz, J = 7.0 Hz, 16a-H$_2$), 4.29 (dd, 1H, J = 13.5 Hz, J = 7.0 Hz, 16a-H$_2$), 4.83 (s, 2H, Bn-H$_2$), 6.79 (s, 1H, 4-H), 6.87 (d, 1H, J = 8.0 Hz, 2-H), 7.02 (s, 1H, 1-H), 7.08 (t, 1H, J = 7.5 Hz, 4′-H), 7,26 (t, 2H, J = 7.5 Hz, 3′- and 5′-H), 7.32 (d, 2H, J = 7.5 Hz, 2′- and 6′-H), 8.01 (d, 2H, J = 7.5 Hz, 2″- and 6″-H).

2.3.29. 3-Benzyloxy-16β-[4′-(4″-nitro-benzoyloxymethyl)-1′H-1′,2′,3′-triazol-1′-yl]methyestra-1,3,5(10)-trien-17β-ol (25e)

Compound **17** (420 mg, 1 mmol) and propargyl 4-nitrobenzoate (2 mmol, 210 mg) were used for the synthesis as described in Section 2.3. The crude product was chromatographed on silica gel ethyl acetate/CH$_2$Cl$_2$ (5:95 v/v) to yield pure **25e** (480 mg, 77%) as a yellow solid. Mp: 187–189 °C; R_f = 0.45 (ss B). (Found C, 69.32; 5.98. C$_{36}$H$_{38}$N$_4$O$_6$ (622.71) requires C, 69.44; H, 6.15%). ^{1}H NMR (δ, ppm, CDCl$_3$): 0.80 (s, 3H, 18-H$_3$), 2.82 (m, 2H, 6-H$_2$), 3.94 (d, J = 10.0 Hz, 1H, 17-H), 4.32 (dd, 1H, J = 13.0 Hz, J = 6.0 Hz, 16a-H$_2$), 4.72 (t, 1H, J = 6.0 Hz, 16a-H$_2$), 5.03 (s, 2H, Bn-H$_2$), 5.52 (s, 2H, triazol-H), 6.71 (s, 1H, 4-H), 6.78 (d, 1H, J = 8.5 Hz, 2-H), 7.19 (d, 1H, J = 8.5 Hz, 1-H), 7.32 (t, 1H, J = 7.0 Hz, 4′-H), 7.38 (t, J = 7.5 Hz, 2H, 3′- and 5′-H), 7.42 (d, 2H, J = 7.5 Hz, 2′- and 6′-H), 8.22 (d, J = 8 Hz, 2H, 3″- and 5″-H), 8.27 (d, J = 8 Hz, 2H, 2″- and 6″-H). ^{13}C NMR (δ, ppm, CDCl$_3$): 12.3 (C-18), 26.2, 27.4, 29.7, 30.8, 37.4, 38.0, 41.2, 43.8, 44.4 (C-13), 48.7 (C-16), 55.5 (C-16a), 58.7 (linker-CH$_2$), 69.9 (Bn-CH$_2$), 80.7 (C-17), 112.4 (C-2), 114.8 (C-4), 123.5 (C-2′ and -6′), 126.3 (C-1), 127.4 (C-2″ and -6″), 127.8 (C-4′), 128.5 (C-3″ and -5″), 130.9 (C-3′ and -5′), 132.5 (C-10), 135.1 (C-1″), 137.3 (C-1′), 137.8 (C-5), 150.7 (C-4″), 156.8 (C-3), 164.6 (C=O).

2.3.30. 3-Benzyloxy-16β-(4′-hydroxymethyl-1′H-1′,2′,3′-triazol-1′-yl) methylestra-1,3,5(10)-trien-17β-ol (25f)

Compound **25e** (210 mg, 0.5 mmol) was dissolved in methanol (10 ml) containing NaOCH$_3$ (14 mg, 0.25 mmol), and the solution was allowed to stand for 24 h. It was then diluted with water, and the precipitate separating out was filtered off and recrystallized from methanol to afford **25f** (232 mg, 98%) as a white crystalline product. Mp: 283–285 °C; R_f = 0.25 (ss B). (Found C, 73.42; H, 7.35. C$_{29}$H$_{35}$N$_3$O$_3$ (473.61) requires C, 73.54; H, 7.45%). ^{1}H NMR (δ, ppm, DMSO-d_6): 0.77 (s, 3H, 18-H$_3$), 3.77 (dd, 1H, J = 9.5 Hz, J = 3.5 Hz, 16a-H$_2$), 4.15 (t, 1H, J = 12.5 Hz, 16a-H$_2$), 5.12 (d, 1H, J = 5.5 Hz, 17-H), 6.68 (s, 1H, 4-H), 6.74 (d, 1H, J = 8.5 Hz, 2-H), 7.16 (d, J = 8.5 Hz, 1H, 1-H), 7.31 (d, 1H, J = 7.0 Hz, 4′-H), 7.37 (t, 2H, J = 7.0 Hz, 3′- and 5′-H), 7.41 (d, 2H, J = 7.0 Hz., 2′- and 6′-H), 7.98 (s, 1H, triazol-H). ^{13}C NMR (δ, ppm, DMSO-d_6): 12.3 (C-18), 25.8, 26.9, 29.1, 30.0, 36.9, 37.8, 40.4, 43.4, 43.7 (C-13), 47.8 (C-16a), 55.0 (linker-CH$_2$), 68.9 (Bn-CH$_2$), 79.5 (C-17), 112.1 (C-2), 114.4 (C-4), 122.7 (triazol-CH), 126.0 (C-1), 127.4 (C-2′ and -6′), 127.6 (C-4′), 128.3 (C-3′ and -5′), 132.3 (C-10), 137.3 (C-5), 147.6 (triazol-C), 156.0 (C-3).

2.3.31. 3-Benzyloxy-16a-(4′-cyclopropyl-1′H-1′,2,′3′-triazol-1′-yl) methylestra-1,3,5(10)-trien-17β-ol (26a)

Compound **18** (420.0 mg, 1 mmol) and cyclopropylacetylene (2 mmol, 0.22 ml) were used for the synthesis as described in Section 2.3. The crude product was chromatographed on silica gel with ethyl acetate/CH$_2$Cl$_2$ (1:99 v/v) to yield pure **26a** (310 mg, 64%) as a white solid. Mp: 191–193 °C; R_f = 0.35 (ss B). (Found C, 76.82; H, 7.94. C$_{31}$H$_{37}$N$_3$O$_2$ (483.64) requires C, 76.98; H, 7.71%). ^{1}H NMR (δ, ppm, CDCl$_3$): 0.83 (s, 3H, 18-H$_3$), 2.83 (m, 2H, 6-H$_2$), 3.54 (d, J = 7.5 Hz, 1H, 17-H), 4.35 (dd, 1H, J = 13.0 Hz, J = 7.5 Hz, 16a-H$_2$), 4.44 (dd, 1H, J = 13.0 Hz, J = 7.5 Hz, 16a-H$_2$), 5.03 (s, 2H, Bn-H$_2$), 6.71 (s, 1H, 4-H), 6.77 (d, 1H, J = 8.5 Hz, 2-H), 7.19 (d, 1H, J = 8.5 Hz, 1-H), 7.31 (t, 2H, J = 7.5 Hz, 4′-H and triazol-H), 7.38 (t, 2H, J = 7.5 Hz, 3′- and 5′-H), 7.42 (d, 2H, J = 7.5 Hz, 2′- and 6′-H). ^{13}C NMR (δ, ppm, CDCl$_3$): 6.6 (C-1″), 7.8 (C-2″ and -3″), 11.8 (C-18), 26.1, 27.2, 28.2, 29.7, 36.6, 38.4, 43.9, 44.3, 44.3 (C-13), 48.3 (C-16), 54.5 (C-16a), 69.9 (Bn-CH$_2$), 85.2 (C-17), 112.3 (C-2), 114.8 (C-4), 120.0 (triazol-CH), 126.3 (C-1), 127.4

(C-2′ and -6′), 127.8 (C-4′), 128.5 (C-3′ and -5′), 132.6 (C-10), 137.3 (C-1′), 137.8 (C-5), 150.2 (triazol-C), 156.8 (C-3).

2.3.32. 3-Benzyloxy-16α-(4′-cyclopentyl-1′H-1′,2′,3′-triazol-1′-yl) methylestra-1,3,5(10)-trien-17β-ol (26b)

Compound **18** (420 mg, 1 mmol) and cyclopentylacetylene (2 mmol, 0.22 ml) were used for the synthesis as described in Section 2.3. The crude product was chromatographed on silica gel with ethyl acetate/CH$_2$Cl$_2$ (1:99 v/v) to yield pure **26b** (442 mg, 86%) as a white solid. Mp: 268–270 °C; R_f = 0.36 (ss B). (Found C, 77.52; H, 7.93. C$_{33}$H$_{41}$N$_3$O$_2$ (511.70) requires C, 77.46; H, 8.08%). ^{1}H NMR (δ, ppm, CDCl$_3$): 0.83 (s, 3H, 18-H$_3$), 2.83 (m, 2H, 6-H$_2$), 3.19 (s, 1H, 1″-H), 3.46 (d, 1H, J = 7.0 Hz, 17-H), 4.42 (dd, 2H, J = 22.5 Hz, J = 6.5 Hz, 16-H$_2$), 5.03 (s, 2H, Bn-H$_2$), 6.71 (s, 1H, 4-H), 6.76 (d, 1H, J = 8.5 Hz, 2-H), 7.19 (d, 1H, J = 8.5 Hz, 1-H), 7.31 (t, 1H, J = 7.5 Hz, 4′-H), 7 0.37 (t, 3H, J = 7.5 Hz, 3′-, 5′-H and triazol-H), 7.42 (d, 2H, J = 7.5 Hz, 2′- and 6′-H). ^{13}C NMR (δ, ppm, CDCl$_3$): 11.9 (C-18), 25.1 (C-3″ and -4″), 26.1, 27.2, 28.3, 29.7, 33.2 (C-2″ and -5″), 36.6 (2C, C-1″), 36.7, 38.4, 43.9, 44.3 (C-13), 48.4 (C-16), 54.5 (C-16a), 69.9 (Bn-CH$_2$), 85.2 (C-17), 112.3 (C-2), 114.8 (C-4), 126.3 (C-1), 127.4 (C-3′ and -5′), 127.8 (C-4′), 128.5 (C-2′ and -6′), 132.6 (C-10), 137.3 (C-1′), 137.8 (C-5), 156.7 (C-3).

2.3.33. 3-Benzyloxy-16α-(4′-cyclohexyl-1′H-1′,2′,3′-triazol-1′-yl) methylestra-1,3,5(10)-trien-17β-ol (26c)

Compound **18** (420 mg, 1 mmol) and cyclohexylacetylene (2 mmol, 0.22 ml) were used for the synthesis as described in Section 2.3. The crude product was chromatographed on silica gel with ethyl acetate/CH$_2$Cl$_2$ (2.5:77.5 v/v) to yield pure **26c** (386 mg, 76%) as a white solid. Mp: 261–263 °C; R_f = 0.34 (ss B). (Found C, 77.93; H, 8.36. C$_{34}$H$_{43}$N$_3$O$_2$ (525.72) requires C, 77.68; H, 8.24%). ^{1}H NMR (δ, ppm, CDCl$_3$): 0.83 (s, 3H, 18-H$_3$), 2.83 (m, 2H, 6-H$_2$), 3.55 (d, 1H, 17-H), 4.43 (m, 2H, 16-H$_2$), 5.03 (s, 2H, Bn-H$_2$), 6.71 (s, 1H, 4-H), 6.77 (d, 1H, J = 8.5 Hz, 2-H), 7.19 (d, 1H, J = 8.5 Hz, 1-H), 7.31 (t, 2H, J = 7.0 Hz, 4′-H and triazol-H), 7.37 (t, 2H, J = 7.0 Hz. 3′- and 5′-H), 7.42 (d, 2H, J = 7 Hz, 2′- and 6′-H). ^{13}C NMR (δ, ppm, CDCl$_3$): 11.9 (C-18), 25.9 (C-4″), 26.1 (C-3″ and -5″), 27.2, 28.3, 29.7 (C-2″ and -6″), 32.9, 33.0, 36.6, 38.4, 43.9, 44.2, 44.3 (C-13), 48.4 (C-16), 54.5 (C-16a), 69.9 (Bn-CH$_2$), 85.2 (C-17), 112.3 (C-2), 114.8 (C-4), 126.3 (C-1), 127.4 (C-2′ and -6′), 127.8 (C-4′), 128.5 (C-3′ and -5′), 132.6 (C-10), 137.3 (C-1′), 137.8 (C-5), 156.7 (C-3).

2.3.34. 3-Benzyloxy-16α-(4′-phenyl-1′H-1′,2′,3′-triazol-1′-yl) methylestra-1,3,5(10)-trien-17β-ol (26d)

Compound **18** (420 mg, 1 mmol) and phenylacetylene (2 mmol, 0.22 ml) were used for the synthesis as described in Section 2.3. The crude product was chromatographed on silica gel with ethyl acetate/CH$_2$Cl$_2$ 5:95 v/v) to yield pure **26d** (372 mg, 71%) as a white solid. Mp: 132–134 °C; R_f = 0.38 (ss B). (Found C, 78.63; H, 6.97. C$_{34}$H$_{37}$N$_3$O$_2$ (519.68) requires C, 78.58; H, 7.18%). ^{1}H NMR (δ, ppm, CDCl$_3$): 0.84 (s, 3H, 18-H$_3$), 2.83 (m, 2H, 6-H$_2$), 3.58 (d, 1H, J = 7.5 Hz, 17-H), 4.46 (dd, 2H, J = 13.5 Hz, J = 8.0 Hz, 16a-H$_2$), 4.55 (dd, 1H, J = 13.5 Hz, J = 8.0 Hz, 16a-H2) 5.03 (s, 2H, Bn-H$_2$), 6.71 (s, 1H, 4-H), 6.78 (d, 1H, J = 8.5 Hz, 2-H), 7.19 (d, 1H, J = 8.5 Hz, 1-H), 7.30–7.86 (m, 11H, 2′-, 6′-, 3′-, 5′-, 4′-, 2″-, 6″-, 3″-, 5″-, 4″- and triazol-H). ^{13}C NMR (δ, ppm, CDCl$_3$): 11.8 (C-18), 26.1, 27.2, 28.2, 29.6, 36.5, 38.4, 43.9, 44.3, 48.3 (C-16), 54.6 (C-16a), 62.1, 69.9 (Bn-CH$_2$), 85.2 (C-17), 112.3 (C-2), 114.8 (C-4), 123.8 (triazol-CH), 125.7 (C-2′ and -6′), 126.3 (C-1′), 127.4 (C-2″ and -6″), 127.8 (C-4′), 128.2 (C-4), 128.5 (C-3″ and -5″), 128.8 (C-3′ and -5′), 130.4 (C-10), 132.6 (C-1″), 137.3 (C-1′), 137.8 (C-5), 156.8 (C-3).

2.3.35. 3-Benzyloxy-16α-[4′-(4″-nitro-benzoyloxymethyl)-1′H-1′,2′,3′-triazol-1′-yl]methylestra-1,3,5(10)-trien-17β-ol (26e)

Compound **18** (420 mg, 1 mmol) and propargyl 4-nitrobenzoate (2 mmol, 210 mg) were used for the synthesis as described in Section

2.3. The crude product was chromatographed on silica gel with ethyl acetate/CH$_2$Cl$_2$ (5:95 v/v) to yield pure **26e** (484 mg, 77%) as a yellow solid. Mp: 94–96 °C; R_f = 0.40 (ss B). (Found C, 69.73; H, 5.94. C$_{36}$H$_{38}$N$_4$O$_6$ (622.71) requires C, 69.44; H, 6.15%). ^{1}H NMR (δ, ppm, DMSO-d_6): 0.70 (s, 3H, 18-H$_3$), 3.33 (m, 2H, 6-H$_2$), 4.38 (dd, 1H, J = 13.5 Hz, J = 9.0 Hz, 16a-H$_2$), 4.52 (dd, 1H, J = 13.5 Hz, J = 5.0 Hz, 16a-H$_2$), 4.86 (d, 1H, J = 5 Hz, 17-H), 5.02 (s, 2H, Bn-H$_2$), 5.47 (s, 2H, linker-H$_2$), 6.64 (d, 1H, J = 2.0 Hz, 4-H), 6.72 (dd, 1H, J = 8.5 Hz, J = 2.0 Hz, 2-H), 7.10 (d, 1H, J = 8.5 Hz, 1-H), 7.31 (t, 1H, J = 7.0 Hz, 4′-H), 7.37 (t, 2H, J = 7.0 Hz, 3′- and 5′-H), 7.42 (d, 2H, J = 7.0 Hz, 2′- and 6′-H), 8.16 (d, 2H, J = 9.0 Hz, 3″- and 5″-H), 8.28 (d, 2H, J = 9.0 Hz, 2″- and 6″-H), 8.32 (s, 1H, triazol-H). ^{13}C NMR (δ, ppm, DMSO-d_6): 11.7 (C-18), 25.7, 26.6, 27.1, 29.0, 30.6, 36.4, 37.9, 43.4, 43.4 (C-13), 43.7 (C-16), 53.1 (C-16a), 58.6 (linker-CH$_2$), 68.9 (Bn-CH$_2$), 82.8 (C-17), 112.1 (C-2), 114.3 (C-4), 123.7 (C-2′ and -6′), 125.1 (triazol-CH), 125.9 (C-1), 127.4 (C-2″ and -6″), 127.5 (C-4′), 128.3 (C-3″ and -5″), 130.6 (C-3′ and -5′), 132.1 (C-10), 134.7 (C-1″), 137.2 (C-1′), 137.3 (C-5), 141.1 (triazol-C), 150.1 (C-4″), 155.9 (C-3), 163.9 (C=O).

2.3.36. 3-Benzyloxy-16α-(4′-hydroxymethyl-1′H-1′,2′,3′-triazol-1′-yl) methylestra-1,3,5(10)-trien-17β-ol (26f)

Compound **26e** (210 mg, 0.5 mmol) was dissolved in methanol (10 ml) containing NaOCH$_3$ (14 mg, 0.25 mmol), and the solution was allowed to stand for 24 h. It was then diluted with water, and the precipitate separating out was filtered off and recrystallized from a mixture of acetone/hexane to afford **26f** (190 mg, 89%) as a white crystalline product. Mp: 152–154 °C; R_f = 0.20 (ss B). (Found C, 73.72; H, 7.63. C$_{29}$H$_{35}$N$_3$O$_3$ (473.61) requires C, 73.54; H, 7.45%). ^{1}H NMR (δ, ppm, DMSO-d_6): 0.71 (s, 3H, 18-H$_3$), 2.73 (m, 2H, 6H$_2$), 3.29 (d, J = 8.0 Hz, 1H, 17-H), 4.28 (dd, 2H, J = 13.0 Hz, J = 10.0 Hz, 16a-H$_2$), 4.47 (dd, 1H, J = 13.0 Hz, J = 4.5 Hz, 16a-H$_2$), 4.51 (s, 2H, Bn-H$_2$), 4.87 (s, 1H, linker-H$_2$), 5.03 (s, 2H, triazol-H$_2$), 5.15 (s, 1H, linker-H$_2$), 6.68 (s, 1H, 4-H), 6.74 (d, 1H, J = 8.5 Hz, 2-H), 7.15 (d, 1H, J = 8.5 Hz, 1-H), 7.31 (t, 1H, J = 7.0 Hz, 4′-H), 7.37 (t, 2H, J = 7.0 Hz, 3′- and 5′-H), 7.41 (d, 2H, J = 7.0 Hz, 2′- and 6′-H), 7.97 (s, 1H, triazol-H). ^{13}C NMR (δ, ppm, DMSO-d_6): 11.8 (C-18), 25.8, 26.7, 27.3, 29.1, 36.4, 38.1, 43.4, 43.5 (C-13), 43.9, 47.5 (C-16), 53.1 (C-16a), 54.9 (linker-CH$_2$), 68.9 (Bn-CH$_2$), 83.0 (C-17), 112.1 (C-2), 114.4 (C-4), 122.7 (triazol-CH), 126.0 (C-1), 127.4 (C-2′ and -6′), 127.6 (C-4′), 128.3 (C-3′ and -5′), 132.3 (C-10), 137.3 (C-1′), 137.4 (C-5), 147.6 (triazol-C), 156.0 (C-3).

2.3.37. 3-Benzyloxy-16β-(4′-cyclopropyl-1′H-1′,2′,3′-triazol-1′-yl) methylestra-1,3,5(10)-trien-17α-ol (27a)

Compound **19** (420.0 mg, 1 mmol) and cyclopropylacetylene (2 mmol, 0.22 ml) were used for the synthesis as described in Section 2.3. The crude product was chromatographed on silica gel with ethyl acetate/CH$_2$Cl$_2$ (5:95 v/v) to yield pure **27a** (454 mg, 93%) as white crystals. Mp: 199–201 °C; R_f = 0.38 (ss B). (Found C, 77.15; H, 7.62. C$_{31}$H$_{37}$N$_3$O$_2$ (483.64) requires C, 76.98; H, 7.71%). ^{1}H NMR (δ, ppm, CDCl$_3$): 0.77 (s, 3H, 18-H$_3$), 0.87 and 0.98 (2 × s, 2 × 2H, 2″- and 3″-H$_2$), 2.05 (s, 1H, 1″-H), 2.84 (m, 2H, 6-H$_2$), 3.66 (s, 1H, 17-H), 4.42 (m, 2H, 16a-H$_2$), 5.03 (s, 2H, Bn-H$_2$), 6.71 (s, 1H, 4-H), 6.78 (d, 1H, J = 8.5 Hz, 2-H), 7.21 (d, 1H, J = 8.5 Hz, 1-H), 7.31 (t, 1H, J = 7.0 Hz, 4′-H), 7.38 (t, 2H, J = 7.0 Hz, 3′- and 5′-H), 7.43 (d, 2H, J = 7.0 Hz, 2′- and 6′-H). ^{13}C NMR (δ, ppm, CDCl$_3$): 6.7 (C-1″), 7.7 (C-2″ and -3″), 17.9 (C-18), 25.9, 27.9, 29.7, 30.4, 31.8, 38.5, 43.3, 45.1 (C-13), 48.9, 49.1 (C-16), 62.1 (C-16a), 69.9 (Bn-CH$_2$), 82.6 (C-17), 112.3 (C-2), 114.8 (C-4), 126.3 (C-1), 127.4 (C-2′ and -6′), 127.8 (C-4′), 128.5 (C-3′ and -5′), 132.7 (C-10), 137.3 (C-1′), 137.9 (C-5), 156.7 (C-3).

2.3.38. 3-Benzyloxy-16β-(4′-cyclopentyl-1′H-1′,2′,3′-triazol-1′-yl) methylestra-1,3,5(10)-trien-17α-ol (27b)

Compound **19** (420 mg, 1 mmol) and cyclopentylacetylene (2 mmol, 0.22 ml) were used for the synthesis as described in Section 2.3. The
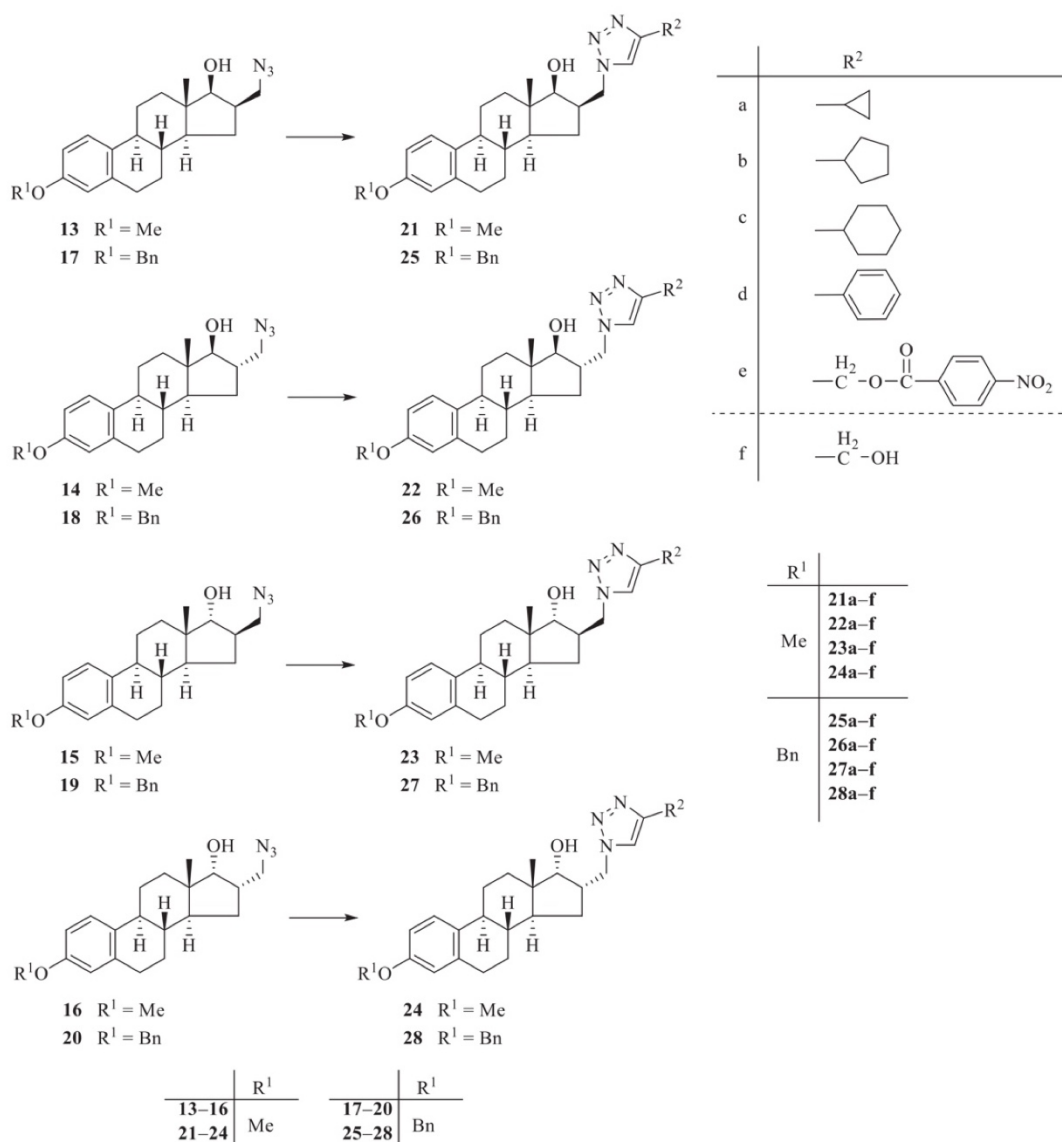
Scheme 2. Reagents and conditions: (i) appropriate alkyne, TEA, CuI, CH_2Cl_2, 40 °C, 24 h; (ii) NaOMe, MeOH, 24 h.

crude product was chromatographed on silica gel with ethyl acetate/ CH_2Cl_2 (5:95 v/v) to yield pure **27b** (408 mg, 79%) as white crystalline. Mp: 220–222 °C; $R_f = 0.40$ (ss B). (Found C, 77.32; H, 7.93. $C_{33}H_{41}N_3O_2$ (511.70) requires C, 77.46; H, 8.08%). ^{1}H NMR (δ, ppm, $CDCl_3$): 0.76 (s, 3H, 18-H_3), 2.84 (m, 2H, 6-H_2), 3.20 (s, 1H, 1″-H), 3.67 (s, 1H, 17-H), 4.43 (m, 2H, 16a-H_2), 5.03 (s, 2H, Bn-H_2), 6.72 (s, 1H, 4-H), 6.78 (dd, 1H, $J = 8.5$ Hz, $J = 2.0$ Hz, 2-H), 7.21 (d, 1H, $J = 8.5$ Hz, 1-H), 7.31 (t, 1H, $J = 7.0$ Hz, 4′-H), 7.38 (t, 3H, $J = 7.0$ Hz, 3′- and 5′-H, triazol-H), 7.43 (d, 2H, $J = 7.0$ Hz, 2′- and 6′-H). ^{13}C NMR (δ, ppm, $CDCl_3$): 18.0 (C-18), 25.1 (C-3″ and -5″), 25.9, 28.0, 29.7, 30.4, 31.8 (C-2″ and -6″), 33.2, 36.7, 38.5, 43.3, 45.1 (C-13), 48.9 (C-16), 49.1 (C-1″), 54.3 (C-16a), 69.9 (Bn-CH_2), 82.6 (C-17), 112.3 (C-2), 114.8 (C-4), 126.3 (C-1), 127.4 (C-2′ and -6′), 127.8 (C-4′), 128.5 (C-3′ and -5′), 132.7 (C-10), 137.3 (C-1′), 137.9 (C-5), 156.7 (C-3).

*2.3.39. 3-Benzyloxy-16β-(4′-cyclohexyl-1′H-1′,2′,3′-triazol-1′-yl) methylestra-1,3,5(10)-trien-17α-ol (**27c**)*

Compound **19** (420 mg, 1 mmol) and cyclohexylacetylene (2 mmol, 0.22 ml) were used for the synthesis as described in Section 2.3. The crude product was chromatographed on silica gel with ethyl acetate/ CH_2Cl_2 (5:95 v/v) to yield pure **27c** (360 mg, 68%) as white crystalline product. Mp: 243–245 °C; $R_f = 0.38$ (ss B). (Found C, 77.54; H, 8.38. $C_{34}H_{43}N_3O_2$ (525.72) requires C, 77.68; H, 8.24%). ^{1}H NMR (δ, ppm, $CDCl_3$): 0.75 (s, 3H, 18-H_3), 2.84 (m, 2H, 6-H_2), 3.68 (s, 1H, 17-H), 4.44 (m, 2H, 16a-H_2), 5.03 (s, 2H, Bn-H_2), 6.72 (s, 1H, 4-H), 6.78 (d, 1H, $J = 8.5$ Hz, 2-H), 7.21 (d, 1H, $J = 8.5$ Hz, 1-H), 7.32 (t, 1H, $J = 7.0$ Hz, 4′-H), 7.38 (t, 3H, $J = 7.0$ Hz, 3′- and 5′-H, triazol-H), 7.43 (d, 2H, $J = 7.0$ Hz, 2′- and 6′-H). ^{13}C NMR (δ, ppm, $CDCl_3$): 17.9 (C-18), 25.9 (C-4″), 26.0, 26.1 (C-3″ and -5″), 27.9, 29.7, 30.4, 31.8 (C-2″ and -6″), 32.1, 32.9 (C-1″), 38.5, 43.3, 45.1 (C-13), 48.9, 49.1 (C-16), 62.1 (C-16a), 69.9 (Bn-CH_2), 82.5 (C-17), 112.3 (C-2), 114.7 (C-4), 126.3 (C-1), 127.4 (C-2′ and -6′), 127.8 (C-4′), 128.5 (C-3′ and -5′), 132.7 (C-10),

9

Table 1
Antiproliferative activities of compounds **21a-f, 22a-f, 23a-f** and **24a-f**.

Growth Inhibition, % ± SEM [calculated IC$_{50}$ (µM)]

	Conc. (µM)	HeLa	SiHa	MCF-7	MDA-MB-231
21					
a	10	< 20	21.28 ± 1.88	< 20	< 20
	30	< 20	28.71 ± 2.20	46.42 ± 1.47	< 20
b	10	< 20	< 20	< 20	< 20
	30	39.86 ± 0.38	< 20	57.42 ± 1.77	29.88 ± 1.57
c	10	< 20	< 20	< 20	< 20
	30	40.22 ± 1.02	< 20	70.84 ± 1.55	37.96 ± 1.55
d	10	< 20	< 20	< 20	< 20
	30	44.16 ± 0.48	< 20	54.93 ± 1.78	38.28 ± 1.84
e	10	< 20	23.91 ± 1.61	34.23 ± 3.10	< 20
	30	37.18 ± 1.65	54.72 ± 0.48	76.26 ± 0.72	35.93 ± 2.13
f	10	< 20	28.06 ± 1.99	29.45 ± 1.67	< 20
	30	41.03 ± 0.77	57.69 ± 1.12	70.23 ± 1.35	34.81 ± 2.88
22					
a	10	< 20	25.55 ± 1.01	< 20	< 20
	30	< 20	34.78 ± 2.47	57.43 ± 1.91	< 20
b	10	< 20	< 20	< 20	< 20
	30	< 20	26.57 ± 2.26	67.59 ± 1.65	< 20
c	10	< 20	< 20	< 20	< 20
	30	< 20	29.90 ± 2.59	69.68 ± 0.77	< 20
d	10	< 20	< 20	< 20	< 20
	30	< 20	29.96 ± 1.79	70.75 ± 1.05	14.54 ± 1.32
e	10	< 20	< 20	< 20	< 20
	30	< 20	38.69 ± 2.09	63.12 ± 2.14	< 20
f	10	< 20	< 20	22.02 ± 1.61	< 20
	30	< 20	37.79 ± 1.04	50.94 ± 1.55	< 20
23					
a	10	< 20	< 20	< 20	< 20
	30	31.14 ± 1.28	< 20	28.72 ± 0.93	25.08 ± 3.15
b	10	< 20	< 20	< 20	< 20
	30	58.25 ± 2.03	< 20	48.01 ± 1.31	< 20
c	10	< 20	30.97 ± 2.69	< 20	< 20
	30	< 20	33.89 ± 2.35	< 20	< 20
d	10	< 20	< 20	< 20	< 20
	30	26.90 ± 2.15	< 20	63.27 ± 0.82	< 20
e	10	< 20	< 20	< 20	< 20
	30	< 20	37.53 ± 3.00	33.94 ± 0.75	28.19 ± 0.96
f	10	< 20	29.13 ± 1.59	< 20	< 20
	30	26.61 ± 0.57	43.85 ± 3.32	38.45 ± 1.93	43.85 ± 3.32
24					
a	10	< 20	< 20	< 20	< 20
	30	89.01 ± 0.47	< 20	78.65 ± 0.78	46.21 ± 1.54
b	10	< 20	< 20	< 20	< 20
	30	34.18 ± 0.81	< 20	31.07 ± 2.36	< 20
c	10	< 20	< 20	< 20	< 20
	30	49.11 ± 0.55	< 20	43.22 ± 1.52	< 20
d	10	< 20	< 20	< 20	< 20
	30	42.13 ± 1.66	< 20	55.41 ± 0.76	< 20
e	10	< 20	< 20	< 20	< 20
	30	83.66 ± 0.34	42.06 ± 2.50	70.11 ± 1.06	50.27 ± 2.00
f	10	< 20	< 20	22.34 ± 2.06	< 20
	30	84.77 ± 1.18	29.80 ± 1.66	68.27 ± 1.19	47.74 ± 1.21
cisplatin	10	42.61 ± 2.33	86.84 ± 0.50	53.03 ± 2.29	20.84 ± 0.81
	30	99.93 ± 0.26	90.18 ± 1.78	86.90 ± 1.24	74.47 ± 1.20
		[12.43]	[7.84]	[5.78]	[19.13]

137.2 (C-1′), 137.9 (C-5), 156.7 (C-3).

2.3.40. 3-Benzyloxy-16β-(4′-phenyl-1′H-1′,2′,3′-triazol-1′-yl)methylestra-1,3,5(10)-trien-17α-ol (27d)

Compound **19** (420 mg, 1 mmol) and phenylacetylene (2 mmol, 0.22 ml) were used for the synthesis as described in Section 2.3. The crude product was chromatographed on silica gel with ethyl acetate/CH$_2$Cl$_2$ (10:90 v/v) to yield pure **27d** (487 mg, 93%) as white crystals. Mp: 202–204 °C; R_f = 0.45 (ss B). (Found C, 78.68; H, 7.38. C$_{34}$H$_{37}$N$_3$O$_2$ (519.68) requires: C, 78.58; H, 7.18%). ^{1}H NMR (δ, ppm, CDCl$_3$): 0.79 (s, 3H, 18-H$_3$), 2.84 (m, 2H, 6-H$_2$), 3.72 (s, 1H, 17-H), 4.48 (dd, 1H, J = 13.5 Hz, J = 7.5 Hz, 16a-H$_2$), 4.56 (t, 1H, J = 13.5 Hz, 16a-H$_2$), 5.03 (s, 2H, Bn-H$_2$), 6.72 (s, 1H, 4-H), 6.78 (d, 1H, J = 8.5 Hz,

2-H), 7.21 (d, 1H, J = 8.5 Hz, 1-H), 7.33 (t, 1H, J = 7.5 Hz, 4′-H), 7.38 (t, 2H, J = 7.5 Hz, 3′- and 5′-H), 7.42 (d, J = 3.5 Hz, 4H, 2′- and 6′-H, 3″- and 5″-H), 7.84 (d, 2H, J = 7.5 Hz, 2″- and 6″-H), 7.88 (s, 1H, triazol-H). ^{13}C NMR (δ, ppm, CDCl$_3$): 17.9 (C-18), 25.9, 27.9, 29.7, 30.4, 31.8, 38.5, 43.3, 45.2 (C-13), 48.9, 49.1 (C-16), 54.6 (C-16a), 69.9 (Bn-CH$_2$), 82.6 (C-17), 112.3 (C-2), 114.8 (C-4), 119.6 (triazol-CH), 125.7 (C-2′ and -6′), 126.3 (C-1′), 127.4 (C-2″ and -6″), 127.8 (C-4′), 128.2 (C-4″), 128.5 (C-3″ and -5″), 128.8 (C-3′ and -5′), 130.5 (C-10), 132.64 (C-1″), 137.3 (C-1′), 137.9 (C-5), 147.7 (triazol-C); 156.8 (C-3).

2.3.41. 3-Benzyloxy-16β-[4′-(4″-nitro-benzoyloxymethyl)-1′H-1′,2′,3′-triazol-1′-yl]methylestra-1,3,5(10)-trien-17α-ol (27e)

Compound **19** (420.0 mg, 1 mmol) and propargyl 4-nitrobenzoate (2 mmol, 210 mg) were used for the synthesis as described in Section 2.3. The crude product was chromatographed on silica gel with ethyl acetate/CH$_2$Cl$_2$ (10:90 v/v) to yield pure **27e** (550 mg, 88%) as yellow crystals. Mp: 177–179 °C; R_f = 0.48 (ss B). (Found C, 69.55; H, 5.93. C$_{36}$H$_{38}$N$_4$O$_6$ (622.71) requires: C, 69.44; H, 6.15%). ^{1}H NMR (δ, ppm, DMSO-d_6): 0.65 (s, 3H, 18-H$_3$), 2.73 (m, 2H, 6-H$_2$), 4.40 (dd, 1H, J = 13.0 Hz, J = 8.5 Hz, 16a-H$_2$), 4.56 (dd, 1H, J = 13.5 Hz, J = 7.5 Hz, 16a-H$_2$), 4.63 (d, 1H, J = 5.0 Hz, 17-H), 5.04 (s, 2H, Bn-H$_2$), 5.47 (s, 2H, triazol-H$_2$), 6.68 (s, 1H, 4-H), 6.74 (d, 1H, J = 8.5 Hz, 2-H), 7.16 (d, 1H, J = 8.5 Hz, 1-H), 7.31 (t, 1H, J = 7.0 Hz, 4′-H), 7.37 (t, 2H, J = 7.0 Hz, 3′- and 5′-H), 7.41 (d, 2H, J = 7.0 Hz, 2′- and 6′-H), 8.18 (d, 2H, J = 8.5 Hz, 3″- and 5″-H), 8.33 (d, 3H, J = 6 Hz, 2″- and 6″-H, triazol-H). ^{13}C NMR (δ, ppm, DMSO-d_6): 17.5 (C-18), 25.6, 27.5, 29.2, 29.6, 31.8, 38.2, 42.9, 44.5 (C-13), 48.2, 49.1 (C-16), 53.6 (C-16a), 58.7 (linker-CH$_2$), 68.9 (Bn-CH$_2$), 80.8 (C-17), 112.1 (C-2), 114.4 (C-4), 123.8 (C-2′ and C-6′), 125.0 (triazol-CH), 126.1 (C-1), 127.4 (C-2″ and -6″), 127.6 (C-4′), 128.3 (C-3″ and -5″), 130.6 (C-3′ and -5′), 132.3 (C-10), 134.7 (C-1″), 137.3 (C-5 and C-1′), 141.1 (triazol-C), 150.2 (C-4″), 160.0 (C-3), 163.9 (C=O).

2.3.42. 3-Benzyloxy-16β-(4′-hydroxymethyl-1′H-1′,2′,3′-triazol-1′-yl)methylestra-1,3,5(10)-trien-17α-ol (27f)

Compound **27e** (210 mg, 0.5 mmol) was dissolved in methanol (10 ml) containing NaOCH$_3$ (14 mg, 0.25 mmol), and the solution was allowed to stand for 24 h. It was then diluted with water, and the precipitate separating out was filtered off and recrystallized from methanol to afford **27f** (273 mg, 99%) as a white crystalline product. Mp: 172–174 °C; R_f = 0.25 (ss B). (Found C, 73.68; H, 7.66. C$_{29}$H$_{35}$N$_3$O$_3$ (473.61) requires C, 73.54; H, 7.45%). ^{1}H NMR (δ, ppm, DMSO-d_6): 0.67 (s, 3H, 18-H$_3$), 2.74 (m, 2H, 6-H$_2$), 3.43 (s, 1H, 17-H), 4.34 (m, 1H, 16a-H$_2$), 4.50 (m, 3H, 16a-H$_2$ and Bn-H2), 4.61 (brs, 1H, OH), 5.04 (s, 2H, triazol-H$_2$), 5.16 (brs, 1H, OH), 6.69 (s, 1H, 4-H), 6.74 (d, 1H, J = 8.5 Hz, 2-H), 7.17 (d, 1H, J = 8.5 Hz, 1-H), 7.31 (d, 1H, J = 7.0 Hz, 4′-H), 7.37 (t, 2H, J = 7.0 Hz, 3′- and 5′-H), 7.41 (d, 2H, J = 7.0 Hz, 2′- and 6′-H), 8.00 (s, 1H, triazol-H). ^{13}C NMR (δ, ppm, DMSO-d_6): 17.5 (C-18), 25.6, 27.5, 29.2, 29.6, 31.9, 38.2, 43.0, 44.5 (C-13), 48.2, 49.1 (C-16), 53.5 (C-16a), 55.0 (linker-CH$_2$), 61.6, 68.9 (Bn-CH$_2$), 80.8 (C-17), 112.2 (C-2), 114.4 (C-4), 122.6 (triazol-CH), 126.6 (C-1), 127.4 (C-2′ and -6′), 127.6 (C-4′), 128.3 (C-3′ and -5′), 132.4 (C-10), 137.3 (C-5 and C-1′), 147.6 (triazol-C), 156.0 (C-3).

2.3.43. 3-Benzyloxy-16α-(4′-cyclopropyl-1′H-1′,2′,3′-triazol-1′-yl)methylestra-1,3,5(10)-trien-17α-ol (28a)

Compound **20** (420.0 mg, 1 mmol) and cyclopropylacetylene (2 mmol, 0.22 ml) were used for the synthesis as described in Section 2.3. The crude product was chromatographed on silica gel with ethyl acetate/CH$_2$Cl$_2$ (1:99 v/v) to yield pure **28a** (305 mg, 63%) as white crystals. Mp: 143–144 °C; R_f = 0.40 (ss B). (Found C, 77.15; H, 7.53. C$_{31}$H$_{37}$N$_3$O$_2$ (483.64) requires C, 76.98; H, 7.71%). ^{1}H NMR (δ, ppm, CDCl$_3$): 0.74 (s, 3H, 18-H$_3$), 0.87 and 0.97 (2 × s, 2 × 2H, 2″- and 3″-H$_2$), 2.85 (m, 2H, 6-H$_2$), 3.63 (d, 1H, J = 5.0 Hz, 17-H), 4.26 (dd, 1H, J = 13.5 Hz, J = 5.5 Hz, 16a-H$_2$), 4.60 (t, 1H, J = 13.5 Hz, 16a-H$_2$),

Table 2

Antiproliferative activities of compounds 25a-f, 26a-f, 27a-f and 28a-f.

Growth Inhibition, % ± SEM [calculated IC_{50} (μM)]

Conc. (μM)		HeLa	SiHa	MCF-7	MDA-MB-231	NIH-3 T3
25						
a	10	44.94 ± 1.04	21.17 ± 2.05	41.71 ± 0.64	47.32 ± 1.15	44.91 ± 1.36
	30	52.45 ± 2.39	66.23 ± 0.86	64.32 ± 0.56	71.49 ± 0.75	91.28 ± 0.50
b	10	51.49 ± 3.62	49.36 ± 1.69	44.58 ± 1.50	93.00 ± 0.26	44.81 ± 1.50
	30	62.58 ± 2.21	73.94 ± 2.04	50.52 ± 3.26	93.71 ± 0.09 [3.33]	59.09 ± 0.73
c	10	54.70 ± 1.88	49.58 ± 2.11	44.04 ± 3.32	77.13 ± 1.07	
	30	53.66 ± 2.56	61.83 ± 2.77	59.33 ± 2.99	88.81 ± 0.55 [5.91]	
d	10	64.14 ± 0.86	70.88 ± 1.03	73.41 ± 1.22	95.04 ± 0.16	95.60 ± 0.25
	30	90.12 ± 0.99 [2.28]	94.14 ± 0.29 [4.05]	80.16 ± 3.40 [3.91]	95.60 ± 0.06 [3.65]	98.22 ± 0.04 [3.34]
e	10	< 20	< 20	41.63 ± 2.83	21.96 ± 0.73	
	30	92.12 ± 0.25	89.25 ± 0.68	97.00 ± 0.11	95.22 ± 0.91	
f	10	45.08 ± 0.72	41.26 ± 1.25	55.41 ± 1.26	55.57 ± 1.50	
	30	39.39 ± 0.49	52.60 ± 1.31	62.52 ± 0.67	88.92 ± 0.99	
26						
a	10	37.98 ± 2.68	< 20	72.42 ± 2.19	46.43 ± 2.05	85.50 ± 1.22
	30	96.56 ± 0.11	96.71 ± 0.17	98.72 ± 0.09 [6.11]	97.96 ± 0.17	97.63 ± 0.12 [5.97]
b	10	38.55 ± 1.32	< 20	31.80 ± 1.35	17.13 ± 2.36	
	30	43.97 ± 2.23	< 20	84.44 ± 0.71	37.72 ± 2.28	
c	10	36.30 ± 1.45	< 20	24.95 ± 2.15	< 20	
	30	35.53 ± 1.24	< 20	74.73 ± 1.00	< 20	
d	10	< 20	< 20	47.25 ± 1.78	45.55 ± 2.63	
	30	22.15 ± 1.29	< 20	57.30 ± 0.77	59.79 ± 1.22	
e	10	< 20	< 20	68.51 ± 0.71	89.24 ± 0.70	31.41 ± 2.21
	30	96.98 ± 0.33	96.91 ± 0.14	99.12 ± 0.07 [6.53]	97.73 ± 0.23 [5.69]	99.01 ± 0.05 [11.75]
f	10	21.62 ± 3.46	< 20	29.14 ± 2.06	40.46 ± 2.98	10.00 ± 1.01
	30	30.79 ± 2.92	27.28 ± 1.90	43.28 ± 1.53	76.93 ± 1.60	23.40 ± 0.60
27						
a	10	24.26 ± 2.63	34.00 ± 1.43	58.38 ± 3.20	56.24 ± 0.98	25.56 ± 2.21
	30	85.22 ± 1.32	82.68 ± 1.25	97.21 ± 0.10	84.18 ± 0.44	99.24 ± 0.07
b	10	37.10 ± 1.77	39.59 ± 1.17	51.92 ± 1.00	56.44 ± 0.98	
	30	52.08 ± 2.08	69.54 ± 1.24	65.12 ± 1.91	71.81 ± 0.96	
c	10	38.89 ± 2.60	64.05 ± 1.24	49.68 ± 1.66	72.37 ± 1.27	13.99 ± 1.79
	30	55.93 ± 2.39	83.34 ± 1.31 [9.29]	61.26 ± 1.72	85.81 ± 1.04 [6.74]	29.56 ± 1.17
d	10	34.23 ± 1.39	30.04 ± 2.07	47.03 ± 1.25	55.77 ± 1.03	
	30	47.74 ± 0.78	39.96 ± 2.34	42.43 ± 1.69	57.71 ± 1.00	
e	10	< 20	21.53 ± 1.81	35.74 ± 1.33	< 20	
	30	99.06 ± 0.09	96.91 ± 0.06	98.50 ± 0.93	99.01 ± 0.52	
f	10	< 20	24.65 ± 1.46	25.50 ± 2.93	24.79 ± 2.20	
	30	98.72 ± 0.13	96.04 ± 0.25	98.41 ± 0.15	98.79 ± 0.16	
28						
a	10	35.48 ± 1.91	46.07 ± 1.13	52.88 ± 0.82	25.61 ± 2.84	
	30	63.44 ± 1.79	69.86 ± 0.55	73.39 ± 0.74	52.16 ± 2.52	
b	10	39.75 ± 2.45	< 20	43.51 ± 1.85	42.28 ± 1.44	44.86 ± 0.93
	30	47.34 ± 1.62	< 20			43.73 ± 2.25
c	10	56.71 ± 0.57	39.93 ± 3.14	48.56 ± 0.48	30.30 ± 1.64	
	30	58.21 ± 0.73	31.15 ± 2.86	49.93 ± 1.33	31.60 ± 3.08	
d	10	74.18 ± 1.15	76.88 ± 0.49	75.97 ± 0.89	86.12 ± 0.33	70.18 ± 1.15
	30	91.17 ± 0.33 [2.30]	87.39 ± 0.86 [4.14]	88.99 ± 0.25 [3.87]	90.72 ± 1.00 [3.89]	91.12 ± 1.64 [3.71]
e	10	27.42 ± 2.16	< 20	52.86 ± 1.30	29.58 ± 1.69	
	30	92.94 ± 0.17	91.91 ± 0.23	96.38 ± 0.07	94.09 ± 0.43	
f	10	30.97 ± 1.02	39.85 ± 1.24	50.60 ± 0.65	31.89 ± 2.92	
	30	91.88 ± 0.26	90.94 ± 0.18	95.12 ± 0.10	92.56 ± 0.34	
cisplatin	10	42.61 ± 2.33	86.84 ± 0.50	53.03 ± 2.29	20.84 ± 0.81	94.20 ± 0.39
	30	99.93 ± 0.26 [12.43]	90.18 ± 1.78 [7.84]	86.90 ± 1.24 [5.78]	74.47 ± 1.20 [19.13]	96.44 ± 0.17 [3.23]

5.03 (s, 2H, Bn-H₂), 6.72 (d, 1H, $J = 2.0$ Hz, 4-H), 6.78 (dd, 1H, $J = 8.5$ Hz, $J = 2.5$ Hz, 2-H), 7.22 (d, 1H, $J = 8.5$ Hz, 1-H), 7.32 (t, 1H, $J = 7.5$ Hz, 4′-H), 7.38 (t, 3H, $J = 7.5$ Hz, 3′- and 5′-H, triazol-H), 7.43 (d, 2H, $J = 7.5$ Hz, 2′- and 6′-H). ^{13}C NMR (δ, ppm, CDCl₃): 6.5 (C-1″), 7.9 (2C, C-2″ and -3″), 17.1 (C-18), 26.0, 27.9, 28.9, 29.8, 31.2, 38.9, 42.3, 43.5, 46.3 (C-16a), 47.0 (C-16), 50.7 (C-13), 69.9 (Bn-CH₂), 78.7 (C-17), 112.2 (C-2), 114.8 (C-4), 120.8 (triazol-CH), 126.3 (C-1), 127.4 (C-2′ and -6′), 127.4 (C-4′), 128.5 (C-3′ and -5′), 132.5 (C-10), 137.2 (C-1′), 137.9 (C-5), 149.6 (triazol-C), 156.7 (C-3).

2.3.44. 3-Benzyloxy-16a-(4′-cyclopentyl-1′H-1′,2′,3′-triazol-1′-yl) methylestra-1,3,5(10)-trien-17a-ol (28b)

Compound **20** (420.0 mg, 1 mmol) and cyclopentylacetylene (2 mmol, 0.22 ml) were used for the synthesis as described in Section

2.3. The crude product was chromatographed on silica gel with ethyl acetate/CH_2Cl_2 (2.5:97.5 v/v) to yield pure **28b** (417 mg, 82%) as white crystals. Mp: 197–199 °C; R_f = 0.42 (ss B). (Found: C, 77.62; H, 7.85. $C_{33}H_{41}N_3O_2$ (511.70) requires C, 77.46; H, 8.08%). ^{1}H NMR (δ, ppm, $CDCl_3$): 0.76 (s, 3H, 18-H_3), 2.85 (m, 2H, 6-H_2), 3.20 (s, 1H, 1″-H), 3.66 (d, 1H, J = 5.0 Hz, 17-H), 4.29 (dd, 1H, J = 13.5 Hz, J = 5.5 Hz, 16a-H_2), 4.62 (dd, 1H, J = 13.5 Hz, J = 9.5 Hz, 16a-H_2), 5.04 (s, 2H, Bn-H_2), 6.72 (s, 1H, 4-H), 6.78 (dd, 1H, J = 8.5 Hz, J = 2.5 Hz, 2-H), 7.21 (d, 1H, J = 8.5 Hz, 1-H), 7.31 (t, 1H, J = 7.0 Hz, 4′-H), 7.37 (t, 2H, J = 7.0 Hz, 3′- and 5′-H), 7.43 (d, 2H, J = 7.0 Hz, 2′- and 6′-H). ^{13}C NMR (δ, ppm, $CDCl_3$): 17.3 (C-18), 25.2 (2C), 26.1, 28.0, 29.1, 29.8 (2C), 31.3, 33.2, 36.8 (C-1″), 39.0, 42.4, 43.6, 46.4 (C-16a), 47.2 (C-16), 50.6 (C-13), 70.1 (Bn-CH_2), 79.0 (C-17), 112.4 (C-2), 115.0 (C-4), 126.3 (C-1), 127.4 (C-2′ and -6′), 127.8 (C-4′), 128.5 (C-3′ and -5′), 133.0 (C-10), 137.5 (C-1′), 137.9 (C-5), 156.9 (C-3).

2.3.45. 3-Benzyloxy-16a-(4-cyclohexyl-1H-1,2,3-triazol-1-yl)methyl-estra-1,3,5(10)-trien-17α-ol (28c)

Compound **20** (420.0 mg, 1 mmol) and cyclohexylacetylene (2 mmol, 0.22 ml) were used for the synthesis as described in Section 2.3. The crude product was chromatographed on silica gel with ethyl acetate/CH_2Cl_2 (2.5:97.5 v/v) to yield pure **28c** (200 mg, 76%) as a white crystals. Mp: 223–225 °C; R_f = 0.44 (ss B). (Found C, 77.82; H, 8.35. $C_{34}H_{43}N_3O_2$ (525.72) requires C, 77.68; H, 8.24%). ^{1}H NMR (δ, ppm, $CDCl_3$): 0.75 (s, 3H, 18-H_3), 2.84 (m, 3H, 6-H2, 1″-H), 3.64 (s, 1H, 17-H), 4.37 (m, 1H, 16a-H_2), 4.69 (m, 1H, 16a-H_2), 5.03 (s, 2H, Bn-H_2), 6.72 (d, 1H, J = 1.5 Hz, 4-H), 6.78 (dd, 1H, J = 8.5 Hz, J = 2.5 Hz, 2-H), 7.22 (d, 1H, J = 8.5 Hz, 1-H), 7.32 (t, 1H, J = 7.0 Hz, 4′-H), 7.38 (t, 2H, J = 7.0 Hz, 3′- and 5′-H), 7.43 (d, 2H, J = 7.0 Hz, 2′- and 6′-H

2.3.46. 3-Benzyloxy-16a-(4-phenyl-1H-1,2,3-triazol-1-yl)methyl-estra-1,3,5(10)-trien-17α-ol (28d)

Compound **20** (420.0 mg, 1 mmol) and phenylacetylene (2 mmol, 0.22 ml) were used for the synthesis as described in Section 2.3. The crude product was chromatographed on silica gel with ethyl acetate/CH_2Cl_2 (5:95 v/v) to yield pure **28d** (337 mg, 64%) as a white solid. Mp: 205–206 °C; R_f = 0.46 (ss B). (Found C, 78.42; H, 7.32. $C_{34}H_{37}N_3O_2$ (519.68) requires C, 78.58; H, 7.18%). ^{1}H NMR (δ, ppm, $CDCl_3$): 0.76 (s, 3H, 18-H_3), 2.87 (m, 2H, 6-H_2), 3.68 (d, 1H, J = 5.0 Hz, 17-H), 4.41 (dd, 1H, J = 13.5 Hz, J = 5.5 Hz, 16a-H_2), 4.69 (t, 1H, J = 13.5 Hz, 16a-H_2), 5.04 (s, 2H, Bn-H_2), 6.73 (s, 1H, 4-H), 6.79 (dd, 1H, J = 8.0 Hz, J = 2.0 Hz, 2-H), 7.22 (d, 1H, J = 8.0 Hz, 1-H), 7.38 (m, 8H, 2′-, 3′-, 4′-, 5′- and 6′-H, 3″-, 4″- and 5″-H), 7.84 (d, 2H, J = 7.5 Hz, 2″- and 6″-H), 7.89 (s, 1H, triazol-H). ^{13}C NMR (δ, ppm, $CDCl_3$): 17.1 (C-18), 26.0, 27.9, 29.8, 31.2, 38.9, 42.2, 43.5, 46.4 (C-13), 47.0 (C-16), 50.8 (C-16a), 69.9 (Bn-CH_2), 78.8 (C-17), 112.3 (C-2), 114.8 (C-4), 120.7 (triazol-CH), 125.7 (C-2′ and -6′), 126.3 (C-1), 127.4 (C-2″ and -6″), 127.8 (C-4′), 128.3 (C-4″), 128.5 (C-3″ and -5″), 128.9 (C-3′ and -5′), 130.2 (C-10), 132.8 (C-1′), 137.3 (C-1″), 137.9 (C-5), 147.1 (triazol-C), 156.7 (C-3).

2.3.47. 3-Benzyloxy-16a-[4′-(4″-nitro-benzoyloxymethyl)-1′H-1′,2′,3′-triazol-1′-yl]methylestra-1,3,5(10)-trien-17α-ol (28e)

Compound **20** (420 mg, 1 mmol) and propargyl 4-nitrobenzoate (2 mmol, 210 mg) were used for the synthesis as described in Section 2.3. The crude product was chromatographed on silica gel with ethyl acetate/CH_2Cl_2 (5:95 v/v) to yield pure **28e** (610 mg, 98%) as a yellow solid. Mp: 75–77 °C; R_f = 0.45 (ss B). (Found C, 69.57; H, 61.32. $C_{36}H_{38}N_4O_6$ (622.71) requires C, 69.44; H, 6.15%). ^{1}H NMR (δ, ppm, DMSO-d_6): 0.66 (s, 3H, 18-H_3), 2.71 (m, 2H, 6-H_2), 3.57 (s, 1H, 16-H), 4.29 (dd, 1H, J = 13.5 Hz, J = 8.5 Hz, 16a-H_2), 4.47 (dd, 1H, J = 13.5 Hz, J = 8.5 Hz, 16a-H_2), 4.85 (d, 1H, J = 5.0 Hz, 17-H), 5.44 (s, 2H, Bn-H_2), 6.65 (s, 1H, 4-H), 6.72 (d, 1H, J = 8.5 Hz, 2-H), 7.14 (d, 1H, J = 8.5 Hz, 1-H), 7.29 (t, 1H, J = 7.5 Hz, 4′-H), 7.35 (t, 2H, J = 7.5 Hz, 3′- and 5′-H), 7.40 (d, 2H, J = 7.5 Hz, 2′- and 6′-H), 8.17 (d, 2H, J = 8.5 Hz, 3″- and 5″-H), 8.28 (s, 1H, triazol H), 8.31 (d, 2H,

J = 8.5 Hz, 2″- and 6″-H). ^{13}C NMR (δ, ppm, DMSO-d_6): 16.9 (C-18), 25.6, 27.5, 28.4, 29.2, 31.1, 38.5, 39.8, 39.9, 43.2, 45.9 (C-16a), 46.2 (C-16), 53.4 (C-13), 58.7 (linker CH_2), 68.9 (Bn-CH_2), 78.0 (C-17), 112.1 (C-2), 114.4 (C-4), 123.8 (C-2″ and -6″), 125.0 (triazol CH), 126.1 (C-1), 127.4 (C-2′ and -6′), 127.5 (C-4′), 128.3 (C-3′ and -5′), 130.6 (C-3″ and -5″), 132.3 (C-10), 134.7 (C-1′), 137.3 (C-5), 141.0 (C-1″), 150.2 (triazol C), 156.0 (C-3), 163.9 (C=O).

2.3.48. 3-Benzyloxy-16a-(4′-hydroxymethyl-1′H-1′,2′,3′-triazol-1′-yl)methylestra-1,3,5(10)-trien-17α-ol (28f)

Compound **28e** (220 mg, 0.5 mmol) was dissolved in methanol (10 ml) containing $NaOCH_3$ (14 mg, 0.25 mmol), and the solution was allowed to stand for 24 h. It was then diluted with water, and the precipitate separating out was filtered off and recrystallized from methanol to afford **28f** (126 mg, 53%) as a white crystalline product. Mp: 86–88 °C; R_f = 0.25 (ss B). (Found C, 73.68; H, 7.63. $C_{29}H_{35}N_3O_3$ (473.61) requires C, 73.54; H, 7.45%). ^{1}H NMR (δ, ppm, DMSO-d_6): 0.68 (s, 3H, 18-H_3), 2.74 (m, 2H, 6-H_2), 3.58 (brs, 1H, OH), 4.26 (t, 1H, J = 8.5 Hz, 16a-H_2), 4.43 (dd, 1H, J = 13.0 Hz, J = 7.0 Hz, 16a-H_2), 4.51 (d, 2H, J = 5.0 Hz, linker H_2), 4.85 (d, 1H, J = 4.0 Hz, 17-H), 5.04 (s, 2H, Bn-H_2), 5.13 (brs, 1H, OH), 6.68 (s, 1H, 4-H), 6.74 (d, 1H, J = 8.5 Hz, 2-H), 7.17 (d, 1H, J = 8.5 Hz, 1-H), 7.31 (d, 1H, J = 7.0 Hz, 4′-H), 7.37 (t, 2H, J = 7.0 Hz, 3′- and 5′-H), 7.42 (d, 2H, J = 7.0 Hz, 2′- and -6′-H), 7.97 (s, 1H, triazol H). ^{13}C NMR (δ, ppm, DMSO-d_6): 16.9 (C-18), 25.6, 27.5, 28.5, 29.2, 31.1, 38.5, 40.7, 43.2, 45.9, 46.2 (C-16), 47.9 (C-13), 50.6 (C-16a), 55.0 (linker CH_2), 68.9 (Bn-CH_2), 78.0 (C-17), 112.1 (C-2), 114.4 (C-4), 122.7 (triazol CH), 126.1 (C-1), 127.4 (C-2′ and -6′), 127.6 (C-4′), 128.3 (C-3′ and -5′), 132.4 (C-10), 137.3 (C-1′), 137.4 (C-5), 147.6 (triazol C), 156.0 (C-3).

2.4. Determination of the antiproliferative activities

The growth-inhibitory effects of the compounds were tested *in vitro* by means of the MTT assay against a gynecological panel containing two breast cancer cell lines (MCF-7, MD-MB-231) and two cell lines isolated from cervical malignancies (HeLa, SiHa) [11]. All cell lines were obtained from the European Collection of Cell Cultures (Salisbury, UK). The cells were maintained in minimal essential medium supplemented with 10% fetal bovine serum (FBS), 1% non-essential amino acids and an antibiotic–antimycotic mixture (AAM). All chemicals, if otherwise not specified, were purchased from Sigma-Aldrich Ltd. (Budapest, Hungary). All cell lines were grown in a humidified atmosphere of 5% CO_2 at 37 °C. For pharmacological investigations, 10 mM stock solutions of the tested compounds were prepared with dimethyl sulfoxide (DMSO). The highest applied DMSO concentration of the medium (0.3%) did not have any substantial effect on the determined cellular functions. Cells were seeded into 96-well plates (5000 cells/well), allowed to stand overnight under cell culturing conditions, and the medium containing the tested compounds at two final concentrations (10 or 30 μM) was then added. After a 72-hour incubation viability was determined by the addition of 20 μl 3-(4,5-dimethylthiazol-2-yl)-2,5-diphenyltetrazolium bromide (MTT) solution (5 mg/ml). The formazan crystals precipitated in 4 h were solubilized in DMSO and the absorbance was determined at 545 nm with an ELISA plate reader utilizing untreated cells as controls. The most effective compounds eliciting at least 60% growth inhibition at 10 μM were tested again with a set of dilutions (0.3–30 μM) in order to determine the IC$_{50}$ values by means of Graphpad Prism 4.0 (Graphpad Software; San Diego, CA, US). These promising compounds were additionally tested using nonmalignant murine fibroblasts (NIH-3 T3) to obtain preliminary data concerning cancer selectivity of the tested molecules. Two independent experiments were performed with 5 parallel wells and cisplatin (Ebewe GmbH, Unterach, Austria), an agent administered clinically in the treatment of certain gynecological malignancies, was used as reference compound.

91

3. Results and discussion

3.1. Synthetic studies

To prepare novel steroid triazoles via 1,3-dipolar cycloaddition, we chose the 3-methoxy- and 3-benzyloxy-16-hydroxymethylestra-1,3,5(10)-trien-17-ol diastereomers (**5–8** and **9–12**). The synthesis strategy for the preparation of the starting diols (**21–28**) is illustrated in Scheme 1. The synthesis of steroidal 1,2,3-triazoles by CuAAC is outlined in Scheme 2.

Stereoselective tosylation of **5–8** and bromination of **9–12** gave **5b–8b** and **9c–12c**, respectively, which then underwent facile S_N2 substitution with NaN_3 in *N,N*-dimethylformamide to furnish the corresponding 16-azidomethyl compounds (**13–16** and **17–20**).

The 16-azido compounds were subjected to the azide–alkyne CuAAC reaction with different alkyl- and aryl-acetylenes. The azide–alkyne reactions of these compounds were carried out with CuI as catalyst in the presence of Et_3N in CH_2Cl_2 under reflux conditions to obtain the required 3-methoxy- and 3-benzyloxyestra-1,3,5(10)-trien-16-(1',4'-substituted 1',2',3')-triazolyl derivatives (**21–24** and **25–28**).

3.2. Determination of the antiproliferative properties of the 16-triazolylmethyl diastereomers

We have published recently that introduction of a substituted triazole moiety onto different positions of the estrane skeleton might increase the antiproliferative properties of estrone derivatives [12]. It was also established that the presence of certain alkyl or aralkyl protecting groups at the phenolic OH function is advantageous. Concerning that 16-hydroxymethylene-17-hydroxy derivatives of estrone-3-methyl ether or 3-benzyl ether (**5a-12a**) displayed substantial cytostatic potential against different types of breast cancer cell lines, these compounds might be suitable for directed modifications with the aim of developing potentially more active antiproliferative steroidal derivatives [13]. In the light of the above-mentioned recent observations, here we aimed to combine the substituted triazole and the 16,17-disubstituted estrone 3-ether moieties. The present study included an evaluation of the direct antiproliferative capacities of the newly synthesized heterocyclic compounds (**21a-f, 22a-f, 23a-f, 24a-f** and **25a-f, 26a-f, 27a-f, 28a-f**). The antiproliferative activities were determined *in vitro* by means of MTT assays against human adherent cervical (SiHa, HeLa) and breast cancer (MCF-7 and MDA-MB-231) cell lines.

The antiproliferative activities of the newly synthesized heterocyclic compounds depended on the nature of the protecting group at the 3-hydroxy function and on the orientation of the substituents at C-16 and C-17. In general, the 3-methyl ethers (**21–24**) exhibited weak antiproliferative action; none of them exerted any substantial effect at 10 µM (Table 1). All diastereomers of the 3-benzyl ether series (**25–28**) proved to be more potent in comparison with their 3-methyl ether counterparts (Table 2). This is in agreement with our earlier results [14]. Based on the substantial difference of the two groups, i.e. that of 3-methyl ethers and 3-benzyl ethers, it can be concluded that only the latter derivatives are promising from pharmacological point of view.

Concerning the orientation of the substituents at position C-16 and C-17, the 16β,17β-derivatives (**25a-f**) displayed outstanding growth-inhibitory properties. Two derivatives bearing similar cycloalkyl groups at position C-4' displayed substantial selective antiproliferative action against the triple-negative breast cancer cell line MDA-MB-231 with IC_{50} values in the low micromolar range. It should be underlined that **25b** and **25c** did not significantly influence the proliferation of other cell lines tested, including the non-cancerous fibroblast. Although both the 4'-cyclohexyl (**25c**) and the 4'-phenyl derivative (**25d**) have six-membered substituents, their cytostatic behavior is completely different. This might be attributed to the different steric structure of the two rings (chair or planar) at C-4'. Compound **25d** exerted potent antiproliferative action against all tested cell lines without any selectivity.

The *cis*-16α,17α-3-benzyl ethers (**28a–f**) were less potent than their β,β-counterparts (**25a–f**), except for **28d**, which behaved similarly to its diastereomer **25d**. The *trans*-16β,17α-isomers (**27a–f**) exhibited activity exclusively on the breast cancer cell lines. Surprisingly, the tendency observed earlier (in the case of compounds **25a–f**) concerning the nature of C-4' substituent was not valid here. Only **26a** and **26e** inhibited cell growth markedly, but with no tumor selectivity. It's worth mentioning that *trans*-16α,17β isomer **26c** was the sole compound, which inhibited the proliferation of HPV 16 + squamous cell carcinoma SiHa, showing an IC_{50} value comparable with that of cisplatin.

In view of the cell lines, it should be noted that triple-negative breast cancer cell line MDA-MB-231 proved to be the most sensitive and all calculated IC_{50} values were lower than that of the reference agent cisplatin (19.1 µM).

Regarding the present and earlier results obtained for 16,17-disubstituted 3-benzyl ethers, it can be stated that introduction of a substituted triazolyl moiety onto the C-16 methylene group of the *cis* isomers proved to be advantageous. In the case of compounds **25b** and **25c**, both the antiproliferative potential and the tumor selectivity were markedly improved.

Appendix A. Supplementary data

Supplementary data to this article can be found online at https://doi.org/10.1016/j.steroids.2019.108500.

References

[1] L.F. Tietze, H.P. Bell, S. Chandrasekhar, Natural product hybrids as new leads drug discovery, Angew Chem. Int. Ed. 42 (2003) 3996–4028.
[2] G. Mehta, V. Singh, Hybrid system through natural product leads: An approach towards new molecular entities, Chem. Soc. Rev. 31 (2002) 324–334.
[3] J. Adamec, R. Beckert, D. Weiß, V. Klimešová, K. Waisser, U. Möllmann, J. Kaustová, V. Buchta, Hybride molecules of estrone: new Compound with potential antibacterial, antifungal and antiproliferative activities, Bioorg. Med. Chem. 15 (2007) 2898–2906.
[4] S.D. Kuduk, F.F. Zheng, L. Sepp-Lorenzino, N. Rosen, S.J. Danishefsy, Synthesis and Evaluation of geldanamycin-estradiol hybrids, Bioorg. Med. Chem. 9 (1999) 1233–1238.
[5] A. Gupta, P. Saha, C. Descôteaux, V. Leblanc, É. Asselin, G. Bérubé, Design, synthesis and biological evaluation of estradiol-chlorambucil hybrids as anticancer agents, Bioorg. Med. Chem. Lett. 20 (2010) 1614–1618.
[6] Schneider Gy, A. Vass, I. Vincze, P. Sohár, Neighbouring group partcipation in the 16-hydroxymethyl-3-methoxyestre-1,3,5(10)-trien-17β-ol series, Liebigs Ann. Chem. (1988) 267–273.
[7] Schneider Gy, L. Hackler, P. Sohár, Preparation of 16α-hydroxymethyl-3-methoxy-estra-1,3,5(10)-trien 17α-ol and solvolysis investigation, Liebigs Ann. Chem. (1988) 679–683.
[8] P. Tapolcsányi, J. Wölfling, G. Falkay, Á. Márki, R. Minorics, Schneider Gy, Synthesis and receptor-binding examination of 16-hydroxymethyl-3,17-estradiol stereoisomers, Steroids 67 (2002) 671–678.
[9] M. Meldal, C.W. Tornøe, Cu-catalyzed azide–alkyne cycloaddition, Chem. Rev. 108 (2008) 2952–3015.
[10] Á. Szájli, J. Wölfling, E. Mernyák, R. Minorics, Á. Márki, G. Falkay, G.y. Schneider, Neighbouring group participation Part 16. stereoselective synthesisi and receptor-binding examination of the four stereoisomers of 16-bromomethyl-3,17-estradiols, Steroids 71 (2006) 141–153.
[11] T. Mosmann, Rapid colorimetrc assay for cellular growth and survival: application to prolyferation and cytotoxicity assay, J. Immunol. Methods 65 (1983) 55–63.
[12] E. Mernyák, I. Kovács, R. Minorics, P. Sere, I. Czégány Sinka, Wölfling, G. Schneider, Z.s. Újfaludi, I. Boros, I. Ocsovszki, Varjj ga M, Zupkó I., Synthesis of

trans-16-triazolyl-13α-methyl-17-estradiol diastereomers and the effects of structural modifications on their in vitro antiproliferative activities, J. Steroid Biochem. Mol. Biol. 150 (2015) 123–134.

[13] I. Sinka, A. Kiss, E. Mernyák, E. Wölfling, G. Schneider, I. Ocsovszki, C.Y. Kuo, H.C. Wang, I. Zupkó, Antiproliferative and antimetastatic properties of 3-benzyloxy-16-hydroxymethylene-estardiol analogs agains breast cancer cell lines, Eur. J. Pharm. Sci. 123 (2018) 362–370.

[14] E. Frank, J. Molnar, I. Zupko, Z. Kadar, J. Wölfling, Synthesis of novel steroidal 17α-triazolyl derivatives via Cu(I)-catalyzed azide-alkyne cycloaddition, and an evaluation of their cytotoxic activity in vitro, Steroids 76 (2011) 1141–1148.

93